Volume 50
Number 2
21 January 2021
Pages 693–1470

Chem Soc Rev

Chemical Society Reviews

rsc.li/chem-soc-rev

ISSN 0306-0012

ROYAL SOCIETY OF CHEMISTRY

REVIEW ARTICLE

Mariateresa Giustiniano *et al.*

Visible light photocatalysis in the late-stage functionalization of pharmaceutically relevant compounds

Chem Soc Rev

REVIEW ARTICLE

View Article Online
View Journal | View Issue

Cite this: *Chem. Soc. Rev.*, 2021, **50**, 766

Visible light photocatalysis in the late-stage functionalization of pharmaceutically relevant compounds†

Rolando Cannalire,[a] Sveva Pelliccia,[a] Luca Sancineto,[b] Ettore Novellino,[a] Gian Cesare Tron[c] and Mariateresa Giustiniano*[a]

Received 8th August 2020

DOI: 10.1039/d0cs00493f

rsc.li/chem-soc-rev

The late stage functionalization (LSF) of complex biorelevant compounds is a powerful tool to speed up the identification of structure–activity relationships (SARs) and to optimize ADME profiles. To this end, visible-light photocatalysis offers unique opportunities to achieve smooth and clean functionalization of drugs by unlocking site-specific reactivities under generally mild reaction conditions. This review offers a critical assessment of current literature, pointing out the recent developments in the field while emphasizing the expected future progress and potential applications. Along with paragraphs discussing the visible-light photocatalytic synthetic protocols so far available for LSF of drugs and drug candidates, useful and readily accessible synoptic tables of such transformations, divided by functional groups, will be provided, thus enabling a useful, fast, and easy reference to them.

Introduction

The availability of effective and general protocols for the direct and selective structural modification of complex biorelevant compounds is of utmost importance in research and development (R&D) campaigns. Actually, they are considered a powerful tool to speed up the optimization of ADME profiles and physical properties such as solubility and stability. Over and above these key issues, late-stage functionalization (LSF) of

[a] *Department of Pharmacy, University of Naples Federico II, via D. Montesano 49, 80131, Napoli, Italy. E-mail: mariateresa.giustiniano@unina.it*
[b] *Department of Pharmaceutical Sciences, University of Perugia, Group of Catalysis, Synthesis and Organic Green Chemistry, via del Liceo 1, 06123 Perugia, Italy*
[c] *Department of Drug's Sciences, University of Piemonte Orientale "A. Avogadro", largo Donegani 2, 20188, Novara, Italy*

† Electronic supplementary information (ESI) available. See DOI: 10.1039/d0cs00493f

Rolando Cannalire

Rolando Cannalire received his PhD in Medicinal Chemistry at the University of Perugia in 2016. During his PhD course, he has been visiting PhD student at University of Lisbon and after at University of Groningen. In 2016, he held a post-doctoral fellowship from Italian National Research Council and, from 2017 to mid-2019, he held postdoctoral fellowships at the Department of Pharmaceutical Sciences of University of Perugia. Since July 2019, he has been appointed Assistant Professor at the Department of Pharmacy of the University of Naples Federico II. His research mainly concerns on the design and synthesis of antiviral, antibacterial, antitumor agents, kinase inhibitors, and development of synthetic methodologies.

Sveva Pelliccia

Sveva Pelliccia graduated summa cum laude in 2008 in Chemistry and Pharmaceutical Technologies at the University of Naples 'Federico II', and in 2013 she obtained a PhD in medicinal chemistry. In 2012, she was a visiting student at University La Sapienza in Rome working in the research laboratories of Professor R. Silvestri. From 2013 to 2020 she was a postdoctoral researcher at the University of Rome and at the University of Naples 'Federico II'. Her research interests range from the discovery of novel multicomponent reactions to the study of new anticancer and antiviral agents.

pharmaceutical agents can hasten the identification of structure–activity relationships (SARs), thereby optimizing on-target potency and minimizing undesired off-target effects.[1–5] Even the introduction of small alkyl groups can have dramatic effects on the bioactivity profiles of complex molecular architectures: it is indeed always astonishing to consider how a simple change of a C–H to a C–Me bond can induce up to a 2135-fold boost in the potency of a drug candidate thanks to both conformational changes and hydrophobic effects, thereby leading to the postulation of the so-called *magic methyl effect*.[6] Groundbreaking avenues in the field of LSF have been unearthed by Baran lab in 2012 who devised sodium and zinc sulfinate based reagents[7] (known with the commercial name of Baran Diversinates™) and by Sharpless lab in 2014 with the development of sulfur(VI) Fluoride Exchange (SuFEx) chemistry.[8] To this end, visible-light photocatalysis (Vis-PC) offers unique opportunities to achieve smooth and clean functionalization of drugs by unlocking site-specific reactivities under generally mild reaction conditions.[9] As a matter of fact, fine-tuneable settings relying on single-electron transfer processes (SET) mediated by excited-state organic or metal-based photosensitizers, hydrogen atom transfer (HAT) catalysts, or the formation of electron–donor–acceptor (EDA) complexes, have been rescuing open-shell intermediates from being considered untamed species, thereby further extending the scope of radical chemistry to LSF and supporting the translational potential of radical species.[10,11] Additionally, the possibility of unravelling unexpected reactivities far beyond the classical ionic chemistry triggered by thermal activation provided new stimulating perspectives in the synthesis of drugs.[12–14] In order to promote the application of photosynthetic approaches to the synthesis of target compounds, recently, König, prompted by the lack of bachelor and master courses focused on photochemistry and

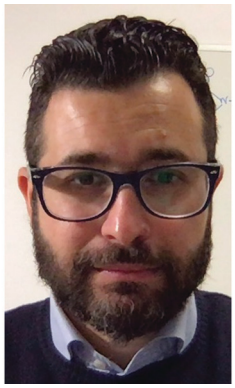

Luca Sancineto

Luca Sancineto obtained his PhD degree in medicinal chemistry in 2012 with a thesis focused on anti-HIV agents. He was visiting researcher at the ICGEB of Trieste (2010). In 2017, he was awarded with the Marie Curie Fellowship in the frame of the Polonez grant by the Polish-NCN and he moved to the Centre of Molecular and Macromolecular studies of the Polish Academy of Sciences in Lodz, Poland for a 2 year stay. In 2018 he got National Academic Qualification as associate professor in medicinal and organic chemistry. Presently, he is assistant professor in Organic Chemistry at the University of Perugia.

Ettore Novellino

Ettore Novellino graduated in 1974 in Pharmacy summa cum laude at the University of Naples "Federico II". Since November 1994 he has been Full Professor of Medicinal Chemistry. He has been Dean of the Faculty of Pharmacy and then Chair of the Department of Medicinal Chemistry; since 2013 he has been Chair of the Department of Pharmacy of the University of Naples "Federico II". In 2009 the Italian Chemical Society awarded Prof. Novellino with the Pratesi Medal. Since 1986 he has spent numerous research periods abroad (USA; Germany; Switzerland).

Gian Cesare Tron

Gian Cesare Tron is full professor of medicinal chemistry at the Università del Piemonte Orientale. He received his degree in Chimica e Tecnologia Farmaceutiche in 1994 and his PhD in Organic Chemistry in 2001 from the Università di Torino (Italy) under the supervision of Prof. Appendino. He has spent sabbatical leaves in the laboratories of Prof. J. Zhu (Institut de Chimie des Substances Naturelles, Gif-sur-Yvette, France), V. Aggarwal (School of Chemistry, Bristol, UK), and V. Fokin (The Scripps Research Institute, La Jolla, USA). His research interests concern the discovery of new multicomponent reactions and their application in the field of medicinal chemistry.

Mariateresa Giustiniano

Mariateresa Giustiniano graduated in 2007 in Chimica e Tecnologia Farmaceutiche at the University of Naples-Federico II, and in 2010 she obtained her PhD in medicinal chemistry (Supervisor: Prof. E. Novellino). She was visiting student in the laboratories of Prof. G. C. Tron (Università del Piemonte Orientale, Novara) and Prof. J. Zhu (CNRS, Gif-sur-Yvette, Paris). From 2011 to 2016 she held post-doctoral fellowships at University of Naples Federico II and in 2016 she became assistant professor (RTDB). In 2018 she got National Academic Qualification as associate professor in medicinal chemistry. Her research interests focus on multicomponent reactions, visible-light photocatalysis, medicinal chemistry.

photoredox catalysis, issued specific retrosynthetic disconnections with informative schemes, availability of the catalysts and reagents, and functional group tolerance.[15] The widening of knowledge in the field to an even broader readership including medicinal chemist practitioners is a priority for scientists committed to the advancement of such a chemistry domain. The innate green features arising from being inspired by Nature's exploitation of light radiation as primary energy source throws vibrant brushstrokes of colors in the landscape of industrial-scale synthesis of drugs.[16–19] Yet, while advancements in the field of Vis-PC have been recurrently reviewed,[20–29,30–37] a comprehensive highlight of exclusive opportunities provided by Vis-PC for the late-stage modification of pharmaceuticals has not been reported so far. Accordingly, the present review aims to bridge this gap by selecting visible light promoted transformations which have been applied to bioactive substrates as chemical inputs, thus demonstrating to be enough mild, robust, and general to become part of the existing LSF toolboxes. To this end, original articles published from 2014 up to June 2020 have been covered. [#] The manuscript is organized in paragraphs and subparagraphs on the basis of the key-reactive functional groups directly engaged in the visible light promoted processes and either already present on the drug scaffolds or formerly introduced to provide a suitable handle for the derivatization. The section dealing with arenes C(sp^2)–H functionalization includes also heteroarenes when they have been enclosed in the scope of the protocol, while the section addressing heteroarenes C(sp^2)–H functionalization covers methodologies limited to such a class of aromatic substrates. Furthermore, synoptic tables divided by functional groups can be found as ESI,† in order to provide a useful, fast, and easy reference to the transformations discussed in the text. Notwithstanding the efforts of including all the relevant reports in the field, the authors apologise for any unintentional omission.

1. Functionalization of C=C bonds

The reductive addition of carbon-centered radicals to electron-poor olefins, also known as Giese-type addition, is one of the most exploited photocatalyzed transformations enabling the redox-neutral construction of C–C bonds.[38,39] In particular, in the first reports by Minisci *et al.* and by Giese *et al.* the intermediate C-centered radicals were generated by using either metal salts and diacyl peroxides or alkyl-mercury salts and $NaBH_4$, respectively. At the time, this kind of transformation was mainly exploited for the synthesis of tailor-made polymers, and in order to develop more controllable reaction conditions suitable for the creation of polyfunctionalized small molecules, the influence of substituents at both the olefin and the radical center on reactivity as well as regio- and stereo-selectivities were largely investigated.[40] With the burgeon of visible light photocatalytic methods, a plethora of mild synthetic protocols have spread out in the literature, thus enabling ever increasing applications of Giese-type reactions to the construction of diverse and complex linear and cyclic scaffolds. Thanks to the identification of suitable and often bench stable radical precursors, olefins have been reported to smoothly undergo alkylation and arylation, as well as the introduction of functional groups such as fluoromethyl[41] or perfluoroalkyl, halogens, amines, amides, sulfonamides, *etc.*, thus providing an easy access to chemical useful intermediates. Worthy of note, as highlighted hereafter, the scope of such a powerful transformation, has been extended in recent years to convergent three-component processes and to the achievement of enantioenriched scaffolds *via* the use of asymmetric either metal-based photocatalysts or organocatalysts. Additionally, the merging of photoredox and transition metal catalysts, empowered the obtainment of functionalized olefins *via* crosscoupling pathways following the photoinduced generation of open-shell intermediates.

1.1 Formation of C(sp^2)–C(sp^3) bonds

1.1.1 Alkylation and alkylarylation. Electron-deficient olefins can react with both alkyl- and aryl-carbon-radicals generated from either boronic acids or esters to form their alkylated or arylated derivatives.[42] This transformation was promoted by a dual catalytic system comprising a Lewis base (LB) catalyst such as quinuclidin-3-ol and an iridium-based photocatalyst. The reaction proceeded under mild conditions, in a 1 : 1 mixture of acetone and methanol, under 14 W blue LEDs irradiation at 30 °C for 24 h. Interestingly, the use of quinuclidin-3-ol as additive is required to enhance boronic acids and esters reactivity, characterized by high oxidation potentials, by engaging their vacant p-orbital in a dative bond with the n-orbital of the Lewis base. A single-electron oxidation of the complex boronic acid/ester-LB, with a reductive quenching cycle of the photocatalyst, allowed the smooth generation of the carbon-radical, which will then add to the alkene. The reaction scope was widely demonstrated with electron-deficient olefins, with both alkyl- and aryl-boronic acids, and with alkyl-boronic esters, while aryl-boronic esters were found to be substantially less reactive. Late-stage functionalization of ixazomib **4**, an orally available drug for the treatment of multiple myeloma, was shown in Scheme 1.

A rapid and mild protocol for alkylarylation of alkenes was described by X.-L. Lv *et al.*[43] as a multicomponent approach involving α-bromocarbonyls (**5**) and boronic acids (**7**) under 30 W blue LEDs irradiation at room temperature and by means of both iridium (*fac*-Ir(ppy)$_3$) and copper(I) catalysis (CuI). From a mechanistic point of view, the process represented an elegant example of radical relay (Scheme 2). This directing-group-free protocol enabled the access to a wide range of γ-arylated esters, ketones, and amides with excellent functional group tolerance as exemplified in the late-stage modification of γ-tocopherol containing alkene **9**.

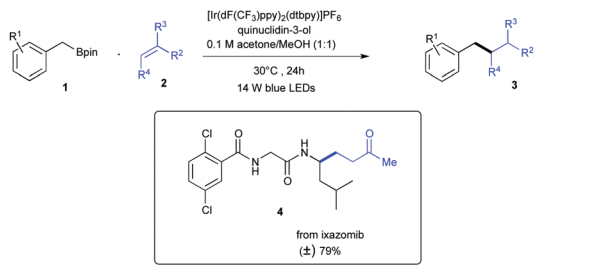

Scheme 1 Olefins alkylation with boronic acids.

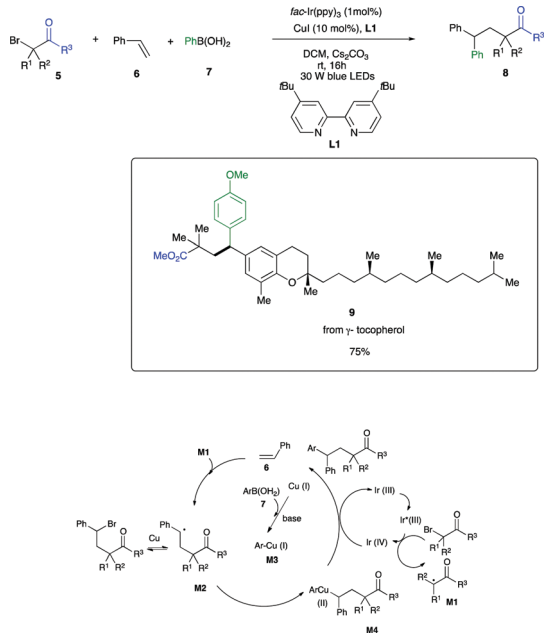

Scheme 2 Alkylarylation of olefins.

A three-component olefin dicarbofunctionalization (DCF) can be accomplished by merging photoredox and nickel catalysis.[44] Regioselective alkylation and arylation of alkenes was enabled by a Giese-type addition of an alkyl radical onto an olefin to give a radical intermediate able to generate an alkyl-nickel adduct. The latter finally underwent oxidative addition of aryl halides, followed by reductive elimination to give the DCF product and restore the Ni^{I} species. Alkyltrifluoroboronates (**10**, Scheme 3) were used as efficient source of alkyl radicals while vinyl borates (**11**) were employed as competent olefins. More in detail, the reaction was promoted by Ni(bpy)Br_2, an iridium catalyst, and K_2HPO_4 in THF, using blue LEDs as the photons source at room temperature for 16 h. The aryl bromide scope was wide, and sensitive functional groups such as acidic, electrophilic, and homolytically labile C–H bonds were well tolerated. Suitable tertiary alkyltrifluoroborates included polycyclic ones, while secondary radicals gave satisfactory yields,

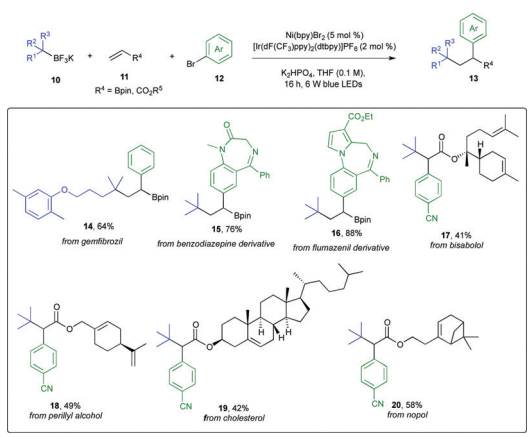

Scheme 3 Dicarbofunctionalization of olefins.

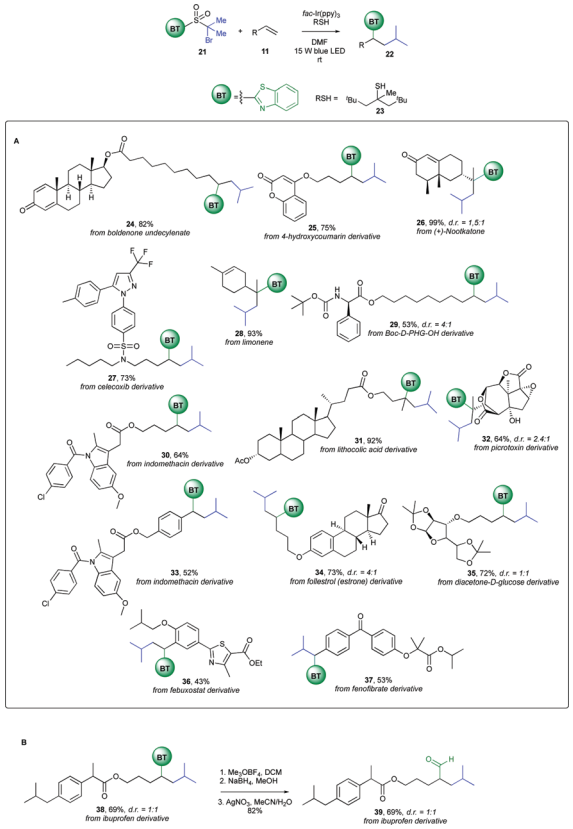

Scheme 4 Polarity umpolung alkylation of electron-rich olefins.

partially affected by a direct cross-coupling as a major competing reaction pathway. Moreover, other electronically deficient alkenes, bearing ester and nitrile functional groups, could be incorporated into the reaction scope. To further prove the robustness of this protocol, late-stage functionalization of gemfibrozil, a benzodiazepine derivative, flumazenil, bisabolol, perillyl alcohol, cholesterol, and nopol was reported (**14**–**20**, Scheme 3).

Recently, the group of C. Zhu reported a polarity umpolung strategy to accomplish radical alkylation of alkenes using a wide array of easily accessed, difunctional alkylating agents (Scheme 4).[45]

The reaction design relied on the replacement of the nucleophilic alkyl radicals with electrophilic sulfone-bearing surrogates **21**, thereby providing a polarity-matched process in the reaction with electron-rich aliphatic alkenes **11**. More in detail, an alkyl and a migratory group were tethered to the sulfone-based alkylating agent **21**, so that, after formation of an alkyl radical and docking onto the alkene double bond, an intramolecular heteroaryl or oximino migration occurred, along with SO_2 extrusion. The transformation required *fac*-Ir(ppy)$_3$ as a photoredox catalyst, *tert*-dodecylthiol **23** as both the hydrogen source and the reductant, K_2CO_3 as a base to neutralize the *in situ* formed HBr, DMF as the solvent, under irradiation with 15 W blue LEDs at room temperature. The mild reaction conditions enabled a wide scope and a broad functional group tolerance, which was showcased also in the late-stage functionalization of drugs and biorelevant compounds **24**–**37** (Scheme 4A). Additionally, the synthetic

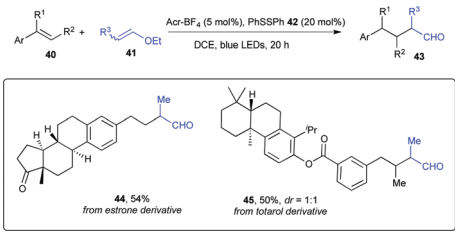

Scheme 5 Synthesis of aldehydes.

utility of the benzothiazole group as aldehyde precursor was shown in the conversion of ibuprofen derivative **38** into carbonyl-adduct **39** (Scheme 4B).

1.1.2 Synthesis of aldehydes. By reacting styrenes (**40**, Scheme 5) with vinyl ethers (**41**) in the presence of an acridinium salt as photocatalyst and a disulfide HAT agent **42** under blue LEDs irradiation it was possible to get polysubstituted alkyl aldehydes (**43**).[46] From a mechanistic point of view, this transformation relied on an anti-Markovnikov hydroformylation process, enabled by a SET oxidation of an electron-rich olefin, which formed a radical cation intermediate. The latter could be intercepted regioselectively at the less substituted carbon by a vinyl ether. The mild reaction conditions developed were applied to a number of diversely substituted styrenes, which were readily converted into linear, β-branched, and β,γ-dibranched aldehydes, while tolerated functional groups included ethers, halogens, esters, and alkynes. Remarkably, 2-substituted enol vinyl ethers were shown to be competent reaction partners, thus extending its scope to α-branched, α,β-dibranched, and α,β,γ-substituted aldehydes. As examples of complex biorelevant structures an estrone-derived alkene and a styryl analogue of totarol were converted into derivatives **44** and **45**, respectively (Scheme 5).

1.1.3 Three-component coupling of styrenes with oxime esters and boronic acids. An oxime ester, *e.g.* **46** (Scheme 6) when irradiated with visible-light in the presence of an appropriate photocatalyst, was able to generate an iminyl radical **46A**, which was prone to undergo a subsequent C–C bond cleavage to form a cyanoalkyl radical **46B**.[47] The latter added to a styrene **6** to afford a benzylic radical **46C**, whose coupling with a boronic acid derived $ArCu^{II}$ complex gave a 1,1-diaryl-methane-containing alkylnitrile **47**. In order to achieve such a transformation, reaction conditions required $Cu(CH_3CN)_4PF_6$, dtbbpy as a ligand, Na_2CO_3 as a base, in MeOH as a solvent, under 7 W blue LEDs irradiation at room temperature for 10 h. The scope of both alkenes and boronic acids was good, with a functional group tolerance embodying silyl, esters, ketone, thioether, ether, and halogens. Heteroaromatic boronic esters, as well as internal alkenes participated to the reaction, as well as nonsymmetrical cyclobutanone- and 3,3-disubstituted *O*-acyl oxime esters. Estrone derivative **48** was obtained in a good 58% yield and 1:1 d.r. (Scheme 6).

1.1.4 Synthesis of GABA derivatives. J. Ma *et al.* reported a photocatalytic enantioselective approach for the synthesis of β-substituted γ-aminobutyric acid derivatives *via* a conjugate addition of α-amino alkyl radicals, generated from glycine derivatives, to alkenes.[48] Remarkably, the reaction did not require a photocatalyst, whereas *N*-methyl-*N*-Boc glycines protected as

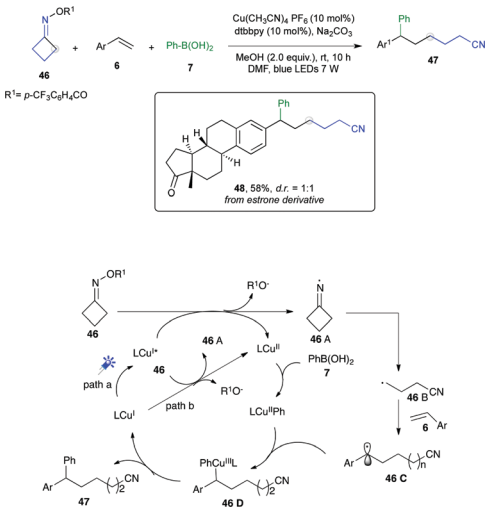

Scheme 6 Three-component alkylarylation of olefins.

N-(acyloxy)phthalimides (**50**) either were directly reduced by a photoexcited Hantzsch ester (HE) or a photoexcited Rh-complex first oxidized the HE and then transferred a single electron to the phthalimide substrate. The reaction proceeded in acetone at room temperature for 16 h under irradiation with a 23 W CFL. As radical acceptors, a wide array of α,β-unsaturated *N*-acylpyrazoles (**49**) took part to the reaction giving the corresponding GABA derivatives in good to excellent yields. Estrone derivative **52** stood for the potential of this synthetic methodology to functionalize complex biorelevant substrates (Scheme 7).

1.1.5 Synthesis of elongated esters. Alkenes could be converted into elongated esters *via* addition of an (alkoxycarbonyl)-methyl radical intermediate generated from an ester-stabilized phosphorous ylide **53** (Scheme 8) upon SET reduction mediated by an excited state photoredox catalyst.[49]

More in detail, after optimization of reaction conditions, *fac*-Ir(ppy)$_3$ resulted the most efficient photocatalyst, while ascorbic acid and pentafluorobenzenethiol **54** were required as additives in 1,2-dimethoxyethane (DME)/H_2O 1:1 mixture under blue LEDs irradiation at room temperature for 40 h. Monosubstituted alkenes underwent the hydro(alkoxycarbonyl)-methylation with excellent regioselectivities, including vinyl acetate, vinyltriethylsilane, and vinylboronic acid pinacol ester. Five- to eight-membered cyclic and acyclic 1,2-disubstituted alkenes gave the desired esters with high to moderate yields. Late-stage functionalization of biologically active complex substrates

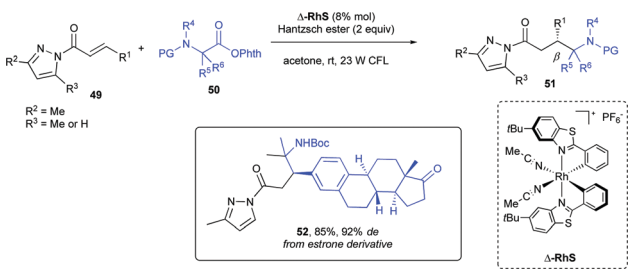

Scheme 7 Synthesis of GABA derivatives.

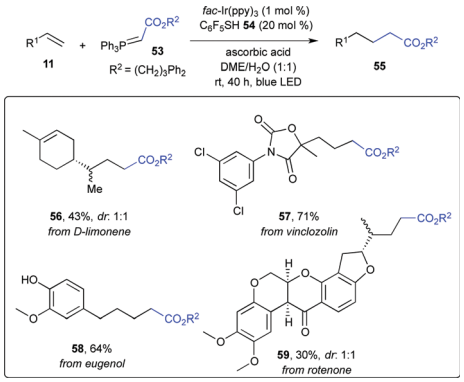

Scheme 8 Synthesis of elongated esters.

such as eugenol, vinclozolin, D-limonene, and rotenone was also accomplished as shown in Scheme 8 (compounds **56–59**).

1.1.6 Hydrodifluoromethylation. Alkenes can be hydrodifluoromethylated with difluoroacetic acid **61** and phenyliodine(III) diacetate (PIDA) in THF under visible light (Scheme 9).[50] Here, THF had three different roles: (1) as a solvent; (2) as a hydrogen atom donor, and (3) as an electron-donor in a SET to form, after decarboxylation, the key radical intermediate $^{\bullet}CF_2H$. The reaction presented a wide scope and full tolerance towards a variety of functional groups such as esters, amides, alcohols, aldehydes, halides, and nitriles. Likewise, vinyl sulfones, vinyl silanes, and even alkynes proved to be competent substrates. Alkene-containing biologically relevant compounds were also investigated: *O*-estrone, uracil, *N*-allyl caffeine, vinclozolin, and bioallethrin were all aptly hydrodifluoromethylated to give compounds **63–67** (Scheme 9).

One more protocol to achieve hydrodifluoromethylation was reported by Q.-Y. Lin *et al.* and exploited *fac*-Ir(ppy)$_3$ as the photoredox catalyst, bromodifluoromethylphosphonium bromide **68** (Scheme 10) as precursor of difluorocarbene, H_2O and THF as hydrogen sources.[51] In addition, triphenylphosphine, sodium iodide and an inorganic base were also essential to promote such a transformation. The scope was wide, covering terminal alkenes such as styrenes, α,β-unsaturated esters and sulfones, and geminally substituted alkenes. Tolerated functional groups ranged from hydroxy, ether, aldehyde, carboxylic acids, and esters, to halogens and phosphine oxide.

Complex biorelevant substrates included estrone, umbelliferone, the fungicide vinclozolin, and two insecticides rotenone, and bioallethrin (**66**, **70–74**, Scheme 10).

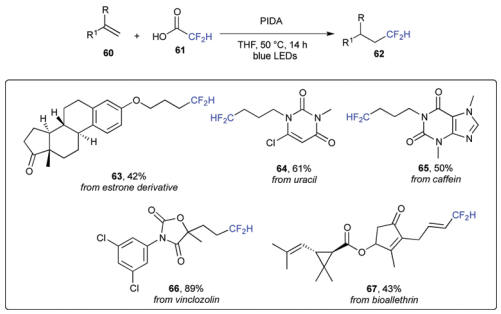

Scheme 9 Hydrofluoromethylation of olefins with difluoroacetic acid.

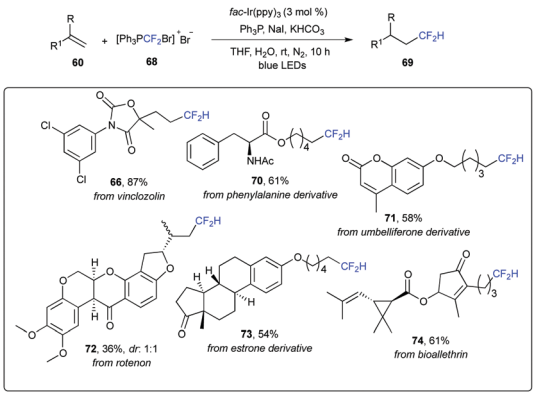

Scheme 10 Hydrofluoromethylation of olefins with bromodifluoromethylphosphonium bromide **68**.

1.1.7 Trifluoromethylation. Trifluoromethylation of alkenes, alkynes, and electron-rich heterocycles under metal-free photoredox catalytic conditions was reported by S. P. Pitre *et al.* Thoroughly, methylene blue was employed as photosensitizer, Togni's reagent **76** (Scheme 11) as CF_3 radical source, and TMEDA (*N*,*N*,*N*′,*N*′-tetramethylenediamine) as electron-donor, in DMF under warm white LEDs irradiation.[52] Trifluoromethylation of electron-rich heterocycles such as indoles, pyrroles, and thiophene tolerated aldehydes, esters, and free primary amines. Internal *vs.* terminal alkenes orthogonality was remarkably shown for biorelevant carvone **78** (TMEDA was replaced by DBU).

An alternative mild and general protocol to achieve photocatalytic trifluoromethylation of styrenes (**79**) was reported by N. J. W. Straathof *et al.*[53] The authors employed *fac*-Ir(ppy)$_3$ as the photocatalyst, CF_3I **81** as the trifluoromethyl radical source, CsOAc as an additive, DMF as a solvent, under visible light irradiation at room temperature (Scheme 12). When 4-hydroxythiophenol was used as an additive, the starting olefins underwent an hydrotrifluoro-methylation. The reaction scope was wide,

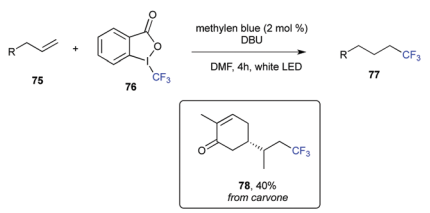

Scheme 11 Trifluoromethylation of olefins with Togni's reagent.

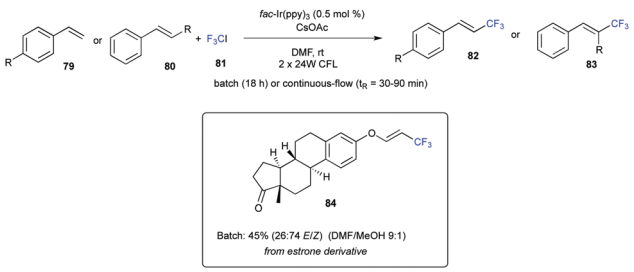

Scheme 12 Trifluoromethylation of olefins with trifluoroiodomethane.

including a variety of substituted styrenes, internal alkenes, and vinyl heterocycles (*e.g.* pyridines, pyrazine, and thiazole). Interestingly, following the observation that *E*/*Z* ratio could be increased by short reaction times, the authors demonstrated that the formation of the *Z* isomer, occurring *via* isomerization of the *E* isomer promoted by an energy transfer mechanism, could be decreased by performing the reaction in a continuous flow microreactor. As example of complex substrate, an estrone derived vinyl ether was converted, in batch conditions, into **84** in 45% and 26 : 74 *E*/*Z* ration (Scheme 12).

1.1.8 Hydrocarbomethoxydifluoromethylation. Methyl fluorosulfonyldifluoroacetate ($FO_2SCF_2CO_2Me$, Chen's reagent, **85** Scheme 13) could be employed as carbomethoxydifluoromethylating reagent with unactivated alkenes, styrenes, and heteroarenes under visible light photoredox conditions.[54]

This protocol featured exceptionally mild reaction conditions, with *fac*-Ir(ppy)$_3$ as the photoredox catalyst, NMP as a solvent at room temperature for 20 hours. Investigation of the alkene substrates revealed orthogonality with respect to unprotected alcohols, aldehydes, epoxides, ethers, esters, tosylate, and imides. Remarkably, the late-stage functionalization of an estrone-derived terminal olefin was carried out in 89% yield (**87**, Scheme 13).

1.1.9 Alkynyldifluoroalkylation. W. Jin *et al.* developed a general and mild approach to β-difluoroalkylated alkynes (**90**) *via* a three-component reaction involving the difluoroalkyl bromide **89**, unactivated alkenes (**2**), and alkynyl sulfones (**88**, Scheme 14).[55] Optimized reaction conditions employed *fac*-Ir(ppy)$_3$, Et_3N as an additive, in DMF under blue LEDs irradiation at room temperature. Terminal alkenes with a wide range of functional groups (alcohols, ethers, bromides, ketones, epoxides, amides, TBS, Bpin, and TMS) were competent substrates, as well as 1,1-disubstituted and internal alkenes. Electron-rich alkynyl sulfones gave better yields than electron-poor ones. In addition to $BrCF_2CO_2Et$, bromodifluoroacetamide and perfluoroalkyl iodides also provided β-difluoroalkylated and β−perfluoroalkylated alkynes in good yields. An estrone-derived alkene was used as complex test substrate and converted into derivative **91** in a good yield.

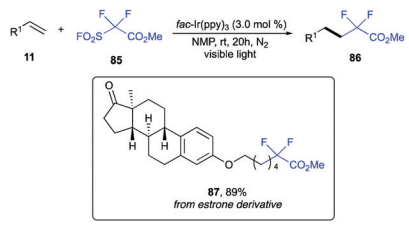

Scheme 13 Hydrocarbomethoxydifluoromethylation of olefins.

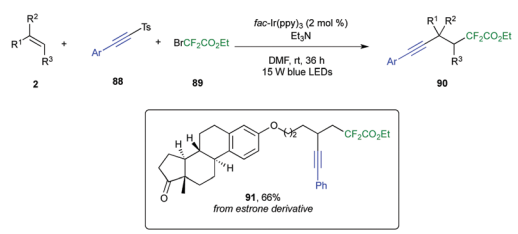

Scheme 14 Alkynyldifluoroalkylation of olefins.

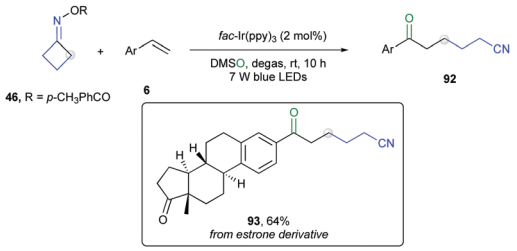

Scheme 15 Synthesis of ketoalkylnitriles.

1.1.10 Synthesis of ketoalkylnitriles. Styrenes could be functionalized as ketoalkylnitriles (**92**) *via* an iminyl radical triggered C–C bond cleavage of a cycloketone oxime ester **46** to give a C-centered cyanoalkyl radical intermediate, followed by the addition of the latter to the double bond to form a benzyl radical intermediate (Scheme 15).[56] Oxidation to carbocation and Kornblum oxidation with DMSO enabled the installation of the keto-functional group. The procedure features mild conditions, with *fac*-Ir(ppy)$_3$ as the photoredox catalyst and 7 W blue LEDs irradiation at room temperature for 10 hours. The broad substrate scope and functional group tolerance was further proved in the derivatization of an estrone-derived terminal alkene to **93** in 64% yield, albeit longer reaction times (20 hours) were requested (Scheme 15).

1.1.11 Synthesis of indole terpenoid-like compounds. α,β-Unsaturated enones **94** (Scheme 16) could undergo an intermolecular conjugate addition of pyrroloindoline/furoindoline radicals to afford indole terpenoid-like derivatives **96**.[57] As reported by S. Zhou and coworkers the reaction was efficiently promoted by $[Ir(ppy)_2(dtbbpy)]PF_6$, in the presence of Et_3N, in DMF as a solvent under blue LEDs irradiation. Conjugated adducts of a variety of electron-deficient olefins were obtained in good yields and as a single diastereomer or as diastereomeric mixtures at C-2, while the stereochemistry of the pyrroloindoline/furoindoline moiety was retained thanks to its structural rigidity.

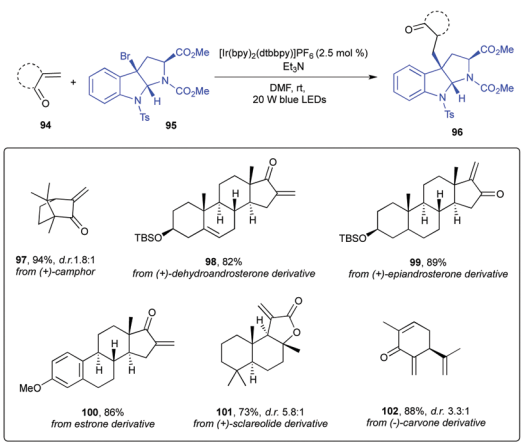

Scheme 16 Synthesis of indole terpenoid-like compounds.

As example of complex substrates, enones derived from (+)-camphor, (+)-dehydroandrosterone, (+)-epiandrosterone, (+)-estrone, (+)-sclareolide, and (−)-carvone, respectively, smoothly reacted with the optically active bromopyrroloindoline to give compounds **97–102** (Scheme 16).

1.2 Introduction of functional groups

1.2.1 Haloalkylation. Olefins could undergo intermolecular atom-transfer radical addition (ATRA) with a variety of haloalkanes under irradiation with a fluorescent light bulb and in the presence of *p*-anisaldehyde **104** (Scheme 17) as photocatalyst in acetonitrile at room temperature.[58] As revealed by mechanistic investigations, the aldehyde catalyst (20 mol%) was able to generate the reactive alkyl radicals by sensitization of the organic halides through an energy-transfer pathway. The haloalkanes scope included α-bromoesters but also substrates such as bromoacetonitrile, carbon tetrachloride, and perfluorohexyl iodide. Furthermore, both terminal olefins and internal alkenes proved to be suitable reaction partners and showed a good tolerance for halogens, unprotected or silyl protected alcohols, carbamates, and epoxides. Besides simple olefins, electron-rich silyl enol ethers and naturally occurring (*R*)-limonene and (−)-β-pinene smoothly reacted under standard conditions affording for example derivatives **106** and **107** (Scheme 17).

1.2.2 Chlorotrifluoromethylation. Alkenes (**2**) could be chlorotrifluoromethylated by using $Ru(phen)_3Cl_2$ as photoredox catalyst, CF_3SO_2Cl **108** (Scheme 18) as a source of both a $^{\bullet}CF_3$ radical and a chloride ion, K_2HPO_4 as a base in MeCN at room temperature under visible-light irradiation.[59] Terminal alkenes showed higher reactivities (76–99% yields) with respect to internal ones (54–78% yields), tolerating functional groups such as *N*-tosyl- and *N*-Boc-protected amines, unprotected hydroxyl and formyl groups, ethers, esters, amides, and heterocyclic rings such as phthalimide and quinoline. The scope of internal alkenes was further tested on complex scaffolds such as carvone, the pesticide rotenone, and the insecticide (+)-nootkatone (**110–112**, Scheme 18).

1.2.3 Bromodifluoromethylation. Difluoromethyltriphenylphosphonium bromide **113** (Scheme 19) could be used as CF_2H radical precursor to accomplish bromodifluoromethylation of alkenes.[60] The reaction was efficiently catalyzed by *fac*-$Ir(ppy)_3$ in DMF as a solvent under visible light irradiation at room temperature for 10 hours. Additionally, the use of $CuBr_2$ was essential to inhibit the competing formation of a hydrodifluoromethylated adduct, thus leading to optimum yields (see reaction mechanism, Scheme 19). The scope of the transformation embodied terminal alkenes bearing a range of functional groups such as alcohols, ethers, aldehydes, carboxylic acids, esters, alkyl bromides, and phosphine oxide. Late-stage bromodifluoromethylation of the fungicide vinclozolin, and pesticides bioallethrin and rotenone, was carried out in 82% yield (**115–117**, Scheme 19).

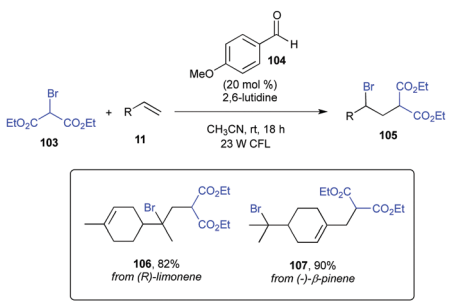

Scheme 17 Haloalkylation of olefins.

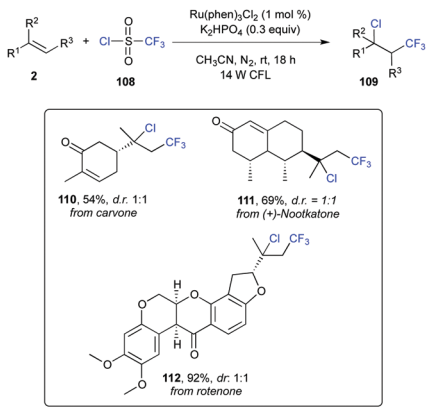

Scheme 18 Chlorotrifluoromethylation of olefins.

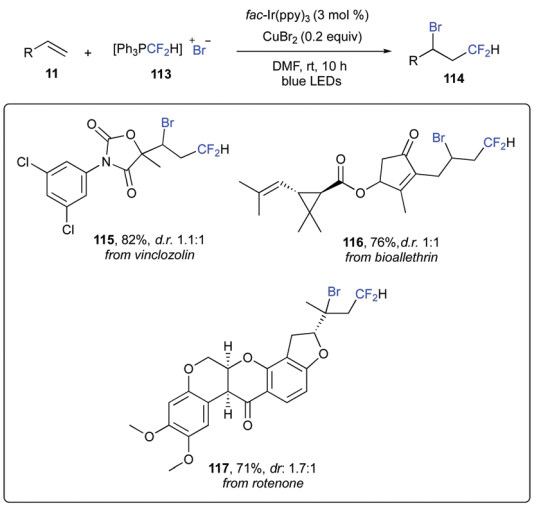

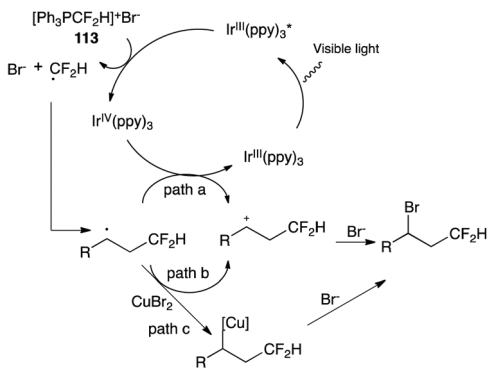

Scheme 19 Bromodifluoromethylation of olefins.

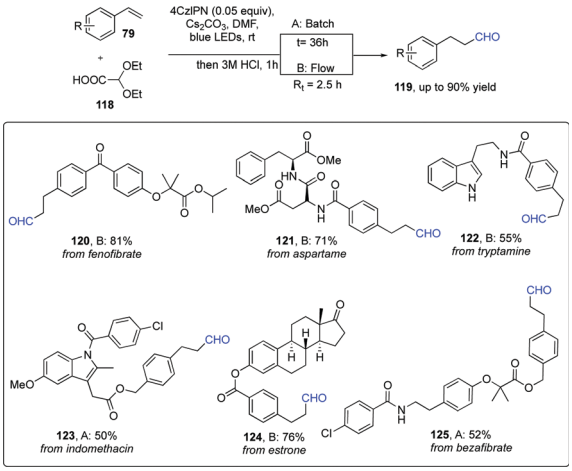

Scheme 20 Hydroformylation of olefins.

1.2.4 Hydroformylation. Styrenes (**79**, Scheme 20) were reported to undergo a chemo- and regioselective, organo-photoredox catalyzed hydroformylation reaction into aldehydes (**119**) with diethoxyacetic acid **118** as the formylation reagent.[61] More specifically, a formyl radical equivalent, produced from 2,2-diethoxyacetic acid *via* a 1,2,3,5-tetrakis-(carbazolyl)-4,6-dicyanobenzene (4CzIPN) visible light photo-catalyzed oxidation–decarboxylation sequence, added in an anti-Markovnikov fashion to the C=C bond of aryl olefins. The benzylic radical formed was then reduced by SET from the anion radical of 4CzIPN, to afford a benzylic anion. Finally, protonation and acid catalyzed hydrolysis of the acetal produced the target aldehyde, regioselectively, in up to 90% yield.

A broad array of functional groups was tolerated under the mild reaction conditions employed: a dye photocatalyst, Cs_2CO_3 as the base, DMF as the solvent, under blue LEDs irradiation at room temperature. Generally, continuous flow technology was applied in order to minimize competitive polymerization of styrenes. Reaction conditions were kept identical, except for reaction times, which could be reduced to 2.5 hours. On the other hand, under flow-conditions, styrenes with electron-neutral and -donating substituents gave poor yields: in these cases, the batch method gave satisfactory yields, thanks to the lower concentration of the styrene partner. The robustness of this synthetic methodology was proved by the successful hydroformylation of complex bioactive substrates, such as fenofibrate and bezafibrate used to reduce cholesterol and triglycerides in the blood, tryptamine, the NSAID indomethacine, estrone, and aspartame **120–125** (Scheme 20).

1.2.5 Hydroacylation. E. Voutyritsa and C. G. Kokotos reported a metal-free protocol to achieve hydroacylation of unactivated olefins in water by using phenylglyoxylic acid **128** (Scheme 21) as photoinitiator under irradiation with CFL.[62] The authors observed that, since the reaction did not proceed under neat conditions, it probably could benefit from the "on water" rate acceleration. The substrate scope included both linear and branched α,α-disubstituted aldehydes, which are considered a challenging class of aldehydes, as, after conversion into acyl radical, the latter are prone to decarbonylation to give a stable secondary

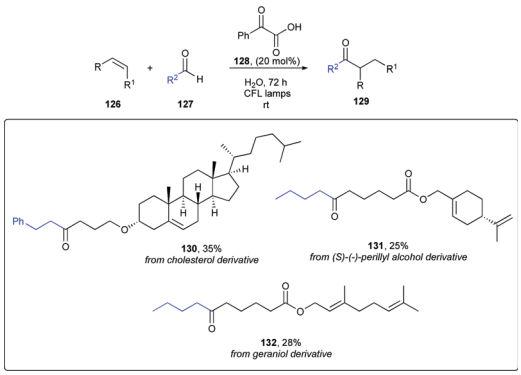

Scheme 21 Hydroacylation of olefins.

alkyl radical. The scope was also extended to aromatic aldehydes, albeit with moderate yields. As for the alkene partner, terminal substituted alkenes and non-terminal alkenes proved to react efficiently, while attempted conversion of styrenes led to unproductive polymerizations. Late-stage functionalization of pharmaceutically relevant molecules such as cholesterol, (*S*)-(−)-perillyl alcohol, and geraniol was reported (**130–132**, Scheme 21).

1.2.6 Hydro- and deuteroamidation. Unactivated alkenes (**134**) could undergo anti-Markovnikov hydro- and deuteroamidation by merging photoredox and thiol HAT catalysis with either water or D_2O.[63] This transformation exploited the addition of an electrophilic CbzHN-radical (Cbz = carbobenzyloxy), generated by a SET oxidation of an α-Cbz-amino-oxy acid (**133**) to an alkene. The resulting radical intermediate was then reduced by catalytic thiophenol, which mediated the H-transfer from the stoichiometric formal radical-reducing agents, *i.e.* either water or D_2O. Standard conditions, as shown in Scheme 22, were successfully applied to a broad array of alkenes, including naturally occurring multifunctionalized scaffolds such as (±)-linalool, (−)-menthol, α-pinene, and sclareol (**136–139**, Scheme 22).

1.2.7 Diamidation and conversion to α-aminoketones. A photoredox difunctionalization of alkenes with *O*-acyl hydroxylamines **140**, **141** and **146–148** (Scheme 23), as precursors of *N*-centered radicals, was reported by Q. Qin.[64] Interestingly, the solvent had a dramatic effect on the fate of this reaction, as diamidation (Ritter reaction) and oxidative amidation

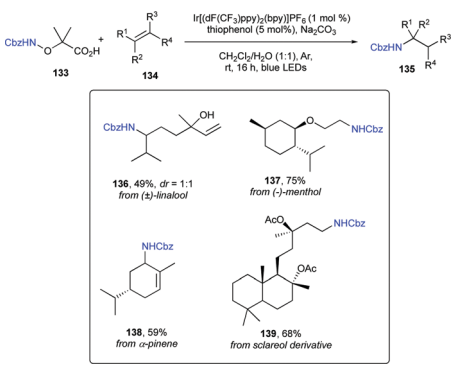

Scheme 22 Hydro- and deuteroamidation of olefins.

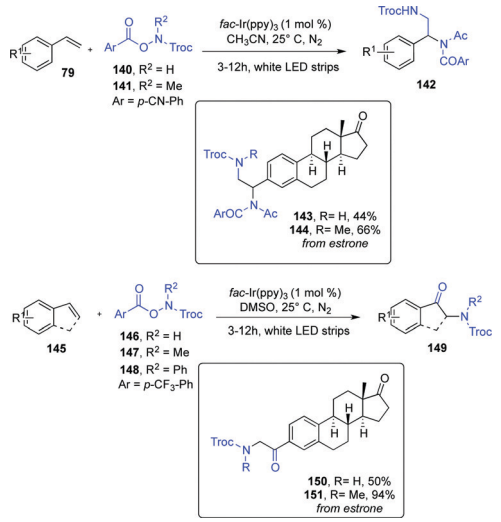

Scheme 23 Diamidation of olefins and conversion to α-ketoamides.

(Kornblum oxidation) were achieved in CH_3CN and DMSO, respectively. A variety of 1,2-diamidates **142** and α-amino ketones **149** were prepared using *fac*-Ir(ppy)$_3$ as the photocatalyst under nitrogen atmosphere, room temperature, and white LEDs irradiation for 3–12 h. The reaction proved to be quite general, as styrenes, naphthalene- and thiophene-derived alkenes, and indene smoothly gave the desired α-aminoketones in medium yields. Modified biologically valuable molecules, such as **143**, **144**, **150**, and **151** derived from estrone (Scheme 23), were also feasible.

1.2.8 Conversion to sulfonamides. Electron-deficient alkenes **152** (Scheme 24) are suitable substrates for a single-step hydrosulfamoylation *via* a challenging single electron reduction of sulfamoyl chlorides (for dimethylsulfamoyl chloride **153** E_{red} = −1.59 V *vs.* saturated calomel electrode (SCE) in MeCN).[65]

In order to smoothly generate the sulfamoyl radical intermediate, a Cl-atom abstraction was accomplished by a silyl radical, formed from tris(trimethylsilyl)silane precursor and photocatalyst Eosin Y, under blue LEDs irradiation. This practical and cost-effective methodology was applied to a wide range of electron-deficient olefins, as well as to diverse primary, secondary, and tertiary, sulfamoyl chlorides, including cyclic ones. Various functional groups, such as esters, amides, carboxylic acids, amines, ethers, halides, nitro and nitriles were tolerated. The derivatization of estrone and ibrutinib derivatives **155** and **156** were reported with good yields of 78 and 69%, respectively (Scheme 24).

A diverse set of substituted sulfonamides **158** (Scheme 25) could be obtained from unactivated alkenes using primary or secondary sulfonamides (*e.g.* **157**), an iridium photocatalyst, a dialkyl phosphate base, and a thiol hydrogen atom donor under blue LEDs irradiation as reported by the group of R. R. Knowles.[66] The proposed mechanism relied on a proton-coupled electron transfer (PCET), where an *N*-centered sulfonamidyl radical **162A** gave an anti-Markovnikov addition to the olefin double bond. The so formed benzyl radical **162B** abstract a hydrogen atom from the thiol to give the final compounds **158**. The authors reported

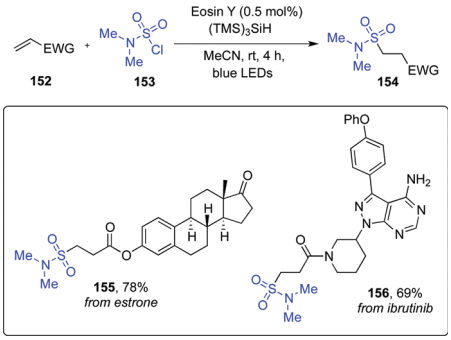

Scheme 24 Conversion of olefins to sulfonamides.

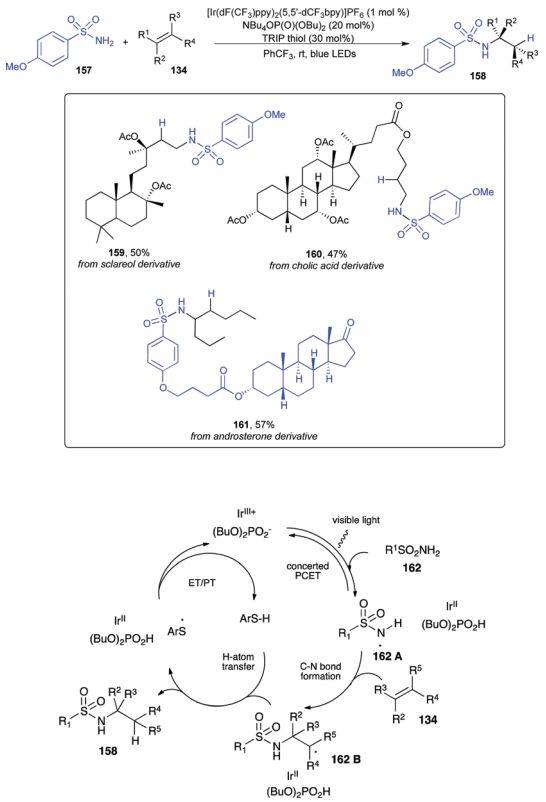

Scheme 25 Conversion of olefins to sulfonamides.

more than 60 examples, including both acyclic and cyclic sulfonamides, and complex bioactive substrates such as cholic acid, sclareol, and androsterone (**159–161**, Scheme 25).

More recently, the same group reported an intramolecular enantioselective amination of alkenes with sulfonamides (Scheme 26).[67] The reaction mechanism underpinning the asymmetric induction relied on noncovalent interactions between a neutral sulfonamidyl radical and a chiral phosphoric acid **CP1** generated in a PCET event, similar to the above described one. By using [Ir(dF(CF$_3$)ppy)$_2$(5,5′-dCF$_3$bpy)]PF$_6$ as a photoredox catalyst, the chiral phosphate **CP1**, and catalytic quantities of TRIP thiophenol as HAT catalyst, in PhCF$_3$ under blue LEDs irradiation at −20 °C for 24 hours, a wide range of amination products **164** were obtained in medium to excellent yields and with e.r. up to 98 : 2.

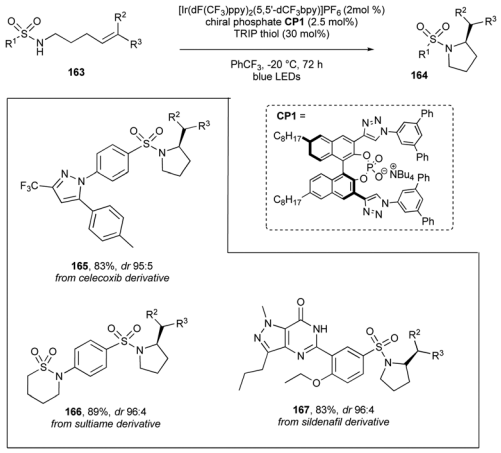

Scheme 26 Intramolecular sulfonamidation of olefins.

The extraordinary functional group tolerance was further showcased in the late-stage modification of celecoxib-, sultiame-, and sildenafil-derived sulfonamides (**165–167**, Scheme 26).

1.2.9 Dual carbosulfonylation with allylsulfones. Allylsulfones **168** (Scheme 27) could act both as carbon and sulfone functional groups sources, suitable for the conversion of alkenes (**6**) to difunctionalized adducts (**169**).[68] The protocol harnessed the visible-light mediated generation of a neutral nitrogen-centered radical (NCR) from the *N*-(2-acetylphenyl)-benzenesulfonamide catalyst (**NCR cat**, Scheme 27), able to activate allyl sulfones **168** by forming a *N*-sulfonamide intermediate while releasing a key sulfonyl radical. By using $[Ir(ppy)_2(dtbbpy)]PF_6$ as the photocatalyst, the above-mentioned NCR precursor, K_2CO_3 as a base, and 7 W blue LEDs irradiation in DMSO as solvent at room temperature, a wide range of both electron-rich and electron-poor styrenes **6**, along with heteroaromatics such as 2-pyridyl- and 2-indolyl-moieties were readily difunctionalized to **169** with medium to good yields (40–75%). Furthermore, internal and simple aliphatic alkenes were also competent substrates, albeit with lower yields. An estrone derived alkene and febuxostat were selected as examples of complex bioactive substrates (**170** and **171**, Scheme 27).

1.2.10 Arylsulfonylation. Simultaneous sulfonylation/arylation of styrenes (**172**) was achieved in a photoredox catalyzed three-component reaction involving sulfinate salts (**173**) and cyanopyridines (**174**) (Scheme 28).[69] From a mechanistic point of view, the process relied on the oxidative formation of a sulfur-centered electrophilic radical, followed by its addition

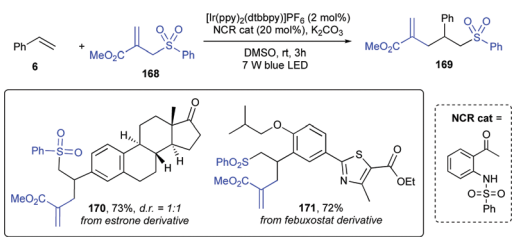

Scheme 27 Dual carbosulfonylation of olefins.

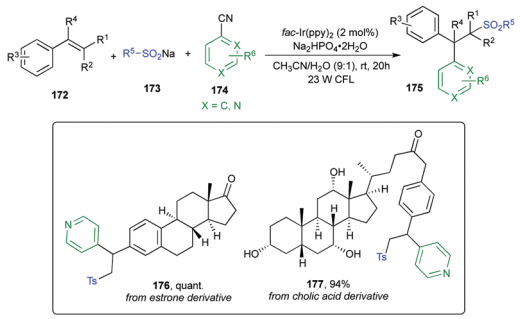

Scheme 28 Arylsulfonylation of olefins.

onto styrenes (**172**) to form a benzyl radical intermediate. The latter was eventually trapped with a persistent radical anion coming from the reduction of the cyanopyridine partner. Experimentally, the reaction required *fac*-$Ir(ppy)_3$ as the photocatalyst, $Na_2HPO_4{\cdot}2H_2O$ as a base, and it was run in a 9 : 1 mixture of $MeCN/H_2O$ under a 23 W CFL irradiation at room temperature for 20 h. The wide scope was demonstrated with a library of 47 examples, with yields up to quantitative. Functionalized cholic acid with a *p*-aminostyrene link, and an estrone vinyl derivative were also converted into derivatives **176** and **177** in excellent yields.

1.2.11 Amination and aziridination. Organic azides could be used as nitrogen source to achieve $C(sp^3)$–H amination and alkene aziridination by using iron porphyrin as a dual photosensitizer and as a catalyst forming a reactive iron-nitrene intermediate (Scheme 29).[70]

Remarkably, the use of such a catalyst enabled the chemo- and regio-selective formation of C–N bonds under mild conditions, whereas visible light driven nitrene transfer and insertion reactions usually lacked selectivity due to a free nitrene intermediate reactivity. Investigated of C–H amination scope of indane with different organic azides revealed that electron-withdrawing substituents led to higher yields with respect to electron-rich substrates. The scope of hydrocarbons embodied a range of inputs including benzylic and tertiary C–H bonds. Additionally, intramolecular C–H amination of

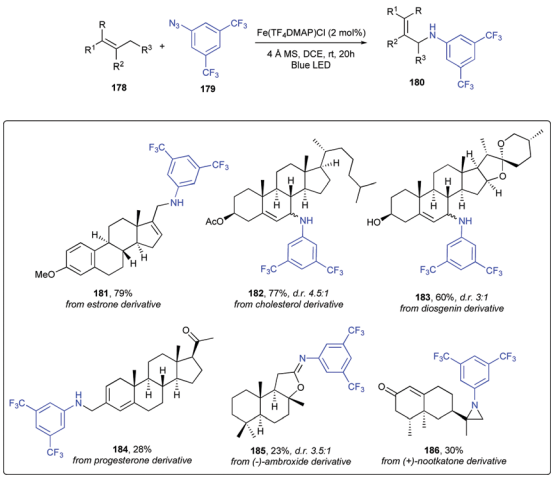

Scheme 29 Amination and aziridination of olefins.

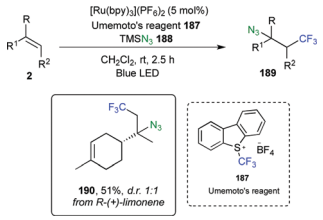

Scheme 30 Azidotrifluoromethylation of olefins.

N-containing alkyl azides and α-azidoketones led to imidazolines and to nitrogen bridged bicyclic moieties, respectively. As for the alkene aziridination, a good stereospecificity was observed, albeit with a limited scope. Derivatization of natural biorelevant products such as estrone, Ac-cholesterol, Bz-diosgenin, progesterone, (−)-ambroxide, and (+)-nootkatone was accomplished in moderate to good yields by using $Fe(F_{20}TPP)Cl$ or $Fe(TF_4DMAP)Cl$ in DCE as a solvent at 25–30 °C under blue LEDs irradiation (**181–186**, Scheme 29).

1.2.12 Azidofluoromethylation, azidofluoroalkylation, and azidohydroxylation. Alkenes could be converted into their corresponding azidotrifluoromethylated adducts **189** (Scheme 30) by using Umemoto's reagent **188** as the CF_3 source, $[Ru(bpy)_3](PF_6)_2$ as the photoredox catalyst, and $TMSN_3$ **187** in CH_2Cl_2 as a solvent.[71] Blue LEDs irradiation at room temperature afforded the desired final azides in short reaction times (typically 2.5 hours). Remarkably, the replacement of $TMSN_3$ with primary aromatic amines, carbamates, amides, sulfonamides, and hydrazines led to the formation of aminotrifluoromethylated products. Among suitable 1,1-disubstituted alkenes, the natural terpene derivative (*R*)-(+)-limonene reacted smoothly to give the tertiary alkyl azide **190** in 51%.

Same years later, it was shown that in the presence of fluoroalkyl iodides (*e.g.* **191**, Scheme 31) and sodium azide **192**, alkenes can undergo a direct and regioselective azidofluoroalkylation (Scheme 31).[72]

This transformation was promoted by $Ru(bpy)_3Cl_2{\cdot}6H_2O$ as the photocatalyst, and by $BnEt_3NBr$ as phase-transfer agent, while a sub-stoichiometric amount of sodium iodide was also needed to improve reaction yields. Excellent selectivities, mild reaction conditions, ready availability of perfluoroalkyl precursors, and broad substrate scope were all valuable issues of this synthetic approach. In order to test the applicability of this approach to complex bioactive molecules, an estrone-derived alkene was converted to azide **194** in a good 52% (Scheme 31).

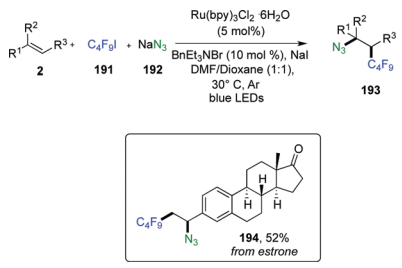

Scheme 31 Azidofluoroalkylation of olefins.

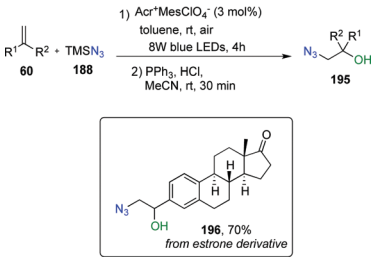

Scheme 32 Azidohydroxylation of olefins.

B. Yang and Z. Lu reported the conversion of alkenes (**60**) into their corresponding hydroxyazide derivatives (**195**) under metal-free aerobic reaction conditions in two steps (Scheme 32).[73] The first photocatalyzed step afforded the 1-azido-2-peroxytrimethylsilane derivatives, which were converted into β-amino alcohols after stirring at room temperature for 30 minutes the filtered reaction mixtures with triphenylphosphine, HCl (conc.) in acetonitrile (Scheme 32). Standard conditions for the photocatalyzed transformation employed $Acr^+MesClO_4^-$ (9-mesityl-10-methylacridinium perchlorate) as the visible-light photocatalyst, $TMSN_3$ in a solution of toluene at room temperature under the irradiation of 8 W blue LEDs and under air for 4 h. This regioselective olefin 1,2-difunctionalization showed an excellent functional group tolerance, with a broad substrate scope, and it was used for converting estrone-derived styrene into its hydroxyazide derivative **196** in 70% yield.

1.2.13 Azidoarylation. Alkenes could react in a three-component coupling with pyridines (**174**) and $TMSN_3$ **187** under visible light photoredox catalytic conditions (Scheme 33).[74] The protocol exploited a radical addition/radical coupling sequence, enabling the synthesis of β-azidopyridines (**197**). Experimentally the reaction required $[Ir(ppy)_2(dtbbpy)]PF_6$ as a photocatalyst in ^{t}BuOH as the solvent under 90 W blue LEDs irradiation at 36 °C for 1 h. The generality of this process was shown with a wide range of electron-rich, neutral, and poor alkenes, including styrenes, heterocycles-substituted, 1,1-disubstituted, and both acyclic and cyclic internal alkenes. Likewise, the pyridine scope was good including methyl-, perfluoroalkyl-, and halogens functional groups. As examples of complex alkenes, estrone and vitamin E were converted into derivatives **198** and **199** with 78 and 58% yields, respectively (Scheme 33).

1.2.14 Hydro-, silyl-, and alkyl-carboxylation. A regioselective hydrocarboxylation of styrenes with CO_2 was achieved by Q.-Y. Meng *et al. via* the combination of visible light and nickel

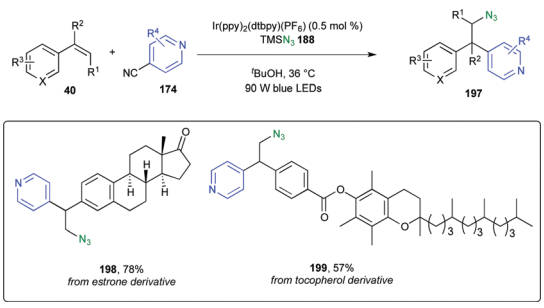

Scheme 33 Azidoarylation of olefins.

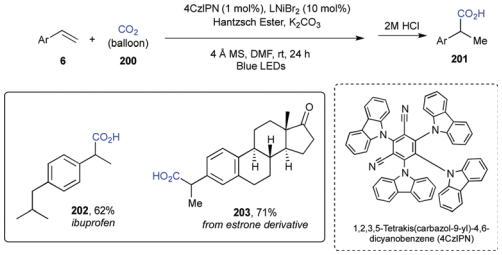

Scheme 34 Hydrocarboxylation of olefins.

catalysis (Scheme 34).[75] More in detail, 4CzIPN was used as the photocatalyst, a ligand complex with $NiBr_2$ as the nickel source, Hantzsch Ester (HE), K_2CO_3 as a base, DMF as a solvent, and 4 Å MS under blue LEDs irradiation for 24 hours at room temperature. Remarkably, the Markovnikov regioselectivity was controlled by using neocuproine as ligand, while the use of 1,4-bis(diphenylphosphino)butane (dppb) favored the formation of anti-Markovnikov adducts. Both electron-rich and electron-poor styrenes were competent substrates affording the carboxylic acid derivatives (**201**) in moderate to good yields. Vinyl-estrone was converted into the Markovnikov derivative **203** in 71% (Scheme 34).

Shortly after, J-Hou *et al.* reported that, by merging photoredox and HAT catalysis, alkenes (**60**) could be functionalized with CO_2 and silanes (**204**) or alkanes to afford either β-silacarboxylic acids (**206**) or acids bearing a γ-heteroatom such as *N*-, *O*-, and *S*- (Scheme 35).[76] Thoroughly, 4CzIPN was used as organic photocatalyst, quinuclidine-3-yl acetate **205** as the HAT agent, and DMSO as the solvent, at room temperature for 4 hours and under 18 W blue LEDs irradiation. The scope of the alkene partner was wide and associated to a broad functional group tolerance including nitrile, ketone, ester, and alkyne. Fully aliphatic silanes reacted more efficiently than their mixed alkyl/aryl analogues, while the scope of the alkenes covered nitrogen, oxygen, and sulfur heterocycles, including 4-, 5-, 6-, and 7-membered ones. An estrone-derived and a tryptamine-derived styryl derivatives were readily difunctionalized under standard conditions to afford **207** and **208**, respectively (Scheme 35).

1.2.15 Synthesis of ketones. According to a protocol developed by M. Zhang *et al.*, alkenes (**11**) could be coupled with an acyl radical generated upon visible light promoted deoxygenation of carboxylic acids (**209**) with triphenylphosphine in aqueous solution, to form ketone derivatives (**210**, Scheme 36).[77]

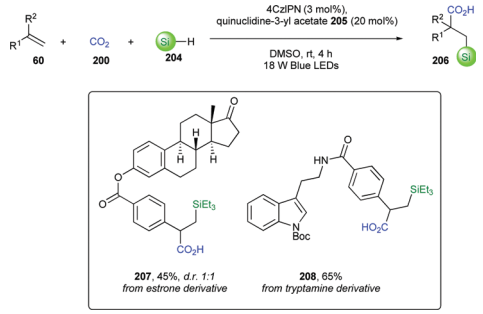

Scheme 35 Silylcarboxylation of olefins.

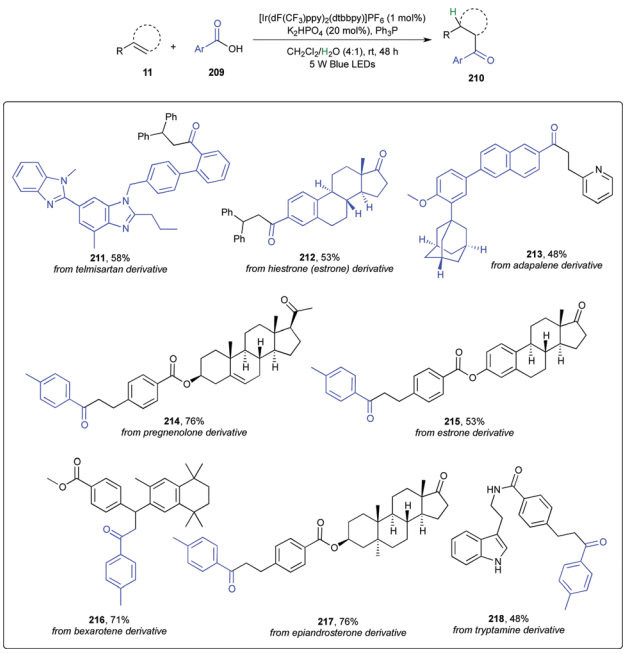

Scheme 36 Synthesis of ketones from olefins.

Thoroughly, in order to carry out such a transformation, $[Ir(dF(CF_3)ppy)_2(dtbbpy)]PF_6$ was used as a photocatalyst, K_2HPO_4 as a base, and Ph_3P was required as an *O*-transfer reagent in a dichloromethane (DCM)/H_2O 4 : 1 mixture under blue LEDs irradiation. Notably, water was employed as the hydrogen source. The carboxylic acid scope was broad including a number of functionalized benzoic acids as well as heteroaromatic substrates. As for the alkene partner, both mono- and difunctionalized olefins proved to be competent acceptors, including aromatic, heteroaromatic, and electron-poor aliphatic alkenes. Additionally, the wide functional group compatibility was showcased in the late-stage functionalization of telmisartan, hiestrone, adapalene, pregnenolone, estrone, bexarotene, epiandrosterone, and tryptamine (**211–218**, Scheme 36).

1.2.16 Alkoxylation. Alkoxy radicals ($RO^{\bullet}$) could be readily generated from *N*-alkoxypyridinium salts **219** and could add to a wide range of styrenes (**79**) under photoredox catalytic conditions in an anti-Markovnikov fashion (Scheme 37).[78,79] This transformation could be carried out under both batch or flow conditions by using *fac*-Ir(ppy)$_3$, $NaH_2PO_4{\cdot}2H_2O$ in wet acetone, or in an acetone/DCM mixture when performed in flow. Interestingly, the radical intermediates involved were

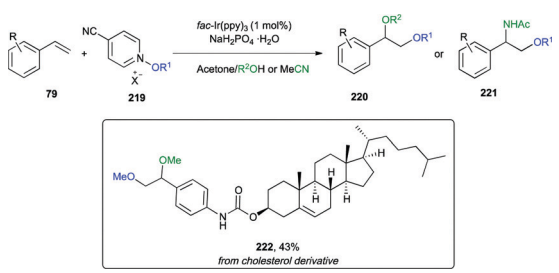

Scheme 37 Alkoxylation of olefins.

characterized by spin trapping with electron paramagnetic resonance (EPR) experiments. The mild conditions allowed for tolerance of a number of functional groups such as halogens, ethers, thioethers, amides, carbamates, and boronic esters, while α-, and β-substituted styrenes and vinyl substituted heteroarenes reacting efficiently. The scope was further extended to aminoalkoxylated adducts *via* a Ritter-type reaction with acetonitrile, and dialkoxylated products by using an appropriate alcohol as a cosolvent as shown for the cholesterol derived alkene (**222**, Scheme 37).

1.2.17 1,2-Dihydroxylation. The same group, developed an efficient visible light promoted metal-free dihydroxylation of styrenes with water and dioxygen (Scheme 38).[80] The protocol was operationally simple, employing abundant and environmentally friendly molecular oxygen and water as the oxygen sources, and $Acr^{+}MesClO_4^{-}$ as organic photocatalyst. A one-pot reduction work-up with triphenylphosphine was needed to reduce a peroxy-intermediate to the final desired alcohol (**223**). The substrate scope was broad and functional group tolerance was proved, as example of relatively complex molecules, on a derivative of DL-menthol (**224**, Scheme 38). Worth of note are the green characteristics of this transformation. Usually, indeed, the direct construction of free 1,2-diols is accomplished with peroxides, hypervalent iodine compounds, periodate salts and selenium dioxide, often used as stoichiometric oxidants, which have explosive characteristics or produce stoichiometric waste.

1.2.18 Hydroxyalkylation. Styrenes (**40**) could be hydroxyalkylated with oxime derivative **225**, which was able to generate key iminyl radicals upon single-electron transfer (SET) under visible light irradiation (Scheme 39).[81]

A subsequent 1,5-HAT generated a *C*-centered radical, able to add to an olefin double bond, and thus afford a benzyl radical intermediate. Oxidation of the latter to carbocation along with the addition of a molecule of water, and hydrolysis of the iminyl function, provided the final hydroxyalkylketones (**226**). The reaction was promoted by *fac*-Ir(ppy)$_3$ in MeCN as a solvent, in the presence of 100 equiv. of water and with a 30 W blue LED lamp as the photons' source. Albeit heteroaromatic styrenes were not compatible, the reaction scope was broad, with a good functional group tolerance as exemplified in the functionalization of the terminal olefins derived from estrone to **227** and **228** (Scheme 39).

1.2.19 Hydroxymonofluoromethylation. Alkenes can be hydroxy-monofluoromethylated by using 1,4-bis(diphenylamino)-naphthalene **230** as photoredox catalyst, with a 9 : 1 mixture of acetone/H_2O (as the source of the –OH function), under blue LEDs irradiation at room temperature for 12 h (Scheme 40).[82] In this synthetic strategy, endowed with a broad functional-group tolerance, the monofluoromethyl radical can be easily generated from a sulfoximine-based precursor **229**. The high excitation energy and interchromophoric conjugation conferred a strong reducing power to the photocatalyst, which was easily prepared by the authors on a gram scale with a palladium-catalyzed Buchwald–Hartwig amination and from readily available starting materials. Late-stage functionalization was reported for vinyl estrone and for the anticancer agent bexarotene (**232** and **233**, respectively, Scheme 40).

1.2.20 Hydroxytrifluoromethylation. Hydrofluoroalkylation of alkenes can be accomplished by using *N*-hydroxybenzimidoyl chloride (NHBC) redox-active esters **234** as fluoroalkyl radical precursors (Scheme 41).[83] The latter provided indeed a general leaving group assisted strategy for a decarboxylative hydrofluoroalkylation, *via* a fluorocarbon radical pathway, along with heteroarylation of unactivated terminal and internal olefins.

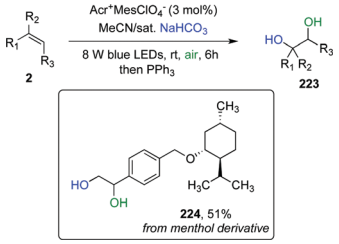

Scheme 38 1,2-Dihydroxylation of olefins.

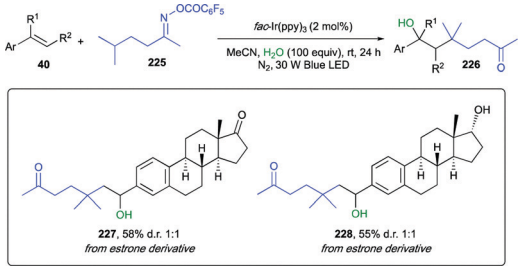

Scheme 39 Hydroxyalkylation of olefins.

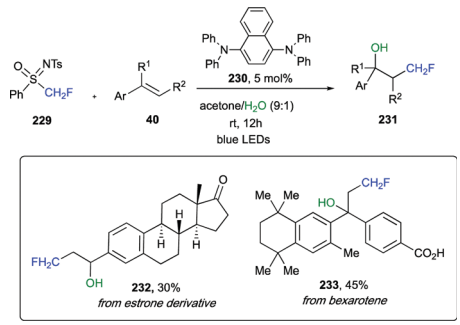

Scheme 40 Hydroxymonofluoromethylation of olefins.

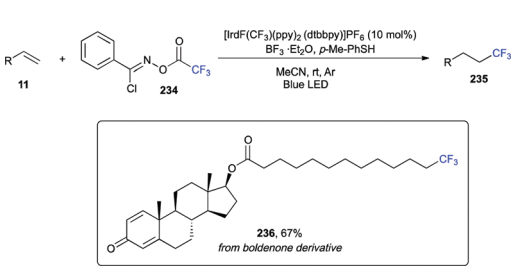

Scheme 41 Hydroxytrifluoromethylation of olefins.

The protocol required $BF_3{}^{\bullet}OEt_2$, *p*-toluenethiol, and an iridium catalyst $[Ir(dF(CF_3)ppy)_2(dtbbpy)]PF_6$ in MeCN at room temperature under blue LEDs irradiation. Trifluoromethylation tolerated amide, ester, sulfonamide, sulfonate, carboxylic acids, and ethers. Difunctionalization of unactivated olefins, with both a CF_3 and a heteroaryl group was also carried out in high yields. Furthermore, simultaneous introduction onto alkenes of fluoroalkyl groups such as CF_2H, CF_3, C_2F_5, and C_3F_7 and heteroaryl substituents can be operated with a slight modification of the reaction conditions. A boldenone-derived terminal alkene showed to be compatible with the protocol affording derivative **236** in 67% yield (Scheme 41).

1.2.21 Aminotrifluoromethylation. Aminotrifluoromethylation of terminal alkenes was achieved by using a ruthenium-based photocatalyst, the Umemoto's reagent **187** as CF_3 radical source, in an $MeCN/H_2O$ mixture as a solvent system under blue LEDs irradiation at room temperature in 3–5 hours as reaction times (Scheme 42).[84,85] The addition of the $^{\bullet}CF_3$ radical to the alkene double bond led to the formation of an intermediate alkyl radical, which oxidated to form a carbocation. The latter reacted with acetonitrile to enable a Ritter-type amination. The scope of this transformation involved *ortho*-, *meta*-, and *para*-substituted styrenes, bearing methyl-, halogen atoms, aldehydes, esters, protected amino groups, and boronic acid esters. Likewise, internal alkenes gave good yields, and moderato to high diastereoselectivities. Application to late stage aminotrifluoro-methylation of vinylestrone afforded derivative **238** in a good 56% yield.

1.2.22 Hydrothiolation. Olefins could undergo an anti-Markovnikov hydrothiolation with a broad range of thiols by using a cheap and non-toxic bismuth oxide photocatalyst (Bi_2O_3) (Scheme 43).[86]

Additionally, this thiol–ene click reaction required bromotrichloromethane ($BrCCl_3$) as an electron acceptor able to promote the generation of the key thiyl radical, which then added onto the olefin double bond. Optimum yields were obtained in DMF as a solvent and with a 25 W light bulb as the photon source. The reaction scope was exceptionally wide, including bulky tertiary alkyl- and benzyl-thiols, and acidic thiols such as methyl thioglycolate, to cite a few. Late-stage diversification of complex substrates such the *S*-acetyl protected precursor of NCH-31 (a potent antitumor agent), the cyclic tetrapeptide SCOP (a potent HDAC inhibitor), and the glycosyl sulfonamide (a potent carbonic anhydrase) (hCA IX and hCA XII) inhibitor was achieved even on a gram scale (**241–243**, Scheme 43).

1.2.23 Thiotrifluoromethylation. Terminal alkenes can be 1,2-thiotrifluoromethylated with benzene sulfonothioates **244** and sodium triflinate **245** as reported by W. Kong *et al.* (Scheme 44).[87] The reaction was characterized by an unconventional reductive quenching cycle, where CF_3SO_2Na (**245**, Langlois reagent) was used as CF_3 radical source, replacing the expensive Umemoto's and Togni's reagents, and benzene sulfonothioates as source of electrophilic sulfur. The transformation demonstrated a robust scope with a variety of *S*-aryl benzenesulfonothioates as well as with different terminal alkenes, including phenyl allyl ethers, and alkenes bearing epoxy- and hydroxy-functional groups. (−)-Borneol and estrone derivatives were suitable complex substrates (**247** and **248**, respectively, Scheme 44).

1.2.24 Trifluoromethylthiolation. J. He and coauthors reported a three-component coupling of olefins, alkyl halides (*e.g.* **89**, Scheme 45), and trifluoromethylthiolate **249** to generate trifluoromethyl-thioethers (**250**).[88]

This process was promoted by a copper catalyst (CuI/binap) under blue LEDs irradiation in MeCN at −40 °C to room temperature. The success of this transformation relied on the proper combination of an alkyl electrophile, an olefin, and a nucleophile.

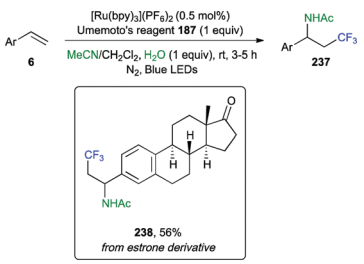

Scheme 42 Aminotrifluoromethylation of olefins.

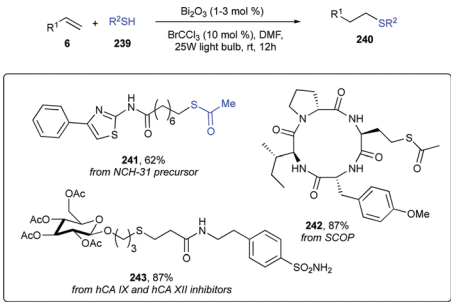

Scheme 43 Hydrothiolation of olefins.

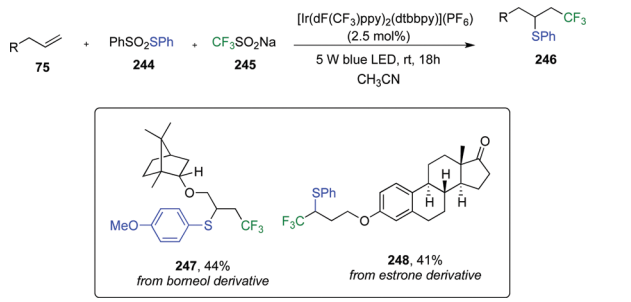

Scheme 44 Hydrothiolation of olefins.

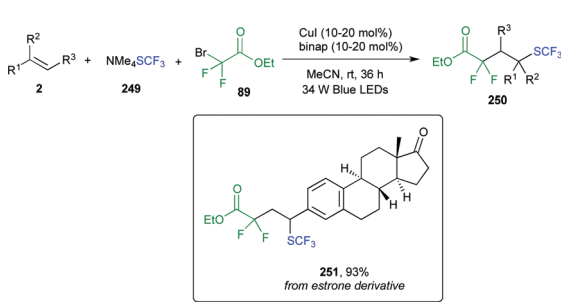

Scheme 45 Trifluoromethylthiolation of olefins.

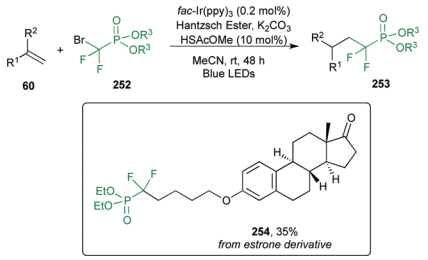

Scheme 46 Hydrophosphonodifluoromethylation of olefins.

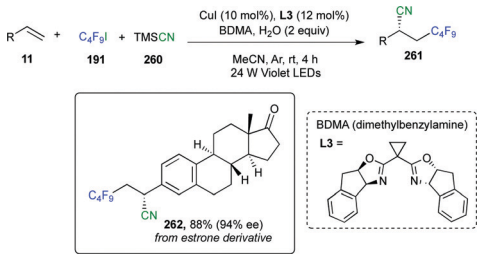

Scheme 48 Cyanofluoroalkylation of olefins.

Suitable olefins included styrenes, di-, and tri-substituted substrates, with functional groups such as bromide, cyanide, and azide being well tolerated. As example of structurally complex and bioactive scaffold, estrone-derived alkene was difunctionalized to **251** in an exquisite 93% yield (Scheme 45).

1.2.25 Hydrophosphonodifluoromethylation. Mono- and di-substituted alkenes could be converted into their corresponding hydrophosphonodifluoromethylated analogues **253** (Scheme 46) under photoredox catalytic conditions by using bromodifluoromethanephosphonate (**252**).[89] Optimized reaction conditions required *fac*-Ir(ppy)$_3$ as the photocatalyst, an Hantzsch ester (Et-HE) as the terminal reductant, HSAcOMe forming *in situ* a thiyl radical as HAT agent, and K_2CO_3 as a base in MeCN under blue LEDs irradiaton at room temperature for 48 h. A number of structurally diverse alkenes, including the bioactive estrone-derived alkene, efficiently reacted affording the desired difunctionalized adducts (for estrone see derivative **254**, Scheme 46) in good to high yields.

1.2.26 Cyanodifluoromethylation and cyanoperfluoroalkylation. A practical and efficient protocol for incorporation of both CN and HCF_2 into alkenes was developed by M. Zhang *et al.* (Scheme 47).[90] $Ph_3P^+CF_2CO_2^-$ **255**/$NaNH_2$ **256** system was employed as a dual CN and HCF_2 source, so that a cyanide anion was generated *in situ*, avoiding the need for toxic cyanation reagents. *fac*-Ir(ppy)$_3$, CuI, DMAc as solvent, and blue LEDs irradiation were all found essential to promote the transformation. A wide range of both electron-rich and electron-poor alkenes was cyanodifluoromethylated under standard reaction conditions, with tolerated functional groups involving ether, ester, ketone, halogens, boronic acid ester, and amide. Two different estrone derivatives further highlighted the utility of this method as a tool for late-stage functionalization of complex substrates (**258** and **259**, Scheme 47).

A procedure for the copper-catalyzed photoredox enantioselective cyanofluoroalkylation of alkenes was reported by Q. Guo *et al.* (Scheme 48).[91] Here, the chiral Cu-based catalyst, generated *in situ*, acted as both the photoredox and the cross-coupling catalyst for the C–CN bond formation.

Worthy of note, the reaction did not require an external oxidant, and exploited low-cost fluoroalkyl iodides (*e.g.* **191**) as carbon-centered fluoroalkyl radical precursors, enabling the introduction of $-CF_3$, $-CF_2CO_2Et$, $-C_4F_9$, $-C_6F_{13}$, and $-C_8F_{17}$ onto terminal alkenes. Additionally, TMSCN **260** was used as CN source and DIPEA as a basic additive, whereas optimum yields were obtained by performing the reaction in MeCN at room temperature under 24 W violet LEDs (390–410 nm) irradiation. Alkenes conjugated to both electron-rich and electron-poor aromatic moieties, regardless *ortho*-, *meta*-, and *para*-substitution patterns afforded the desired products with good yields and excellent ee values, while nonconjugated alkenes gave only trace amounts of products. Functional group tolerance was also confirmed in the derivatization of an estrone derivative (**262**, Scheme 48).

1.2.27 Difluoropropargylation. J. Chen *et al.* reported a visible light-induced hydrodifluoropropargylation of alkenes from silyl-protected bromodifluoropropyne **263** catalyzed by a thiyl radical (Scheme 49).[92] Thoroughly, benzothiazoline **264** was used as a critical reductant, while diphenylsulfide **42** provided the key thiyl radical able to give H abstraction from benzothiazoline, affording an intermediate acting as electron donor in SET reduction of the bromopropargylic substrate. Optimum yields were obtained with DMF as a solvent and blue LEDs irradiation. The simple and mild conditions provided a wide functional group tolerance. Allyl-estrone was readily converted in 40% yield into derivative **266** (Scheme 49).

1.2.28 Difluoromethylation–heteroarylation. Despite the huge progresses in the field, the radical-mediated difunctionalization of

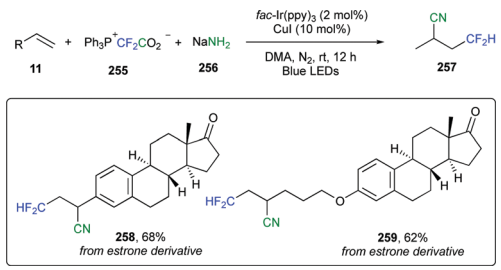

Scheme 47 Cyanodifluoromethylation of olefins.

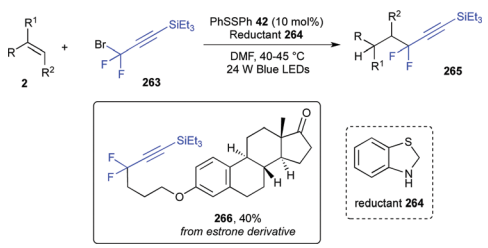

Scheme 49 Difluoropropargylation of olefins.

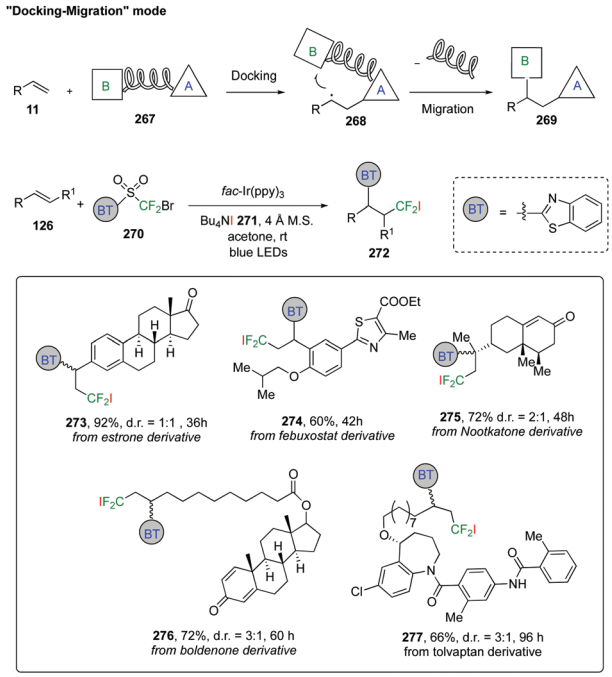

Scheme 50 Difluoromethylation–heteroarylation of olefins.

unactivated alkenes is still considered to be very challenging. A docking-migration strategy was reported by J. Yu *et al.* (Scheme 50).[93]

Conceptually, it was based on the use of a dual-function reagent **267**, containing both a radical donor (part A) and an acceptor (part B). The donor, upon "docking" onto the alkene generated a transient alkyl radical **268** able to attack intramolecularly the radical acceptor and trigger a functional group migration. More specifically, the authors chose difluoroalkyl bromides (*e.g.* **270**, Scheme 50) as the radical donor, which formed an electrophilic difluoroalkyl radical, and a migratory heteroaryl as the radical acceptor. Donor and acceptor were finally tethered by a sulfonyl group as a traceless linker released during the migratory process as SO_2. The reaction was performed under mild conditions, using *fac*-Ir(ppy)$_3$, Bu_4NI **271**, 4 Å MS, acetone, and blue LEDs irradiation at room temperature. A vast array of functional groups was compatible offering an efficient approach for the late-stage functionalization of complex natural products and drug molecules such as estrone, the veterinary drug boldenone, febuxostat used long-term in the treatment of high uric acid levels associated with gout, nootkatone, the most important and expensive aromatic of grapefruit, with repellent/insecticide properties and approved as food additive, and the aquaretic drug tolvaptan (**273–277**, Scheme 50).

1.2.29 Carbopyridylation and trifluoromethylative pyridylation. A similar approach with a bifunctional reagent was recently reported by G. R. Mathi *et al.* (Scheme 51).[94]

The authors found that *N*-alkenoxypyridinium salts (**278**) were able to generate α-carbonyl radicals **278A** after cleavage of the *N–O* bond, so that unactivated alkenes could simultaneously incorporate α-keto and pyridyl groups. This transformation afforded, in mild reaction conditions and with a broad substrate

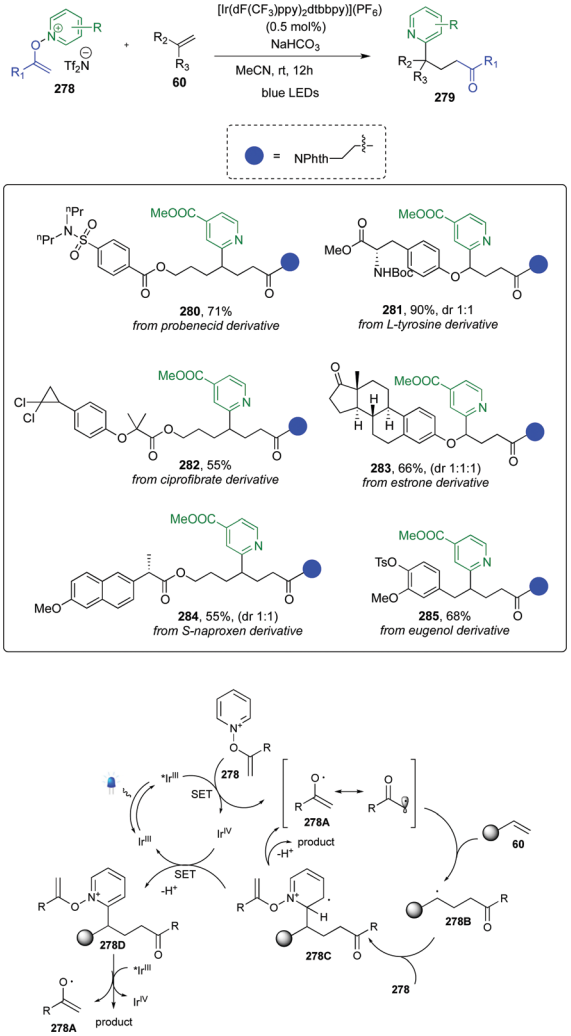

Scheme 51 Carbopyridylation of olefins.

scope a variety of γ-pyridyl ketones (**279**). Typically, the conversion proceeded with a low loading of an iridium catalyst (0.5 mol%) and Na_2CO_3 as the base, in acetonitrile, under blue LEDs irradiation for 12 h. The good functional-group compatibility was shown also with complex bioactive molecules such as probenecid, used treat gout and hyperuricemia, estrone, ciprofibrate, the NSAID (*S*)-naproxen, and eugenol, a natural compound with prosthodontic applications in dentistry (**280–285**, Scheme 51).

The same group also developed a site-selective trifluoromethylative pyridylation of unactivated alkenes (Scheme 52).[95] In detail, the process was initiated by the selective addition of a CF_3 radical to the *N*-alkenoxypyridinium salts (**286**) to provide a nucleophilic alkyl radical intermediate; a subsequent *ortho*-selective migration on a pyridyl ring provided C2-fluoroalkyl functionalized pyridines (**287**).

Both secondary and tertiary alkyl radicals were well-suited, and the method was also successfully applied to *P*-centered radicals. The robustness of this transformation was further demonstrated by the LSF of complex bioactive molecules such as the anticancer drug vismodegib, roflumilast, orally bioavailable drug used to treat inflammatory conditions of the lungs

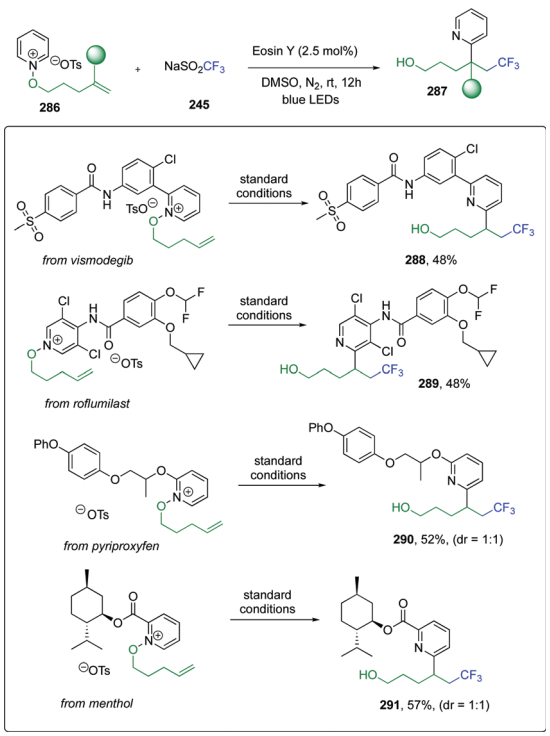

Scheme 52 Trifluoromethylative pyridylation of olefins.

(*e.g.* chronic obstructive pulmonary disease, COPD), the pesticide pyriproxyfen, and menthol (**288–291**, Scheme 52).

Similar reaction conditions (Scheme 53) were already shown to be effective in a three-component coupling involving unactivated alkenes (**11**), *N*-methoxypyridinium salts (**292**), and $NaSO_2CF_3$ **245** as CF_3 source.[96] Opposite to the migrative transformation reported above, here a methoxy radical ($^{\bullet}OMe$) was released from the pyridinium salt and subsequently reduced to methoxide anion by $NaSO_2CF_3$ with concomitant chain formation of the CF_3 radical. This protocol was efficiently applied to the LSF of selected biologically active compounds such as L-tyrosine, oxaprozin, eugenol, estrone, and β-D-glucopyranoside derivatives (**294–298**, Scheme 53).

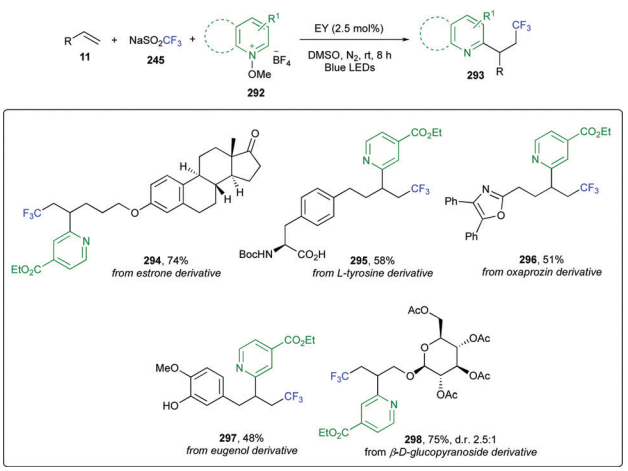

Scheme 53 Three-component trifluoromethylative pyridylation of olefins.

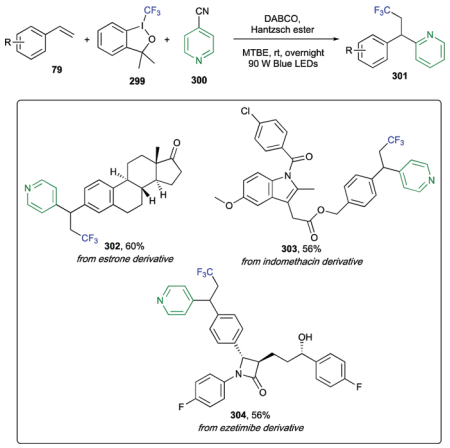

Scheme 54 Three-component trifluoromethylative pyridylation of olefins.

One more intermolecular approach to achieve carbopyridylation of alkenes was reported by D. Chen *et al.* (Scheme 54).[97] In this protocol cyanopyridines (**300**) were chosen as the coupling partners, Togni's II reagent **299** as the $^{\bullet}CF_3$ source, and Hantzsch ester **201** as the stoichiometric photoreductant, without the need for an exogenous photocatalyst. The reaction proceeded in MTBE as a solvent, in the presence of DABCO as additive, under 90 W blue LEDs irradiation at room temperature. The mild three-component protocol developed proved to be efficient with a number of vinylarenes and heteroarenes, with a wide functional group tolerance including halogens, alkynes, ethers, sulfones, carbamates, esters, and amides. Cyanopyridines functionalized at the 2- or 3-position with alkyl-, halogens, aryl, and cyano-groups afforded the corresponding products (**301**) in good to high yields. The potentiality of this synthetic protocol in the late-stage functionalization of drugs was showcased with indomethacin, estrone, and ezetimibe (**302–304**, Scheme 54).

1.2.30 Aminopyridylation. *N*-Aminopyridinium salts **306** can be straightforwardly used as both aminating and pyridylating reagents for alkenes (**305**), quickly increasing molecular complexity and affording aminoethyl pyridine derivatives under mild reaction conditions (Scheme 55).[98]

The generation of *N*-centered radicals in photocatalytic systems from *N*-aminopyridinium salts was already known, but usually the fragmentation of the prefunctionalized *N*-radical precursor by single electron transfer (SET) reduction resulted in the loss of pyridine as chemical waste. Here, the authors were able to engage alkenes in an efficient difunctionalization forming at the same time a new C–*N* bond and a new Csp_3–Csp_2 bond with the pyridyl ring. Reaction conditions featured eosin Y as the photocatalyst, K_3PO_4 as the base, and DMSO as the solvent, at room temperature under blue LEDs irradiation for 3 h. This transformation was characterized by an excellent C4-regioselectivity (with respect to the pyridyl ring), a broad substrate scope, and a good functional group compatibility. Late-stage functionalization of biorelevant estrone, β-citronellol, pyriproxyfen, and bisacodyl was accomplished in good yields (**308–311**, Scheme 55).

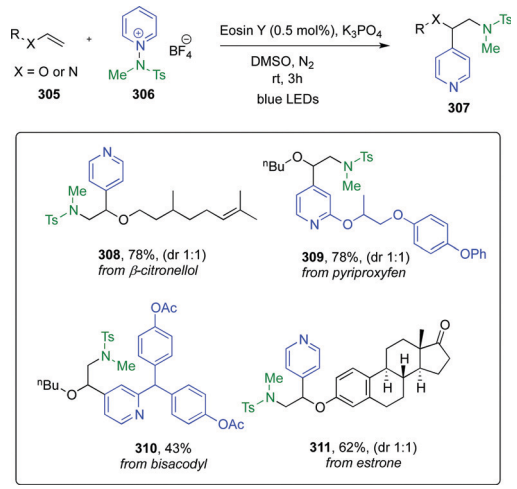

Scheme 55 Aminopyridylation of olefins.

1.2.31 Azolylation. A. Arora *et al.* described a photocatalytic reductive coupling of unactivated alkenes (**126**) with heteroaryl bromides (**312**) in the presence of *fac*-Ir(ppy)$_3$ as the photocatalyst, a tertiary amine as electron donor and final reductant, HCO_2H as an acidic additive in MeCN as a solvent and at 45 °C under blue LEDs irradiation for 12–22 hours (Scheme 56).[99]

From a mechanistic point of view, the reaction proceeded *via* a photoinduced electron transfer from the tertiary amine to the heteroaryl bromide, to provide an aryl radical intermediate, which added to the alkene double bond. A wide range of bromo azoles, including thiazole, benzothiazole, and benzimidazole reacted with moderate to excellent yields, whereas heterocycles such as 2-bromooxazole failed to react under standard conditions. The potential application of this protocol in the late-stage functionalization of complex substrates was showcased with the thiazolation of cholesterol, and in the ring-opening of vinyl cyclobutanes such as the antibacterial (+)-α-pinene and the anti-inflammatory, anticarcinogenic, antimicrobial, antioxidative, and analgesic (−)-caryophyllene oxide (**314–316**, Scheme 56).

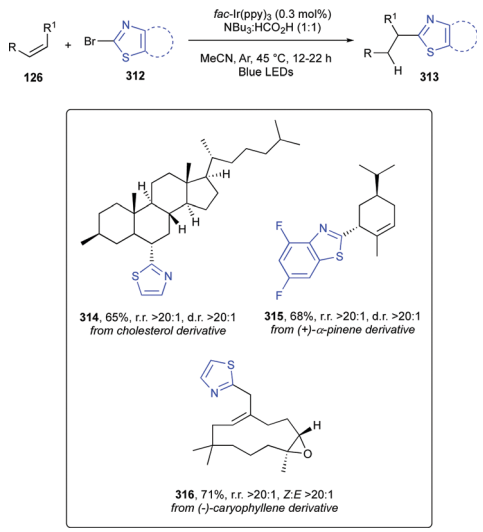

Scheme 56 Azolylation of olefins.

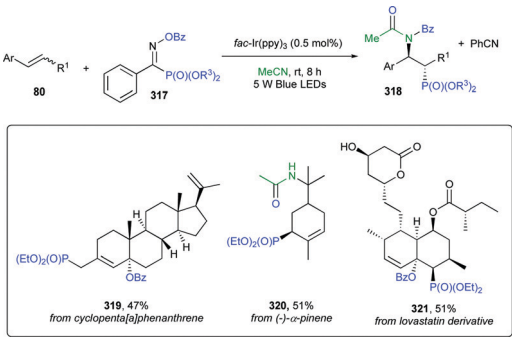

Scheme 57 Synthesis of β-aminophosphonates from olefins.

1.2.32 Synthesis of β-aminophosphonates. Y.-H. Li *et al.* synthesized a novel type of multifunctional oxime phosphonates (**317**) and harnessed its reactivity in an intermolecular cascade radical addition to alkenes under photoredox catalytic conditions (Scheme 57).[100] Thoroughly, the formation of an *N*-centered unstable iminyl radical from the phosphine source, along with the release of a benzoxyl anion, unlocked a selective C–*P* single bond cleavage forming a *P*-centered radical. Addition of the latter to the alkene afforded a benzyl radical intermediate, which was oxidized to carbocation and attacked by acetonitrile in a Ritter-type reaction. Eventually, the so formed nitrilium ion intermediate was intercepted by the benzoyl anion, followed by acyl migration to afford the β-aminophosphinoylation products (**318**). The reaction, performed in exceptionally mild conditions (*fac*-Ir(ppy)$_3$ in MeCN) showcased a wide reaction scope as proven for example in the late-stage functionalization of (−)-α-pinene, a steroid derivative, and esterified lovastatin (**319–321**, Scheme 57).

1.2.33 Formation of *gem*-bis(boryl)alkanes. Alkenyl diborate complex **322**, formed *in situ* from alkenyl Grignard reagents and bis(pinacolato)diboron (B_2Pin_2), could react with alkyl bromides (**232**) under ruthenium–photoredox catalysis to afford *gem*-bis(boryl)alkanes (Scheme 58).[101] Actually, alkyl radicals, generated upon SET reduction of alkyl bromides (**232**), added

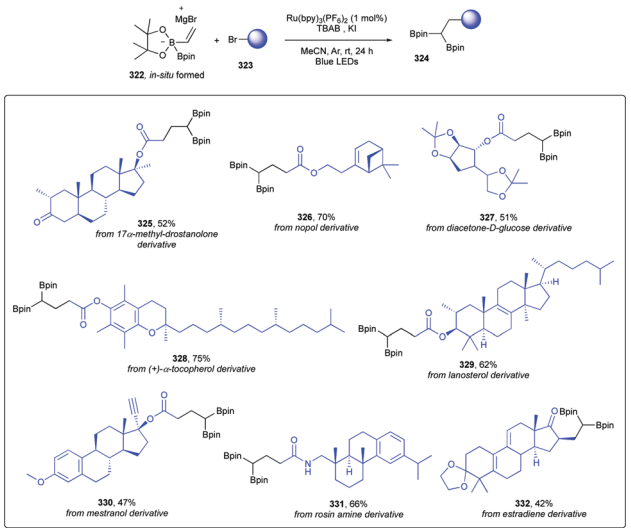

Scheme 58 Formation of *gem*-bis(boryl)alkanes from olefins.

to the alkenyl diboronate complex **322**, so that the resulting radical anions underwent a radical-polar crossover through a 1,2-boryl-anion shift from boron to the sp^2 α-carbon. Optimum yields were obtained with $[Ru(bpy)_3](PF_6)_2$ as the photocatalyst, TBAB (tetrabutylammonium bromide) and KI as additives, in MeCN at room temperature for 24 h under blue LEDs irradiation. The scope of alkyl halides encompassed 2-bromoacetophenone derivatives as well as substrates bearing aliphatic esters, amides, fluoroalkyl- and cyano-groups. Derivatives of bioactive compounds such as drostanolone, Nopol, (+)-α-tocopherol, D-glucose, lanosterol, mestranol, rosin amine, and estradiene were selected to test the robustness of the method in the LSF of complex substrates (**325–332**, Scheme 58).

1.2.34 Fluorocarboborylation. Recently, the group of Y. Pan developed a radical difunctionalization of alkenes and alkynes to attain fluorine-containing alkylboronates **335** and vinylboronates, respectively, with a redox active and bench-stable imidazolium sulfonate cationic salt, IMDN-SO_2R_F **333** (Scheme 59).[102]

The use of such a reagent in the presence of *fac*-Ir(ppy)$_3$, B_2cat_2 **334** as a diboron reagent in a 1 : 3 v/v MeCN/EtOAc solvent mixture at room temperature under irradiation with 30 W blue LEDs provided a scalable and efficient protocol to achieve fluoroalkylation–borylation of unsaturated hydrocarbons with high regio- and stereo-selectivities (typically $E/Z > 20:1$). The scope of the difunctionalization was demonstrated with a range of substituted terminal alkynes providing high yields also with heteroaromatic substituents, while aliphatic inputs reacted less efficiently. On the other hand, a wide array of structurally diverse olefins afforded the target fluoroalkyl borylated adducts in good to high yields and with an exceptional functional group tolerance as highlighted in the LSF of bioactive boldenone, lanosterol, (+)-α-tocopherol, and estrone (**336–339**, Scheme 59).

1.2.35 Synthesis of complex secondary amines. Recently, T. Opatz and coworkers reported a four-component reaction involving styrenes (**172**), primary amines (**340**), aldehydes (**341**), and sodium sulfonate salts (**173**) affording substituted γ-sulfonylamines under photoredox catalytic conditions (Scheme 60).[103] This straightforward multicomponent approach enabled the simultaneous formation of one C–C, one C–N, and one C–S bond in a single synthetic step, providing multifunctionalized secondary amines (**342**) with a high structural diversity and in a high atom-economy. The mild conditions developed featured *fac*-Ir(ppy)$_3$ as the photocatalyst, $NaHSO_4{\cdot}H_2O$ as an additive in a 9 : 1 mixture of MeCN/H_2O under irradiation with a 23 W CFL at room temperature for 24 hours. A library of 48 examples witnessed the broad scope involving diverse substrates from the all four components. To cite a few, complex biomolecules such as styrene-functionalized cholic acid and biotin derivatives yielded adducts **343** and **344**, respectively (Scheme 60).

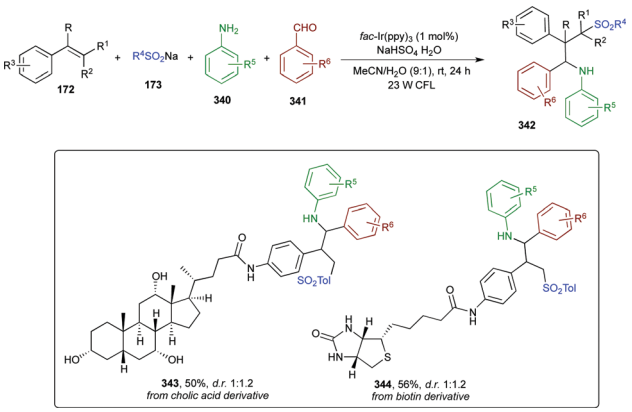

Scheme 60 Synthesis of complex secondary amines from olefins.

1.3 Formation of cyclic systems

1.3.1 Cyclopropanation. J. P. Phelan *et al.* developed a bench stable bifunctional reagent **345** (Scheme 61) for the redox-neutral cyclopropanation of olefins, by using 4CzIPN as the photocatalyst in DMSO and under 30 W blue LEDs irradiation for short reaction times (3 hours).[104] Such a reagent, triethylammonium bis(catecholato)-iodomethylsilicate **345** could be easily prepared on a multigram scale and enabled the formation of an interesting halomethyl radical, which added onto the olefin double bond to form an alkyl radical intermediate. Reduction of the latter afforded a carboanion, responsible of a 3-*exo-tet* ring closure to cyclopropane, thus enabling a radical/polar crossover mechanism. The additive-free conditions allowed a high functional group tolerance and a wide scope including caffeine and menthol as substrates (**347** and **348**, respectively, Scheme 61).

At the same time, Guo *et al.*[105] reported a similar protocol exploiting chloromethyl silicate **350** as a methylene transfer

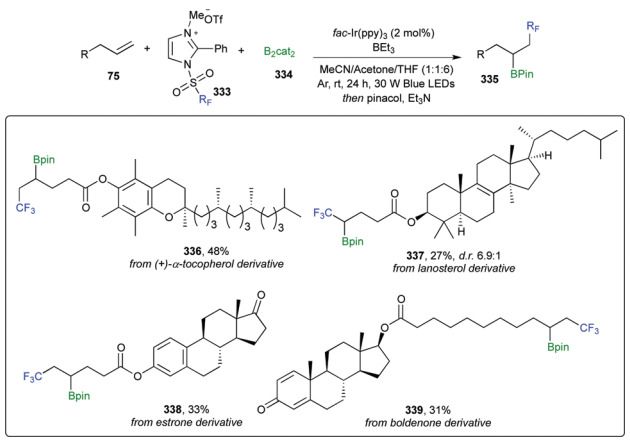

Scheme 59 Fluorocarboborylation of olefins.

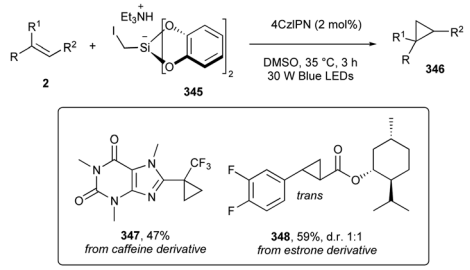

Scheme 61 Cyclopropanation of olefins.

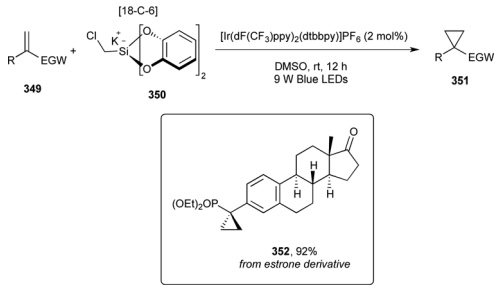

Scheme 62 Cyclopropanation of olefins with chloromethyl silicate.

agent to accomplish cyclopropanation of alkenes (Scheme 62). Optimum yields were achieved with an iridium-based photoredox catalyst, DMSO as a solvent and 9 W blue LEDs irradiation for 12 hours at room temperature. By applying these conditions, a range of Michael acceptors (**349**) including α-substituted vinylphosphonates, α,β-unsaturated acrylate, ketone, amide, and sulfone smoothly underwent cyclopropanation in good to excellent yields. Tolerated functional groups involved halogens, ketones, esters, nitro-, ethers, and cyano-functionalities. Additionally, estrone-derived vinyl phosphonate was cyclopropanated in 92% yield (**352**, Scheme 62), highlighting the applicability of this method for the late-stage functionalization of pharmaceuticals.

Alternatively, styrenes can be cyclopropanated by using *gem*-diiodomethyl carbonyl reagents **354** and **355** with excellent chemoselectivity and functional group tolerance (Scheme 63).[106] Interestingly, the reaction did not need any photocatalyst and was simply promoted by visible light (CFL as source), as *gem*-diiodomethyl carbonyl reagents, endowed with more absorbance in the visible region, could provide a photoinduced generation of iodomethyl carbonyl radicals. The cyclopropyl carboxylate generated, not possible to obtain in a direct manner by current catalytic strategies relying on metal-carbene (carbenoid), could also be further diversified by well-documented decarboxylative strategies. The authors synthesized 1-adamantanyl 2,2-diiodoacetate **354** as new cyclopropanating agent on a 12-gram scale from

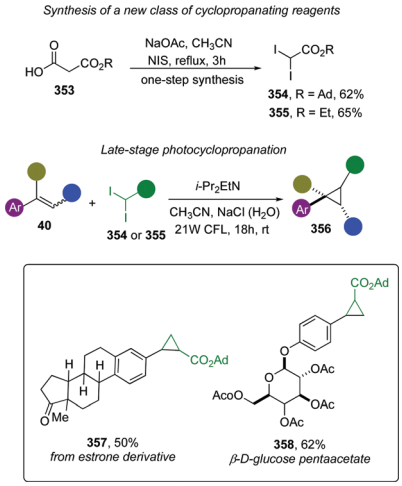

Scheme 63 Cyclopropanation of olefins with *gem*-diiodomethyl carbonyl reagents.

3-(adamantan-1-yloxy)-3-oxopropanoic acid and *N*-iodosuccinimide (NIS). Interestingly, this compound is a white solid, much more stable than its parent ethyl 2,2-diiodoacetate **355**, which has to be stored in a freezer (< −20 °C) and in solution (0.5 M CH_3CN). The broad substrate scope was also demonstrated in the LSF of biomolecule derivatives, such as estrone and β-D-glucose pentaacetate (**357** and **358**, respectively, Scheme 63; the conversion of the protecting-group free β-D-glucose was also possible, with a lower 30% yield).

1.3.2 Formation of cyclobutanes. A wide range of dienes and alkenes, including an enyne, a vinyl ether, and styrenes were reported to be good substrates to form cyclobutanes with three contiguous stereogenic centers (**360**), with excellent d.r. (up to >20:1 d.r.) and e.e. (up to >99%) upon reaction with α,β-unsaturated carbonyl compounds (**359**) (Scheme 64).[107] In this transformation, a substrate-bound chiral Lewis acid complex absorbed visible light and generated an excited state that directly reacted with a cosubstrate in a highly stereocontrolled fashion. In particular, a chiral rhodium complex was used as the photocatalyst, and reaction conditions optimization suggested acetone as solvent, 24 W blue LEDs irradiation and room temperature. In this report, modification of an estrone-derivative was accomplished in an excellent 97% yield (**361**, Scheme 64).

1.3.3 Formation of cyclopentanes. Alkyl chlorides with tethered alkenes (*e.g.* **362**, Scheme 65) could afford substituted cyclopentanes (**363**) upon a metallaphotoredox intramolecular 5-*exo*-*trig* cyclization.[108] The cleavage of the strong C(sp^3)–Cl bond was mediated by a highly nucleophilic low-valent cobalt or nickel intermediate generated *in situ* upon SET reduction mediated by a copper photocatalyst. Optimal reaction conditions made use of $\mathbf{PC_{Cu}/1^{H}Co}$ catalyst system, Et_3N, EtOH/MeCN (3:2) as a solvent mixture under 1 W blue LEDs irradiation for 24 h at 30 °C. The copper/cobalt catalyst showed very efficient in promoting the reductive cyclization of several diethyl malonates, while more challenging linear alkyl chlorides were efficiently converted into their corresponding five-membered carbocyclic products with a dual copper/nickel catalyst $\mathbf{PC_{Cu}/1^{H}Ni}$. The reaction scope proved to be wide with several complex substrates, including an estrone derivative (**364**, Scheme 65).

Formation of cyclopentanes (or cyclopentenes) from alkenes (or from alkynes) was also achieved *via* a [3+2] photocycloaddition with cyclopropanes (Scheme 66).[109] Valuably, the use of a bis-cyclometalated chiral-at-metal rhodium complex **Δ-RhS** enabled

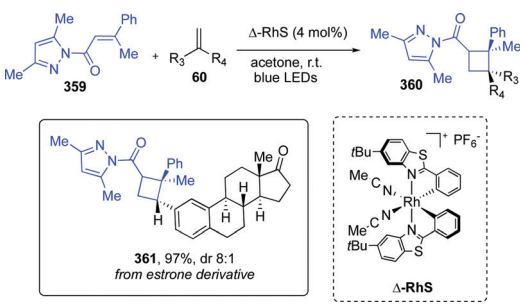

Scheme 64 Formation of cyclobutanes from olefins.

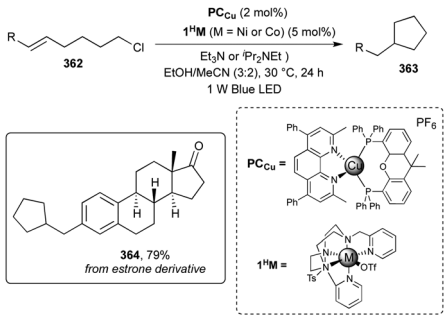

Scheme 65 Formation of cyclopentanes from unsaturated alkyl chlorides.

excellent enantioselectivities of up to >99% ee, along with yields in a 63–99% range. This catalyst, besides being responsible of the overall stereocontrol, after coordination to the cyclopropane, generated a visible light absorbing complex lowering the reduction potential of the cyclopropane and thus enabling its mild SET reduction. With alkenes, the reaction was performed in acetone in the presence of DIPEA as a base, while with alkynes optimum yields were achieved in THF and TEA as organic base. In all the cases the reaction proceeded at room temperature under blue LEDs irradiation. The robustness of this synthetic methodology was showcased with a number of complex multifunctionalized, and enantioenriched cyclopentanes including derivatives coming from fenofibrate and estrone, (**369** and **370**, respectively, Scheme 66).

Vinylcyclopentanes **373** (Scheme 67) could be achieved by applying a recently reported protocol for [3+2] cycloaddition of diversely substituted vinyl- and ethynylcyclopropanes *e.g.* **371** with a broad range of alkenes **11**.[110]

The method exploited a mild bromine radical catalysis enabled by a triplet-state cinnamyl bromide, which excited upon energy transfer process from an organic photocatalyst, gave a β-fragmentation to generate bromine radicals in a controlled manner. Awfully, the reaction proceeded in the presence of parts per million-level of 4CzIPN photocatalyst and 1–2 mol% of cinnamyl bromide precatalyst in DMSO at 30 °C under blue LEDs irradiation. These conditions were applied to a broad range of vinylcyclopropanes **371** and alkenes **11** with formation of the desired vinylcyclopentanes **373** in moderate to excellent yields and with diastereomeric ratios (dr) ranging from 50 : 50 to 95 : 5. Tolerated functional groups included fluorine, epoxide, ketone, carboxylic acid, aldehyde, and nitrile. The substrate scope was further extended to complex bioactive scaffolds such as 4-vinylbenzylated theophylline, a phosphodiesterase inhibitor,

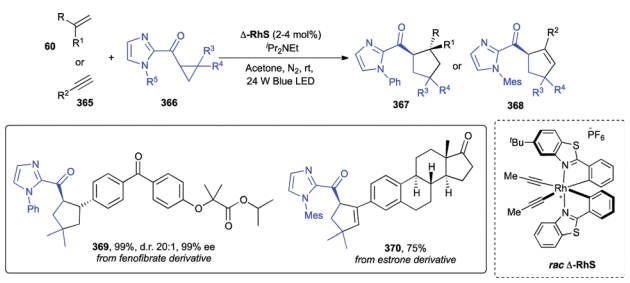

Scheme 66 Formation of cyclopentanes from alkenes and cyclopropanes.

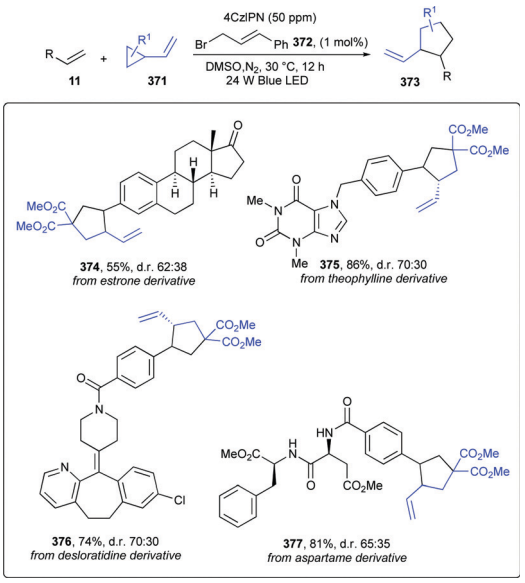

Scheme 67 Formation of vinylcyclopentanes from alkenes and vinylcyclopropanes.

estrone, aspartame, and 4-vinyl benzoylated desloratadine (**374–377**, Scheme 67).

In the meantime, the group of J.-R. Cheng investigated the feasibility of a [3+2] cyclization of vinylcyclopropanes and *N*-tosyl vinylaziridines **378** (Scheme 68) with alkenes by harnessing a tunable hydrazone as a nitrogen radical catalyst (**NCR**) precursor.[111] Mechanistic studies suggested that the photogenerated hydrazone nitrogen radical added to vinylcyclopropanes and *N*-tosylaziridines to trigger their ring opening *via* C–C and C–N bond cleavage, respectively, forming a new C- or N-centered radical. The latter further added to alkenes, thereby enabling subsequent cyclization along with elimination of the hydrazone nitrogen radical. The reaction was efficiently promoted by [Ir(ppy)$_2$(dtbbpy)]PF$_6$, the NCR catalyst, K$_2$CO$_3$ as a base in MeCN under irradiation with 7 W blue LEDs at room temperature. Variation of both the cyclopropane and the *N*-tosyl vinylaziridine inputs, as well as of the alkene partners provided a wide scope with yields of vinylcyclopentanes up to 92% and pyrrolidines **379** up to 87%. Vinyl estrone and D-vinyl menthol also showed to be amenable to undergo [3+2] cycloaddition providing the corresponding pyrrolidines **380** and **381** in 53% and 86% yields, respectively (Scheme 68).

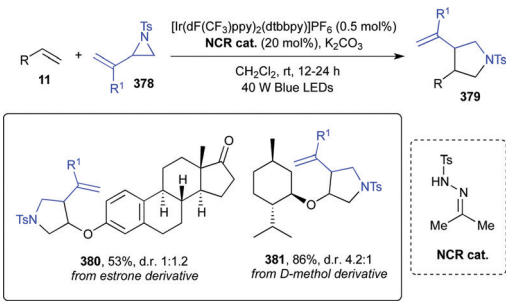

Scheme 68 Formation of vinylcyclopentanes from alkenes and *N*-tosyl vinylaziridines.

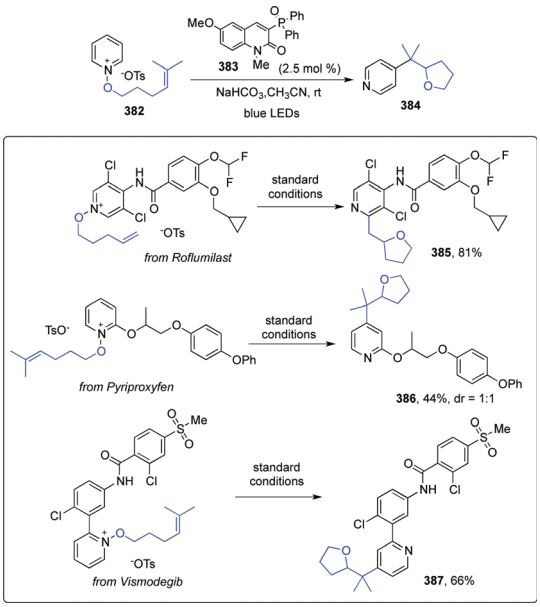

Scheme 69 Formation of tetrahydrofurans from olefins.

1.3.4 Formation of tetrahydrofurans. The exploitation of bifunctional reagents, as already shown for **278** and **286**, allowed the same group to identify a novel visible-light-enabled alkoxy radical ring-closure and pyridylation from *N*-alkenyloxypyridinium salts (Scheme 69).[112] The latter served as both alkoxy radical precursors and heteroaryl sources in a tandem radical process involving their fragmentation, a radical cyclization, and a final pyridylation. To achieve effective and rapid fragmentation of the pyridinium salt, 3-phosphonated quinoline **383** was employed as the photocatalyst, in MeCN as the solvent, under blue LEDs irradiation at room temperature. In contrast, the use of Ru- and Ir-based catalysts led to partial decomposition of the substrates and subsequent low yields. Worthy of note, after the reaction, about 90% of catalyst **383** can be recovered by column chromatography. The mild metal-free conditions and the functional group compatibility were tested on the *N*-alkenyloxypyridinium derivatives of Roflumilast, Pyriproxyfen, and Vismodegib to get, in medium to good yields compounds **385–387** (Scheme 69).

1.3.5 Formation of cyclic amides and carbamates. A photocatalytic method for olefin hydroamidation to afford γ-lactams and cyclic *N*-acyl amines **389** was described by S. T. Nguyen *et al.* (Scheme 70).[113] It relied on the formation of a transient amidyl radical *via* proton-coupled electron transfer (PCET) activation of *N*–H bonds in *N*-alkyl amides promoted by an excited-state iridium photocatalyst and a dialkyl phosphate base.

Given the high bond dissociation free energies (BDFEs) of about 110 kcal mol^{-1}, the abstraction of a $^{\bullet}$H from amide *N*–H is considered challenging, with the resulting amidyl being highly reactive species capable of numerous nonproductive pathways. Here, the use of [Ir(dF(CF$_3$)ppy)$_2$(5,5′-d(CF$_3$)bpy)]PF$_6$ as the photocatalyst, tetrabutylphosphonium dibutylphosphate as a base, and the hydrogen atom transfer (HAT) catalyst 2,4,6-triisopropyl thiophenol (TRIP thiol) at room temperature in fluorobenzene and under blue light irradiation provided an

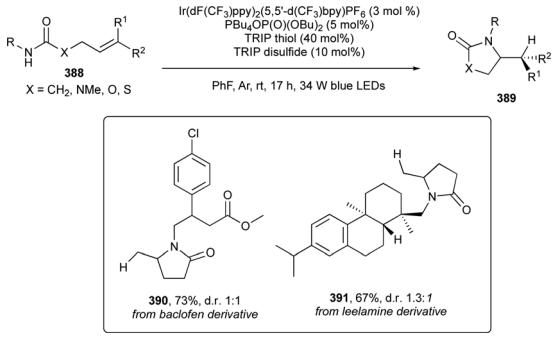

Scheme 70 Formation of cyclic amides and carbamates from olefins.

efficient protocol to carry out olefin derivatization to lactams, cyclic *N*-acylamines, and carbamates. The muscle relaxant baclofen and a leelamine-derived substrate were efficiently hydroamidated (**390** and **391**, Scheme 70, 67 and 91% yield, respectively).

Previous reports from the same group focused on the intramolecular hydroamidation of unactivated alkenes by using *N*-arylamides **392** and a similar ternary catalytic system formed by an iridium photocatalyst, a weak phosphate base, and a H-donor (Scheme 71).[114,115] Thoroughly, the reaction proceeded *via* a concerted proton-coupled electron transfer (PCET), enabling the formation of a *N*-centered radical, which attacked intramolecularly the alkene double bond to form an alkyl radical intermediate. A final H-atom transfer afforded the final cyclic amides. Optimum yields were achieved with thiophenol as the H-atom donor, CH_2Cl_2 as a solvent under blue LEDs irradiation for 20 hours at room temperature. The reaction scope was wide encompassing both acyclic and cyclic systems, with tolerated functional groups including ethers, esters, cyano, halogens. High diastereoselectivities were achieved in most cases, as shown for a progesterone-derived carbamate giving derivative **394** as a single detectable diastereoisomer, and for a carbamate derived from the bridgehead alcohol of giberellic acid providing the polycyclic oxazolidinone **395** in 68% yield (Scheme 71).

1.3.6 Formation of imino-heterocycles. Conversion of olefins into polyfunctionalized nitrogen heterocycles **399** can be easily accessed by a visible-light-mediated radical cascade process reported by J. Davies *et al.* (Scheme 72).[116] The oxidative

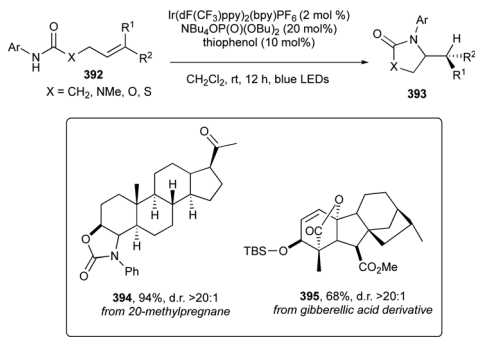

Scheme 71 Intramolecular hydroamidation of olefins.

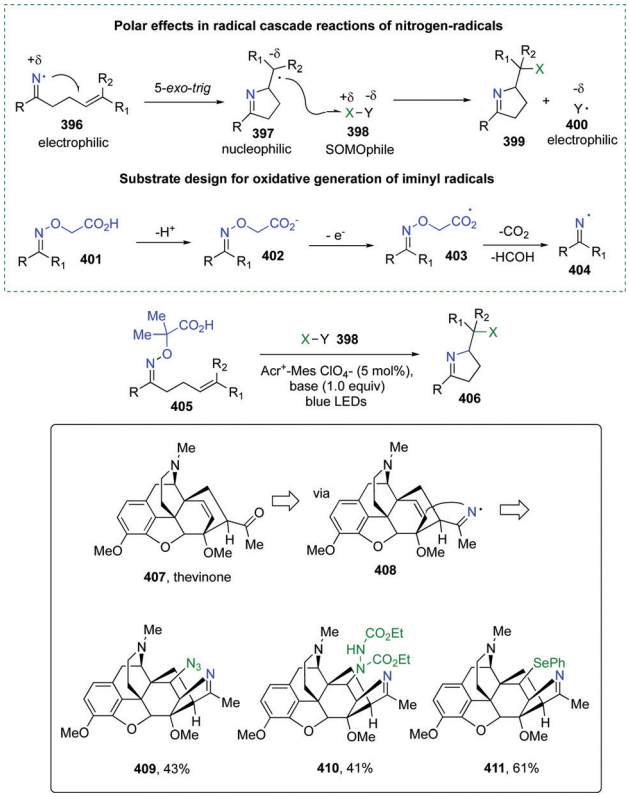

Scheme 72 Formation of imino-heterocycles from olefins.

generation of an iminyl radical **396** followed by 5-*exo-trig* cyclization/radical trapping with a wide range of SOMOphiles X–Y **398** (Scheme 72) enabled the access to a wide range of imino-derivatives such as: hydroxy-, chloro-, bromo-, iodo-, and fluoro-, azido-, amino-, thioether-, seleno-, cyano-, but also Michael adducts, and olefins and alkynyl-derivatives. Iminyl radicals **404** were generated *in situ* from oxime **401** upon deprotonation and SET oxidation, which allowed two subsequent β-scissions with loss of CO_2 and HCOH (Scheme 72). The reaction conditions employed methyl acridinium perchlorate as organic photocatalyst under blue LEDs irradiation at room temperature; the base, the solvent, and the reaction concentration had to be optimized with respect to the different imino functionalizations. In general, inorganic bases Cs_2CO_3 and K_2CO_3, and the solvents dichloromethane and toluene provided maximum efficiency. As an example of LSF the authors tested their procedure on the complex thevinone, a morphane structurally related to thebaine, which successfully gave azido- (**409**, Scheme 72), amino- (**410**), and seleno- (**411**) derivatives in medium yields.

1.3.7 Formation of furans. Akenes can be 1,2-difunctionalized through reaction with *gem*-dibromides (*e.g.* **412**, Scheme 73) under redox neutral photocatalytic conditions.[117] On the basis of the electronic effect of alkenes **79** either 1,2-carboxygenation, with the formation of furan derivatives **413**, and 1,2-carbohalogenation are predictable, regardless of steric effect. Specifically, strong electron-rich alkenes underwent 1,2-carboxygenation (electron-push effect on benzyl radical intermediate), whereas electron-poor and weak electron-rich styrenes afforded their 1,2-carbohalogenated

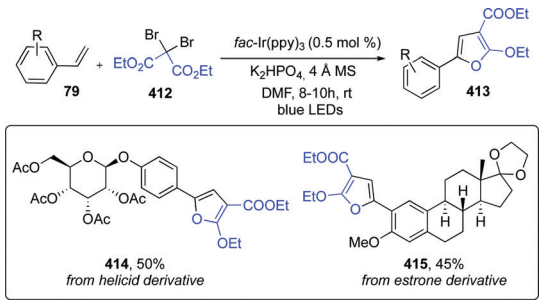

Scheme 73 Formation of furans from olefins.

congeners (electron-pull effect on benzyl radical intermediate). Optimal reaction conditions were identified as the following: *fac*-Ir(ppy)$_3$, K_2HPO_4, 4 Å MS, DMF, blue LEDs irradiation for 8–10 h at room temperature. Regioselectivity and functional group compatibility were good, and LSF of helicid, a natural compound reported to alleviate neuropathic pain and to treat sleep disturbances,[118] and an estrone derivative was accomplished (**414** and **415**, respectively, Scheme 73).

1.4 Conversion to functionalized vinylic, allylic, and other unsaturated systems

1.4.1 Functionalized allylic systems. D. Kurandina *et al.* reported the first visible light-induced Pd-catalyzed Mizoroki–Heck reaction of α-heteroatom substituted alkyl iodides and bromides **416** (Scheme 74) with vinyl arenes/heteroarenes **417**, enabling the synthesis of functionalized allylic systems, such as allylic silanes **418**, boronates, germanes, stannanes, pivalates, phosphonates, phthalimides, and tosylates.[119]

This transformation involved the use of $Pd(OAc)_2$ as catalyst, xantPhos as ligand, Cs_2CO_3 as the base and toluene as solvent under 34 W blue LEDs irradiation for 12 h. Worth of note, the synthesis of the latter substrates was not possible under thermally induced Pd-catalyzed conditions, proving the need of visible light catalysis. This light-induced Heck reaction was tested, as an example of complex substrate, on a vinyl derivative of estrone, giving the desired adduct **419** in a good 81% yield (Scheme 74). Similar results were published at the same time by G.-Z. Wang *et al.*, with primary, secondary, and tertiary alkyl bromides, and mainly styrene substrates. Their catalytic system involved $Pd(PPh_3)_2Cl_2$ as the catalyst, Xantphos as the ligand, K_2CO_3 as the base, water and DMA as solvents, at room temperature and under 36 W blue LEDs irradiation for 15 h.[120]

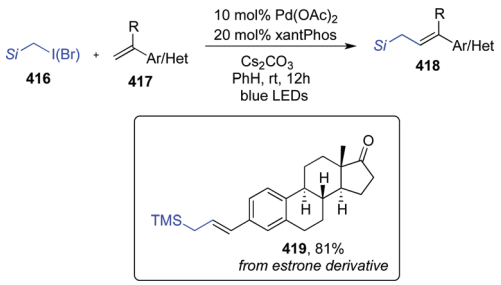

Scheme 74 Synthesis of functionalized allylic systems.

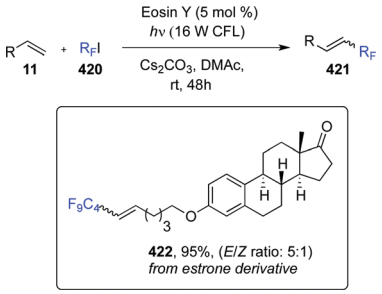

Scheme 75 Perfluoroalkenylation of olefins.

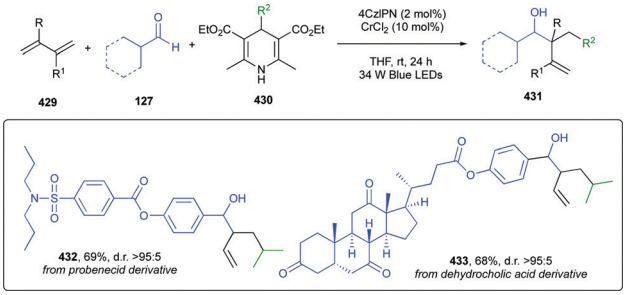

Scheme 77 Three-component dialkylation of 1,3-dienes.

1.4.2 Perfluoroalkenylation. Terminal alkenes **11** can be perfluoroalkenylated *via* an atom transfer radical addition elimination (ATRE) reaction with perfluoroalkyl halides **420** under visible light.[121] The photoredox catalysis was accomplished with the organic dye eosin Y, irradiating with a 16 W fluorescent lamp at room temperature for 48 h, and by using dimethylacetamide (DMA) as the solvent and Cs_2CO_3 as the base. The reaction scope was quite broad, with functional groups having only a minor effect on the reaction outcome, as exemplified by estrone-derived alkene leading to product **422** in 95% yield (Scheme 75).

1.4.3 Synthesis of homoallylic amines. Conjugated dienes **424** (Scheme 76) were shown to couple with photoredox-generated α-amino radicals using a dual cobalt and iridium catalytic system to generate a variety of homoallylic amines from simple commercially available starting materials.[122] Standard conditions were identified as the following ones: cobalt(II) bromide and $[Ir(dF(CF_3)ppy)_2(dtbbpy)](PF_6)$ as the catalysts, dppp as diphosphine ligand, and CsOPiv as the base, MeCN as solvent, at room temperature and under blue LEDs irradiation for 12–20 h. The scope of tertiary amines was quite broad, tolerating a wide variety of functionalized anilines, including aryl bromides and terminal alkynes, as well as fully aliphatic amines. Diversely, electron-poor dienes participated efficiently in the reaction, while electron-rich dienes were typically low-yielding. Structurally complex linear dienes such as pseudoionone, myrcene, and piperine demonstrated to be suitable substrates, affording their amino-alkylated analogues **426–428** (Scheme 76) in medium to good yields.

1.4.4 Dialkylation of 1,3-dienes. More recently, the group of F. Glorius developed a dual photoredox/chromium catalysis enabling a regioselective and diastereoselective three-component dialkylation of 1,3-dienes **429** starting from Hantzsch esters **430** and aldehydes **127** and affording homoallylic alcohols **431** (Scheme 77).[123] Optimum yields were obtained by employing 4CzIPN as the organic photosensitizer, $CrCl_2$ as the chromium source, in THF at room temperature under 34 W blue LEDs irradiation for 24 hours. The robustness of the method was demonstrated by a wide range of both aliphatic and aromatic aldehydes, as well as diverse alkyl Hatzsch esters, and four different 1,3-dienes including myrcene. The exquisite functional group tolerance embodied free alcohols, double bonds, halogens, ethers, Boc-protected amines, and imides. Additionally, enantioselectivity could be achieved by using chromium–bisoxazoline complexes. Application of the standard conditions to probenecid- and dehydrocholic acid-derived aldehydes led to derivatives **432** and **433** in good 69% and 68% yields, respectively, with excellent dr $>95:5$ (Scheme 77).

1.4.5 Synthesis of enones. β-Selective aroylation of activated alkenes can be accomplished *via* a non-chain-radical aroyl chlorination upon a 1,3-chlorine atom shift to form β-chloroketones as masked enones (Scheme 78).[124] The formation of the latter, which afforded the final enones **435** after work-up, avoided the occurrence of undesired pathways, such as double aroylation, *E*/*Z* isomerization, and enone [2+2] cycloaddition, thus leading to good reaction yields. The transformation was accomplished by using *fac*-$Ir(ppy)_3$ as the photocatalyst, 2,6-di^{t}Bu-4-MePy as an additive, in MeCN under 30 W blue LEDs irradiation at room temperature for 16 h. The substrate scope was wide, as proven by more than 55 examples, with a high functional group

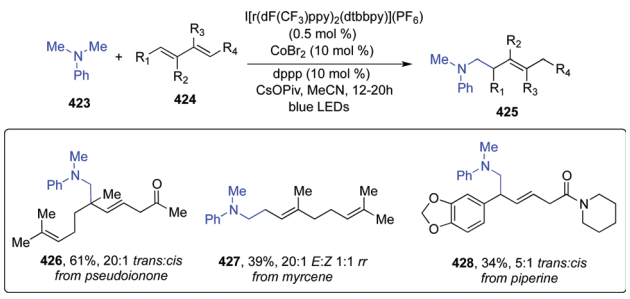

Scheme 76 Synthesis of homoallylic amines from olefins.

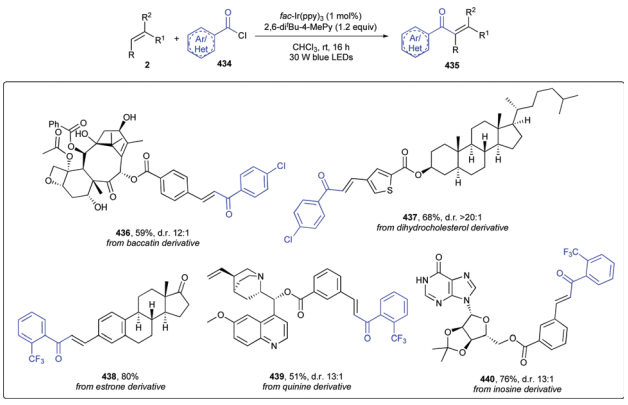

Scheme 78 Synthesis of enones.

compatibility. LSF of baccatin, precursor to the anti-cancer drug paclitaxel, dihydrocholesterol, estrone, quinine, and inosine, among other biorelevant substrates, was also efficiently reported (**436–440**, Scheme 78).

1.4.6 Synthesis of δ-allyl-derivatives. Electron-deficient allyl sulfones **442** can be reacted as δ-carbon radical acceptors generated from aliphatic amide derivatives **441** under photoredox catalytic conditions (Scheme 79).[125]

In particular, pre-functionalized amides **441**, in the presence of eosin Y as a photocatalyst and green LEDs irradiation, afforded amidyl radicals **441B** *via* a SET reduction. A subsequent 1,5-HAT gave a carbon centered radical **441C**, which added onto alkenes, thus providing δ-allyl-derivatives **443**.

Optimized reaction conditions required DIPEA as an additive (here, as a sacrificial electron donor to regenerate the photoactive catalyst eosin Y), and CH_2Cl_2 as the solvent. The scope of the amide enclosed substituted benzoyl-, aromatic-, *N*-acetyl, and *N*-cyclopentyl-carbonyl-substrates, to cite a few, as well as carbamates. Remarkably, a variety of secondary C(sp^3)–H bonds was functionalized in excellent yields. As for the radical acceptors, besides electron-poor allyl sulfones, more complex substrates such as cholesterol and carbohydrates were easily converted to the corresponding derivatives **444** and **445**, respectively (Scheme 79).

1.4.7 Synthesis of allylsilane derivatives. Alkenes could be converted into their corresponding allylsilane derivatives **448** by combining photoredox, hydrogen-atom-transfer, and cobalt

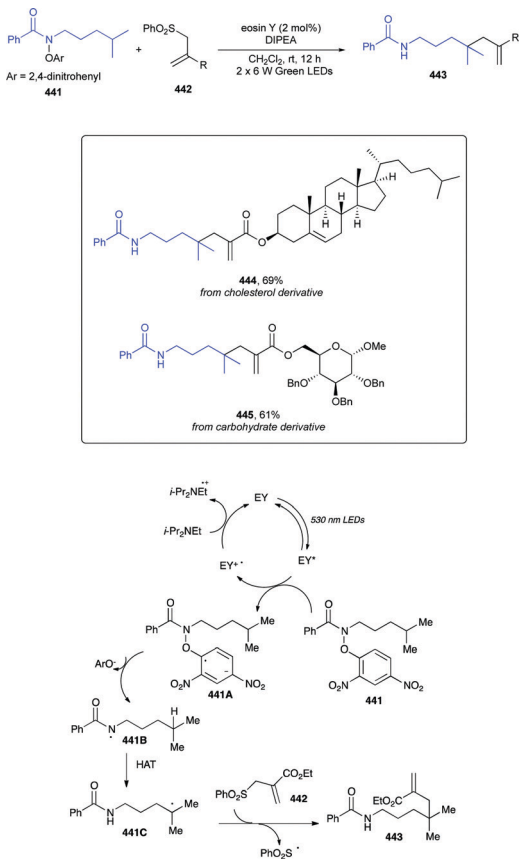

Scheme 79 Synthesis of δ-allyl-derivatives.

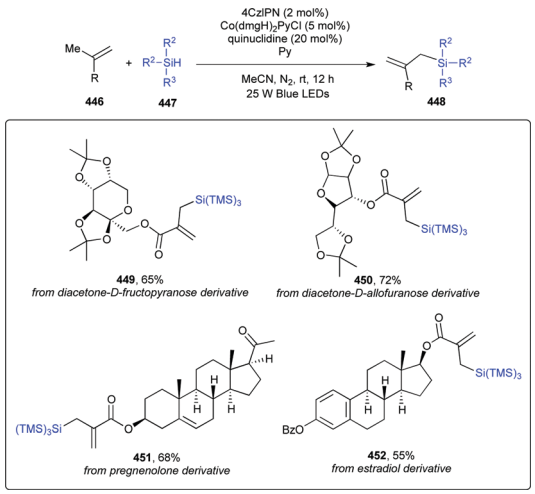

Scheme 80 Synthesis of allylsilane derivatives.

catalysis (Scheme 80).[126] More in detail, to avoid hydrosylilation and the formation of vinyl silanes adducts, this synergistic approach required 4CzIPN as photosensitizer, $Co(dmgH)_2PyCl$ as metal catalyst, quinuclidine as HAT agent, and pyridine as a base, while tris(trimethylsilyl)silane (TTMSS), triethyl-, triisopropyl-, and *tert*-butyldimethyl-silanes acted as stable and commercially available silyl-source. The reaction was performed in MeCN, at room temperature, and under blue LEDS irradiation for 24 h. The alkene scope was wide, including methacrylamides, alkyl acrylates, and heterocyclic aromatic alkenes; on the other hand, monosubstituted alkenes and α,β-unsaturated ketones failed to afford the expected products. Complex and biologically relevant unsaturated substrates such as diacetone-D-fructopyranose, diacetone-D-allofuranose, and steroids were suitable candidates (derivatives **449–452**, Scheme 80), even on a 1 mmol reaction scale as shown for **451** (60% yield, Scheme 80).

1.4.8 Pyridylation of olefins. Branch-selective pyridylation of alkenes could be accomplished *via* a sulfinate assisted photoredox catalytic protocol to afford valuable vinyl pyridines **453** (Scheme 81).[127] Actually, the reaction involved alkenes **80**, cyanopyridines (*e.g.* **300**), and sodium methanesulfinate, together with an iridium photocatalyst such as *fac*-Ir(ppy)$_3$. The latter, in its excited state, operated a SET reduction of cyanopyridine **300** to pyridyl radical anion **300A**, thereby forming an Ir^{IV} species, which could then oxidize sodium methanesulfinate to form an electrophilic sulfonyl radical. Radical addition of the *S*-centered radical to the alkene **80** generated a nucleophilic benzylic radical **80A**, further undergoing a radical–radical coupling with the persistent pyridyl radical anion **300A**, to eventually forge β-sulfonyl pyridine derivatives **300B**. Given the ability of sulfone of acting as a leaving group, the alkyl sulfone intermediate finally underwent a base mediated E1 elimination to α-branched alkenylpyridines **453**. Remarkably, in this last step, methanesulfinate was fully regenerated and could be recycled. Standard reaction conditions involved DBU as the base, and a mixture of MeCN/EtOH as solvent system, at 40 °C and under 90 W blue LEDs irradiation. The scope of the alkenes was broad, embodying both electron-rich and electron-poor aromatics, as well as heteroaromatics. As examples of complex

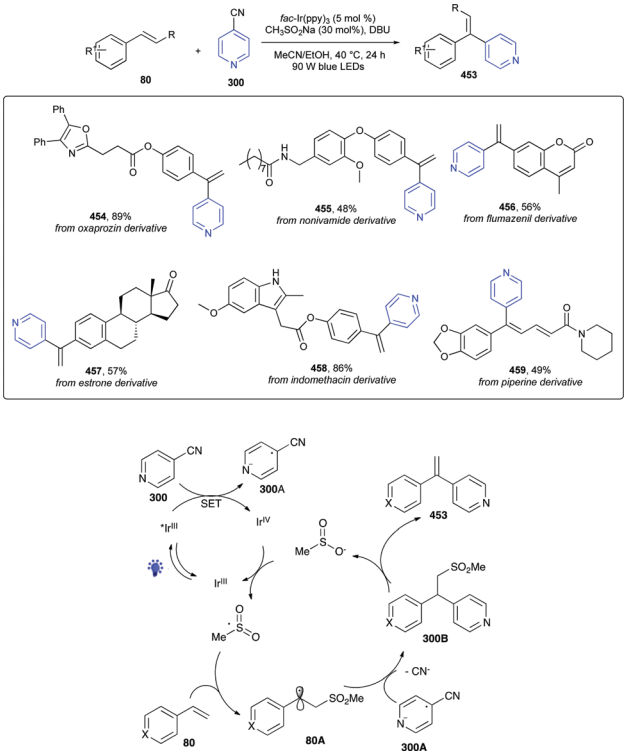

Scheme 81 Pyridylation of olefins.

bioactive compounds, oxaprozin, nonivamide, hymecromone, estrone, indomethacin, and piperine were readily functionalized to derivatives **454–459** (Scheme 81) with medium to good yields.

1.4.9 Sulfonylation of vinyl arenes. Vinyl arenes **79** could be converted into their corresponding vinyl sulfones **461** by using bench-stable and readily available arylsulfonate phenol esters **460** as precursors of sulfonyl radical intermediates (Scheme 82).[128] Remarkably this protocol did not require any metal catalyst, as the base-assisted formation of electron donor–acceptor (EDA) complex between arylsulfonate phenol ester **460** and a molecule of DMA (used as the reaction solvent) enabled, upon visible light excitation, a SET event leading to the formation of the key sulfonyl radical intermediate. Addition of the latter to styrene afforded a benzyl radical, which underwent a HAT to give the final vinyl sulfone. The transformation proved to be viable with *ortho*-, *meta*-, and *para*-electron-rich or electron-poor vinyl arenes, as well as with vinyl heteroarenes. Likewise, diversely substituted or heteroaromatic sulfone moieties

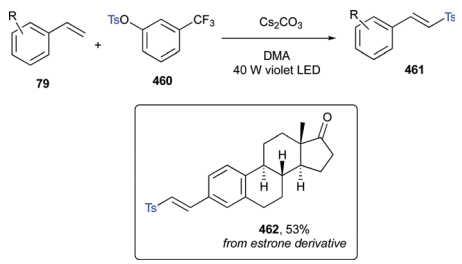

Scheme 82 Sulfonylation of vinyl arenes.

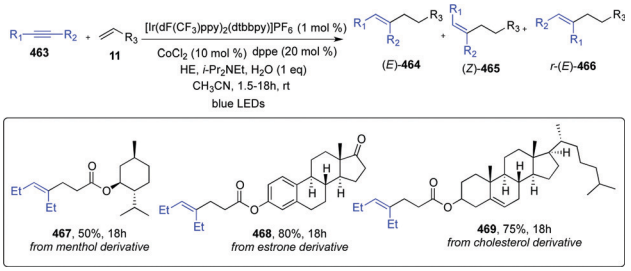

Scheme 83 Ene–yne coupling reaction (467: NMR yield).

gave excellent yields. As an example of a complex bioactive alkene, vinyl estrone, was readily converted into derivative **462** in 53% yield (Scheme 82).

1.4.10 Ene–yne coupling. P. Rai *et al.* reported an ene–yne coupling reaction enabled by a dual catalytic system based on an iridium photocatalyst and $(dppe)_2CoCl_2$ as high valent transition-metal co-catalyst (Scheme 83).[129]

A 1 : 2 mixture of $^{i}Pr_2NEt$/Hantzsch ester (HE) as organic sacrificial reductants, and water as a proton source, were also essential for the transformation. The latter proceeded under blue LEDs irradiation at room temperature in MeCN as the solvent. The mild conditions enabled functional group tolerance and broad substrate scope as demonstrated with 39 examples, with yields up to 99%. For a large number of alkenes, including for example aliphatic and benzyl-acrylates, enones, and acrylonitrile, yields were good, and, in all the cases, the (*E*)-stereoisomer was formed selectively. Functional groups such as F-, Cl-, Br-, and pyridine rings were orthogonal to reaction conditions. As for alkyne partners, while for unsymmetrical alkynes, the regioselectivity was controlled by the cobalt catalyst, diarylacetylenes gave a stereoisomeric mixture due to *E*/*Z* isomerization *via* a triplet–triplet energy transfer. As examples of bioactive substrates, menthol, estrone and cholesterol were successfully converted into derivatives **467–469** with 50, 80, and 75% yields, respectively (Scheme 83).

1.5 Structural modification of functionalized alkenes

1.5.1 From trifluoromethyl-substituted alkenes. S. B. Lang *et al.* described a scalable route to access *gem*-difluoroalkenes **472** starting from trifluoromethyl-substituted alkenes **470** and different carbon-radical precursors **471** (Scheme 84).[130] *Gem*-difluoroalkenes

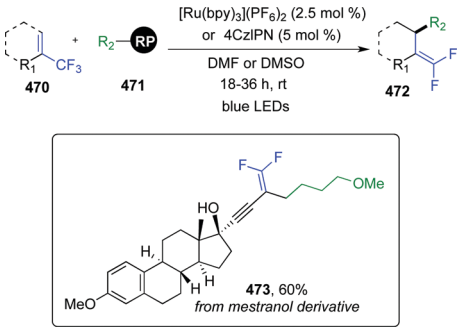

Scheme 84 Synthesis of *gem*-difluoroalkenes.

472 are considered valuable functional groups in medicinal chemistry as they have been demonstrated to behave as isosters of the metabolically unstable ketones, which are reduced to their corresponding alcohols during phase I metabolism, being inactivated and leading to poor bioavailability. The *gem*-difluoroethylene moiety proved to be a good mimic of the carbonyl-one, preserving its geometry and electronics: it is indeed an isopolar analogue still able to be engaged in H-bonding. This radical defluorinative alkylation was accomplished by using $Ru(bpy)_3(PF_6)_2$ (2.5 mol%) or 1,2,3,5-tetrakis(carbazol-9-yl)-4,6-dicyanobenzene (4CzIPN, 5 mol%), DMF or DMSO (0.05–0.1 M), at room temperature irradiating with blue LEDs (6 to 40 W) for 18–36 h. The process was also extended to perfluoroalkyl-substituted alkenes and non-stabilized primary, secondary, and tertiary radicals can be all used to install a wide range of functional groups. As an example of complex substrate, mestranol, a pro-drug of ethinylestradiol, used in birth control pills, menopausal hormone therapy, and in the treatment of menstrual disorders, was readily converted into its *gem*-difluoroalkenyl-derivative **473** (Scheme 84) in a good 60% yield, showing that the tertiary alcohol is orthogonal to standard reaction conditions.

1.5.2 Alkylation of *gem*-difluoroalkenes. Electron-rich *gem*-difluoroalkenes **474** can undergo a F-nucleophilic addition, *via* a prior photoredox single-electron oxidation of the aryl system to radical cation, to afford CF_3-embedded tertiary and quaternary carbon centers **475** (Scheme 85).[131] Thoroughly, this strategy provided α-CF_3-substituted benzylic radical intermediates, which added to an allyl sulfone coupling partner. Experimentally, the reaction required $Et_3N{\cdot}3HF$ as the fluoride source, $[Ir(dF(CF_3)ppy)_2(5,5'\text{-}dCF_3bpy)](PF_6)$ as the photocatalyst in MeCN as the solvent, under blue LEDs irradiation at room temperature. *gem*-Difluoroalkenes with electron-donating groups reacted with moderate to excellent yields, whereas substrates with relatively high oxidation potentials, *e.g.* alkyl-, halogen-, and trifluoromethoxy-substituted ones, required a switch to photocatalyst Acr^+-Mes. Yet, substrates with electron-withdrawing groups such as ester, cyano, nitro, and ketone were not suitable, while heteroaromatics and extended aromatic systems reacted uneventfully. As example of late-stage modification, tocopherol-derived *gem*-difluoroalkene, menthol and epiandrosterone allyl sulfone derivatives were readily converted into compounds **476–478** (Scheme 85).

1.5.3 Monofluoroalkenylation of thiols with *gem*-difluoroalkenes. A protocol for the defluorinative cross-coupling of *gem*-difluoroalkenes (*e.g.* **479**) with aryl, benzyl, and alkyl thiols **239** under photoredox catalytic conditions was developed by J. Wang *et al.* (Scheme 86).[132] Tri- and tetra-substituted monofluoroalkenes *e.g.* **480** could be smoothly synthesized by using $[Ir(dF(CF_3)ppy)_2(dtbpy)]PF_6$ as a photocatalyst, K_2CO_3 as a base, either toluene or MeCN as a solvent, under 15 W blue LEDs irradiation at room temperature. The alkene partners included mono- and di-substituted aromatic and heteroaromatic substrates, tolerating a wide range of functional groups such as ethers, esters, and halogens, while diversely substituted thiophenols as well as benzylic and aliphatic thiols reacted cleanly under standard reaction conditions. Late-stage modification of dehydrocholic acid and diosgenin to **481** and **482**, was accomplished in 55 and 82% yields, respectively, as shown in Scheme 86.

1.5.4 From vinylazides. Vinyl azides **483**, as reported by W.-L. Lei *et al.*,[133] can be reacted with ammonium thiocyanate **484** to give 4-alkyl/aryl-2-aminothiazoles **485** (Scheme 87). The reaction is catalyzed by copper salts and blue LEDs irradiation at room-temperature (Scheme 87). Interestingly, the in situ-formed $Cu(NCS)_2^-$ played a dual catalytic role: as photocatalyst, through energy-transfer of its excited state, in the activation of vinyl azides, and as Lewis acid to promote the ring opening of intermediate 2*H*-azirines with thiocyanide. The process was characterized by high yields, mild reaction conditions, low catalyst loadings, and a wide functional group tolerance. Furthermore, copper is inexpensive, earth-abundant, and readily available so that this transformation can be considered sustainable and environmentally benign. In order to prove the robustness of this synthetic procedure, the authors chose cholesterol as a complex substrate, which readily gave the thiazole derivative **486** in a good 61% yield (Scheme 87).

1.5.5 Alkylation of enol silyl ethers. K. Ohmatsu *et al.* identified a catalytic system based on an iridium photosensitizer

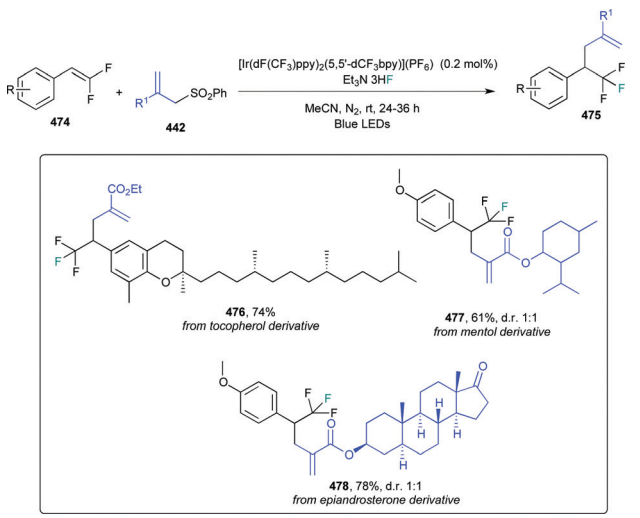

Scheme 85 Alkylation of *gem*-difluoroalkenes.

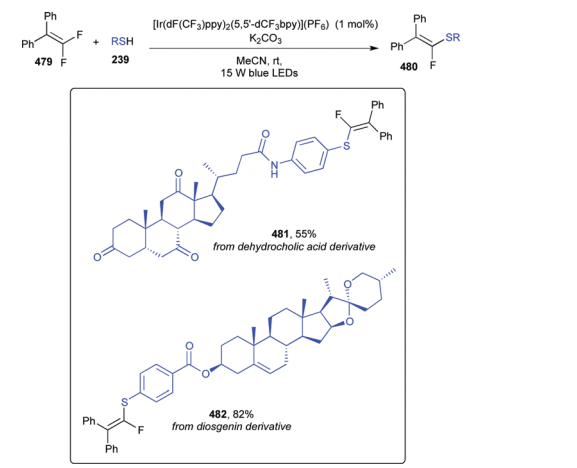

Scheme 86 Monofluoroalkenylation of thiols with *gem*-difluoroalkenes.

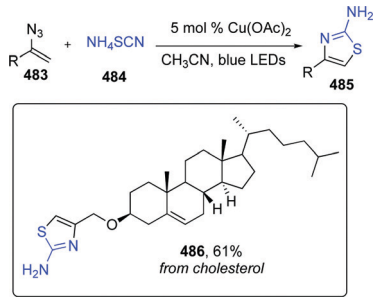

Scheme 87 Synthesis of 4-alkyl/aryl-2-aminothiazoles.

to generate nucleophilic allylic radicals from enol silyl ethers **487** through a SET oxidation/deprotonation sequence under visible light irradiation (Scheme 88).[134] The resultant allylic radical added onto electron-deficient alkenes, thus enabling their selective allylic C–H alkylation and rapidly affording complex carbonyl compounds after desilylation. Optimum yields were obtained by employing $[Ir(dF(CF_3)ppy)_2(4,4'\text{-}dCF_3bpy)]PF_6$ as the photocatalyst, 2,4,6-collidine as a base, in MeCN as the solvent, and blue LEDs as the photon source. As electrophilic acceptors a range of arylidene malononitriles, α,β-unsaturated ketones and sulfones, were competent substrates, while alkylidene malononitriles led to moderate efficiencies. Also, 6-, 7-, and 8-membered cyclic enol silyl ethers, as well as primary alkyl ketone and mesityl ketone-derived enol silyl ethers smoothly reacted under standard conditions in good to excellent yields. Functional group compatibility covered, among others, chlorine, ether, ester, amide and nitrile, and it was further tested in the conversion of an estrone-derived silyl enol ether into derivative **490** in an excellent 92% yield (Scheme 88).

1.5.6 Fluoroarylation of allenoates. Fluoroarylation of allenic esters **491** leading to β-fluoroalkyl-containing cinnamate derivatives **493** could be accomplished under visible-light-promoted gold redox catalytic conditions starting from arenediazonium salts **492** (Scheme 89).[135] The reaction exploited $Et_3N{\cdot}3HF$ as fluorine source, Ph_3PAuCl as the gold-based catalyst, and proceeded in a MeCN/DCE solvent mixture under irradiation with 15 W blue LEDs at room temperature. By applying these conditions, incorporation of fluorine and aryl groups into a wide range of allenoates was achieved in medium to excellent yields, and with exquisite regio- and stereo-selectivities. Late-stage modification of bioactive structurally complex scaffolds was performed with epiandrosterone-derived allenoate (**494**, Scheme 89), and arenediazonium salts derived from L-menthol, vitamin E, and estrone (**495–497**, Scheme 89).

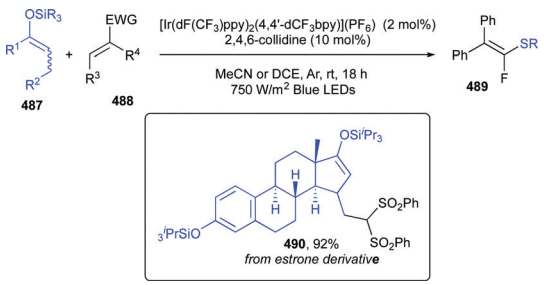

Scheme 88 Alkylation of enol silyl ethers.

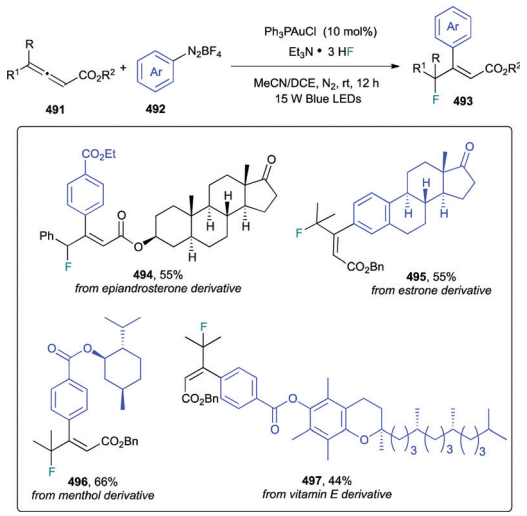

Scheme 89 Fluoroarylation of allenoates.

1.6 Controllable isomerization of alkenes

Thermodynamic and kinetic isomerization of alkenes can be attained by a dual photoredox-nickel catalytic system (Scheme 90).[136]

In the presence of 4CzIPN as photosensitizer and Xantphos as a ligand, the protocol led to the most stable isomers, while the use of DPEphos enabled the isomerization of terminal alkenes over other positions. Furthermore, exocyclic alkenes **498** can be converted into the corresponding endocyclic products **499** upon treatment with 4CzIPN and $Co(acac)_2$ and without any additional ligand (Scheme 90). Mechanistic investigations showed that the cobalt catalyst was involved in the generation of a Co-hydride, likely to add to the alkene, thus initiating the isomerization process. As examples of complex biorelevant scaffolds, cholesterol derivative **500** and (−)-β-pinene **502** were converted into **501** (96% yield) and (−)-α-pinene **503** (98% yield), respectively.

1.7 C=C bond cleavage towards α-ketoesters

A photoredox catalytic metal-free protocol for the α−oxoesterification of enaminone (**504**) C=C double bonds with primary and secondary

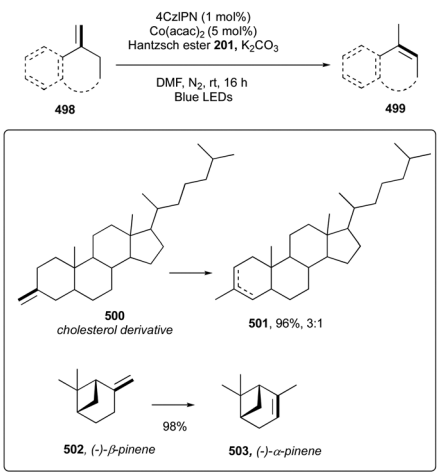

Scheme 90 Controllable isomerization of alkenes.

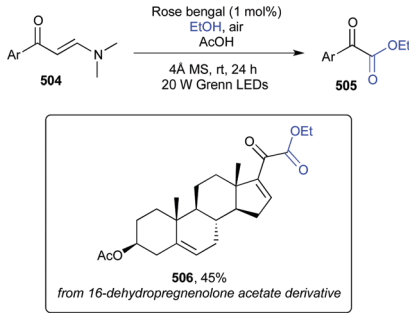

Scheme 91 C≡C bond cleavage towards α-ketoesters.

alcohols was reported by Q. Yu *et al.* (Scheme 91).[137] The authors exploited the use of the organic dye rose bengal (RB) under air as oxidant and green LEDs irradiation. After optimization, it was found that acetic acid as an additive and ethanol as the solvent gave the most efficient conditions. Aryl enaminones with electron donating groups at the phenyl ring gave better results than their electron-poor analogues, while the substitution pattern (*ortho*-, *meta*-, or *para*-) did not exert substantial effects on the outcome of the reaction. Furthermore, enaminones with double phenyl-, fused aryl-, and heteroaryl-substituents afforded α-ketoesters with good yields. Remarkably, scope of the alcohols included both primary and secondary linear and branched substrates, haloalkyl-, cyclic-, and alkynyl-alcohols, to cite a few. Post elaboration of the naturally occurring 16-dehydropregnenolone acetate gave derivative **506** in a moderate 45% yield.

2. Functionalization of C≡C bonds

Similar to alkenes, albeit at a less extent, alkynes have been widely used as radical acceptors in both intra- and intermolecular radical additions, triggering cascade processes and enabling the access to complex and often polycyclic molecular frameworks.[138–140] The synthetic value of this transformation relies on the formation of highly reactive vinyl radicals as key intermediates, which can be trapped by cyclization, or react through addition onto other π systems or *via* HAT/ATRA events, thus granting C(sp^2)–X bonds' formation. Typically, anti-Markovnikov addition, giving more stable vinyl radicals, was obtained exclusively due to the Kharasch effect.[141,142] However, albeit considered challenging, methods enabling a direct synthesis of α-substituted vinyl compounds from intermolecular radical addition to terminal alkynes were also reported (Section 2.2.1). Also, dual synergic systems based on photoredox/transition metal catalysts as well as copper-based photoactive complexes promoted radical crosscoupling pathways to achieve functionalization of terminal alkynes or [4+2] annulation to all-carbon aromatic compounds (Section 2.1.2).

2.1 Formation of C(sp^2)–C(sp^2) bonds

2.1.1 Alkenes' synthesis. A photocatalytic C_{aryl}–F alkenylation reaction of alkynes **463** and fluorinated arenes **507** was reported by A. Singh *et al.* (Scheme 92).[143] Remarkably, the choice of the photocatalyst, acting *via* both electron and energy transfer, allowed to selectively obtain *E* or *Z* isomers. Thoroughly, *Z*-alkenylation was

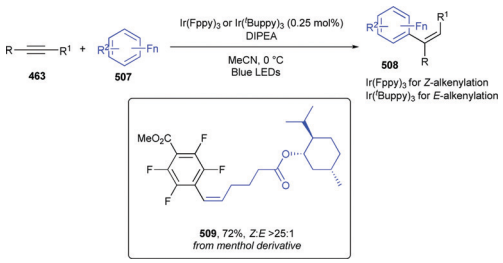

Scheme 92 Alkene's synthesis.

accomplished by using Ir(Fppy)$_3$, while the *E*-isomers were obtained by employing Ir(*t*Buppy)$_3$. Accordingly, it was suggested that the differences in the energy transfer process depended also in the internuclear distances, so that the steric volume of the photocatalyst could dramatically influence such a process. In particular the authors found that as the steric volume of the photocatalyst increased, the isomerization decreased. The transformation required DIPEA as an additive and was run in MeCN at 45 °C under blue LEDs irradiation. The reaction scope was wide, with a good functional group tolerance including halogens, alcohols, and esters. A menthol-derived alkyne was converted into **509** in 78% yield and with $Z:E$ ratio $>25:1$.

Recently, the group of M. Rueping reported the metallaphotoredox regioselective hydroalkylation and arylalkylation of alkynes **365** with carboxylic acids **510** and aryl bromides **12** (Scheme 93).[144]

The anti-Markovnikov-type hydroalkylation was promoted by an iridium photocatalyst and $NiCl_2$·glyme as a metal-based catalyst, in the presence of Cs_2CO_3 as a base in a MeCN/DMF solvent mixture under blue LEDs irradiation at room temperature for 12 hours. On the other hand, the arylalkylation required a slight variation of the reaction conditions (Scheme 93B). Both transformations were successfully accomplished with a wide

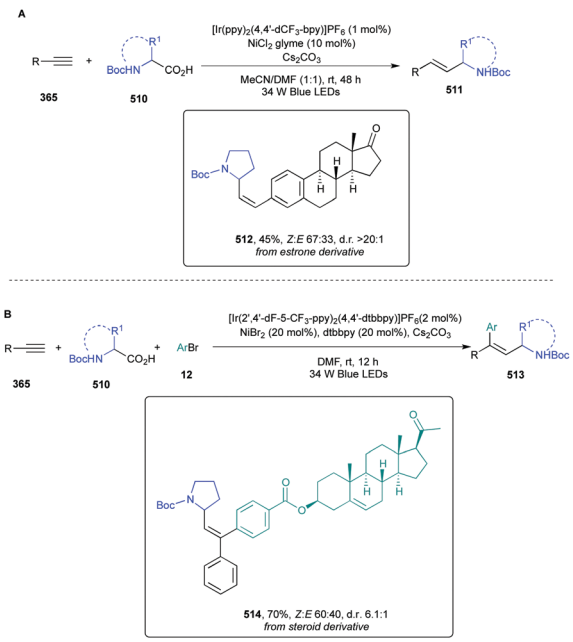

Scheme 93 Hydroalkylation of alkynes.

number of both alkynes and carboxylic acids, and the good functional group tolerance was further tested by using an estrone-derived alkyne and steroid-derived bromide (**512** and **514**, respectively, Scheme 93).

In this context, *cis*-selective transfer semihydrogenation of alkynes (**365**) could be achieved thanks to the synergic combination of $[Ir(dF(CF_3)ppy)_2(dtbbpy)]PF_6$ as a photoredox catalyst and $CoBr_2$/*n*-Bu_3P as a proton-reducing catalyst, while $^iPr_2NEt$/AcOH was used as the hydrogen source (Scheme 94).[145]

Notably, the semihydrogenation protocol showed a good selectivity towards *Z* isomers and avoided over-reduction. Based on mechanistic studies, the photosensitizer acted with the dual role of promoting a SET event and controlling the stereoselectivity *via* an energy transfer process (EnT). The reaction scope included both terminal and internal alkynes, and functional group tolerance was observed for a wide range of functional groups such as halogen, cyano, and ester. Ethisterone and ethinylestradiol were selected as examples of bioactive complex substrates and reduced in quantitative yields to derivatives **515** and **516** (Scheme 94).

2.1.2 [4+2] annulation. Alkynes (**463**) could react with styrenes (**40**) *via* a [4+2] annulation to give aromatic compounds (**517**, Scheme 95). The reaction was performed under external-oxidant-free conditions, by merging photoredox and cobaloxime catalysis at room temperature.[146] More in detail, $AcrMes^+ClO_4^-$ was used as photocatalyst and $Co(dgmH)_2py_2PF_6$ as the cobaloxime co-catalyst, in DCE as solvent and using a blue LEDs light source at room temperature for 24 hours. These conditions efficiently enabled a scaling up to a gram scale and provided a wide scope as showcased for the annulation of vinyl estrone to derivative **518** in 64% yield (Scheme 95).

Shortly after, the same group reported an elegant and versatile protocol enabling the synthesis of substituted benzene rings **520** *via* a visible light induced [4+2] annulation of alkynes **463** and thiophenes (*e.g.* **519**, Scheme 96).[147] Mechanistically, the latter was driven by an *in situ* generated thiophene radical cation, which added into the carbon–carbon triple bond to give a *S*-bridged bicyclic radical intermediate. Final benzene derivatives were obtained after one more SET event, and loss of sulfur as $\frac{1}{8}S_8$. Remarkably, this intermolecular desulfurative annulation of thiophenes did not require any external oxidant and was efficiently catalyzed by Mes-Acr^+ClO4^- under blue LEDs irradiation in MeCN at room temperature. Thiophene substrates tolerated alkyl, acetoxy, methoxy, and halogen groups at the C3-position, while

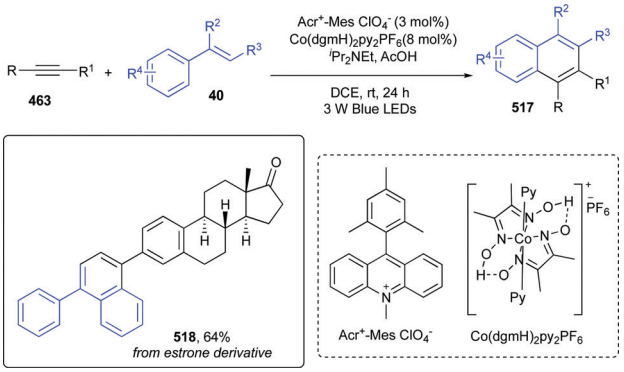

Scheme 95 [4+2] annulation of alkynes and styrenes.

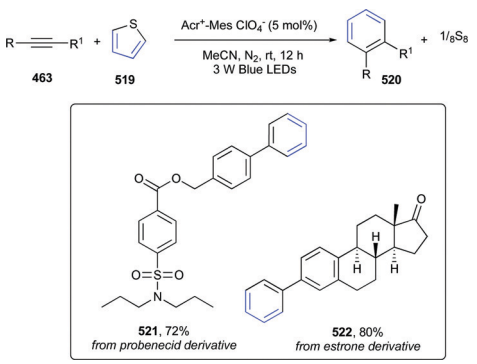

Scheme 96 [4+2] annulation of alkynes and thiophenes.

substituents at the C2-led to moderate yields due to the steric hindrance. The scope of alkynes embodied both electron-poor and electron-rich phenylacetylenes, heterocyclic ethynes as well as enyne, alkynol, aliphatic alkynes, and, interestingly, internal alkynes. Complex bioactive alkyne derivatives of probenecid and estrone afforded the desired adducts **521** and **522** in 72 and 80% yield, respectively.

More recently, L.-Z. Wu and coworkers developed a strategy to generate a transient α-carbonyl radical and persistent ketyl radical from aromatic β-ketoesters **523** by using *fac*-$Ir(ppy)_3$ as a photoredox catalyst and without the need for stoichiometric external oxidant nor reductant (Scheme 97).[148] A series of

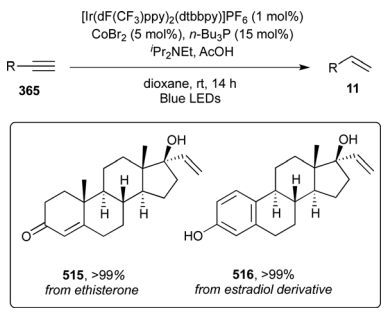

Scheme 94 Semihydrogenation of alkynes.

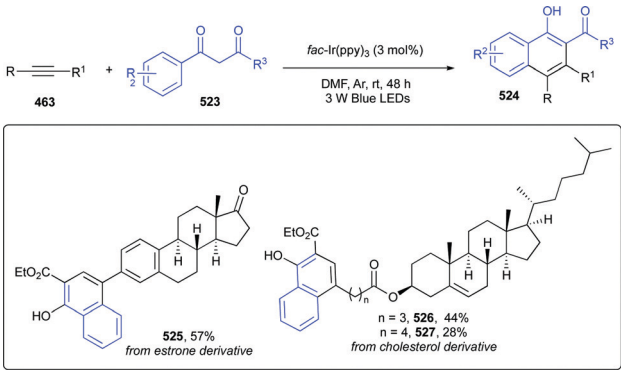

Scheme 97 Synthesis of 1-naphthols.

highly functionalized 1-naphthols **524** were generated upon pinacol coupling of ketyl radicals and benzannulation of α-carbonyl radicals with alkynes. The reaction conditions were exceptionally mild, requiring only the photocatalyst in DMF under blue LEDs irradiation for 48 hours at room temperature. In order to highlight the good functional-group tolerance of the protocol, estrone and cholesterol derivatives were used as examples of complex molecules (**525–527**, Scheme 97).

2.2 Formation of C(sp)–C(sp^3) bonds

Terminal alkynes (**365**) were also reported to be suitable substrates in a photoinduced copper-catalyzed three-component radical cross-coupling with alkenes **6** and cycloketone oxime esters **528**, to provide access to cyanoalkyl-propargylic derivatives **529** (Scheme 98).[149] The cycloketone oxime esters were valuable precursors of iminyl radicals, which readily underwent ring-opening *via* β-C–C bond cleavage, forming a cyanoalkyl radical **530**. The latter could add to alkenes, forming a benzyl radical **531**, which could finally react through a cross-coupling with the *in situ*-formed copper acetylide complex. Remarkably, in this transformation, three new C–C bonds were formed, with exceptional atom economy. Standard reaction conditions required CuI, dtbbpy (4,4′-di-*tert*-butyl-2,2′-bipyridine) as a ligand, K_2CO_3, DMF as the solvent, under blue LEDs irradiation at 30 °C for 10 h. A range of neutral styrenes, as well as functionalized ones with both electron-donating (*e.g.* Ph, OMe, OAc) or electron-withdrawing (*e.g.* Bpin, Br, CO_2Me) groups gave good yields (36–76%). To prove the utility of the developed catalytic system in LSF of pharmaceutical compounds, estrone, febuxostat, and gibberellic-acid derivatives were selected as starting alkenes, and ethynyl estradiol and a diacetone-D-glucose-derivative as starting alkynes. A smooth conversion to derivatives **534–538** was accomplished (Scheme 98).

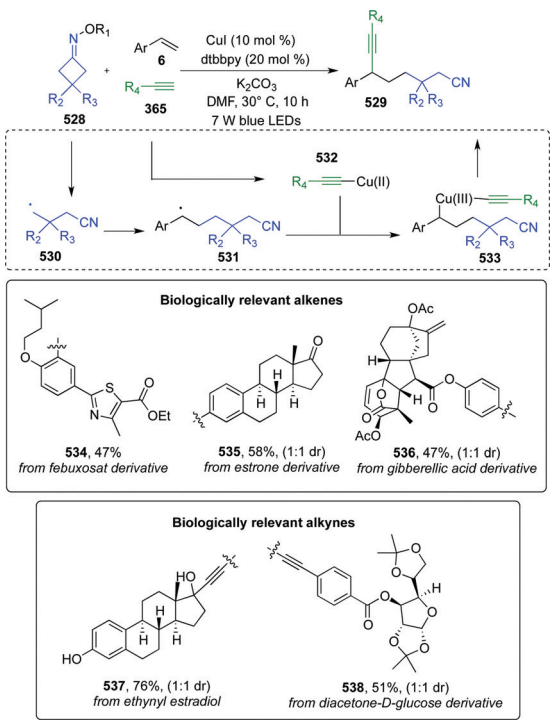

Scheme 98 Synthesis of cyanoalkyl-propargylic derivatives.

2.3 Formation of C(sp^2)–C(sp^3) bonds

A protocol for the functionalization of both terminal and internal alkynes (*e.g.* **539**, Scheme 99) with THF **540** was reported in 2015 by J. Li *et al.*[150]

This transformation exploited the synergistic actions of eosin Y as an organic photocatalyst, *tert*-butyl hydroperoxide (*t*-BuOOH) as an oxidant, and HCOOH as an acidic additive, in the presence of 4 Å MS, under irradiation with a 45 W household lightbulb in a 1 : 1 mixture of MeCN/THF at room temperature for 36 hours. The reaction scope proved to be wide, with a good functional group tolerance including esters, ethers, halogens, and aliphatic alkyl chains as well as aromatic heterocycles, with *E*/*Z* ratios ranging from 0.3 to 1.6. Late-stage elaboration of a diosgenin derivative afforded **542** in a good 53% yield.

More recently, it was shown that terminal alkynes **543** could be functionalized with different cyclic ethers **544** to give 2-vinyl heterocycles **545** under visible light irradiation in presence of a Cu-catalyst (Scheme 100).[151]

Interestingly, the Cu(I)-acetylide formed *in situ* had the dual role of activating the C–H bond of terminal alkynes, and of serving as photocatalyst as it exhibited visible-light absorption: no additional noble metals or organic dyes were indeed required. *tert*-Butyl hydroperoxide (TBHP) was also essential as a HAT agent, to generate the key α-oxy-carbon centered radical from THF. By applying optimized reaction conditions, a series of vinyl tetrahydrofurans were isolated in good yields, with *E*/*Z* isomeric ratios ranging from 0.1 to 4.1. electron-donating/-withdrawing

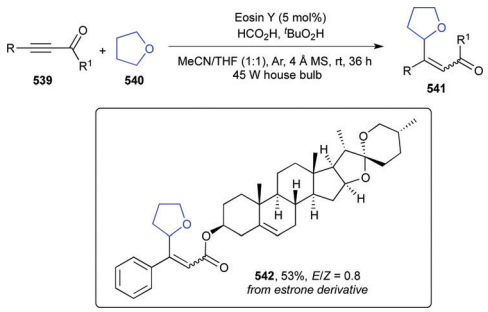

Scheme 99 Functionalization of alkynes with tetrahydrofuran.

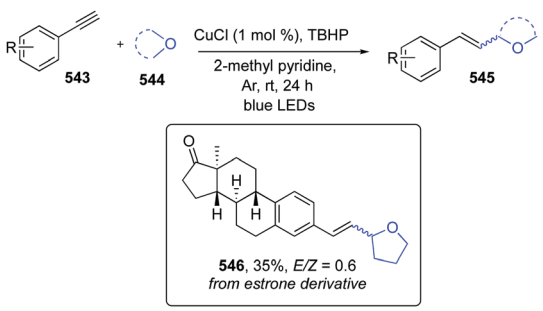

Scheme 100 Functionalization of alkynes with ethers.

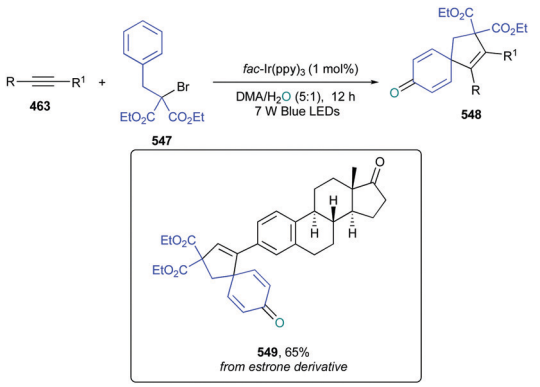

Scheme 101 Reaction of alkynes with 2-benzyl-2-bromomalonate.

properties and substitution patterns (*ortho*-, *meta*-, *para*-) did not affected a generally good reactivity. Besides THF, dioxane, dioxolane, and tetrahydropyran were suitable starting ethers. Bioactive estrone was easily functionalized to give **546** with an *E*/*Z* ratio of 0.6 (Scheme 100).

Meantime, W. Dong *et al.* experienced that reaction of alkynes **463** with 2-benzyl-2-bromomalonate **547** under visible light photoredox catalytic condition and in the presence of H_2O led to formation of spiro[4.5]deca-1,6,9-trien-8-ones **548** *via* a 5-*exo*-*dig* radical dearomative cyclization.[152] The protocol was easily scalable to gram quantities thanks to low catalyst loading required (0.1–1.0 mol%) and the absence of both extra oxidant and leaving groups. Optimum yields were obtained by employing *fac*-Ir(ppy)$_3$ as the photocatalyst in a 5 : 1 mixture of DMA/H_2O while irradiating with 7 W blue LEDs at room temperature for 12 hours (Scheme 101). The substrate scope of both the 2-bromocarbonyl compounds and the alkynes was good, with a broad functional group tolerance as shown in the functionalization of estrone-derived alkyne (**549**, Scheme 101).

2.4 Formation of C(sp^2)–X bonds

2.4.1 Formation of C(sp^2)–S bond. In this context, the Lei lab reported a transition-metal free and visible-light mediated Markovnikov addition of sulfinic acids **555** to terminal alkynes **365** through generation of vinyl radicals and cross coupling with sulfonyl radicals (Scheme 102).[153] This α-regioselective transformation was accomplished by using sulfinic acids as sulfinyl radical precursors, eosin Y as the photocatalyst, K_2CO_3 as a base, in DMF at room temperature. The scope of the terminal alkynes included both *ortho*- and *para*-substituted aromatic ones, and heteroaromatics, with halides, carbonyls, and even amines and sulfonamides suitable as functional groups. On the other hand, aliphatic alkynes provided moderate yields. Benzene-, naphthalene-, and heteroaromatic sulfinic acids also proved to be suitable substrates, with a good functional group compatibility (*e.g.* Br-, Cl-, and acetyl-substituents). As example of complex bioactive skeleton, an estrone derived alkyne was converted in a good 65% yield to its α-vinyl parent compound **557** (Scheme 102).

2.4.2 Trifluoromethylthiosulfonylation. Alkynes **463** could be converted into trifluoromethylthio- and difluoromethylthio-functionalized vinylsulfones **559** *via* the merger of photoredox

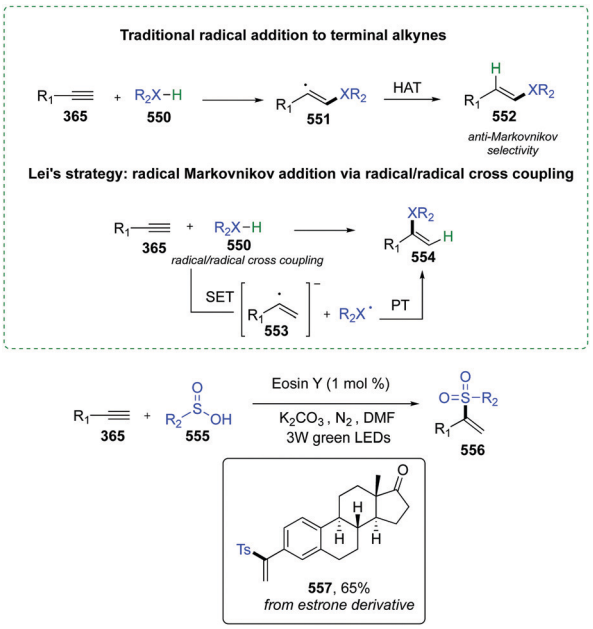

Scheme 102 Formation of C(sp^2)–S bond (PT = proton transfer).

and gold catalysis (Scheme 103).[154] From a mechanistic point of view, this transformation relied on a gold-assisted atom transfer radical addition (ATRA) of a sulfonyl radical to the alkyne. The role of the gold-catalyst is essential to both activate the triple bond and to stabilize the vinyl radical intermediate, thus providing good stereoselectivity. In order to get optimum yields, the reaction required $Ph_3PAuNTf_2$ as a gold-catalyst, $Ru(bpy)_3Cl_2$ as a photoredox catalyst, either $PhSO_2SCF_3$ or $PhSO_2SCF_2H$ as difunctionalization reagents, in dioxan at room temperature and under blue LEDs irradiation. The alkyne scope was broad for both tri- and di-fluoromethylthiosulfonylation, with good functional group tolerance showcased for two pharmaceutical agents such as clofibrate and estrone (**560** and **561**, respectively, Scheme 103).

2.4.3 Iodofluoroalkylation. Recently, a visible light promoted approach to achieve iodofluoroalkylation of unactivated alkynes and alkenes (**463** and **2**, respectively) was devised by Y.-X. Ji *et al.*[155] The reaction design relied on an ATRA process of fluoroalkyl halides such as iododifluoroacetate **562** to alkynes (and alkenes). Remarkably, $Mn_2(CO)_{10}$ was exploited as an

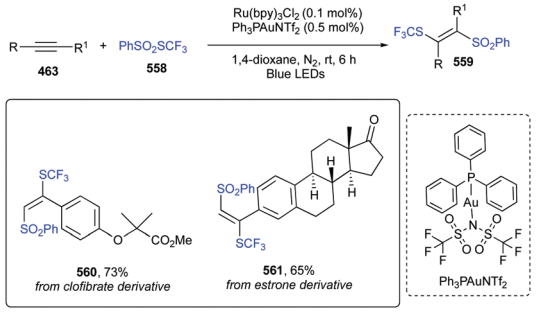

Scheme 103 Synthesis of trifluoromethylthio-functionalized vinylsulfones.

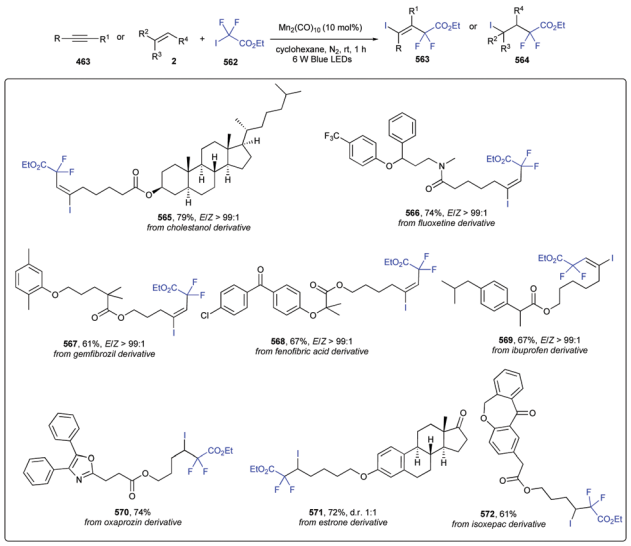

Scheme 104 Iodofluoroalkylation of unactivated alkynes.

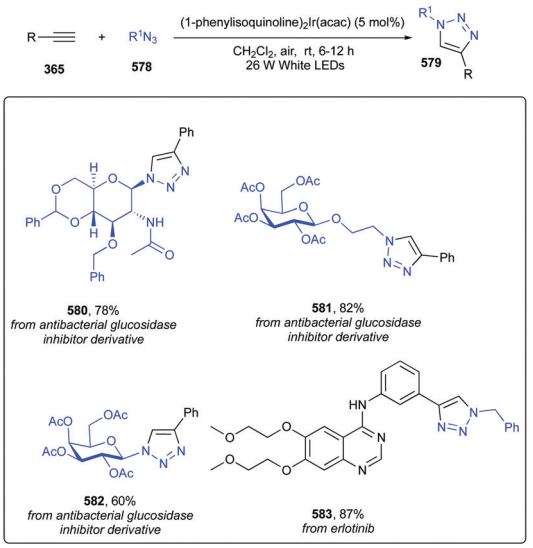

Scheme 106 Azide–alkyne cycloaddition.

abundant and inexpensive manganese catalyst and enabled high efficiency, scalability, and exquisite chemo-, regio-, and *E*/*Z* selectivities. The iodofluoroalkylation was performed in cyclohexane at room temperature for 1 hour and under 6 W blue LEDs irradiation. The wide substrate scope and the high functional group tolerance was demonstrated with a library of more than 40 examples, starting from substrates containing halogens, free-alcohols, ethers, carboxylic acid esters, aldehydes, and boronic esters. The generality of the protocol was further showcased in the LSF of alkyne (or alkene) derivatives of complex bioactive scaffolds such as cholestanol, fluoxetine, gemfibrozil, fenofibric acid, ibuprofen, oxaprozin, isoxepac, and estrone to afford compounds **565–572**, reported in Scheme 104.

2.4.4 Oxidative halogenation. Y. Li *et al.* reported a mild, catalyst-free, synthetic access to dihaloacetophenones (DHAPs) **574** *via* oxidative halogenation of alkynes **573** (Scheme 105).[156] Remarkably, this protocol avoided the need for either corrosive and low compatible molecular halogens or polyamide backbones such as NBS and NCS. Accordingly, either NaBr or LiCl were efficiently exploited as the halogen sources, in the presence of $NaHSO_4{\cdot}H_2O$ in a mixture of MeCN and water as a solvent system under blue LEDs irradiation, air, and at room temperature.

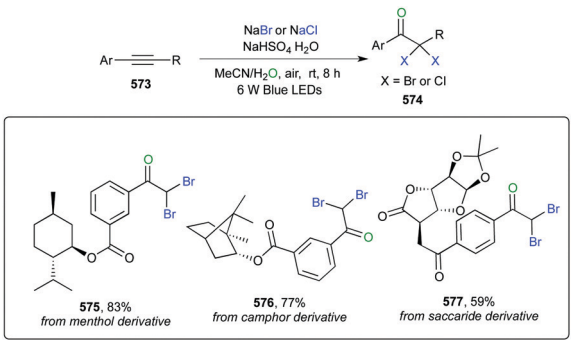

Scheme 105 Synthesis of dihaloacetophenones.

Both terminal and internal, electron-rich and electron-poor alkynes, reacted smoothly under standard conditions affording the corresponding products in good to excellent yields. Functional group tolerance was further tested in the late stage oxyhalogenation of natural compounds such as menthol, camphor, and saccharides (**575–577**, Scheme 105).

2.4.5 Azide–alkyne cycloaddition. Visible light photoredox catalysis provided an efficient and general approach for a highly regioselective azide–alkyne cycloaddition, while avoiding the use of additional reducing agents and ligands as well as cytotoxic copper required by the CuAAC protocol (Scheme 106).[157]

It was recently reported, indeed, the possibility to replace the traditional metal-catalyzed coordination process with a photoredox electron-transfer radical mechanism. Accordingly, by reacting an organic azide (**578**) and a terminal alkyne (**365**) in CH_2Cl_2, in the presence of [$(piq)_2Ir(acac)$] (piq: 1-phenylisoquinoline; acac: acetylacetonate) as the photosensitizer, at room temperature and under irradiation with 26 W white LEDs a wide array of 1,4-triazoles (**579**) were obtained with yields up to 99% and absolute regioselectivity. The transformation was endowed with an excellent atom economy and the possibility of recycling the photocatalyst. The good functional group tolerance was also showcased in the LSF of bioactive molecules and pharmaceuticals such as antibacterial glucosidase inhibitor derivatives converted into compounds **580–582**, and erlotinib into **583** (Scheme 106).

3. Functionalization of arenes

Inter- and intramolecular additions of radicals to aromatic rings are considered useful synthetic transformations to grant access to a large number of structurally diverse molecules.[158] Typically, the reaction mechanism underpinning homolytic aromatic substitutions relied on the addition of an *in situ* generated radical species to the arene, followed by oxidative rearomatization pathways. Photoinduced radical mediated C(sp^2)–H

functionalization protocols offered the great advantage of mild reaction conditions (*e.g.* the exploitation of a photoredox catalyst or a photoactive organic dye under irradiation with low energy photons such as blue LEDs or CFL, and room temperature) with respect to stoichiometric or excess initiators requiring high temperatures. The availability of such experimental methods, together with the advancement in the identification of regioselective approaches, provided unique opportunities to harness radical chemistry for the exploration of a wider chemical space. Accordingly, the following paragraph will focus on progresses in the achievement of regioselective alkylations, arylations, and formation of C(sp^2)-heteroatom bonds, which have been proved enough efficient, mild, and robust to be applicable to the late-stage functionalization of a large number of pharmaceuticals.

3.1 Formation of C(sp^2)–C(sp^3) bonds[159]

3.1.1 *meta*-Selective C(sp^2)–H alkylation. Arenes and heteroarenes (*e.g.* **584**, Scheme 107), when properly functionalized, can be selectively *meta*-alkylated under visible-light irradiation with a dual-function ruthenium cyclometalated complex.[160] The latter, indeed, can act as photoredox catalyst, operating, upon excitation, an outsphere SET to generate alkyl radicals from alkyl iodide precursors (**585**). Additionally, the same metal center can form a ruthenacycle, through its inner coordination sphere, with an endocyclic nitrogen of the arene, thus directing the substitution at the *meta*-position of the aryl ring. This mild protocol required $[RuCl_2(p\text{-cymene})]_2$ as dual metallaphotocatalyst, KOAc, 2Me-THF as solvent, 5 equiv. of H_2O, under blue LEDs irradiation at room temperature, and under a nitrogen atmosphere. Reaction scope of both alkyl iodides and hetero(arenes) was wide, with a good functional group tolerance as shown in the synthesis of the *meta*-alkylated biorelevant purine **587** in an outstanding 90% yield.

3.1.2 Regioselective Nicewicz C(sp^2)–H alkylation. Recently, the group of D. A. Nicewicz developed a transition metal-free protocol to achieve alkylation of arenes (**588**) with moderate to good regioselectivities (Scheme 108).[161] More in detail, an excited-state organic photoredox catalyst was engaged in a SET oxidation of the arene to generate an arene cation radical, which underwent polar nucleophilic addition of ethyl diazoacetate **588** to form a distonic radical cation. Subsequent reduction to norcaradiene was followed by a SET event triggering the ring opening along with the formation of a distonic benzylic radical cation. Further SET reduction and deprotonation provided the rearomatization of product **590**. Experimentally, the reaction

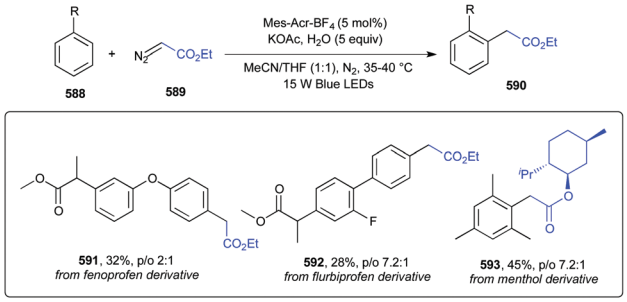

Scheme 108 Regioselective alkylation of (hetero)arenes.

proceeded in the presence of Mes-Acr$^+$BF4$^-$ as the organic photocatalyst, in a 1:1 mixture of MeCN:TFE under irradiation with 465 nm LEDs at room temperature. The substrate scope was investigated with a wide range of simple arenes, anisole derivatives, as well as heterocycles and pharmaceutical scaffolds including fenoprofen methyl ester, flurbiprofen methyl ester, and a menthol-derived diazo-compound (**591–593**, Scheme 108).

3.1.3 Trifluoromethylation. Trifluoromethylation of non-activated arenes **588** and heteroarenes **594** and **595** by means of photoredox catalysis was pioneered by D. A. Nagib and D. W. C. MacMillan in 2011 (Scheme 109).[162] As convenient trifluoromethyl radical source ($^\bullet CF_3$), the authors capitalized on the ability of trifluoromethanesulphonyl chloride **108** (triflyl chloride, TfCl), to undergo, after reduction to radical anion, a fragmentation entropically driven by the release of SO_2 and Cl^-. $Ru(phen)_3Cl_2$ was used as the photocatalyst, K_2HPO_4 as a base, MeCN as the solvent, and a household 26 W fluorescent light was an effective photon source. A wide number of mono- and di-functionalized arenes, along with five-, six-membered, and benzo-fused heterocycles smoothly underwent trifluoromethylation under standard reaction conditions. Uracil and vitamin P underwent selective functionalization, while ibuprofen, lidocaine and Lipitor afforded a mixture of regioisomers (**599–603**, Scheme 109).

A continuous-flow protocol for the trifluoromethylation of both arenes and heteroarenes was developed by I. Abdiaj *et al.*[163] To this end, the solid and bench-stable sodium trifluoromethanesulfinate (**245**, CF_3SO_2Na; Langlois' reagent) was used as the trifluoro-methylating agent and an iridium complex as the photocatalyst (Scheme 110). Residence time was set within 30 minutes, and $(NH_4)_2S_2O_8$ was also essential as an oxidant. A number of (hetero)aromatics was efficiently trifluoromethylated,

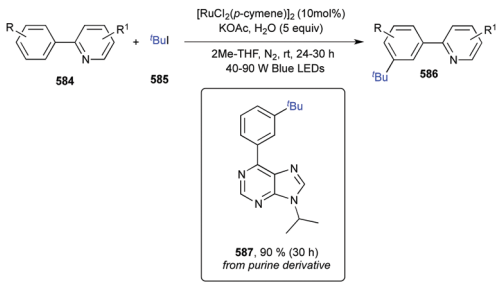

Scheme 107 *meta*-Selective C(sp^2)–H alkylation of arenes.

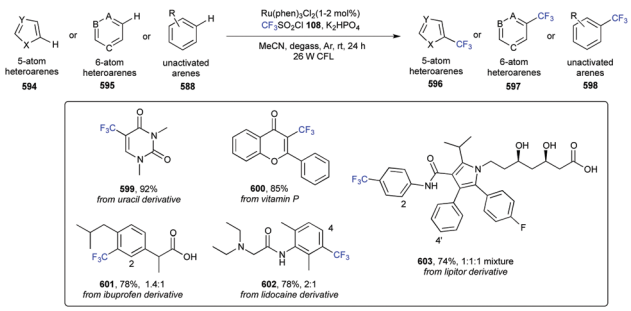

Scheme 109 Trifluoromethylation of non-activated arenes.

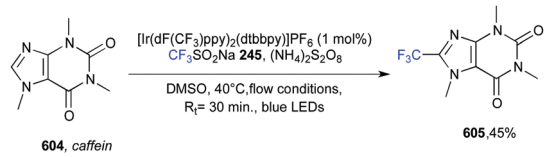

Scheme 110 Trifluoromethylation of (hetero)arenes.

with good functional group tolerance as for example with bromo-, chloro-, and iodo-containing substrates. The sole example of biorelevant scaffold was caffeine **604**, which was regioselectively converted into its C8 trifluoromethyl derivative **605** with a medium 45% yield.

Nevertheless, other efficient protocols to achieve trifluoromethylation of arenes and heteroarenes (**595**) are available in literature. In 2015 J. W. Beatty *et al.*[164] employed trifluoroacetic anhydride as a CF_3 source in the presence of pyridine *N*-oxide **606** and a ruthenium photocatalyst (Scheme 111A). Notably, trifluoromethylation of caffeine was performed on a multigram scale and achieved in a good 54% yield. Later, Y. Ouyang *et al.* exploited trifluoromethanesulfonic anhydride as a low-cost trifluoromethylation agent, under ruthenium-based photoredox catalytic conditions (Scheme 111B).[165] Site-selective functionalization of pentoxyphilline as reported by the authors is shown in Scheme 111B. Alternatively, J. Lin *et al.* developed a photo-driven catalytic process harnessing trifluoroacetic acid as CF_3 source, in the presence of $Na_2S_2O_8$ as an oxidant and Rh-modified TiO_2 nanoparticles as a photocatalyst (Scheme 111C). This protocol was applied to 4 different xanthines, achieving good yields also on a gram scale.[166]

Trifluoromethylation of (hetero)arenes could also be accomplished by using dye-incorporated coordination polymers, such as Zn-TCTA (Scheme 112).[167]

The latter was indeed composed by large π-systems of thiophene-substituted triphenylamine. Importantly, the substrates could be docked near the photoredox-active centers, thus achieving regio- and diastereoselectivity. Optimized reaction conditions employed Zn-TCTA as the photocatalyst, CF_3SO_2Cl

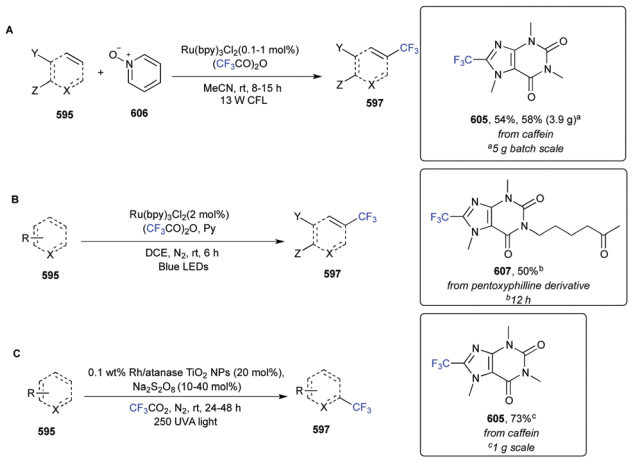

Scheme 111 Trifluoromethylation of (hetero)arenes.

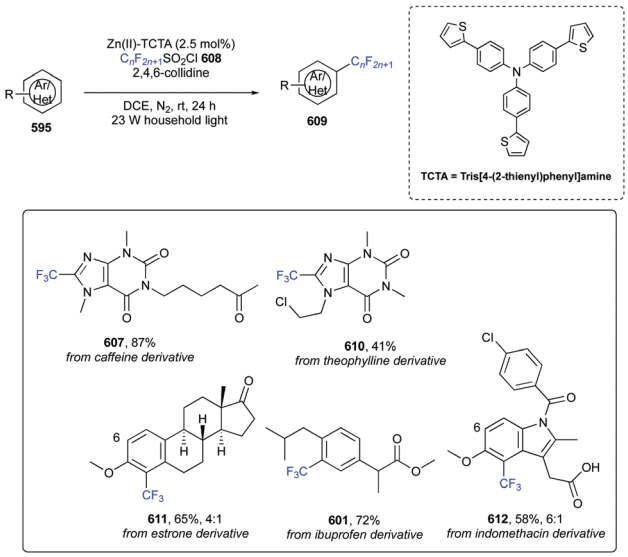

Scheme 112 Trifluoromethylation of (hetero)arenes.

(or perfluoroalkyl analogues **608**) as the CF_3 source, 2,4,6-collidine as a base in MeCN and under 23 W household light irradiation at room temperature. Late stage trifluoromethylation of pentoxyphylline, theophylline, methylestrone, ibuprofen, and indomethacin was accomplished in good yields and with moderate to exclusive regioselectivities (**601**, **607**, **610–612**, Scheme 112).

More or less at the same time, Y. Huang *et al.* reported a mild protocol to access trifluoromethylated and perfluoroalkylated uracils, cytosins, and pyridines (*e.g.* **615**, Scheme 113).[168] This metal-free strategy required trifluoromethyl iodide or perfluoroalkyl iodides, in the presence of Cs_2CO_3 as a base in DMSO as a solvent, and under 12 W blue LEDs irradiation at room temperature for 12 hours. This exceptionally mild protocol showed to be robust and successfully promoted the conversion of a number of functionalized substrates. A selected example is shown in Scheme 113; its synthesis was also performed on a 10 grams scale, with retention of a good yield.

Recently, the group of L. Ackermann reported an electrophotocatalytic approach to achieve (hetero)arenes C(sp^2)–H trifluoromethylation with the Langlois' reagent CF_3CO_2Na **245** (Scheme 114).[169] The synergic combination of electrosynthesis and photoredox catalysis enabled the generation of a CF_3 radical species without requiring external chemical oxidants, thus providing mild reaction conditions along with a wide scope. Optimum yields were obtained by using an undivided cell with a

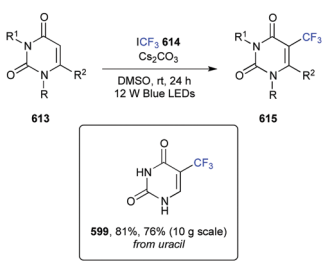

Scheme 113 Trifluoromethylation of (hetero)arenes.

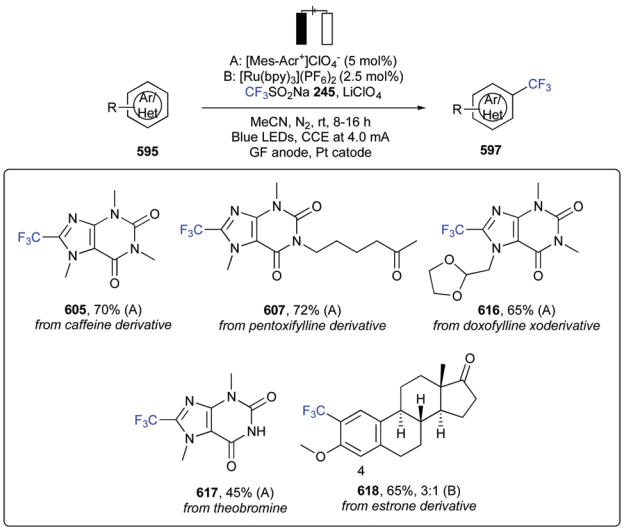

Scheme 114 Trifluoromethylation of (hetero)arenes.

platinum plate cathode and a graphite felt (GF) anode (constant current (CCE) = 4.0 mA), either Mes-Acr^{+}ClO4^{-} or $[Ru(bpy)_3]PF_6$ as a photocatalyst, $LiClO_4$ as additive, and KOAc as a conductive additive in MeCN at room temperature under blue LEDs irradiation. Both arenes and heteroarenes, bearing a range of functional groups, proved to be competent substrates and the robustness of the electrophotocatalytic protocol was shown also in the functionalization of complex biorelevant substrates such as caffeine, pentoxifylline, doxofylline, theobromine, and methyl estrone into the corresponding trifluoromethyl analogues (**605**, **607**, **616–618**, Scheme 114). Additionally, a modular electro-flow-cell equipped with an *in operando* monitoring unit for on-line flow-NMR spectroscopy enabled in-flow trifluoromethylation while providing experimental evidence for the SET events underpinning the reaction mechanism.

3.1.4 Difluoroacetimidation. Unactivated arenes and heteroarenes **595** could undergo difluoroacetimidation by using readily available bromodifluoroacetamides (*e.g.* **619**) under visible light photocatalytic conditions (Scheme 115).[170] In order to achieve optimum yields, the reaction required *fac*-Ir(ppy)$_3$ as a photocatalyst, KOAc as an additive, a 3 W blue LEDs source, in CH_2Cl_2 at room temperature. A wide range of (hetero)arenes showed good to excellent reactivities together with exquisite functional group tolerance including halogens, cyano, aldehyde, ethers, and

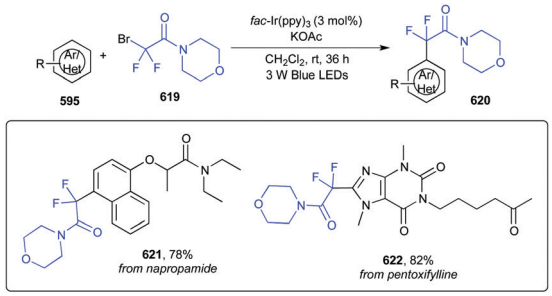

Scheme 115 Difluoromethylation of (hetero)arenes.

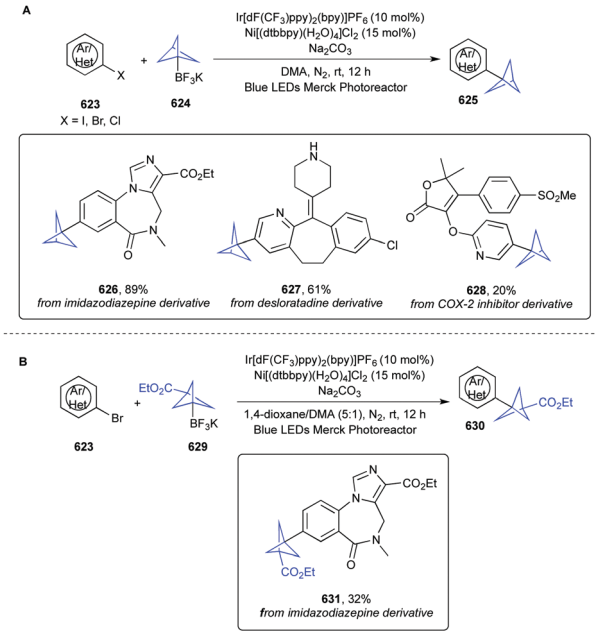

Scheme 116 Difluoromethylation of (hetero)arenes.

amides. Late-stage difluoroacetimidation of napropamide and pentoxifylline was achieved in 78 and 82% yield, respectively (**621** and **622**, Scheme 115).

3.1.5 Introduction of a bicyclo[1.1.1]pentane moiety. Bench-stable bicyclo[1.1.1]pentane trifluoroborate salts (**624** Scheme 116, BCP, BF_3K) were synthesized on a 200 gram scale *via* continuous flow methodology and used in a dual photoredox-nickel catalyzed strategy with aryl and heteroaryl bromides (**623**).[171] This structural motif has gained increasing popularity as *para*-substituted aryl bioisoster in medicinal chemistry thanks to its ability to modulate physicochemical properties and improve pharmacokinetic issues. Actually, it is able to confer increased solubility, permeability, and decreased lipophilicity due to its sp^3 character. The authors applied metallaphotoredox conditions, exploiting Ir[(dF(CF$_3$)ppy)$_2$(bpy)]PF$_6$ as the photocatalyst, Ni[(dtbbpy)(H$_2$O)$_4$]Cl$_2$, Na_2CO_3, in DMA as solvent under blue LEDs irradiation. These reaction conditions were then applied to biorelevant complex substrates in microscale high-throughput experimentation (HTE), where formation of the cross-coupled adducts was observed in 13 out of 18 wells, with a good functional group tolerance. A subset of successful substrates (**626–628**, Scheme 116A) was then scaled up, and the corresponding products were isolated in modest to excellent yields. Ethyl ester BCP **629** was also conveniently installed onto imidazenil modifying the solvent to a 5 : 1 mixture of dioxane:DMA (**631**, Scheme 116).

3.2 Formation of C(sp^2)–C(sp^2) bonds

3.2.1 Benzodiazepine arylation. Privileged 5-phenyl-1,4-benzodiazepine scaffolds **632** were able to react under both palladium- and visible-light catalysis with aryldiazonium salts (**492**) to give *ortho*-arylation on the 5-phenyl-ring (Scheme 117).[172] DFT studies suggested that the palladium/ruthenium photocatalyzed

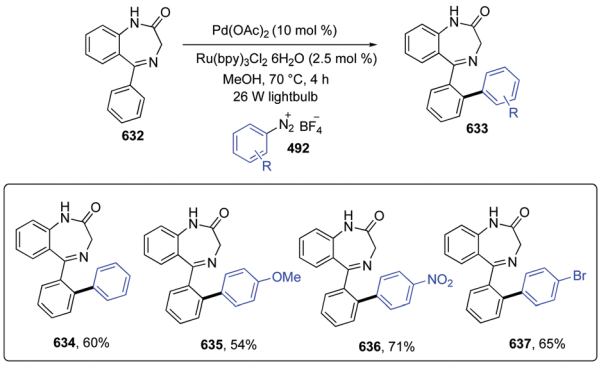

Scheme 117 Benzodiazepine arylation.

mechanism involved a low-energy SET pathway avoiding the high-energy oxidative addition occurring when the reaction was catalyzed by palladium only. As the reaction proceeded in methanol at reflux temperature, when 2- or 4-fluorobenzenediazonium salts were used, both fluoroaryl- and methoxyaryl-adducts were obtained, as resulting from a S_NAr on the fluorobenzene-ring ("nuisance effect"). Three examples with electron-donor (**635**), and electron-withdrawing substituents (**636** and **637**) are reported in Scheme 117.

3.2.2 Perfluoroarylation. Direct arylation of simple arenes with fluorinated aryl bromide **638** under visible-light eosin Y catalysis was reported by A. U. Meyer *et al.* (Scheme 118).[173] The authors reported 17 examples with yields up to 99% and a wide scope in both fluorinated compounds and arenes. From a mechanistic point of view, photoreduction of eosin Y *via* its triplet state by triethylamine afforded eosin Y radical anion, which reduced, *via* a SET event the polyfluorinated bromoarene. The latter then fragmented to polyfluorinated aryl radical and a bromide anion. Addition of the aryl radical to the arene, followed by loss of one electron and a proton gave the final perfluorobiaryl derivatives. The mild reaction conditions enabled the functionalization of the alkaloid brucine **639** in a very good 71% yield without the need for protecting groups (**640**, Scheme 118).

3.2.3 Azolylation. C(sp^2)–H heteroarylation of arenes and heteroarenes **595** could be accomplished by exploiting 2-azolyl radicals' reactivity, generated from 2-bromoazoles **641** (Scheme 119).[174,175] Optimal reaction conditions were verified as the following ones: *fac*-Ir(ppy)$_3$, K_2CO_3, MeCN as the solvent, 30 °C, blue LEDs irradiation under Argon. The use of a bulky and poorly soluble *N*-cyclohexyl-*N*-isobutyl-*N*-cyclohexanamine was essential to induce a reductive quenching cycle of the photocatalyst avoiding undesired reduction of the starting bromoazole to azole *via* a hydrogen atom transfer. The reaction showed broad scope, a good functional group tolerance, and anti-Minisci selectivity. Late-stage azolylation of commercially

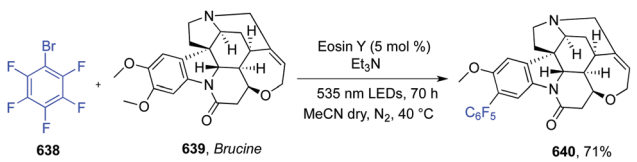

Scheme 118 Perfluoroarylation of arenes.

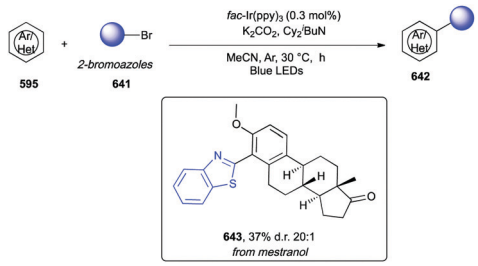

Scheme 119 Azolylation of arenes.

available methylestrone, where carbonyl modification led to an FDA approved oral contraceptive (mestranol), was also reported (**643**, Scheme 119).

3.2.4 Synthesis of (hetero)biaryls. D. J. Procter and coworkers disclosed a photocatalytic selective C–H arylation protocol that did not require prefunctionalized arene partners (Scheme 120).[176]

Amazingly, the method exploited an interrupted Pummerer activation of the arene C(sp^2)–H bond, where the pairing of the organic photoredox catalyst, *i.e.* 10-phenylphenothiazine (PTH), and the intermediate dibenzothiophenium salts enabled a highly chemoselective reduction to form aryl radical species. Ensuing, coupling with an arene trap and SET oxidation eventually led to the aryl–aryl coupling product. Optimization studies led to a one-pot/two-step procedure featuring the use of a dibenzothiophenium salt (DBTSO), triflic anhydride in CH_2Cl_2 at −78 °C to −40 °C for 2 hours, followed by addition of PTH, a trapping agent, in DMSO under blue LEDs irradiation for 18 hours at room temperature. The arene scope embodied a wide array of functionalized inputs, bearing functional groups such as sulfonyl, sulfonamides, halogens, ethers, amides, tertiary aromatic amines, and cyano-. As radical traps diverse pyrroles, furans, thiazoles, pyridines, pyrazines, indoles, benzofurans, and arenes proved to be competent reagents, albeit they were required in 20 equivalent amounts. Application of the protocol to the LSF of pharmaceutical agents fenofibrate, clofibrate, salicilin pentaacetate, boscalid, and *N*-acetylmexiletine led to derivatives **646–650** in medium to good yields (Scheme 120).

3.2.5 Diazomethylation. Carbynes, as monovalent carbons with three non-bonded electrons, enjoy a unique reactivity, as they are characterized by the innate ability to form three new covalent bonds sequentially. Recently, Z. Wang *et al.* showed that diazomethyl radicals can be used as direct equivalents of carbyne species under visible-light irradiation, inducing site-selective C(sp^2)–H cleavage in aromatic rings and so enabling useful arenes diazomethylation, underpinning divergent LSF of bioactive agents (Scheme 121).[177]

Key for an efficient generation of diazomethyl radical was the design of a suitable precursor, with an appropriate redox-active leaving group. To this end, a new bench-stable benziodoxolone and its pseudo-cyclic analogue **651** were prepared and tested for their ability to generate the substituted diazomethyl radical $N_2{=}C(\cdot)$–CO_2Et upon catalytic photoredox activation. Best results were identified by combining **651**, sodium bicarbonate as base, MeCN as solvent, and [Ru(bpy)$_3$(PF$_6$)$_2$] as the photocatalyst (Scheme 121, top side). These conditions were successfully

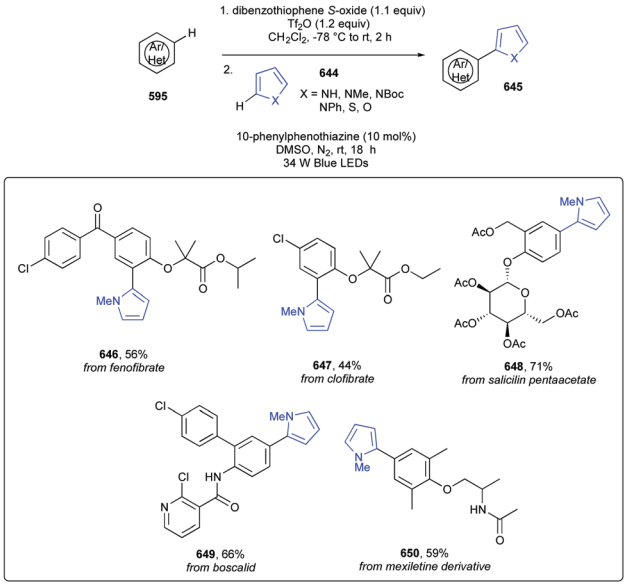

Scheme 120 Synthesis of (hetero)biaryls.

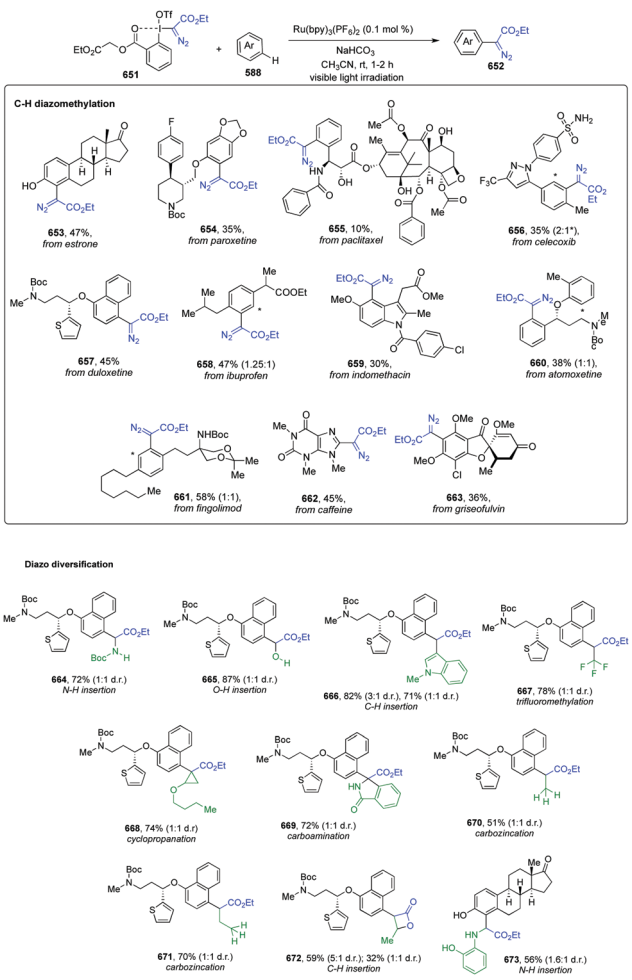

Scheme 121 Diazomethylation and diazodiversification of (hetero)arenes.

applied to a wide range of arenes unsubstituted or decorated with a variety of functional groups, including sterically congested substrates. Di-substituted aromatics preferably reacted at their electron-rich sites; and mono-substituted arenes afforded selectively *ortho*-diazomethylated derivatives. Additionally, five- and six-membered heterocycles also proved to be suitable starting materials. As for the hypervalent iodine reagents, besides ester functional groups, sulfonates, phosphonates, and trifluoromethyl groups can be efficiently transferred. A selection of biorelevant compounds including imatinib and paclitaxel (anticancer), duloxetine and paroxetine (antidepressant), celecoxib, ibuprofen and indomethacin (NSAIDs), atomoxetine (attention deficit hyperactivity disorder-ADHD), griseofulvin (antifungal), and fingolimod (treatment of multiple sclerosis) successfully afforded the corresponding diazomethylated drugs (**653–663**, Scheme 121). Diazo-compounds diversification for duloxetine derivative **657** was also reported, thus highlighting the valuable potential of these synthetic intermediates (Scheme 121, bottom side).

3.3 Formation of C(sp^2)–C(sp) bonds

3.3.1 Cyanation. A direct and metal-free C(sp^2)–H cyanation of arenes *via* organic photoredox catalysis was reported by J. B. McManus *et al.*[178] Aromatic nitriles' synthesis was accomplished by using an acridinium photoredox catalyst **674** (Scheme 122) and trimethylsilyl cyanide (**260**, TMSCN), as inexpensive cyanide source, a 10 : 1 MeCN/pH 9 buffer solvent system, under an aerobic atmosphere and blue LEDs irradiation at room temperature for 24 h.

The reaction was compatible with a variety of electron-donating and electron-withdrawing groups including halogens as well as with nitrogen- and oxygen containing heterocycles. In a good number of cases, cyanation exhibited an exclusive regioselectivity, while substrates such as 3,5-dimethylanisole, 2-allyloxyanisole, 1,3-dimethoxybenzene and heterocyclic *N*-methylindazole gave a mixture of cyanide products. Reaction conditions were successfully applied also to convert complex bioactive scaffolds; as examples naproxen, gemfibrozil, *N*-Boc-melatonin, and fenoprofen smoothly afforded single cyanide regioisomers in good yields (**676–679**, Scheme 122).

3.4 Formation of C(sp^2)–X bonds

3.4.1 Amination. In 2014, the group of M. S. Sanford described the use of *N*-acyloxyphthalimides **680** as precursors

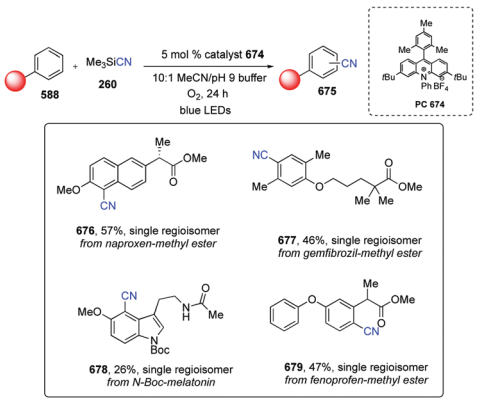

Scheme 122 Cyanation of (hetero)arenes.

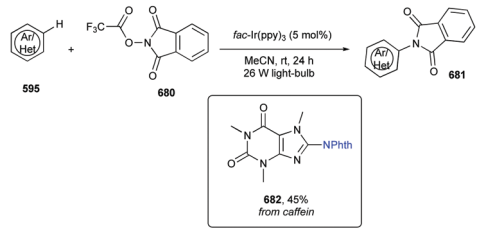

Scheme 123 Amination of (hetero)arenes.

to nitrogen-based radical intermediates in a visible light photocatalyzed amination of arenes and heteroarenes (Scheme 123).[179] The reaction proceeded in the presence of *fac*-Ir(ppy)$_3$, in MeCN as a solvent, at room temperature. The use of *N*-acyloxyphthalimides **680** as versatile reagents, readily prepared from *N*-hydroxyphthalimide and carboxylic acids, has kept growing thanks to their ability to undergo a photocatalyzed SET reduction, followed by a decarboxylative fragmentation to release CO_2, a radical intermediate $^{\bullet}$R, and phthalimide anion. Interestingly, in this seminal paper, the authors showed that the use of more electron-withdrawing R substituents would favor the release of RCO_2^- with the concomitant formation of a PhthN$^{\bullet}$. The latter was then able to provide C–H amination of a range of arenes and heteroarenes, tolerating functional groups such as halogens, methyl-, and ethers. Regioselective amination of caffeine into derivative **682** was carried out in 45% as shown in Scheme 123.

The first report about site-selective amination of aromatics and heteroaromatics by using an organic photoredox catalytic system, along with nitroxyl radicals as co-catalysts, was dated back to 2015 (Scheme 124).[180] In contrast to the Buchwald–Hartwig and Chan–Lam aminations, this strategy avoided the need for pre-functionalization of the substrate as halide, triflate, or boronic acid. Here, the amine **683** formed a σ-adduct with an arene cation radical intermediate **685**, generated upon SET oxidation from an excited-state photocatalyst (Scheme 124); subsequent deprotonation of distonic cation radical **686** and oxidative aromatization of **687** led to aminated arene **684**. Optimized reaction conditions involved the use of 9-mesityl-3,6-di-*tert*-butyl-10-phenylacridinium tetrafluoroborate (**PC1**) as the organic photocatalyst, immobilized TEMPO on polystyrene, DCE as solvent, and blue LEDs irradiation at 33 °C for 20–72 h under air. Site-selective coupling of pyrazole with a variety of functionalized aromatics and heteroaromatics proved the wide scope of the direct amination protocol. As examples of biorelevant complex scaffolds *O*-acetylcapsaicin, naproxen methyl ester, and dihydroquinidine trifluoroacetic acid (DHQD·TFA) were successfully derivatized with pyrazole (**688–690**, Scheme 124), while di-Boc-protected adenine was arylated (**691**, Scheme 124).

An intriguing photoelectrocatalytic method for C(sp^2)–H amination was reported by L. Zhang *et al.* (Scheme 125).[181]

Here the authors exploited photoelectrochemical cells (PECs), usually studied for the conversion of solar energy into chemical fuels, to develop a wide-in-scope methodology for the synthesis of aromatic nitrogen-containing compounds. More in detail, haematite (α-Fe_2O_3), an earth-abundant and robust photoanode was able to generate, upon irradiation, holes, which allowed oxidation of electron-rich arenes (**595**) to radical cations. These latter further reacted with pyrazole **692** to give nitrogen heterocycles (**693**). Interestingly, unusual *ortho*-selectivity was observed, probably due to a hydrogen-bond between the substrate and the hexafluoroisopropanol co-solvent. Moreover, the heterogenous nature of the photoelectrocatalyst allowed longer catalyst lifetime, easier product isolation, and less energy consumption thanks to light harvesting. As examples of drug scaffolds, clofibrate, metaxalone, and benzethonium chloride were converted into their pyrazole derivatives **694–697** (Scheme 125).

The scope of the above reported direct aryl C(sp^2)–H amination methods was then further expanded to primary aliphatic amines as coupling partners with aromatic ethers **698**, by K. A. Margrey *et al.* (Scheme 126).[182]

The mechanistic approach always relied on the excited-photocatalyst mediated oxidation of arenes through a SET event generating the corresponding cation radicals, which were able to act as electrophiles for nitrogen nucleophiles. In particular, aryl amination was accomplished by using Me_2-Mes-Acr$^+$ under

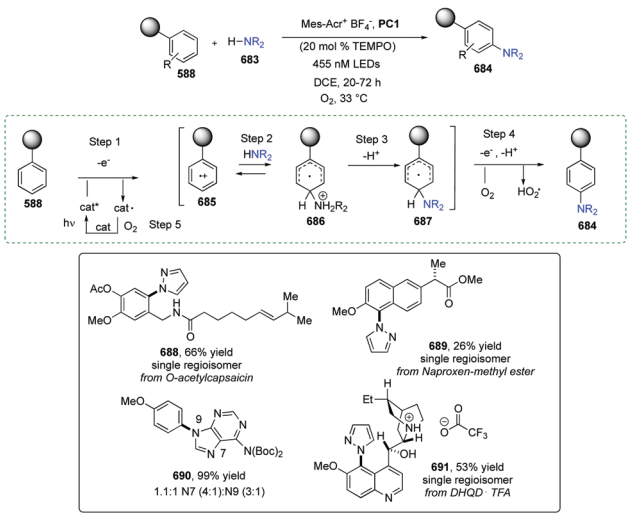

Scheme 124 Amination of (hetero)arenes.

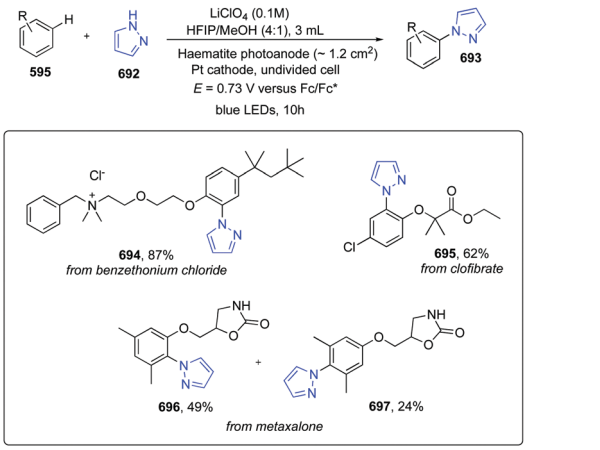

Scheme 125 Amination of (hetero)arenes.

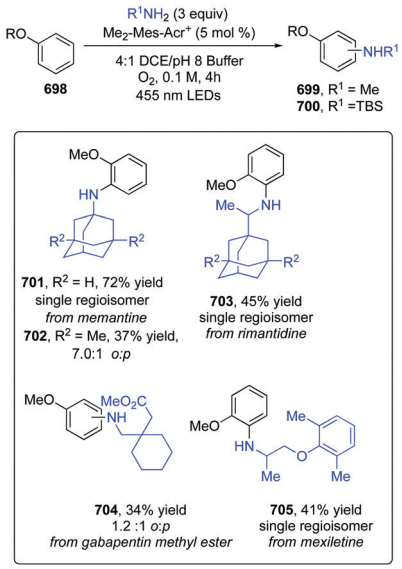

Scheme 126 Amination of (hetero)arenes.

blue LEDs irradiation, and DCE or a mixture of DCE and pH 8 phosphate buffer (if amine hydrochloride salts were employed) as solvent. With anisole as the starting arene, a mixture of *ortho*- and *para*-regioisomers were obtained. Nevertheless, amino acid esters, linear aliphatic amines, bulk amines such as *tert*-butyl amine, halogenated amines, allylamine, benzylamine derivatives, including chiral ones, proved all to be suitable substrates. The scope of pharmaceutically relevant complex amines included adamantylamine and memantine, anti-Parkinson and anti-Alzheimer drugs, respectively; the antiviral rimantadine, gapentin methyl ester, and mexiletine (**701–705**, Scheme 126). As for the arene coupling partner, the regioselectivity of the amination could be altered depending on the substitution pattern on the phenolic ether: more steric encumbered aliphatic (Me, Et, *t*Bu) and silyl-protected (TES, TBS, TBDPS) phenolic ethers led to higher amounts of the *para*-isomer. With halogens on the aromatic ring, a substoichiometric amount of TEMPO was required, and the major product resulted from an *ortho*-addition with respect to the methoxy substituent. In general, 1,2-, 1,3- and 1,4-disubstituted arenes reacted efficiently, and when an additional ring was present, the functionalization only occurred on the more-electron-rich ring. Examples of heterocycles such as 2,6-dimethoxypyridine, *N*-methylindazole, and 7-bromo-*N*-methylindazole all gave single regioisomers. As examples of complex biorelevant arenes the NSAID fenoprofen, gemfibrozil, clofibrate, and bezafibrate were successfully aminated with *tert*-leucine methyl ester or valine methyl ester.

Based on these findings, the same group, reported a predictive model for site-selective aryl and heteroaryl C(sp^2)–H functionalization protocol using electron density calculations.[183] The site selectivity was efficiently predicted for a number of aromatic and heteroaromatic systems commonly present in biologically active compounds, further extending the potential applications of this synthetic methodology for late-stage functionalization. The authors developed a computational model able to predict both reactivity and regioselectivity by considering some innate factors of the aromatic systems such as the redox potentials, the electrophilicity, the electron-density, the representation (*i.e.* delocalized or localized distonic alkene cation radical) of the intermediate aryl cation radical after a SET oxidation from the photocatalyst, and the electronic nature and the position of substituents. These parameters were computationally investigated and compared with experimental data for a wide number of aromatic scaffolds, which were grouped into two main classes: (i) six-membered aromatics such as benzenoids, pyridines and quinolines and (ii) aromatics with at least one five-membered heteroaromatic ring or aromatic bicyclic [4.3.0] core. As general guidelines, for the first group, the site of functionalization matched E_AS selectivity, whereas, for the second category including pyrazoles, indazoles, bridging-nitrogen polyaromatics, benzofurans, indoles and benzazoles, the site of functionalization matched where iminium or oxocarbenium radical character predominated. Remarkably, as several classes of aromatic heterocycles were too electron-deficient and could not be oxidized by the acridinium catalyst, being so unreactive under the developed conditions, selective functionalization of more electron-rich heteroaromatics could be possible (for a flowchart further illustrating general selectivities for heterocycles grouped by class see Fig. 1).

A regioselective amination of arenes using alkyl amines was reported by Leonori's group *via in situ* formation of *N*-chloramines from both primary and secondary aliphatic amines (Scheme 127).[184]

The presence of Brønsted acid afforded protonated *N*-chloramines, well-known strong electrophiles in Friedel–Crafts reactions with aromatics. Nevertheless, key to the success of this strategy, is their diverse reactivity as precursors of aminium radicals, able to undergo highly polarized addition to aromatics. The presence of a Brønsted acid was also essential to the transformation, due to its dual role of activating the *N*-chloroamine and avoiding both undesired aniline over-amination and oxidation. A broad range of functional groups was shown to be compatible with standard reaction conditions, and multigram scale was possible *via* a batch-to-flow protocol. Several structurally complex drugs were successfully aminated, underpinning the application of this methodology as a tool for LSF of pharmaceuticals. Strychnine, fenopren dichloroprop, ramipril, and donezepil, among others were indeed converted into **706–712** (Scheme 127A) with good yields and in some cases as single regioisomers. Functionalization of

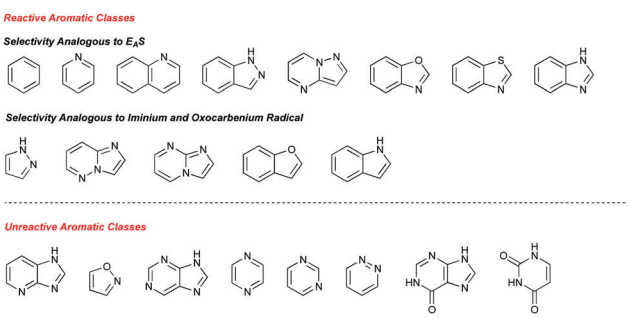

Fig. 1 Predictability for site-selective aryl and heteroaryl C(sp^2)–H functionalization.

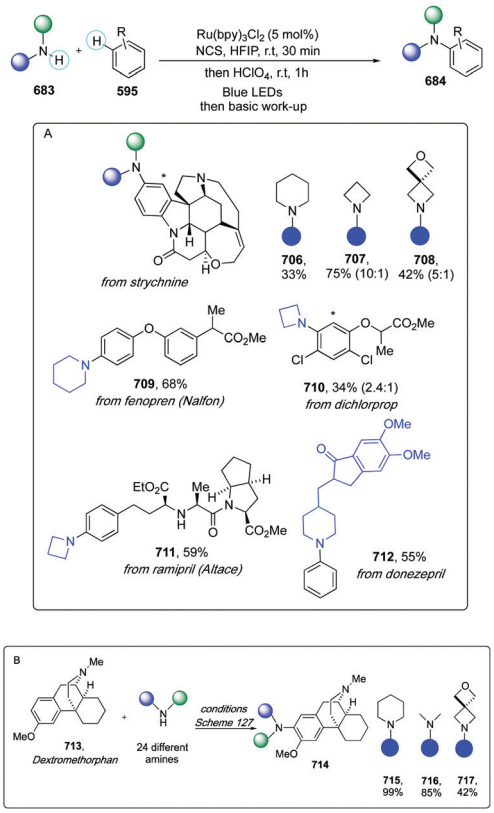

Scheme 127 Amination of (hetero)arenes.

dextromethorphan **713** with 24 different amines was performed in a 24-well parallel photoredox reactor (Scheme 127B).

Site-selective C(sp^2)–N bond formation could also be achieved *via* arenes pre-functionalization as aryl thianthrenium salts **718** (Scheme 128) and reaction of the latter with *N*-nucleophiles as reported by P. S. Engl.[185] Aryl thrianthrenium salts **718** were readily obtained through reaction of simple arenes **595** with commercially available tetrafluorothianthrene-*S*-oxide or thianthrene-*S*-oxide. The authors elaborated two Pd-catalyzed methods enabling C–N cross-couplings with cyclic and acyclic secondary amines, and with aryl amines, amides, carbamates, and ureas. However, primary amines and *N*-heterocylces required a photoredox method in combination with Cu(I).

The robustness of the reaction scope was proved with a range of pharmaceutically representative compounds such as rivaroxaban, etofenprox, pyriproxyfen, nefiracetam, estrone, linezolid, fenubrufen, indomethacin (**720–727**, Scheme 128A) and flurbiprofen (**730–733**, Scheme 128B).

Introduction of a pyridinium ring onto arenes and heteroarenes was reported by S. L. Rossler *et al.* by using *N*-substituted pyridinium reagents **734** as precursors of *N*-pyridyl radical cations (Scheme 129).[186] Interestingly, the *N*-aryl pyridinium adducts enabled divergent access to anilines, dihydropyridines, and substituted piperidines. Optimal reaction conditions were identified as the following: $[Ru(bpy)_3](PF_6)_2$ in anhydrous MeCN, under blue LEDs irradiation for 90 minutes. The reaction was not always regioselective, affording mixtures of pyridinium adducts. As example of complex bioactive scaffold, the fungicide Metalaxyl

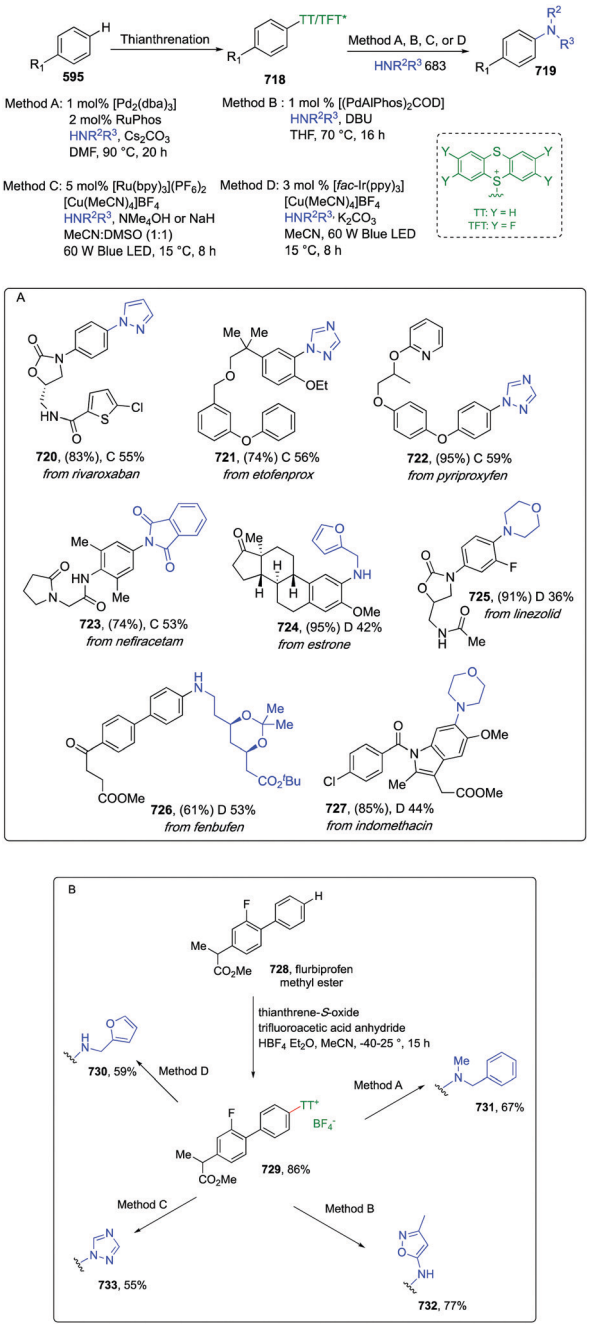

Scheme 128 Amination of (hetero)arenes *via* thianthrenium salts.

was converted into derivative **736** with medium yields and a 2.2 : 1 *meta*-/*para*-regioselectivity (Scheme 129).

An intramolecular C(sp^2)–H amination of azidoformates (**736**) to afford benzoxazolone derivatives (**737**) under iridium-based photoredox catalysis was reported by Y. Zhang and coworkers (Scheme 130).[187]

The reaction exhibited a good chemoselectivity, with C(sp^2)–H amination favored over C(sp^3)–H amination. When azidoformates were *ortho*-functionalized with an allyl-group, [5.1.0] bicyclic aziridines were obtained. From a mechanistic point of view, azidoformates acted as triplet nitrene precursors: upon triplet energy transfer from the excited photocatalyst a triplet

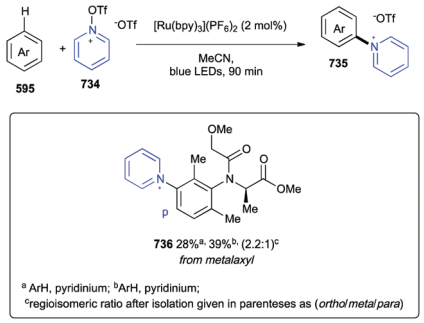

Scheme 129 Formation of pyridinium salts.

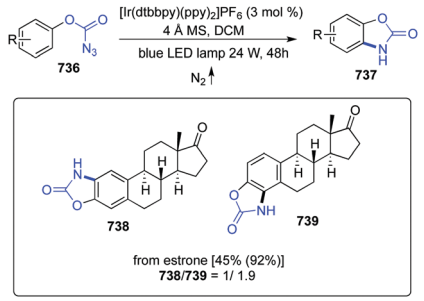

Scheme 130 Formation of benzoxazolone derivatives.

azide was formed, which readily decomposed with loss of N_2. A subsequent intramolecular radical addition, along with 1,2-hydrogen atom transfer and rearomatization led to benzoxazole adducts. The protocol was characterized by mild conditions, as no additional oxidants or reductants are required, and high atom economy, with nitrogen as the sole byproduct. Benzoxazolone estrone derivatives **738** and **739** were obtained in good yield, albeit in a moderate conversion (Scheme 130).

3.4.2 Trifluoromethoxylation and perfluoroalkoxylation (OR_F). Trifluoromethylation of a wide range of arene substrates **588** was reported by B. J. Jelier *et al.* exploiting a pyridinium-based trifluoromethoxylation reagent **740** as a bench-stable precursor of an OCF_3 radical (Scheme 131)[188] (for a recent review about visible light promoted tri- and di-fluoromethoxylated see M. Ngai *et al.*[189]). A ruthenium-based photoredox catalyst, upon visible-light excitation, was indeed able to undergo an oxidative quenching cycle, giving SET reduction of the pyridinium cation, which readily fragmented to afford the *O*-centered radical. The process was driven by the elimination of a thermodynamically favored neutral pyridine. After the addition of the trifluoromethoxyl radical to the arene, the catalytic cycle was closed by oxidation and deprotonation to give the trifluoromethoxylated products. Reaction scope was wide, and exquisite functional group tolerance was demonstrated with arenes bearing a wide variety of substituents, including halides, nitriles, ketones, aldehydes, benzyls, amides, acids, sulfonamides, imides, esters, boronic esters, and phosphonates. LSF of the breast cancer drug Femara®, the fungicide metalaxyl, phenytoin, a reference drug in the treatment of seizures, and procymidone, a fruit fungicide, were converted into derivatives **742–746** (Scheme 131) albeit in low to moderate yields and for **745** and **746** in low regioselectivity.

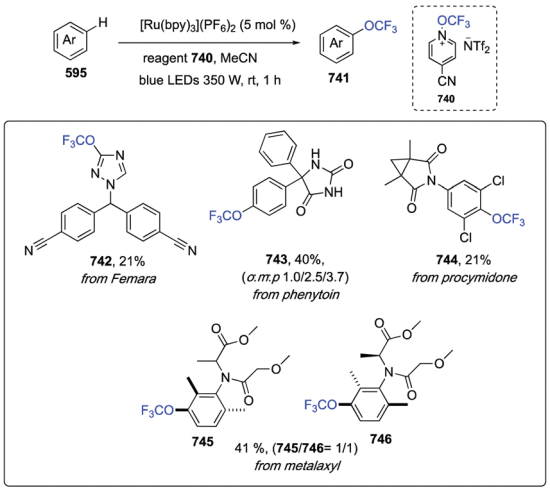

Scheme 131 Trifluoromethoxylation of arenes.

At the same time, W. Zheng *et al.* developed a similar strategy, but that differed by designing and developing a redox-active cationic reagent (benzotriazolium salts **747** and **748**, Scheme 132) enabling the controllable and selective formation of the OCF_3 radical under visible light photocatalytic conditions.[190]

Opposite to the previous protocol, where a minor pathway produced about 15% of undesired arene pyridination products, due to competing formation of a pyridinium radical cation, here exclusive formation of OCF_3 radical species occurred, thus resulting in any formation of *N*-arylated side products.

The generality of this procedure, as shown in Scheme 132, were also tested on complex substrates such as *trans*-androsterone, metronidazole, chlorpropamide, L-menthol, and baclofen to synthesize derivatives **749–753**. Alternatively, a benzimidazole-based OCF_3 reagent **748** (Scheme 132) was developed shortly before by the same group and used under very similar reaction conditions.[191] In this

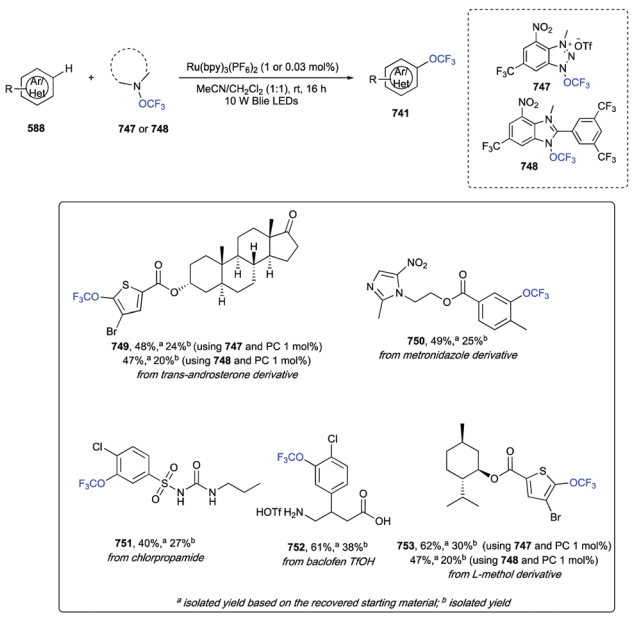

Scheme 132 Trifluoromethoxylation of arenes.

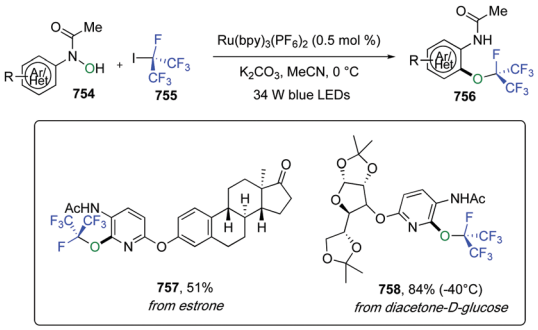

Scheme 133 Synthesis of perfluoroalkoxylated (hetero)arenes.

case, LSF of menthol and estrone were accomplished in 74 and 47% yields, respectively (derivatives **749** and **753**, respectively).

A general method to access perfluoroalkoxylated (hetero)-arenes (**756**, Scheme 133) with commercially available and cost efficient perfluoroalkyl iodides (R_F-I, *e.g.* **755**) was reported by J. W. Lee *et al.*[192] This strategy exploited the ability of *N*-(hetero)-aryl-*N*-hydroxylamides (**756**) to form, in the presence of the *in situ* generated R_F radicals, N-OR_F intermediates, which readily underwent OR_F-migration to afford perfluoroalkoxylated (hetero)-arenes. The reaction was run in the presence of $Ru(bpy)_3(PF_6)_2$ as the photocatalyst and potassium carbonate in MeCN, under 3 W blue LEDs irradiation, at 23 °C for 12 h. Interestingly, due to the persistent radical effect, the coupling of O- and R_F-radicals was more favorable than the direct addiction of the latter to arenes, assuring exclusive chemoselectivity. A wide range of diversely substituted both aromatic and heteroaromatic hydroxylamides were efficient starting materials, as well as trifluoromethyl iodides and perfluoroalkyl iodides, included perfluorohexyl-, smoothly afforded the perfluoroalkoxylated adducts. Complex *N*-pyridinyl-*N*-hydroxylamides derived from estrone and diacetone-D-glucose were subjected to standard reaction conditions in order to get trifluoroalkoxymethylated **757** and **758** in 51 and 84% yield, respectively (Scheme 133).

3.4.3 Phosphonylation. Oxidative phosphonylation of C(sp^2)–H bonds under visible light irradiation, with dual photoredox and cobalt catalysis, and without the need for noble metals and external oxidants was achieved by L. Niu *et al.* (Scheme 134).[193] Methylarenes, anisoles, polycyclic aromatic hydrocarbons, heteroaromatics, anilines and olefins were all suitable starting materials. This strategy relied on the capture of key arenes and olefins radical cations, generated upon SET transfer with an excited photocatalyst. After optimization, standard reaction conditions required triethyl phosphite **759**, $Acr^+MesClO_4^-$ as organic photocatalyst, $Co(dmgH)(dmgH_2)Cl_2$ as transition-metal catalyst, ammonium acetate as an additive, MeCN as the solvent, and 3 W blue LEDs irradiation at room temperature for 24 h. In many of the reported examples, the phosphonylation showed exclusive regioselectivity. LSF of naproxen and gemfibrozil methyl esters was reported in 91 and 60% yields, respectively (**761** and **762**, Scheme 134).

3.4.4 Sulfoxidation and sulfenylation. A dual electron- and energy-transfer photocatalytic process starting from aryliodonium **763** and thiosulfate salts **764** could afford either sulfoxidation or sulfenylation of arenes by simply tuning the reaction conditions (**765**, Scheme 135).[194] In this strategy, stabilization of a sulfur radical was realized through both electronic conjugation and steric hindrance, so that undesired homocoupling and overoxidation could be minimized and yields increased. Standard reaction conditions to get sulfoxidated products employed eosin Y as the photocatalyst, DIPEA, $Zn(OAc_2)$, in a mixture of MeOH/MeCN as the solvent under 18 W green LEDs irradiation, under air. In order to switch the reaction outcome towards sulfenylated adducts, a nitrogen inert atmosphere, together with $Zn(OAc_2)\cdot 2H_2O$, MeOH as the solvent and a 23 W CFL for irradiation were essential. The transformation showed a broad reaction scope, with good functional group tolerance. As examples of complex biorelevant scaffolds furanose, pyranose, and metronidazole successfully underwent sulfoxidation (**766–768**, Scheme 135). Unfortunately, the authors did not report any late-stage sulfenylation of pharmaceutical agents.

3.4.5 Thianthrenation. One of the most straightforward approach to LSF promoted by visible-light catalysis was reported by F. Berger *et al. via* thianthrenation (*i.e.* the conversion to synthetically versatile arylthianthrenium salts, Scheme 136).[195] This kind of arenes' functionalization could allow site-selective aromatic C(sp^2)–H derivatization without requiring specific directing groups. Actually, the reaction of a persistent sulfur-based radical with aromatics afforded thianthrenium salts with excellent chemo- and regio-selectivity. The latter are valuable synthetic linchpins, ready to be further engaged in different transformations, *via* both transition-metal and photoredox catalysis. Thianthrene radical cations can be accessed *in situ* from the new bench-stable thianthrene sulfoxide **769**, prepared

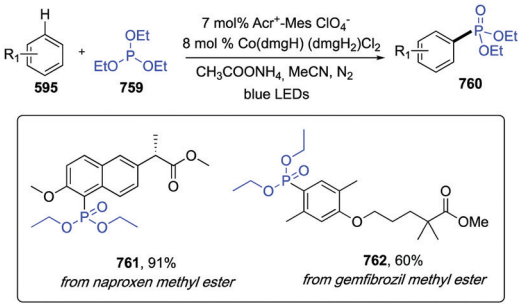

Scheme 134 Phosphonylation of (hetero)arenes.

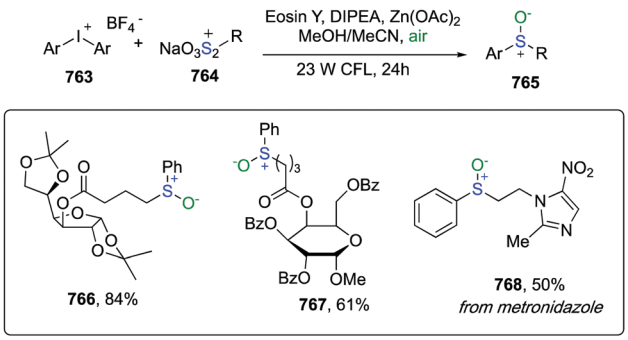

Scheme 135 Sulfoxidation and sulfenylation of (hetero)arenes.

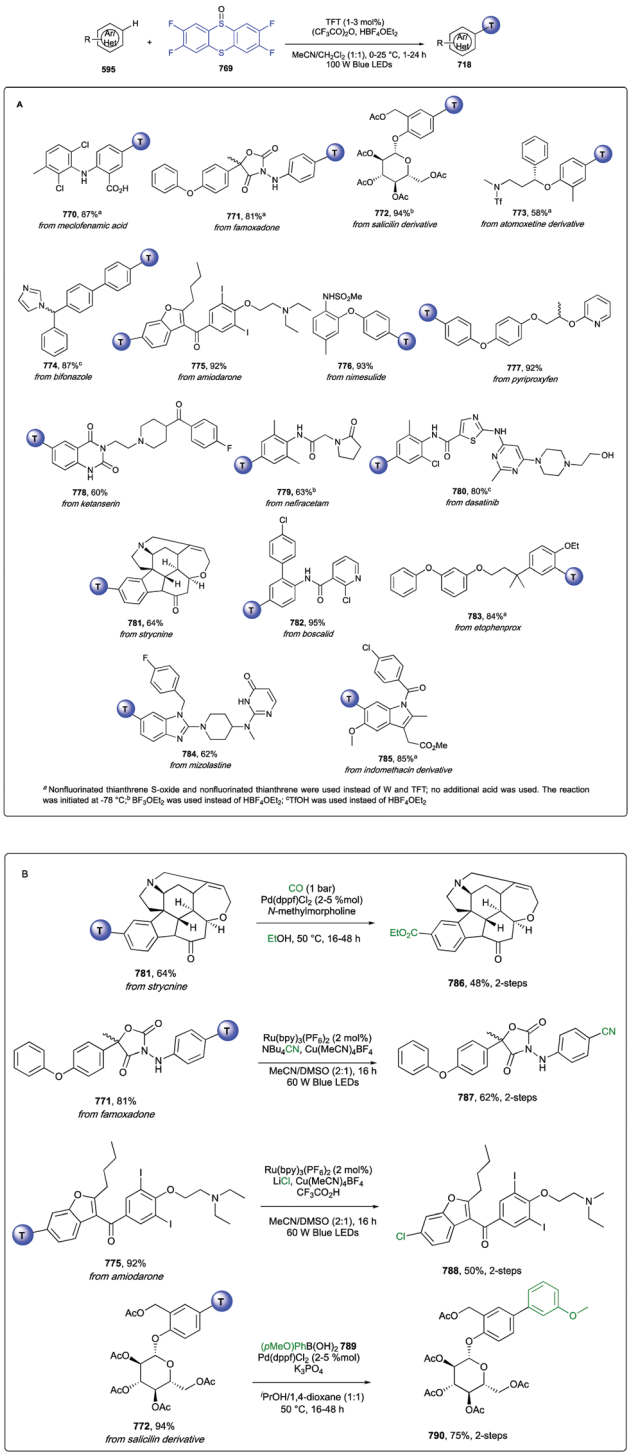

Scheme 136 Thianthrenation of (hetero)arenes.

on scale by the authors in two reaction steps. This reagent enabled successful derivatization of both electron-rich and electron-poor arenes, and reaction conditions were tested on a wide range of bioactive complex substrates such as meclofenamic acid, famoxadone, salicin pentaacetate, atomoxetine, (±)-bifonazole, amiodarone, nimesulide, (±)-pyriproxyphen, ketanserine, nefiracetam, dasatinib, strychnine, boscalid, etofenprox, mizolastine, and indomethacin methyl ester (**770–785**, Scheme 136A). In order to test the chemoselectivity in the further elaboration of thianthrenium salts, some of them were reacted in a number of different reaction conditions, including Negishi, Heck, Suzuki, Sonogashira, to cite a few, to afford their corresponding derivatives. As examples of drug scaffolds, functional-group tolerance was tested with strychnine, amiodarone, (±)-famoxadone, and salicin pentaacetate derivatives (further converted to **786–788**, **790**, Scheme 136B).

Recently, the same group identified a wide scope methodology for the fluorination of thianthrenium salts (**718**) under photoredox conditions (Scheme 137).[196] The protocol required a dual photoredox/copper catalysis, and CsF as fluoride source, acetone as the solvent, 68 W blue LEDs irradiation at 30 °C for 12 h.

These standard conditions were conveniently applied to a wide range of electron-rich and electron-poor arenes, with *ortho*-, *meta*-, and *para*-substitution patterns. Tolerated functional groups included, among others, aldehydes, esters, heterocycles, benzyl ethers, carbamates, alcohols, halides, and tertiary amines. LSF of a number of pharmaceuticals including salicin pentaacetate, flurbiprofen, indomethacin, amiodarone, calone, clofibrate, boscalid, etofenprox, nefiracetam, gemfibrozil, and pyriproxyfen was reported (**793–804**, Scheme 137).

3.4.6 ^{18}F-Fluorination. A mild method for the direct arene C(sp^2)–H ^{18}F-fluorination with an [^{18}F]F^- salt *via* organic photoredox catalysis was developed by W. Chen *et al.* (Scheme 138).[197]

As fluoride source, [^{18}F]F^- was prepared *via* proton bombardment of [^{18}O] water and subsequent elution of ^{18}F-fluoride with tetrabutylammonium bicarbonate to afford [^{18}F]TBAF. Optimized reaction conditions required an acridinium perchlorate as organic dye photocatalyst, TEMPO, a 4 : 1 mixture of MeCN:*t*-BuOH as solvent system, and blue light irradiation for 30 minutes at 0 °C and an O_2 atmosphere. A range of substituted aromatics and heteroaromatics were all efficiently and, most of them regioselectively, labeled, tolerating, among others, halogens and carbonyl-containing functional groups. Radiofluorination of several (hetero)arenes was reported, and selective LSF of bioactive fenoprofen and flurbiprofen (as methyl esters), clofibrate, fenofibrate, DOPA (as protected derivative) was accomplished (**806–810**, Scheme 138).

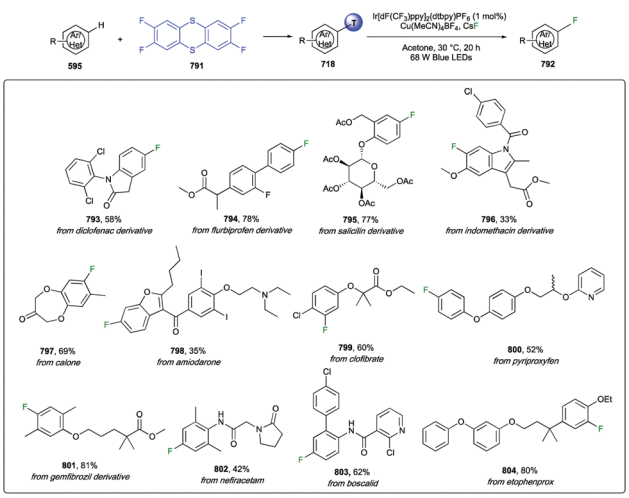

Scheme 137 Fluorination of thianthrenium salts.

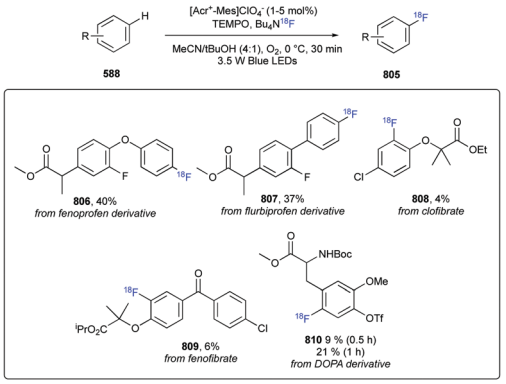

Scheme 138 ^{18}Fluorination of (hetero)arenes.

3.5 Bifunctionalization with organic semiconductor photocatalysts

I. Ghosh *et al.* reported the use of a stable organic semiconductor material, mesoporous graphitic carbon nitride (mpg-CN), as visible-light photoredox catalyst able to promote oxidative and reductive electron transfers to two different substrates for direct twofold carbon–hydrogen functionalization of arenes and heteroarenes (Scheme 139).[198]

The photogenerated hole and electrons on the catalyst surface could either afford arenes functionalized at two distinct C–H sites, or monofunctionalized arenes could be obtained by means of a coupled sacrificial redox process. Here, the authors reported a valuable array of transformations for both arenes and heteroarenes including direct one-pot dual C(sp^2)–C(sp^3)/C(sp^2)–heteroatom and C(sp^2)–C(sp^3)/C(sp^2)–C(sp^3) C–H functionalization and innate (*i.e.* at the inherently reactive positions) or regiospecific C(sp^2)–C(sp^3), C(sp^2)–C(sp^2), or C(sp^2)–heteroatom mono-functionalization with more than 20 different groups.

This catalytic system enabled for example both heteroarenes alkylation with alkyl bromides and dual alkylation/trifluoromethylation in the co-presence of sodium triflinate; mono-trifluoromethylation, perfluoroarylation, and difluoroalkylation (for a recent review about difluoroalkylation see: A. Luxen *et al.*[199]); introduction of halogens, cyano-, thiocyano-, amines, or small molecules such as succinimide and phthalimide. Notably, the catalyst could be efficiently recoverable by simple centrifugation of reaction mixtures for at least 4 times without any loss in efficiency. As examples of biorelevant scaffolds uracil, allopurinol, and melathonin were regioselectively converted into trifluoromethyl derivatives **599**, **813**, and **814** (Scheme 139); caffeine, besides being trifluoromethylated (**605**), was also converted into derivatives **815** and **817**, while theophylline was modified into compound **816**.

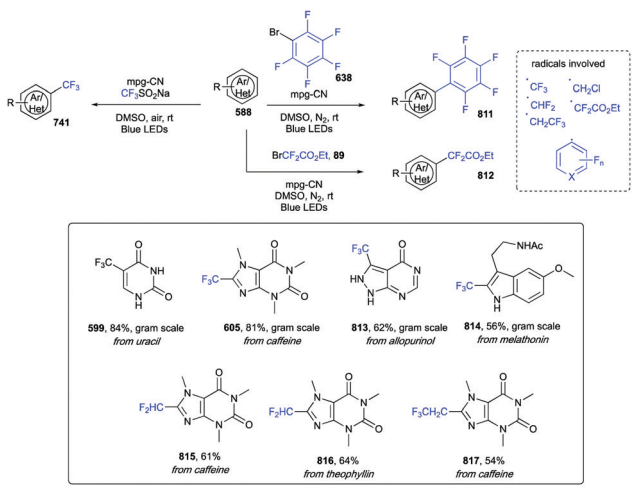

Scheme 139 Bifunctionalization with organic semiconductor photocatalyst.

3.6 Photoreduction of arenes and heteroarenes

A. Chatterjee and B. König showed that the energy accumulation of two visible-light photons could be sufficient to break aromatic stabilization, thus inducing dearomatization of arenes and heteroarenes (Scheme 140).[200] Here, the combination of energy-transfer and electron-transfer mechanistic pathways generated an arene radical anion, which was trapped by hydrogen-atom transfer (HAT) and subsequently protonated to afford the reduced product. More in detail, the sensitizer absorbed a photon and transferred energy to the arene; at the same time the excited photocatalyst was reduced by a sacrificial electron donor and promoted a SET event to form the radical anion species. A fast HAT generated a stable anion, whose protonation gave the final reduced adduct. Reaction conditions were optimized as the following: an iridium catalyst, DIPEA as both a sacrificial electron donor and a source of hydrogen atom, methylammonium chloride as an additive in DMF as solvent under air and blue LEDs irradiation. The reaction scope was demonstrated with a range of both substituted and unsubstituted aromatics, nitrogen-heterocycles, an alkene, an alkyne, and, as drug-like compound, naproxene methyl ester was converted into the two dihydro-derivatives **819** and **820** (Scheme 140).

4. Functionalization of heteroarenes

The most famous transformation relying on the *in situ* generation of a radical species and its subsequent addition to electron-deficient heteroarenes is the monumental Minisci reaction.[201,202] (For recent reviews about Minisci-type reactions see ref. 203.) Back in the '60s Minisci and Barton groups reported that a broad variety of synthetically useful transformations could be realized by harnessing the so called "polar effects" originating from the nucleophilic C-centered radicals in the reaction with protonated heteroaromatic bases. As for other venerable radical transformations, the coming of photoredox catalysis put the Minisci reaction in a new spotlight by

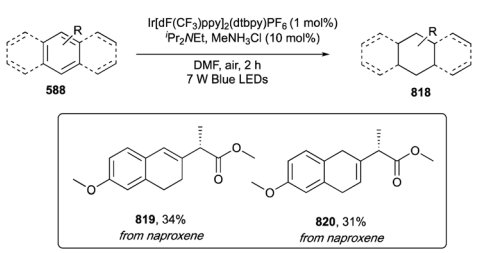

Scheme 140 Photoreduction of arenes and heteroarenes.

expanding its scope to diversely and densely functionalizated heteroarenes, including unactivated aromatic substrates and complex bioactive scaffolds.

4.1 Formation of C(sp^2)–C(sp^3) bonds

The protocols herein reported exploit the use of pre-functionalized reagent. For a direct alkylation with simple unactivated alkanes see Section 10.

4.1.1 Introduction of small alkyl substituents (Me, Et, and c-Pr). The first, to our knowledge, and seminal paper addressing the problem of introducing small and unstable alkyl radicals, *i.e.* Me, Et, and *c*-Pr, into *N*-heteroarenes, with the assistance of visible-light catalysis, was published in 2014 by D. A. Di Rocco (Schemes 141 and 142).[204]

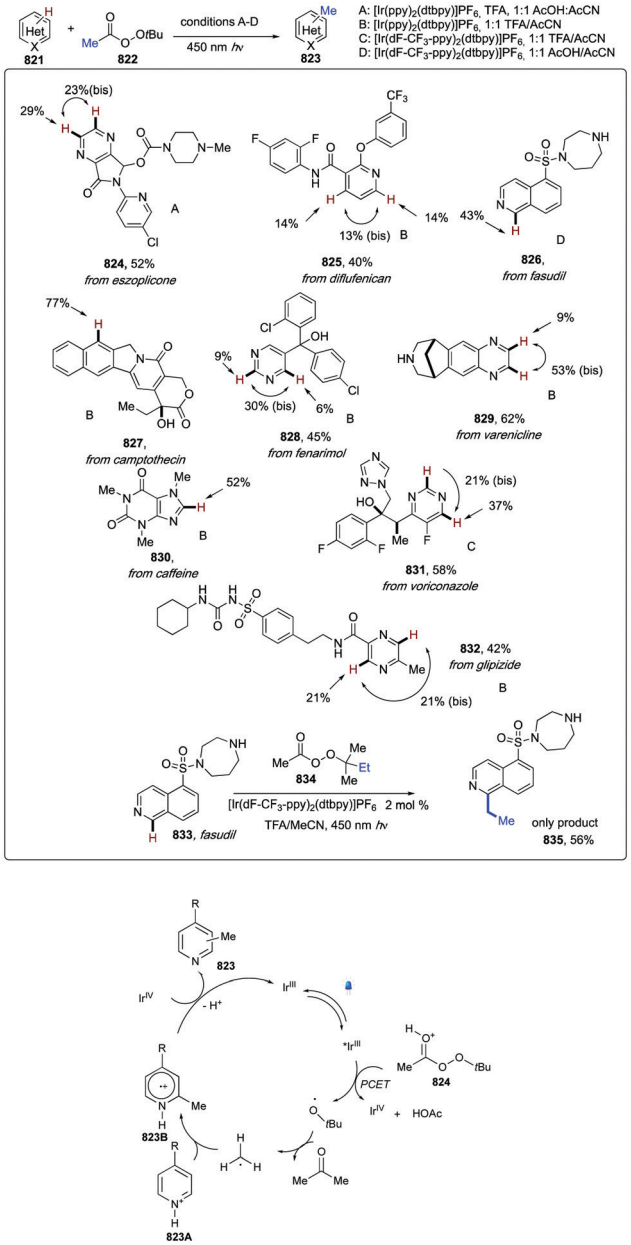

Scheme 141 Methylation of heteroarenes.

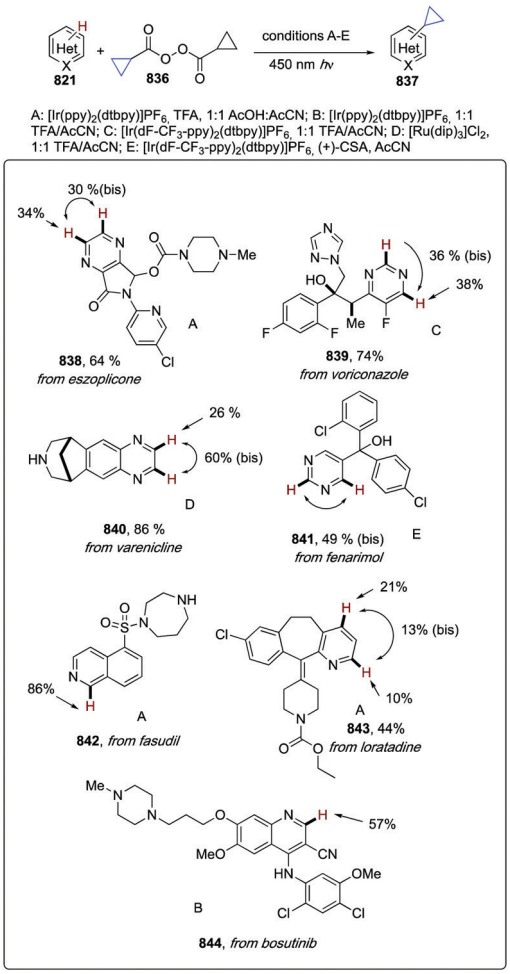

Scheme 142 Alkylation of heteroarenes.

Previously existing methodologies, as reported by Minisci,[205] Baran,[206] Molander,[207] and others, indeed, proved to be efficient in the LSF of a number of marketed drugs but were somehow limited in the scope of smaller alkyl radicals. The authors, here, demonstrated how photocatalytic conditions allowed a slow, controlled generation of reactive radicals reducing undesired side reactions. Optimal conditions were identified by means of a high-throughput screening of 12 photocatalysts and 8 solvents and solvent mixtures with TFA as an additive. As precursor of a methyl radical, *tert*-butylperacetate (**822**, *t*-BPA) was employed: its decomposition was initiated through a SET event from the excited-state photocatalyst, or, more in detail, its protonated form was reduced *via* a proton-coupled electron transfer (PCET). A first decomposition to acetic acid and *tert*-butoxy radical by homolytic cleavage of the weak O–O bond occurred, followed by decomposition of *tert*-butoxy radical to acetone and methyl radical. The reaction efficiency, in terms of cost and practicality, is evident if considering low molecular weight and benign by-products (acetone and acetic acid), and low cost of reagents. To evaluate the applicability of this protocol as a late-stage tool, several medicinal and agrochemical compounds were selected as substrates and conversion to their methylated analogues

(**824–832**, Scheme 141) was generally obtained with good yields; both 6- and 5-membered heterocycles reacted efficiently, with basic heterocycles (*e.g.* imidazole) preferred to the less basic ones such as 1,3,4-triazole as in voriconazole (**831**, Scheme 141). Importantly, amines, alcohols, amides, and esters were orthogonal to reaction conditions avoiding the need for protecting groups. *tert*-Amylperacetate and biscyclopropane-carbonyl peroxide (CPO) were used to generate ethyl and cyclopropyl radicals, respectively. In particular conversion of fasudil **833** into ethyl derivative **835** (Scheme 141) was obtained using *tert*-amylperacetate. On the other hand, the use of biscyclopropane-carbonyl peroxide afforded the cyclopropyl derivatives **838–844**, reported in Scheme 142.

4.1.2 Alkylation from alcohols. In 2015 J. Jin and MacMillan reported *N*-heteroarenes functionalization by using alcohols as alkylating agents (Scheme 143).[208] The authors were inspired by one of the key principles in DNA biosynthesis, *i.e.* the radical-mediated conversion of ribonucleosides to deoxygenated ribonucleosides. During this enzymatic step, a "spin-center shift" occurred, and as a consequence, a β-alcohol C–O bond is cleaved, releasing a carbon-centered radical intermediate and elimination of water. In order to mimic this naturally occurring transformation, a dual catalytic system was designed by merging photoredox catalysis and hydrogen atom transfer (HAT) catalysis. More in detail, by using $[Ir(ppy)_2(dtbbpy)]PF_6$ and ethyl 2-mercaptopropionate **846** as HAT agent, along with *p*-toluenesulfonic acid and blue LEDs irradiation, methyl substituents were introduced into a wide range of heteroaromatics **821** (*e.g.* quinolines, isoquinolines, phthalazines, phenanthridines, and pyridines) starting from methanol as methylating agent.

Besides methanol, a broad array of primary alcohols efficiently provided α-oxy-radicals. Steric bulk in proximity of the –OH function was tolerated, while the presence of an electron-withdrawing trifluoromethyl (CF_3) group distal to the alcohol was detrimental: in this case, the use of a more electrophilic thiol catalyst (*i.e.* 2,2,2-trifluoroethanethiol) restored excellent yields, probably thanks to the polar effect on the HAT transition state. Remarkably, diols were also good substrates and exceptional chemoselectivity, favoring the primary alcohol site, was observed. The robustness of this transformation was further proved in the functionalization of the bioactive compounds fasudil and milrinone (**848** and **849**, Scheme 143).

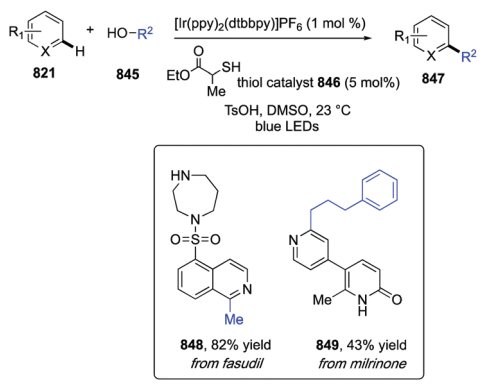

Scheme 143 Alkylation of heteroarenes from alcohols.

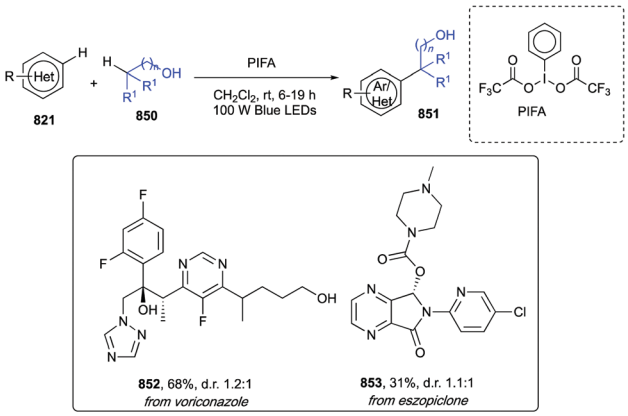

Scheme 144 Alkylation of heteroarenes from alcohols.

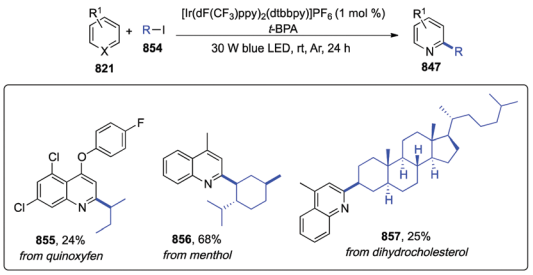

Scheme 145 Alkylation of heteroarenes from alkyl halides.

Heteroaryls **821** could also be hydroxy-alkylated with aliphatic alcohols: in this case an *in situ* generated alkoxy radical triggered a regioselective HAT event, thereby forming an alkyl radical and enabling a remote C–H bond activation (Scheme 144).[209] This challenging transformation (O–H bonds are typically associated with high bond dissociation energies, BDE) was accomplished by using phenyliodine bis(trifluoroacetate) (PIFA) as the only catalyst under visible-light irradiation (100 W blue LEDs) in CH_2Cl_2 as solvent at room temperature. A number of alcohols were shown to be suitable partners, including primary, secondary, and tertiary substrates; remarkably, the regioselective 1,5-HAT occurred even in the presence of more reactive benzylic C–H bonds.

The generality of the protocol was examined with a wide range of nitrogen containing heterocycles, such as quinolines, isoquinolines, pyridines, pyrimidines, and pyrazines to cite a few. The method showed to be amenable also to complex bioactive scaffolds as for voriconazole and eszopiclone, which were converted into their alkyl derivatives **852** and **853** in 68 and 31% yields, respectively (Scheme 144).

4.1.3 Alkylation from alkyl halides. The scope of the DiRocco late-stage alkylation of *N*-heteroarenes was recently further expanded by Z. Wang *et al.* to a wide range of alkyl substituents (Scheme 145).[210] Here the authors used readily available *tert*-butyl peroxyacetate (*t*-BPA) as a radical relay precursor to generate alkyl radicals from alkyl iodides.‡ The reaction was promoted by the

‡ The choice of the period was based on the first report by DiRocco *et al.* (see ref. 204) specifically focused on the late-stage modification of drugs under visible light photocatalytic conditions.

$[Ir(dF(CF_3)ppy)_2(dtbbpy)]PF_6$ photocatalyst. In particular, the methyl radical, generated upon proton coupled electron transfer (PCET) between Ir^{III}* and *t*-BPA, and subsequent β-scission of the *tert*-butoxy radical, was able to abstract an iodine atom from alkyl iodides. The mild protocol, along with broad substrate scope and functional group tolerance, allowed the late-stage functionalization of complex nitrogen-containing natural compounds and drugs such as quinoxyfen, menthol, and dehydrocholesterol (**855–857**, Scheme 145).

P. Nuhant *et al.* developed a visible-light-driven Minisci protocol employing an inexpensive earth-abundant metal catalyst, decacarbonyldimanganese $Mn_2(CO)_{10}$, to generate alkyl radicals from alkyl iodides (Scheme 146).[211] A light-triggered chain reaction mechanism was propagated by $^{\bullet}Mn(CO)_5$, with the rate-limiting step being iodine abstraction from an alkyl iodide. Reaction conditions were compatible with a wide array of sensitive functional groups, including sugar moieties, azetidines, and Boc-groups, to cite a few. High-throughput late-stage C–H functionalization of four drugs including fasudil **833**, varenicline **858**, hydroquinine **859**, and bosutinib **860** was performed with nine different secondary and tertiary alkyl iodides in methanol under 36 W blue LEDs irradiation and in the presence of TFA as acid cocatalyst (Scheme 146).

One more protocol for direct visible-light-mediated Minisci C–H alkylation of heteroarenes with unactivated alkyl halides was reported by J. Dong *et al.* (Scheme 147).[212] Interestingly, molecular oxygen was used as the oxidant, and typical reaction conditions relied on the use of an iridium photocatalyst, tris(trimethylsilyl) silane (TTMS) as the halogen-abstraction agent, TFA, and acetone as the solvent under 36 W blue LEDs irradiation at room temperature for 24 h. The protocol presented broad scope, including (iso)quinolines, pyridines, phenanthrolines, quinazoline, and other heterocyclic compounds, and unactivated primary, secondary, and tertiary alkyl halides. The compatibility with a wide array of sensitive functional groups was efficiently demonstrated also in the late-stage functionalization of seven biorelevant compounds (**862–872**, Scheme 147).

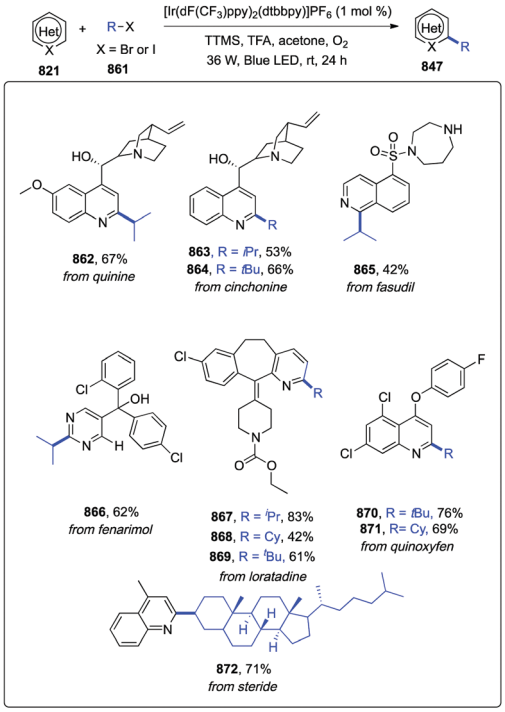

Scheme 147 Alkylation of heteroarenes from alkyl halides.

While J. Dong and co-workers reported the protocol illustrated above, J. J. Perkins *et al.* were working at the development of a very similar method.[213] However, added values of the latter were the absence of any metal photocatalyst and the use a water/MMeCN mixture as reaction solvent, which is ideal for purification under reverse-phase conditions and parallel workflows (Scheme 148).

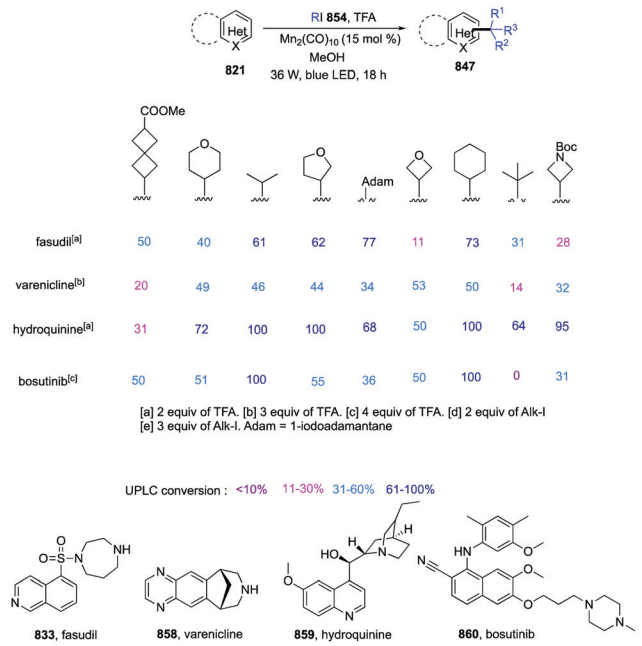

Scheme 146 Alkylation of heteroarenes from alkyl halides.

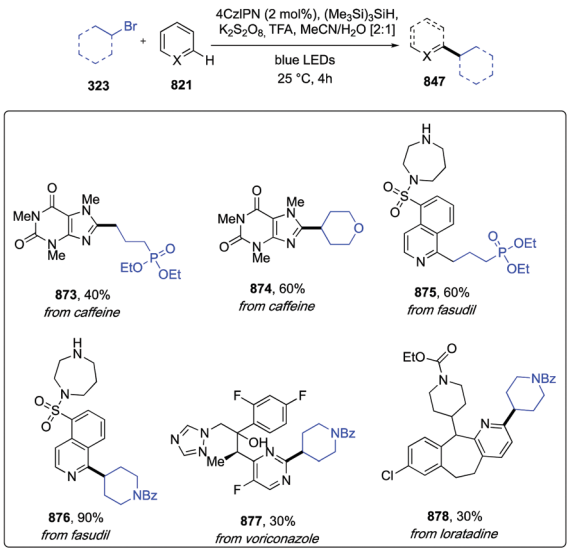

Scheme 148 Alkylation of heteroarenes from alkyl halides.

Moreover, the bubbling oxygen atmosphere required in the Dong protocol could be not always practical for library synthesis. Standard reaction conditions in the Perkin protocol required $(Me_3Si)_3SiH$, 4-CzlPN as the organic photocatalyst, potassium persulfate ($K_2S_2O_8$) as an oxidant, and TFA at room temperature and blue LEDs irradiation for 4 h. The scope of alkyl bromides was explored by using quinazoline: primary, and unactivated secondary alkyl bromides, including unfunctionalized cyclic and linear alkyls and cyclic ethers such as tetrahydrofuran and tetrahydropyran, provided the corresponding products in good yields. The scope of heteroarenes included fused 5-membered rings, *e.g.* benzothiazole and benzoimidazole, 2,4-disubstituted pyridines, and of course classic examples of Minisci C–H substrates such as quinolines and isoquinolines. As examples of biorelevant complex compounds, caffeine, fasudil, the antifungal voriconazole, and the antihistamine loratadine were selected and readily converted in medium yields to their alkylated analogues **873–878** (Scheme 148).

4.1.4 Alkylation from carboxylic acids. A direct decarboxylative C–H alkylation of *N*-heteroarenes can be performed by using inexpensive, stable, naturally abundant, and commercially available aliphatic carboxylic acids **879** as radical precursors (Scheme 149).[214] Functionalization of (iso)quinoline, pyridine, phthalazine, benzothiazole, and other heterocyclic derivatives with both cyclic and acyclic primary, secondary, and tertiary carboxylic acids as well as amino and fatty acids smoothly proceeded under the standard reaction conditions. The reaction was promoted by $[Ir(dF(CF_3)ppy)_2(dtbbpy)]PF_6$ along with ammonium persulfate as oxidant under 5 W blue LEDs irradiation, in DMSO, while times varied from 1.5 to 16 h depending on the substrate complexity. Alkylation of fasudil, a potent vasodilator, was accomplished in 49% yield (**880**, Scheme 149).

A similar procedure for the decarboxylative alkylation of *N*-heteroarenes was reported by J. Wang *et al.* (Scheme 150).[215] $Ru(bpy)_3Cl_2$ was used as the photocatalyst and acetoxybenziodoxole (**881**, BI–OAc) selected as the oxidant. Substrate scope of *N*-heteroarenes involved, among others, quinolines, isoquinolines, quinoxalines, pyridines, and pyridazines, while a wide range of primary, secondary and tertiary alkyl groups were efficiently incorporated. As example of complex substrates, a purine nucleoside, the fungicide quinoxyfen, and fasudil were selectively alkylated at C6, C2, and C1, respectively, with excellent yields (**882–884**, Scheme 150).

Hypervalent iodine-promoted decarboxylation was also exploited in a metal-free decarboxylative C–H alkylation of *N*-heteroarenes (Scheme 151).[216]

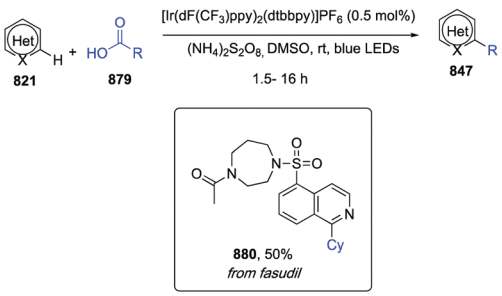

Scheme 149 Alkylation of heteroarenes from carboxylic acids.

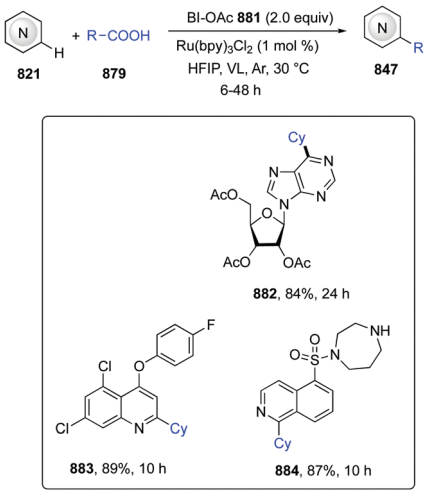

Scheme 150 Alkylation of heteroarenes from carboxylic acids.

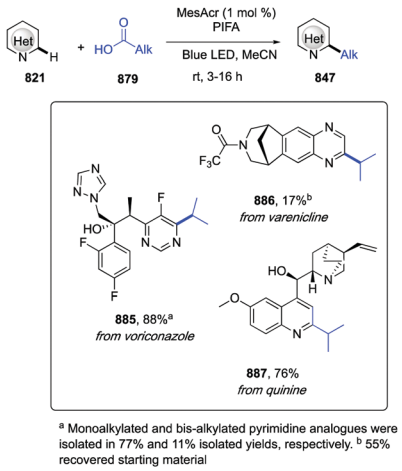

a Monoalkylated and bis-alkylated pyrimidine analogues were isolated in 77% and 11% isolated yields, respectively. b 55% recovered starting material

Scheme 151 Alkylation of heteroarenes from carboxylic acids.

J. Genovino and coworkers employed indeed an organic dye photocatalyst, MesAcr, in the presence of $PhI(TFA)_2$ (PIFA) as the oxidant, in MeCN as solvent under blue LEDs irradiation. 35 examples with yields up to 94% were reported: the wide functional groups tolerance enabled the late-stage functionalization of drugs such as voriconazole, varenicicline, and quinine in 88, 17, and 76% yield (**885–887**, Scheme 151).

A photocatalyst-free decarboxylative coupling of carboxylic acids with *N*-heterocycles was reported instead by X.-Y. Zhang *et al.* (Scheme 152).[217] This protocol, besides providing efficient and general alkylation of substrates, also enabled C–H acylation when α-ketoacids were used. Moreover, alkylation could be accomplished by using either aliphatic carboxylic acids or alcohols and oxalyl chloride, forming *in situ* oxalate derivatives. The authors exploited hypervalent iodine(III) reagents (HIR) as efficient and readily accessible radical source *via* visible-light photolysis. Initiation occurred indeed *via* photo-triggered I–O bond homolysis of HIR that was formed from carboxylic acid by ligand exchange with $PhI(TFA)_2$ (PIFA) to generate the C-radical **PFD** and one equivalent of TFA, which protonated, and so

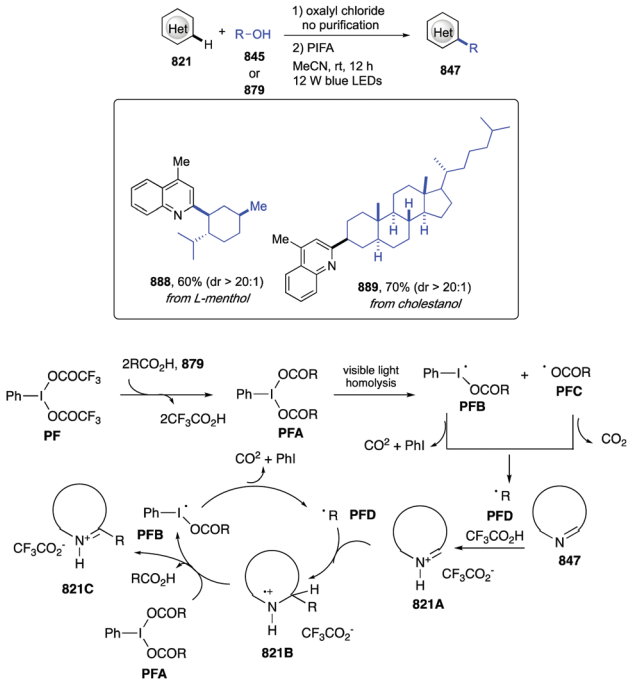

Scheme 152 Alkylation of heteroarenes from carboxylic acids.

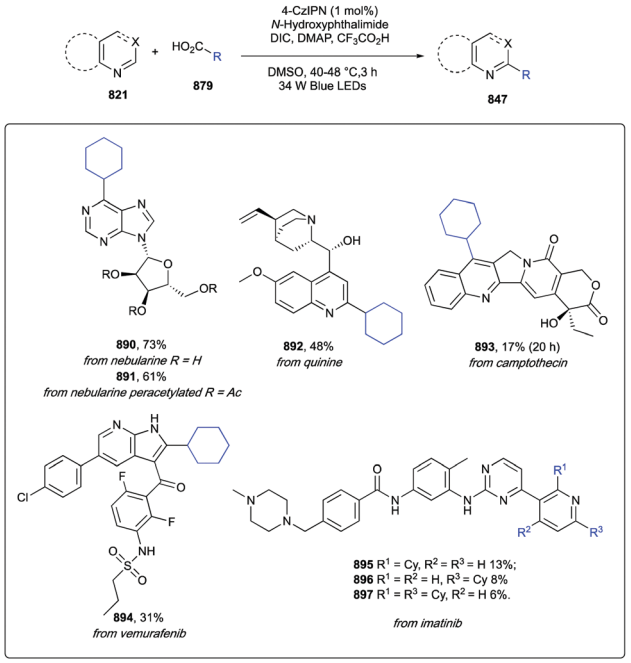

Scheme 153 Alkylation of heteroarenes from carboxylic acids.

activated, the *N*-heterocycle. Overall, the mechanism relied on a radical chain reaction. This metal-free protocol was successfully applied to various *N*-heterocycles and to a broad range of carboxylic acid derivatives, including some complex biorelevant structures such as L-menthol and cholestanol (**888** and **889**, Scheme 152)

Alternatively, carboxylic acids could also be converted *in situ* to *N*-(acyloxy)-phthalimides (NHI) in order to carry out a two-step one-pot alkylation of a broad range of six-membered and fused five-membered heteroarenes (Scheme 153).[218] CzIPN proved to be the optimal photocatalyst, and the use of TFA as acid additive and DMSO as the solvent at 40–48 °C with a 34 W blue LED lamp as the photon source afforded a wide library of 4-methylquinolines regioselectively alkylated at position 2. Conversely, heteroarenes such as pyridines, isoquinolines, purines, and benzimidazole, to cite a few, gave mixtures of regioisomers. Marketed drug scaffold including nebularine and peracetylated nebularine, quinine, camptothecin, vemurafenib, and imatinib, were used as starting materials to demonstrate the potential application of this protocol as a tool for late-stage functionalization of bioactive complex scaffolds (**890–897**, Scheme 153).

4.1.5 Alkylation from aldehydes. A photoredox decarbonylative Minisci-type alkylation of *N*-heteroarenes with aldehydes (**127**) was reported for the first time by Z. Wang *et al.* (Scheme 154).[219]

The developed protocol met some key green principles, as it required the organic dye as photocatalyst (4CzIPN), air as the sole oxidant, and water as solvent at room temperature. Tosic acid hydrate ($TsOH{\cdot}H_2O$) and NaBr were also needed as an acid and an additive, respectively. As for the generality of the reaction, α-branched aldehydes gave excellent yields, while primary alkyl aldehydes and aromatic aldehydes failed to react under this

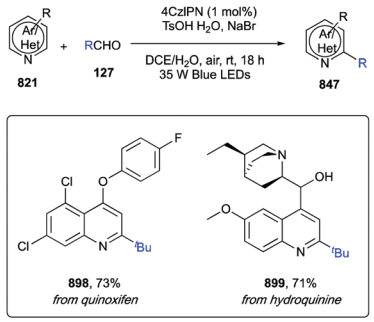

Scheme 154 Alkylation of heteroarenes from aldehydes.

catalytic system, probably due to the relatively high bond dissociation energies of the corresponding acyl radicals. On the other hand, suitable *N*-heteroarenes involved widely substituted quinolines, isoquinoline, pyridine, phenanthridine, and other multi-nitrogen containing heterocycles. As biologically active substrates the authors reported the conversion of quinoxyfen and hydroquinine into their corresponding *tert*-butyl derivatives **898** and **899** with 73 and 71% yield, respectively (Scheme 154).

4.1.6 Alkylation from boronic acids. Hypervalent iodine(III) reagents (HIR) were also used by G.-X. Li in a photoredox Minisci C–H alkylation of *N*-heteroarenes with boronic acids **900** as the radical source (Scheme 155).[220]

Promoted by $[Ru(bpy)_3]Cl_2$ as the photocatalyst and acetoxybenziodoxole (BI-OAc) as oxidant, this transformation allowed incorporation of a broad range of both primary and secondary alkyl groups into quinolines, quinoxalines, pyridines, pyrazines, benzimidazoles, and more complex substrates. As predictable, electron-deficient *N*-heteroarenes show higher reactivity toward alkylation. The excellent reaction scope and the functional

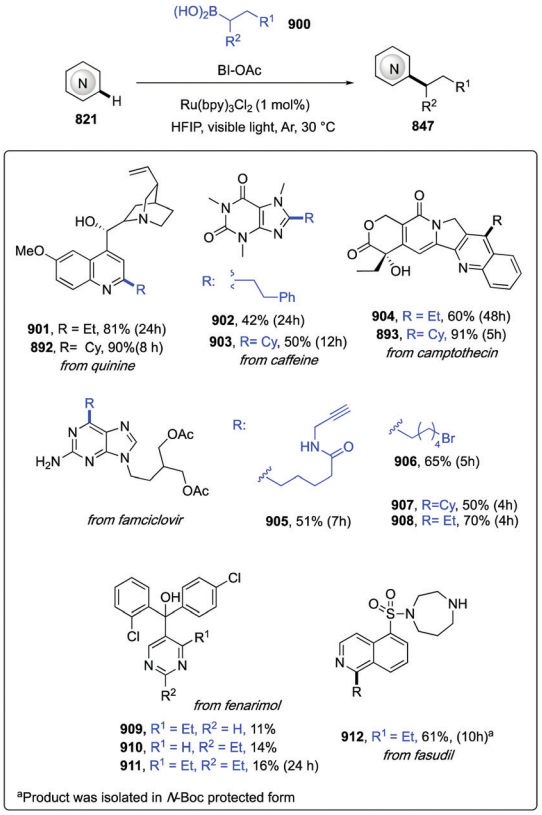

Scheme 155 Alkylation of heteroarenes from boronic acids.

group tolerance offered a valuable tool for late-stage functionalization of drugs as shown for quinine, caffeine, camptothecin, famciclovir, fenarimol, and fasudil: ethyl- and cyclopropyl-moieties were indeed efficiently and, in most cases, regioselectively added (**892**, **893**, **901–912**, Scheme 155).

4.1.7 Alkylation from dimethylsulfoxide. DMSO could act as a versatile alkylating agent for heteroarenes, as reagent-controlled photoredox catalytic conditions could promote methylation, trideuteromethylation, and methylthiomethylation (Scheme 156).[221] Thoroughly, in the presence of $PhPOCl_2$ as a phosphorous-based activator and $[Ir(ppy)_2(dtbbpy)]PF_6$ as the photocatalyst, in DMSO under blue LEDs irradiation, site-selective methylation in good to high yields could be achieved. On the other hand, the replacement of $PhPOCl_2$ with TMSCl as a silicon-based activator, and the use of a DMSO/DMS mixture as the solvent system afforded methylthiomethylated adducts. The reaction scope involved diversely substituted quinolines and isoquinolines, with yields ranging from 45 to 90%. Late-stage site-regioselective methylation of protected fasudil was accomplished in a good 50% yield (**915**, Scheme 156).

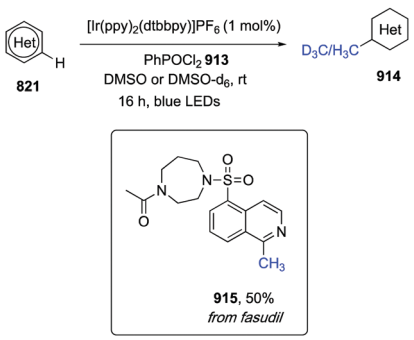

Scheme 156 Alkylation of heteroarenes from dimethylsulfoxide.

4.1.8 Alkylation from organotrifluoroborates. By merging organic electrochemistry and photoredox catalysis H. Yan *et al.* reported C(sp^2)–H alkylation of heteroarenes with organotrifluoroborates (**10**) (Scheme 157).[222] The latter are widely recognized as stable and easily available precursors of alkyl radicals. The developed protocol enabled the introduction of primary, secondary, and tertiary alkyl groups without the need for an additional oxidizing agent. The optimal reaction conditions occurred with $[Mes\text{-}Acr]^+ClO_4^-$ as organic dye photocatalyst, TFA as the acid additive, in a mixed solvent system $MeCN/H_2O$ (2 : 1) at room temperature. The electrolysis was conducted with a constant current (2 mA) in an undivided cell equipped with a reticulated vitreous carbon (RVC) anode and platinum plate cathode, while 20 W blue LEDs were employed as the photon source. A wide range of heteroarenes such as 4- or 2-substituted quinolines, isoquinolines, acridine, phenanthridine, and phatalazine, among others, underwent monoalkylation with excellent regioselectivity. Bioactive voriconazole, camptothecin, fasudil, and quinine proved to be complex competent substrates, demonstrating an exquisite functional group tolerance. Derivatives **865**, **885**, **887** and **916** were obtained (Scheme 157).

4.1.9 Alkylation from alkanes. Heteroarenes could be alkylated with simple alkanes **917** by using Selectfluor as a HAT agent under visible-light irradiation, HCl or TFA as acidic additives, in acetone as the solvent at room temperature (Scheme 158).[223]

The protocol was effective with quinolines, isoquinolines, pyridazines, pyrazines, benzothiazoles, and six-membered

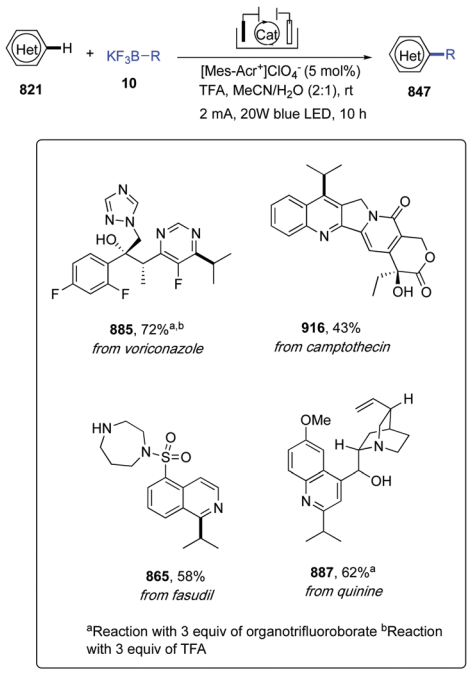

Scheme 157 Alkylation of heteroarenes from organotrifluoroborates.

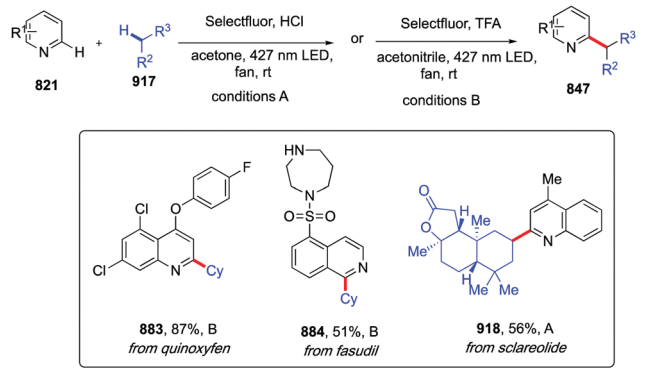

Scheme 158 Alkylation of heteroarenes from alkanes.

heterocycles such as pyridines and pyrimidines, to cite a few. Tolerated functional groups covered esters, halogens, nitriles, and ethers. Interestingly, suitable aliphatic C–H partners included linear, branched, and cyclic alkanes, ketone, esters, and even bridged ethers such as 1,4-epoxycyclohexane. Late-stage functionalization of biologically active quinoxyfen, fasudil, and the natural antifungal sclareolide was accomplished in good yields (**883**, **884**, and **918**, Scheme 158). Heteroarenes could also be alkylated in the presence of a hypervalent iodine oxidant PFBI-OH, which exhibited a high steric sensitivity in the H abstraction of secondary over tertiary C–H bonds (Scheme 159).[224] Accordingly, high selectivity toward penultimate methylene groups was observed for a wide range of linear aliphatic alkanes. Reaction conditions relied on $Ru(bpy)_3Cl_2$ as the photocatalyst, HFIP as the solvent, and a CFL as light source, at 30 °C for 20 h. LSF of fasudil, Bz-protected estrone, and the natural product sclareolide was achieved in good yields, albeit the starting alkane drugs were required in 5 equivalents (**921–923**, Scheme 159).

4.1.10 Programmable double alkylation. 2-Cyano-substituted heteroarenes (**174**) could undergo double *ipso*- and *para*-alkylation with tertiary radicals generated through visible light decarboxylation of carboxylic acids (**879**) (Scheme 160).[225]

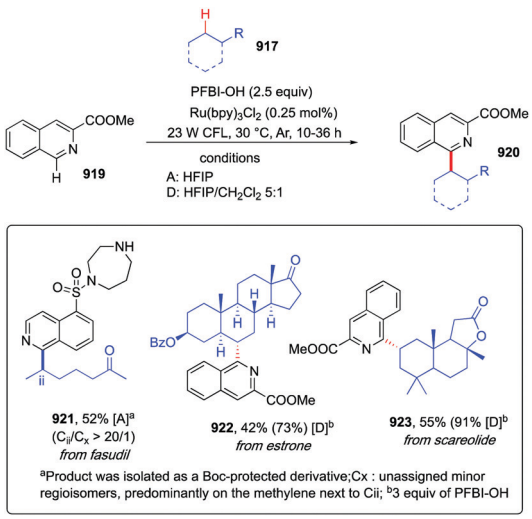

Scheme 159 Alkylation of heteroarenes from alkanes.

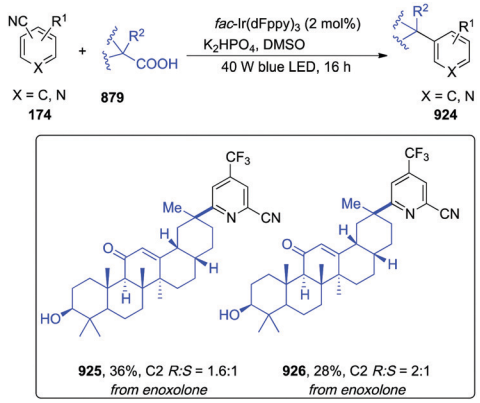

Scheme 160 Programmable double alkylation.

The transformation proceeded in DMSO at room temperature and in the presence of *fac*-Ir(dFppy)$_3$ as a photosensitizer, and K_2HPO_4 as a base, while irradiating with 40 W blue LEDs for 16 hours. Notably, the carboxylic acid inputs included α-amino and α-oxy substrates, thus delivering a wide array of structurally diverse alkylated heteroarenes (**924**) in good to excellent yields. Enoxolone, endowed with a plethora of biological activities such as antiulcer, antitussive, antiviral, antifungal, antiprotozoal, and antibacterial properties, was selected as representative complex scaffold and derivatized into **925** and **926** with moderate yields (Scheme 160).

4.1.11 Difluoromethylation. Heterocycles could be directly difluoromethylated by applying organophotocatalytic conditions using O_2 as a green oxidant while circumventing the need for pre-functionalization of substrates, metals as well as additives (Scheme 161).[226]

Thoroughly, moderate to excellent yields were obtained when sodium difluoromethane sulfonate ($NaSO_2CF_2H$, **927**) was used as difluoromethyl radical precursor, rose bengal as an organic photosensitizer, DMSO as a solvent under irradiation with two 3 W green LEDs. The substrate scope included a wide range of quinoxaline-2(1*H*)-ones bearing functional groups such as halogens, nitro, ethers, alkenes, and alkyl chains. Likewise, a rich array of 5- and 6-membered heteroaromatics embodying pyrazines, pyrrole, imidazole, pyridines, thiadiazole, and purines, to cite a few, underwent difluoromethylation in good yields under the standard conditions. In order to demonstrate the synthetic utility of this method in the late-stage difluoromethylation of complex bioactive molecules, caffeine, uridine, melatonin, allopurinol, uracil, voriconazole, metyrapone, and sulfonylureas' precursor were selected as representative scaffolds and converted into derivatives **815**, **816**, **929–939** (Scheme 161).

4.1.12 ^{18}F-Difluoromethyl labeling. *N*-Heteroaromatics can be labeled with a ^{18}F-difluoromethyl moiety *via* a photoredox flow reaction in a two-step synthesis and in very short reaction times (2 minutes) (Scheme 162).[227] The reaction proceeded by C(sp^2)–H activation avoiding pre-functionalization of the substrate. The radiolabeled *N*-heteroaromatics showed high molar activity, with a great potential as PET tracers for biological *in vivo* studies and clinical applications. It's worth noting that

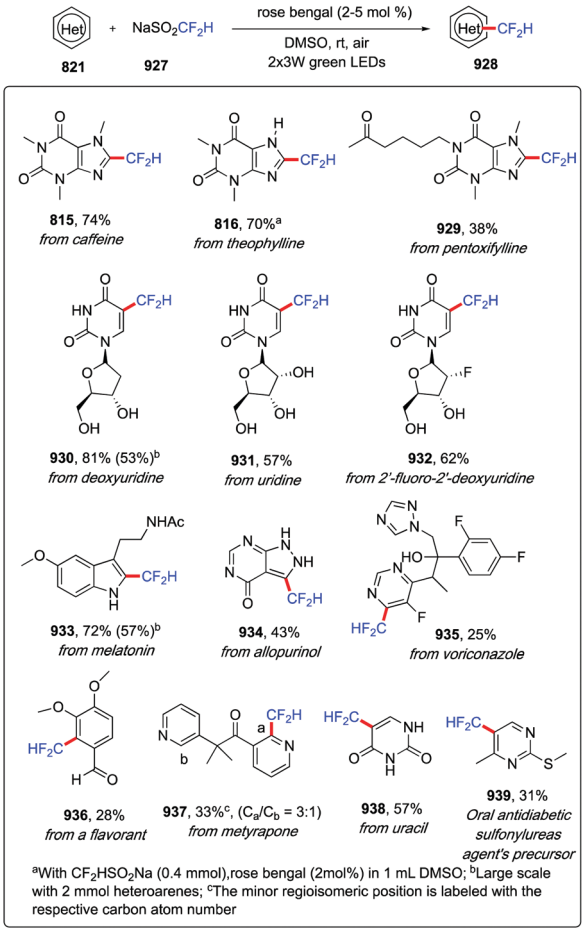

Scheme 161 Difluoromethylation of heteroarenes.

the difluoromethyl group (CHF_2) behaves as a lipophilic bioisoster of the hydroxy group given its ability to act as a hydrogen-bond donor. As precursor of the [^{18}F]-difluoromethyl radical, benzothiazole sulfone was readily prepared over two steps. The ^{18}F-difluoromethylation was conducted using flow chemistry, as anticipated, in DMSO with *fac*-Ir(ppy)$_3$ as a catalyst under blue LEDs irradiation at 35 °C. These reaction conditions smoothly afforded the labeled analogue of acyclovir (**942**), of moxonidine (**943**), a drug used to treat hypertension, and a SV2A ligand (**944**), used as PET tracer, thus showing to be competent substrates (Scheme 162).

4.1.13 Dehydrogenative cross-coupling with ethers, amines, and unactivated alkanes. Recently, Y. Quan *et al.* reported a dehydrogenative cross-coupling of *N*-heteroarenes (**821**) with ethers (**544**), amines, and unactivated alkanes by using metal–organic layers (MOLs) for a synergistic Lewis acid and photoredox catalysis (Scheme 163).[228] MOLs are a free-standing monolayered version of MOFs (metal–organic frameworks), porous materials suitable for tunable heterogenous catalysts with crystalline structures and well-defined active sites. Here, the authors developed a new multifunctional MOL, Hf_{12}-Ir-OTf able to catalyze the dehydrogenative cross-couplings with ethers, amines, and unactivated alkanes with turnover numbers of 930, 790, and 950, respectively. More in detail, Hf_{12}-Ir-OTf is composed of triflate

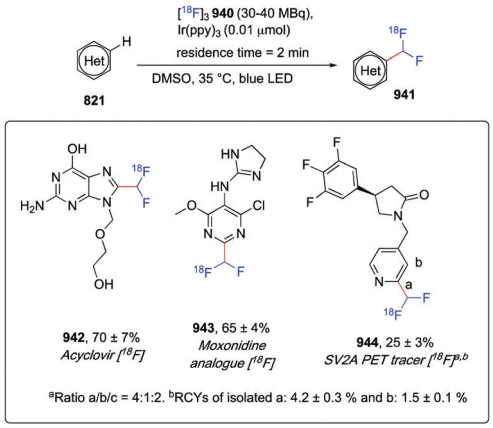

Scheme 162 ^{18}F-Difluoromethyl labeling.

(OTf)-capped Hf_{12}, secondary building units (SBUs) and Ir(DBB)-[dF(CF$_3$)ppy]$_2^+$ bridging ligands. Its superior catalytic performance over a mixture of photoredox and Lewis acid was due to the close proximity (1.2 nm) between photoredox and Lewis acid catalysts, facilitating the reaction between the carbon radical and the activated heteroarene, and accelerating the SET from a nitrogen radical intermediate and the oxidized Ir(IV) species in the catalytic cycle. Reaction scope of both *N*-heteroarenes and the alkylating ethers, amines, and unactivated alkanes was good; LSF of bioactive caffeine, fasudil, and metyrapone was reported (**946–948**, Scheme 163).

4.1.14 α-Aminoalkylation. *N*-Hydroxyphthalimide esters (**949**) of both natural and unnatural amino acids can be used as the α-aminoalkyl radical precursors in order to react with *N*-heteroarenes for a regioselective α-aminoalkylation (into **951** adducts) *via* a dual catalytic system based on an iridium photoredox catalyst with a suitable redox potential, and a BINOL-derived phosphoric acid **950** to increase the electron deficiency of *N*-heteroarenes (Scheme 164).[229] This decarboxylative process required 36 W blue LEDs irradiation, in DMA as solvent, at room temperature for a short time (*e.g.* 3 h). Various amino acid-derived redox-active esters are suitable substrates, and typical *N*-protecting groups in peptide chemistry, such as the *tert*-butyloxycarbonyl (–Boc) and benzyloxycarbonyl (–Cbz) groups were amenable. The absence of any strong acids and oxidants conferred an excellent functional group tolerance to this synthetic approach, as demonstrated by successful LSF of three

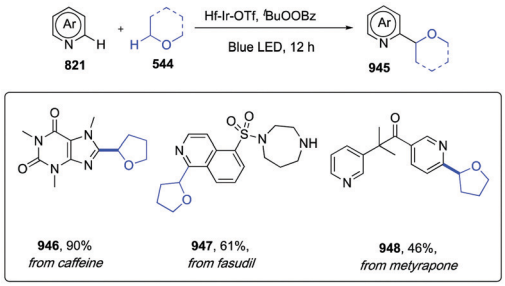

Scheme 163 Dehydrogenative cross coupling with ethers.

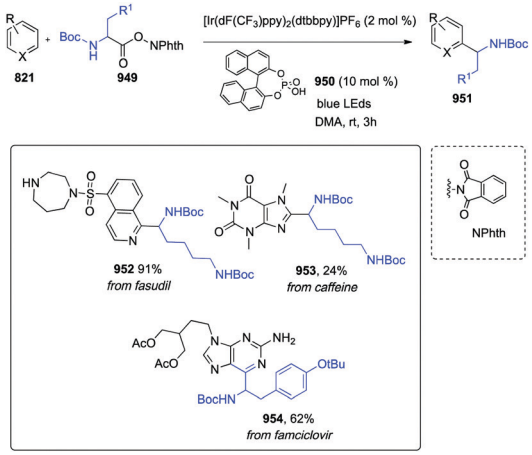

Scheme 164 α-Aminoalkylation of heteroarenes.

drug molecules, fasudil hydrochloride, caffeine, and famciclovir (**952–954**, Scheme 164).

An enantioselective Minisci-type alkylation of pyridines and quinolines harnessing the formation of prochiral α-amino alkyl radicals from NHI esters of amino acids (**955**) was reported by R. S. J. Proctor *et al.* (Scheme 165).[230] Excellent control of both enantioselectivity and regioselectivity were allowed by an enantiopure chiral Brønsted acid catalyst, while an $[Ir(dF(CF_3)ppy)_2(dtbpy)]PF_6$ promoted the required SET processes. The reaction did not require additional additives and proceeded in 1,4-dioxan at room temperature under blue LEDs irradiation. The robustness of this protocol was showcased in the late-stage functionalization of metyrapone and etofibrate, which were converted into derivatives **957** and **958** in good 70 and 86% yields, and 95 and 93% ee, respectively (Scheme 165).

An improved protocol for α-aminoalkylation of *N*-heterocycles was reported by J. Dong *et al.*[231] *via* a photoredox-mediated direct cross-dehydrogenative coupling reaction (Scheme 166). In this case, no substrate prefunctionalization is needed, and the protocol was extended to other hydrogen donors besides amines (*i.e.*, ethers, an aldehyde, a formamide, *p*-xylene, and alkanes). Standard reaction conditions were the following: $[Ir(dF(CF_3)ppy)_2(dtbbpy)]PF_6$ as a photocatalyst, TFA as a proton source, and *tert*-butyl peracetate (*t*-BPA) as an oxidant, acetone as the solvent, and 36 W blue LEDs irradiation at room temperature for 24 h. The substrate scope was broad and gram scale was tested without great loss in efficiency

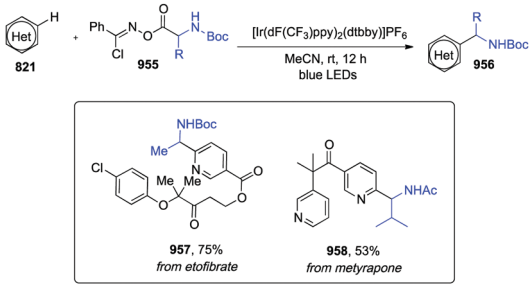

Scheme 165 α-Aminoalkylation of heteroarenes.

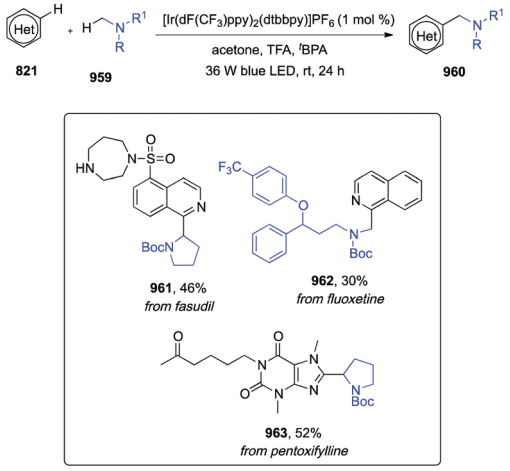

Scheme 166 α-Aminoalkylation of heteroarenes.

(84% yield on 4 mmol scale). As examples of drugs for LSF, the anti-depressant fluoxetine, the vasodilator fasudil, and pentoxifylline-used to treat muscle pain in people with peripheral artery disease- were selected (**961–963**, Scheme 166).

4.1.15 α-Hydroxyalkylation. Quinolines and isoquinolines can be hydroxyalkylated under visible light irradiation *via* a radical path exploiting the excited-state reactivity of 4-acyl-1,4-dihydropyridines as precursors of acyl radicals (Scheme 167).[232] This strategy featured extraordinary mild conditions as compared to the classical oxidative Minisci-type reactions. Here, the excited acyl-DHPs **430*** could act as strong single-electron transfer (SET) reductants, and generate nucleophilic acyl radicals, but the absence of an external oxidant led to hydroxyalkylated adducts in place of the typical Minisci-type acylated products. Acyl-DHPs **430** were readily available substrates, easily synthesized in a one-step procedure.

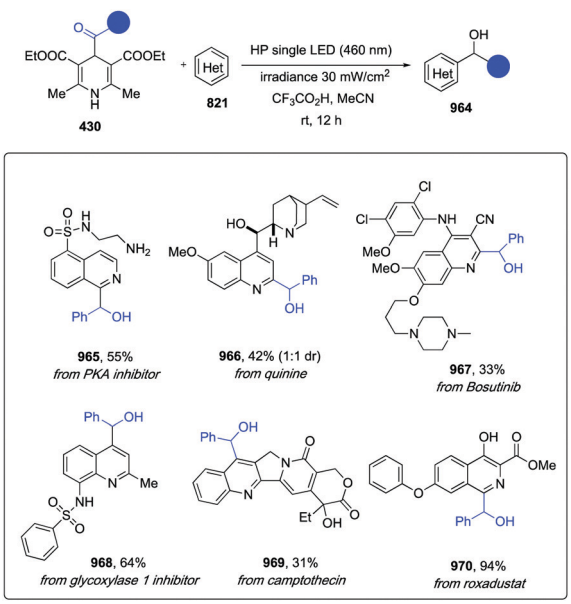

Scheme 167 α-Hydroxyalkylation of heteroarenes.

Typical reaction conditions required TFA, MeCN, and blue LEDs irradiation, at room temperature for 12 h. For quinolines substrates, a 1 : 1 regioisomeric mixture of C2/C4 substituted adducts were obtained, whereas the presence of a substituent directed the functionalization at either the C2 or C4 position. The presence of functional groups likely to suffer from oxidation such as primary amines, diarylamines, and both aliphatic and aromatic alcohols was well tolerated. To prove the efficacy of this protocol in the LSF of complex substrates a variety of bioactive scaffolds was selected and smoothly hydroxylakylated in good yields: a potent PKA inhibitor H-89, roxadustat analogue, quinine, a glycoxylase 1 inhibitor, and the anticancer agents bosutinib and camptothecin **965–970** (Scheme 167).

4.1.16 Oxyfluoroalkylation. Visible-light photocatalyzed (hetero)aryloxytetrafluoroethylation of heteroaromatics with oxyfluoroalkyl reagents was reported by G.-R. Park *et al.* (Scheme 168).[233] Reaction conditions employed $[Ru(Phen)_3]Cl_2$, resulted as the best photosensitizer among those tested, TMEDA, in MeCN and under irradiation with a 23 W CFL for 24 h. Substrate scope of both heteroaromatics and alkenes was good; moreover, this strategy provided a valuable diversity also with respect to the (hetero)aryloxytetrafluoroethyl reagents, which could bear either electron-donating (EDG) or electronwithdrawing (EWG) substituents, as well as heteroaromatic reagents containing for example a dimethylpyrimidine moiety. Bioactive compounds such as 5-aminouracil and caffeine were also successfully oxyfluoroalkylated (**974** and **975**, Scheme 168).

4.1.17 *N*-Alkylsulfonamidation. A Minisci-type δ-selective C(sp^3)–H heteroarylation of sulfonyl-protected primary aliphatic amines with *N*-heteroarenes was reported by Z. Deng and coworkers (Scheme 169).[234] This photoredox-mediated remote functionalization exploited the use of $Ru(bpy)_3Cl_2$ as the photosensitizer, benziodoxole acetate (BI-OAc **881**) as an oxidant and hexafluoroisopropanol (HFIP) as the solvent. Dealing with the amine protecting group, replacing the 4-*tert*-butylphenylsulfonyl group (*t*BP) with other acyl or sulfonyl groups was detrimental, leading to decreased yields. Aliphatic sulfonamides of both linear and cyclic amines (**976**) were compatible with this protocol, and functional groups including ester, carbamate, azido, terminal alkyne, and alkene were tolerated. Besides δ methylene C–H bonds, also the more inert δ-methyl group could be heteroarylated with quinoline **977**, albeit under forced conditions

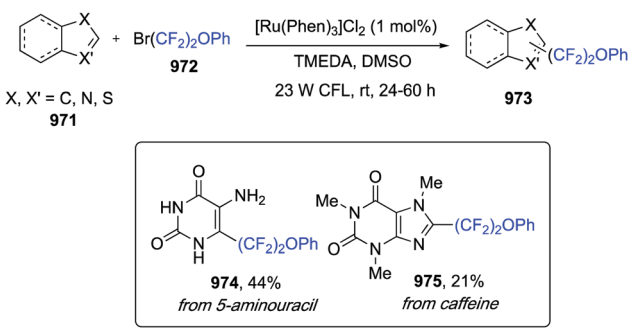

Scheme 168 Oxyfluoroalkylation of heteroarenes.

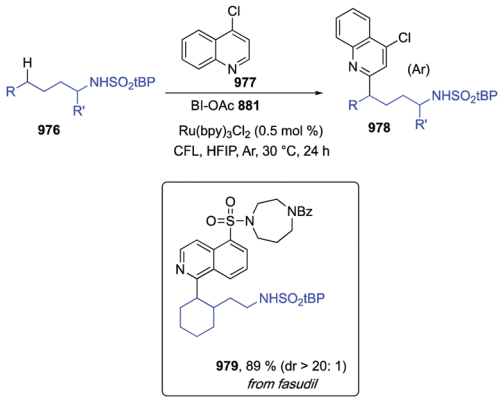

Scheme 169 *N*-Alkylsulfonamidation of heteroarenes.

(3 equiv. of amine substrate and 5 equiv. of BI-OAc). δ-Heteroarylalkylmine derivative of benzoyl protected fasudil was also obtained in an excellent 89% yield (**979**, Scheme 169).

4.1.18 Quinolines perfluoroalkylation. The regioselective perfluoroalkylation of quinoline derivatives was reported by P. B. Arockiam *et al.* (Scheme 170).[235] For quinoline systems, C-2 functionalization is commonly achieved *via* a radical Minisci reaction,[205] while C-3 and C-4 diversification[236,237] may be realized from metal-catalyzed transformations. Importantly, this reaction allowed to functionalize selectively both C-5 and C-8 positions of quinolines. It was compatible with a wide range of substrates, and interestingly did not require any transition metal catalysts or oxidants, fulfilling green chemistry requirements and establishing itself as an ideal tool for late-stage functionalization. A reported example was based on the synthesis of C5-perfluoroalkylated derivative **981** starting from the Boc-protected (±)-primaquine **980** (Scheme 170).

4.1.19 Tryptophols and tryptamines α-carboxyalkylation. Tryptophols and tryptamines **982** could be derivatized with an α-carboxyalkyl moiety under visible-light irradiation using α-bromo-ethyl acetate methyl ester **983** (Scheme 171).[238] Compound **983**, in the presence of an Ir(III) photocatalyst, provided carbon-centered radicals, which readily underwent coupling with indole derivatives. The methodology displayed wide functional group tolerance and excellent regioselectivity; furthermore, it was applied to the LSF of brevianamide F, an indole diketopiperazine alkaloid from holothurian-derived fungus Aspergillus Fumigatus, and to ergot derivatives metergoline and pergolide, psychoactive drugs and long-acting dopamine agonists for the treatment of Parkinson's Disease (**985–987**, Scheme 171).

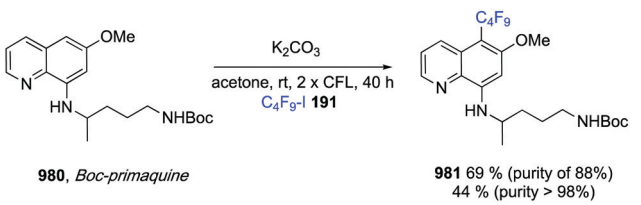

Scheme 170 Quinolines perfluoroalkylation.

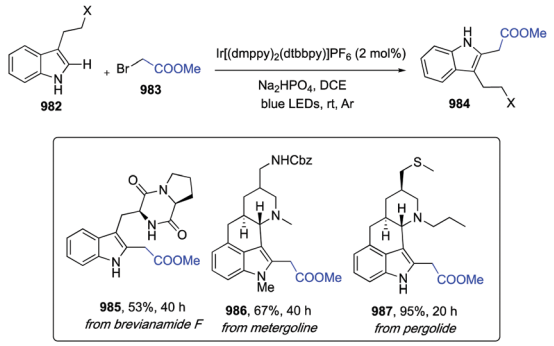

Scheme 171 Tryptophols and tryptamines α-carboxyalkylation.

4.2 Formation of C(sp^2)–C(sp^2) bonds

4.2.1 Formylation. Redox-neutral Minisci C(sp^2)–H formylation of *N*-heteroarenes could be achieved by using 1,3-dioxoisoindolin-2-yl 2,2-diethoxyacetate **988** as a formyl source (Scheme 172).

The experimental conditions featured Ir[dF(CF_3)ppy]$_2$(dtbbpy)PF_6 as a photocatalyst, TFA as an acid additive, DMA as a solvent, 36 W blue LEDs as the photon source at room temperature for 24 hours (Scheme 172).[239] The formyl group was eventually attained *via* treatment with 4 M HCl for 6 hours. The scope of the heteroarenes included a wide range of substituted isoquinolines as well as tricyclic substrates such as phenanthridine and pyrido-indoles, while simple pyridine substrates were not reactive. As an example of complex bioactive scaffold, site-selective formylation of acetylated fasudil was carried out in a good 60% yield (**990**, Scheme 172).

4.2.2 Carbamoylation. Nitrogen-containing heterocycles **821** could be directly carbamoylated by using bench stable and commercially available alkyl oxamate and oxamic acid derivatives **991** under photoredox catalytic conditions (Scheme 173).[240] This transformation was carried out by using 9-mesityl-3,6-di-*tert*-butyl-10-phenylacridin-10-ium tetrafluoro-borate as a photocatalyst, $K_2S_2O_8$ as an external oxidant, TFA as acidic additive in a 1 : 1 mixture of DMSO/H_2O at 30 °C under blue LEDs irradiation for 90 minutes. Worthy of note, these reaction conditions tolerated functional groups generally incompatible with standard amidation protocols such as carboxylic acids and unprotected amines. The oxamate scope was wide, including *N*-alkyl and *N*,*N*-dialkyl carbamoyl groups, sterically encumbered amines, and chiral starting materials, which showed no loss in optical purity. In addition to quinoline, other heterocyclic systems such as isoquinolines, quinoxaline, and phthalazine performed well under standard

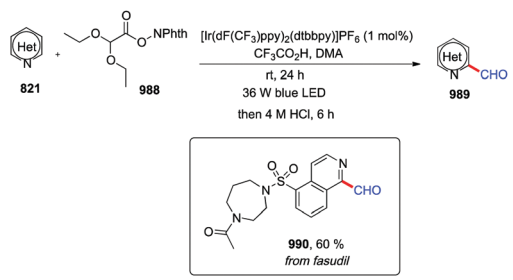

Scheme 172 Formylation of heteroarenes.

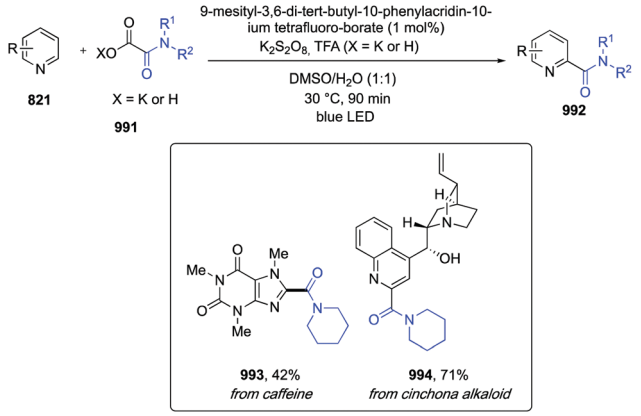

Scheme 173 Carbamoylation of heteroarenes.

conditions. As examples of complex biorelevant scaffolds, the authors explored the late stage carbamoylation of caffeine and cinchona alkaloid (**992** and **994**, Scheme 173).

4.2.3 Acylation of quinoxaline-2(1*H*)-ones. Quinoxalin-2(1*H*)-ones **995** could be acylated at position 3- *via* a visible light promoted decarboxylative process by using α-oxo-carboxylic acids (*e.g.* **996**) as acyl source (Scheme 174).[241]

Notably, the protocol was efficient in an aqueous medium and did not require a photoredox catalyst. Accordingly, the transformation relied on the formation of a hypervalent iodine(III) reagent *via* ligand exchange of a 2-oxo-carboxylic acid with PIDA. A photo-triggered I–O bond homolysis provided an O-centered radical along with a I-centered radical, which upon fragmentation, afforded the key acyl radical intermediate. Addition of the latter to the C=N bond of quinoxaline-2(1*H*)-one formed a N-centered

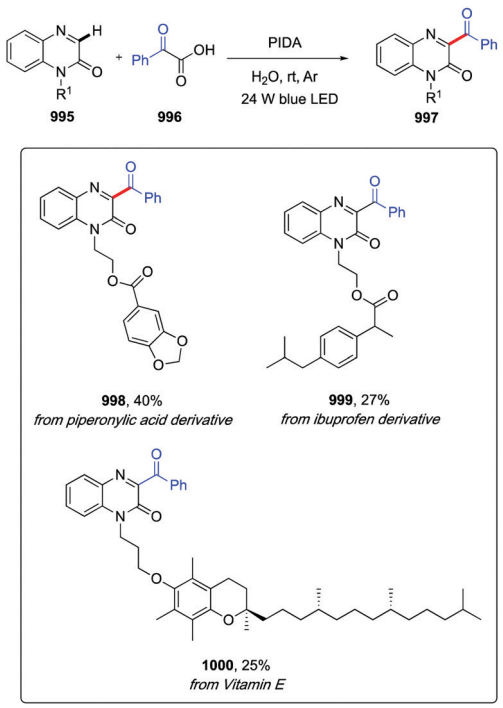

Scheme 174 Acylation of quinoxaline-2(1*H*)-ones.

radical, further undergoing a 1,2-H migration to C-radical and finally oxidative deprotonation to give the acylated heterocycle. The developed protocol proved to be efficient with a wide range of aromatic 2-oxo-carboxylic acids, while aliphatic congeners afforded the corresponding acylated products in poor yields. On the other hand, the usefulness of this method in the late-stage modification of bioactive scaffolds was exemplified with piperonylic acid, ibuprofen, and vitamin E (**998–1000**, Scheme 174).

4.3 Formation of C(sp^2)–X and C(sp^3)–X bonds

4.3.1 Sulfonylation of quinoline N-oxides. L.-Y. Xie *et al.* developed a deoxygenative C2-sulfonylation of quinoline *N*-oxides **1001** with sulfinic acids **1002** promoted by an organic dye photocatalyst (Scheme 175).[242]

The reaction proceeded under exceptionally mild conditions consisting of Na_2 eosin Y as catalyst, an acetone/H_2O (1.5 : 1) mixture as the solvent, under air and 5 W blue LEDs irradiation at room temperature. Various substituted quinoline *N*-oxides were efficiently derivatized with *p*-toluenesulfinic acid, tolerating sterically hindered groups as well as electron-donating or electron-withdrawing groups. The scope of the sulfinic acid also proved to be wide as shown by 16 examples with yields ranging between 63 and 83%. Late-stage functionalization of cloquintocet-mexyl, after prior *m*-CPBA promoted oxidation to *N*-oxide derivative, was also reported in a good 63% yield (**1004**, Scheme 175).

4.3.2 Azolylation. 2-Arylimidazoheterocycles (*e.g.* caffeine **604**, Scheme 176) could be coupled with azoles under photoredox catalytic conditions without requiring any external oxidant.[243] This cross dehydrogenative coupling, endowed with a high regioselectivity, was efficiently promoted by merging photoredox catalysis (Acr^+-Mes ClO_4) and a hydrogen evolution catalyst such as Co(dmgH)(dmgH_2)Cl_2 (**1006**) in DCE as a solvent under 3 W blue LEDs irradiation at room temperature for 24 hours. A number of diverse imidazo[1,2-*a*]pyridines bearing halogens, ester, and sulfone functional groups were smoothly coupled with 3,5-dimethylpyrazoles affording the desired products in excellent yields. Likewise, heterocycles such as imidazole and triazoles proved to be competent substrates, albeit with less efficiency. Azolylation of caffeine with pyrazole derivative **1005** was carried out in a moderate 27% yield (**1007**, Scheme 176).

4.3.3 C(sp^3)–N and C(sp^2)–N bonds formation. A decarboxylative C(sp^3)–N coupling of naturally abundant aliphatic carboxylic acids (**879**) with nitrogen nucleophiles (*e.g.* indazole **1008**) was accomplished by Y. Liang *et al. via* a synergistic combination of copper and photoredox catalysis (Scheme 177).[244]

Standard reaction conditions involved Ir(F-Meppy)$_2$(dtbbpy)PF_6 as the photocatalyst, CuTC (TC = thiophene-2-carboxylate) as the copper catalyst, BPhen or dOMe-Phen (dOMe-Phen = 4,7-dimethoxy-1,10-phenanthroline) as the ligand, BTMG (BTMG = 2-*tert*-butyl-1,1,3,3-tetramethylguanidine) as the base, under exposure to 34 W blue LEDs light. The protocol was efficient with a broad range of primary, secondary, and tertiary alkyl carboxylic acids, through iodonium activation, as well as with a vast array of electron-deficient nitrogen nucleophiles including *N*-heterocycles, aryl amides, aryl sulfonamides, phthalimides, cyclic carbamates, and anilines. The corresponding *N*-alkyl derivatives were obtained in good to excellent yields, at room temperature, in short reaction times, and in high regioselectivity when the substrates contained several amino-groups. Moreover, the mild reaction conditions were compatible with a range of functional groups such as terminal olefins and alkynes, internal alkenes, aryl bromides and iodides, alcohols, ketones, nitro groups, esters, and protected amines. Applications as a tool for late-stage functionalization of pharmaceutical compounds included, but were not limited to celecoxib, vemurafenib, pioglitazone, riluzole and metaxalone (**1004–1017**, Scheme 177).

C(sp^2)–N bond formation between an aryl halide (**1018**) and different nucleophiles could be achieved *via* an S_NAr reaction of

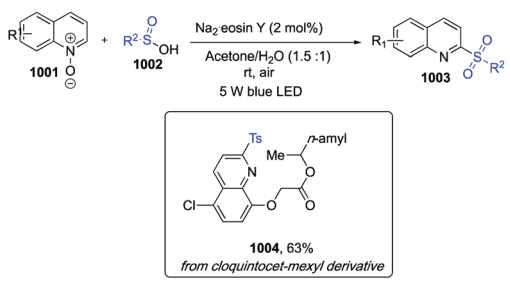

Scheme 175 Sulfonylation of quinoline *N*-oxides.

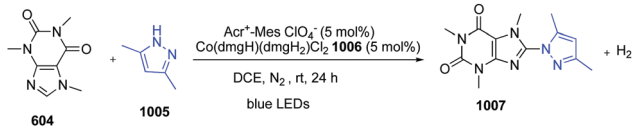

Scheme 176 Azolylation of heteroarenes.

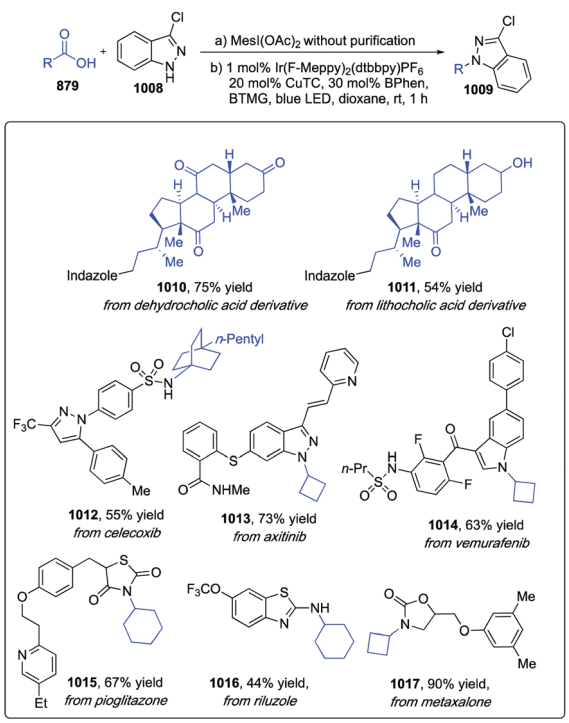

Scheme 177 C(sp^3)–N and C(sp^2)–N bonds formation.

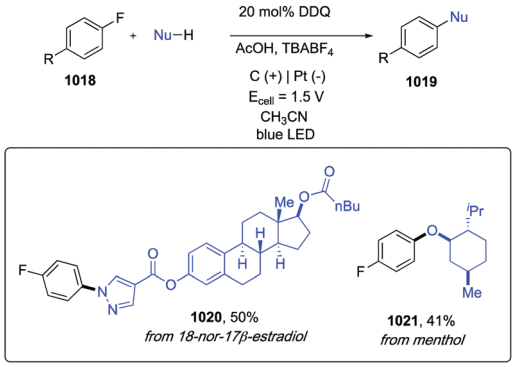

Scheme 178 C(sp^3)–N and C(sp^2)–N bonds formation.

unactivated aryl fluorides under electrophotocatalytic conditions (Scheme 178).[245]

The protocol, developed by H. Huang and T. H. Lambert, exploited 2,3-dichloro-5,6-dicyanoquinone (DDQ) as the photosensitizer, in an undivided cell (E_{cell} = 1.5 V) under irradiation with white light and in the presence of $TBABF_4$ and AcOH in MeCN. By applying these conditions, a wide number of functionalized nitrogen-containing heteroarenes were arylated in moderate to good yields. Likewise, the scope of the fluoroarenes proved to be good, albeit strongly electron-withdrawing groups completely deactivated the substrates. Additionally, replacement of heteroarenes with other nucleophiles such as alcohols provided alkyl arylethers in moderate to good yields. LSF of bioactive molecule derivatives such as 18-nor-17β-estradiol and menthol was also performed (**1020** and **1021**, Scheme 178).

5. Functionalization of alkyl and aryl halides

The use of alkyl and aryl halides as radical precursors is largely documented in both pioneering historic and recent innovative reports.[246] Such radicals, as illustrated above can undergo addition to a plethora of acceptors such as activated and unactivated olefins, including styrenes, silyl enol ethers and enamides to afford linear or cyclic adducts. Addition to a strained carbocycle[1.1.1]propellane enables the introduction of a pharmaceutically valuable bicyclo[1.1.1]pentane moiety (see Section 3.1.5). Derivatization of aryl halides with functional groups such as methyl-, alkyl-, trifluoromethyl-, perfluoroalkyl- as well as the introduction of amino or carbonyl groups have been made possible by the merging of photoredox and transition metal (mainly nickel) catalysis starting from a plethora of bench stable radical precursors, including potassium organotrifluoroborates (Molander crosscoupling), boracene-based alkyl borates, cyclic alcohols, and epoxides, to cite a few.

5.1 Structural modification of alkyl- and alkenyl-halides

5.1.1 Giese addition to electron-poor olefins. Unactivated alkyl iodides could undergo a Giese addition to electron-poor olefins with a manganese catalyst, decacarbonyl dimanganese

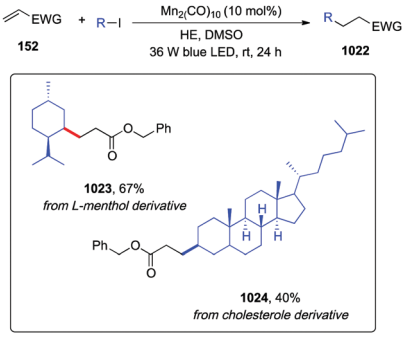

Scheme 179 Giese addition to electron-poor olefins.

$Mn_2(CO)_{10}$, which had the key advantages to be inexpensive, earth-abundant and readily available (Scheme 179).[247]

Under visible-light irradiation such a catalyst homolyzed to form a manganese-centered radical [$^{\bullet}Mn(CO)_5$], able to selectively abstract the iodide atom from an alkyl iodide to afford an alkyl radical intermediate, which could subsequently add to olefins. The reaction proceeded in the presence of a Hantzsch ester as a reductant, in DMSO, and under 36 W blue LEDs irradiation at room temperature at 24 h. The scope of this transformation was further extended to alcohols, *via in situ* generation of the corresponding alkyl iodides with a pretreatment with I_2, PPh_3, and imidazole in DCM (Wittig conditions), as shown in Scheme 179 for transformation of L-menthol and a cholesterol analogue into derivative **1023** and **1024**, respectively.

5.1.2 Addition to silyl enol ethers and enamides. Tertiary, secondary, and primary alkyl bromides (**323**) could be exploited as alkylating agents for silyl enol ethers and enamides (**1025**) in the presence of a palladium catalyst and a dual phosphine ligand system under blue LEDs irradiation (Scheme 180).[248] The reaction delivered stereoselectively α-alkylated ketones and *N*-acyl ketimines (**1026**). Additionally, the latter could be further subjected to chiral phosphoric acid-catalyzed asymmetric reduction with Hantzsch ester to afford the corresponding *N*-acyl-protected α-arylated aliphatic amines in up to 99% enantioselectivity. Experimentally, the alkylative protocol proceeded in 1,4-dioxan at room temperature and in the presence of $Pd(PPh_3)_4$, Xantphos, KOAc, and 10 equiv. of water. Investigation of the substrate scope revealed an extraordinary functional group tolerance with yields up to 94%. The synthesized α-alkylated imines included also steroid derivatives **1027** and **1028** from their corresponding bromide derivatives (Scheme 180).

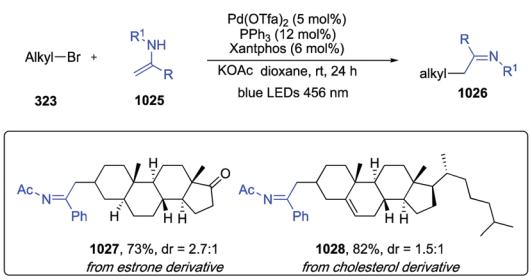

Scheme 180 Addition to silyl enol ethers and enamides.

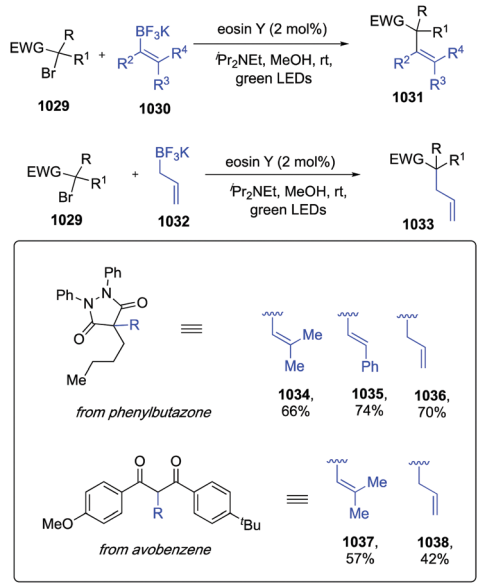

Scheme 181 *ipso*-Vinylation and allylation.

5.1.3 *ipso*-Vinylation and allylation. D. Leonori *et al.* reported a metal-free vinylation and allylation of electrophilic radicals (*e.g.*, malonyl radical), generated from a bromo-precursor (**1029**), with vinyl potassium trifluoroborate reagents (**1030**),[249] which are characterized by chemical stability, ease of preparation, and commercial availability (Scheme 181). The reaction was performed by using an organic photocatalyst such as eosin Y, $^{i}Pr_2NEt$ as the base in MeOH under green LEDs irradiation (530 nm), at RT, overnight (Scheme 181). The process showed good functional group compatibility and was applied to the *ipso*-vinylation and -allylation of the veterinary NSAID phenylbutazone and the sunscreen agent avobenzone (**1034–1038**, Scheme 181).

A protocol to accomplish the alkenylation of unactivated alkyl bromides (**323**) under visible-light irradiation was reported by Q.-Q. Zhou *et al.* (Scheme 182).[250] Such a transformation harnessed $[Ir(dF(CF_3)ppy)_2(dtbbpy)]PF_6$ as a photoredox catalyst and $(TMS)_3SiH$ as the atom transfer agent, K_2CO_3 as a base in MeCN as a solvent, at room temperature for 24 h. These mild conditions enabled the conversion of a wide range of alkyl bromides into their corresponding alkenylated adducts with good efficiency and high chemoselectivity. As example of complex biorelevant substrate an estrone-derived bromide was alkenylated to **1040** in 61% yield (Scheme 182).

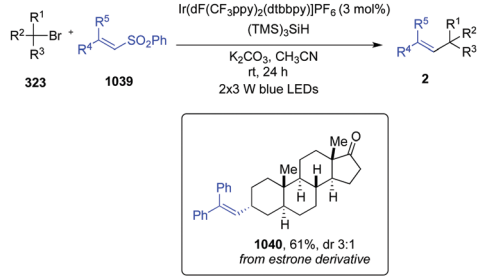

Scheme 182 *ipso*-Vinylation and allylation.

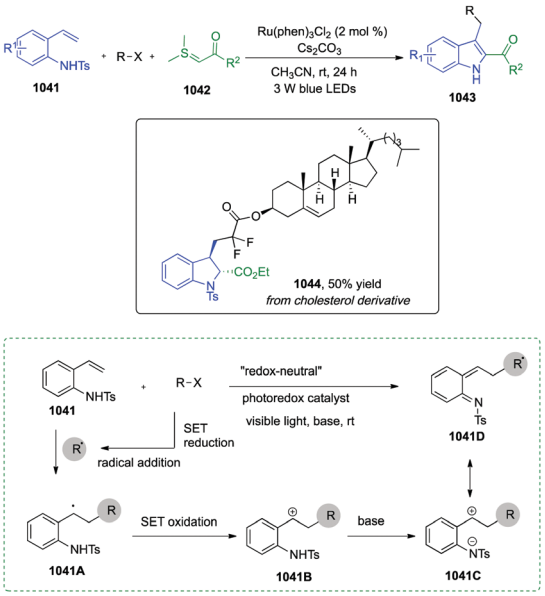

Scheme 183 Formation of heterocyclic adducts.

5.1.4 Formation of (hetero)cyclic adducts. In a three-component visible-light catalyzed reaction involving halides, vinyl anilines **1041** and sulfur ylides **1042**, Y.-Y. Liu *et al.* reported a convergent synthesis of indoles **1043** (Scheme 183).[251]

Here, simple halides could be transformed into electrophilic carbon-radicals upon SET and add to the alkene moiety of a vinylamine, generating a radical intermediate **1041A**, which after another SET and deprotonation led to a zwitterionic species **1041C** in resonance with its neutral aza-*ortho*-quinone-methide structure **1041D** (Scheme 183). The latter underwent a [4+1] cycloaddition with sulfur ylide to give the corresponding indoline; a Cs_2CO_3-mediated E1-elimination and aromatization gave the final indole derivative. The reaction was shown to proceed under mild reaction conditions, using a ruthenium-photocatalyst, an inorganic base such as Cs_2CO_3, and MeCN as the solvent under 3 W blue LEDs irradiation at room temperature for 24 h. Different radical sources, including perfluoroalkyl- and functionalized halides proved to be successfully engaged in the reaction, as well as both aryl- and alkyl-sulfur ylides, and both electron-poor and electron-rich vinyl anilines. As model bioactive scaffold, a cholesterol-derived bromide was transformed into its indoline-derivative **1044**, in a medium yield of 50% and as a single stereoisomer (Scheme 183).

A visible light promoted atom transfer radical cyclization (ATRC) of unactivated alkyl iodides was reported by Y. Shen *et al.* (Scheme 184).[252] The protocol was characterized by a high chemoselectivity, avoiding parasitic hydrogen atom transfer pathways. Usually, ATRCs or atom transfer radical additions (ATRAs) involve activated halides possessing weak C(sp^3)–X bonds adjacent to π-systems, heteroatoms, or electron-withdrawing groups, which favor rapid SET events. Besides, unactivated alkyl halides show very high redox potentials, difficult to match the photocatalysts redox potential. This report was the first one to meet the challenge of a redox-neutral ATRC of unactivated halides. After extensive optimization of reaction conditions, the desired

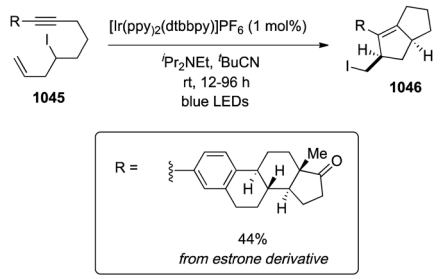

Scheme 184 Formation of heterocyclic adducts.

ATRC was carried out with $[Ir(ppy)_2(dtbbpy)]PF_6$, $^iPr_2NEt$ under blue LEDs irradiation in *t*-BuCN as solvent, at room temperature for 12–48 h. The use of *t*-BuCN in place of the more popular MeCN was essential to achieve high yields and suppress HAT. The reaction scope was wide, as it involved alkyl iodides with silyl groups, nitriles, alkenes, free alcohols, silyl ethers, aldehydes, carbamates, and even alkyl or aryl halides. Interestingly, aromatic- or aliphatic-substituted alkynes did not interfere. Furthermore, secondary alkyl iodides bearing an allyl group led to a 5-*exo-trig* cyclization, followed by rapid interconversion of the *in situ* formed vinyl radicals and a final iodine transfer, resulting in a bicyclic skeleton as exemplified for estrone derivative **1046** (Scheme 184).

5.1.5 Introduction of a bicyclo[1.1.1]pentane moiety into both alkyl and (hetero)aryl iodides. Organic halides can add to carbocycle[1.1.1]propellane **1046** under visible-light catalytic conditions to afford the pharmaceutically relevant bicyclo[1.1.1]-pentane derivatives **1047** (Scheme 185).[253]

Such structural frameworks are routinely used in drug discovery programs as nonclassical bioisosters of aromatic rings, with improved physico-chemical and pharmaco-kinetic properties.

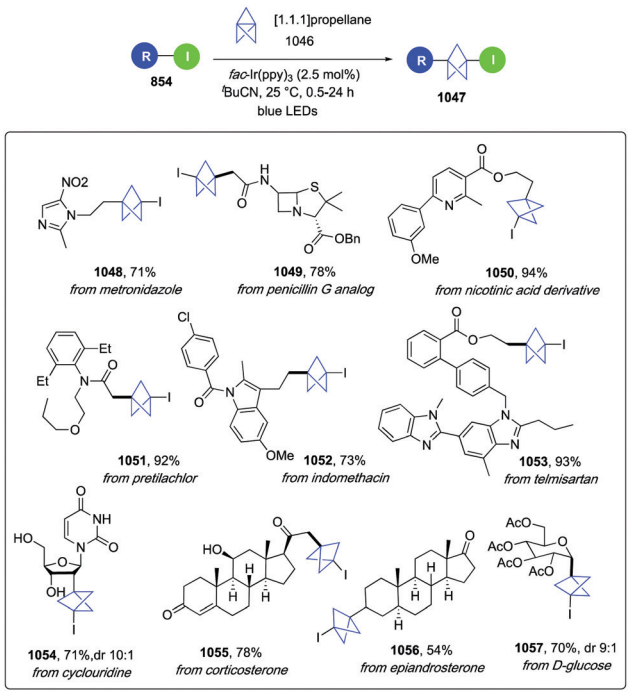

Scheme 185 Introduction of a bicyclo[1.1.1]pentane moiety.

In this report, bicyclopentylation of both sp^2 and sp^3 carbon–halogen bonds proceeded in the presence of *fac*-Ir(ppy)$_3$, *t*-BuCN as the solvent under blue LEDs irradiation at room temperature for 0.5–24 h. The reaction scope was exquisitely wide as a number of functionalized aryl and heteroaryl iodides, primary and secondary alkyl iodides, (hetero)benzylic- and α-electron-withdrawing substituted alkyl iodides smoothly underwent the desired transformation under standard conditions in good to excellent yields. Remarkably, the mechanistic pathway relied on an atom transfer radical addition (ATRA), so that the final compounds bear an iodine substituent, potentially allowing further derivatization. Late-stage bicyclopentylation of drugs and biorelevant molecules, such as metronidazole, penicillin G, nicotinic acid, pretilachlor, indomethacin, telmisartan, cyclouridine, corticosterone, D-glucose, and epiandrosterone afforded derivatives **1048–1057** (Scheme 185).

5.2 Structural modification of alkyl- and alkenyl-halides

5.2.1 Hydrodehalogenation and Br/D exchange. Reductive dehalogenation of unactivated aryl and alkyl bromides and chlorides could be accomplished by using a palladium complex under visible light irradiation (Scheme 186).[254] The scope of the transformation was also extended to reductive cyclization, dehalogenative deuteration, and inter- and intra-molecular radical addition with excellent functional group tolerance and broad substrate scope. The reaction mechanism relied on the direct photoexcitation of the palladium-based catalyst, followed by a SET reduction of the organic halide, which then underwent a fragmentation to generate a C-centered radical. Representative deuteration of a menthol-derived aryl bromide with deuterated isopropanol into compound **1059** was accomplished in 88% yield as shown in Scheme 186.

5.2.2 Methylation of (hetero)aryl chlorides. The group of A. G. Doyle developed a protocol to carry out dual photoredox/nickel catalyzed methylation of (hetero)aryl (**1060**) and acyl chlorides (**1061**) using trimethyl orthoformate $[(MeO)_3CH]$ as a methyl radical source (Scheme 187).[255]

The reaction mechanism relied on the β-scission of a trimethylorthoformate C-centered radical generated upon chlorine-mediated hydrogen atom transfer. Optimum yields were achieved by employing $[Ir(dF(CF_3)ppy)_2(dtbbpy)]PF_6$ as the photosensitizer, $NiCl_2$·glyme and dtbbpy as the nickel source and the ligand, respectively, $[(MeO)_3CH]$ as both the methyl source and the solvent, in the presence of K_3PO_4 as a base under 34 W blue LEDs irradiation at room temperature for 48 hours. The substrate scope was investigated with a wide range of functionalized aryl

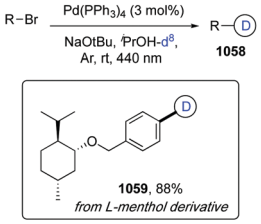

Scheme 186 Hydrodehalogenation and Br/D exchange.

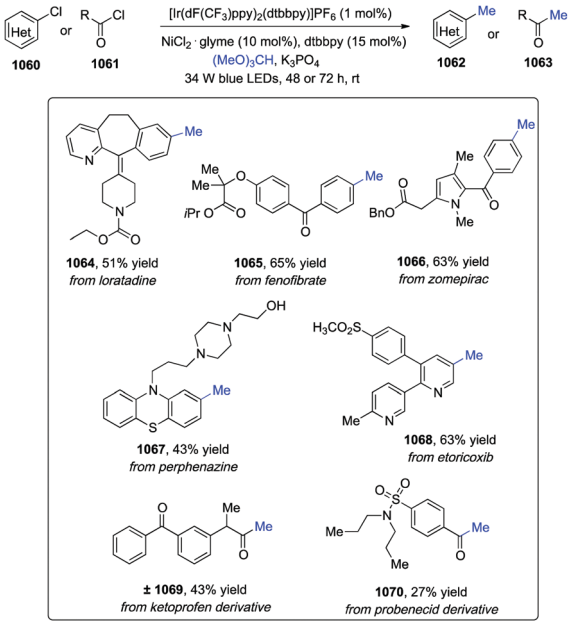

Scheme 187 Methylation of (hetero)aryl chlorides.

and heteroaryl chlorides, as well as acyl chlorides, providing methylated adducts in medium to good yields. The robustness of the method was highlighted in the late-stage methylation of complex aryl chloride- and bromide-containing bioactive scaffolds such as loratadine, fenofibrate, zomepirac, perphenazine, and etoricoxib, which albeit bearing two equivalent aryl chlorides, underwent selective monomethylation in 55%, as a result of the influence of electronic effects on the catalytic system (**1064–1068**, Scheme 187). The method was also applied to the LSF of acid chlorides prepared from drugs such as ketoprofen and probenecid (**1069** and **1070**, Scheme 187).

5.2.3 Deaminative alkylation of (hetero)aryl bromides. Recently, J. Yi *et al.* developed a cross-electrophilic deaminative coupling strategy exploiting Katritzky salts **1071** as alkyl radical precursors under the assistance of a dual photoredox-nickel catalytic system (Scheme 188).[256] The protocol required $NiBr_2$(dtbbpy), the organic dye 4CzIPN, TEA as a base, and THF as the solvent, under blue LEDs irradiation at room temperature for 24 h. These mild reactions were successfully applied to a broad range of both electron-rich and electron-poor functionalized aryl bromides (**12**), including pinacol boronic esters, aryl chlorides, lactones, sulfonamides, difluoroaryl bromides, and several heteroaryl systems. Alkylpyridinium salts **1071** showed as well a wide functional groups tolerance. To demonstrate the synthetic utility of this transformation as a LSF tool, the alkyl pyridinium salt of mexiletine was prepared and cross-coupled with two different aryl bromides to give, for instance, derivatives **1073** and **1074**, while bromoloratadine was employed as an example of complex starting aryl bromide (**1075**, Scheme 188).

5.2.4 Alkylation with neutral C(sp^3)–H bonds. Aryl and heteroaryl bromides have been reported as competent substrates to be alkylated with a set of aliphatic C(sp^3)–H bonds containing organic frameworks *via* the combination of polyoxometalate-facilitated HAT and nickel catalysis under visible-light catalysis (Scheme 189).[257] This dual-catalytic protocol enabled the generation of carbon-centered radicals from strong, neutral C–H bonds, which acted as nucleophiles with aryl bromides to afford their corresponding alkylated cross-coupling adducts. Experimentally, the reaction required TBADT (tetrabutylammonium decatungstate), Ni(dtbbpy)Br_2, K_3PO_4 as a base in MeCN and a 34 W 390 nm (black light) lamp as the photon source at room temperature. These mild conditions provided a wide scope and a good functional group tolerance, as shown in the late-stage alkylation of celecoxib to derivatives **1068–1070** (Scheme 189).

5.2.5 Alkylation with α-aminomethyltrifluoroborates. The same group of G. A. Molander demonstrated that, thanks to the synergistic combination of iridium photoredox and nickel catalysis, it was possible also to convert aryl and heteroaryl bromides (**12**) into benzylamine derivatives (**1083**) starting from the methyltrifluoroborate adducts of readily available Boc-protected amino acid methyl esters (**1081**) (Scheme 190).[258]

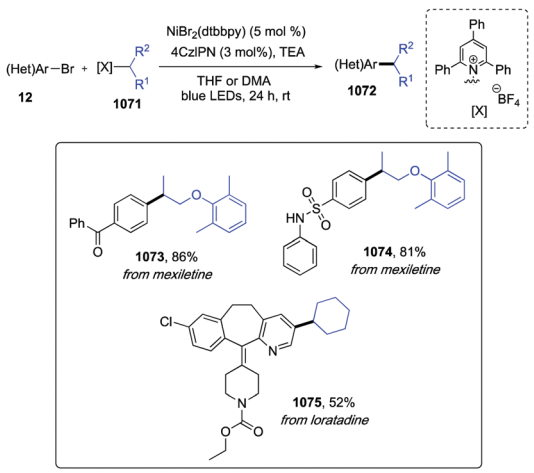

Scheme 188 Deaminative alkylation of (hetero)aryl bromides.

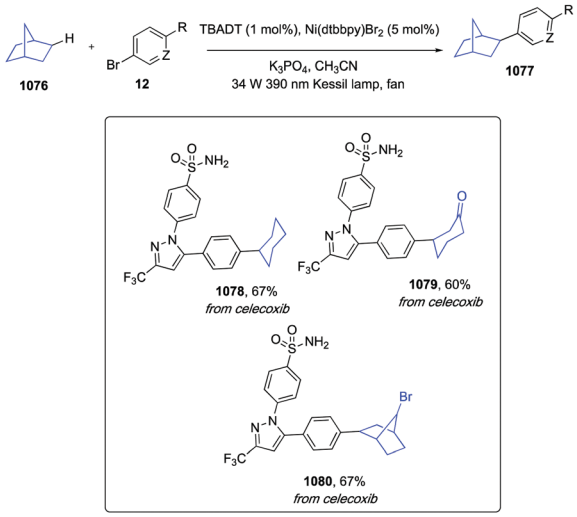

Scheme 189 Alkylation with neutral C(sp^3)–H bonds.

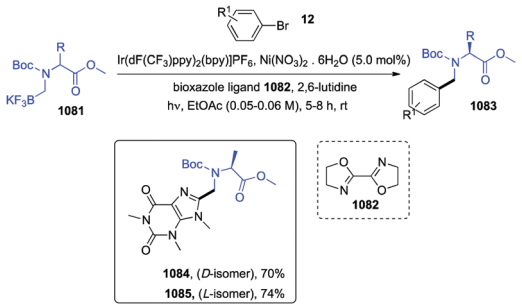

Scheme 190 Alkylation with α-aminomethyltrifluoroborates.

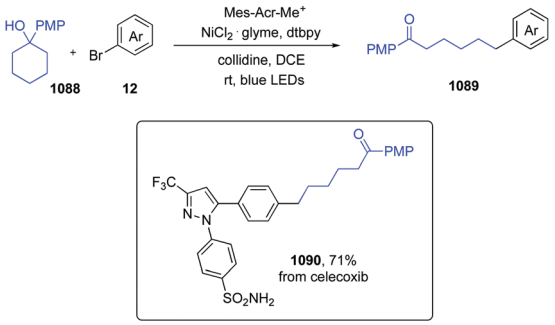

Scheme 192 Alkylation with cyclic alcohols.

The cross-coupling was efficiently carried out by using Ir[dF(CF_3)-ppy]$_2$(bpy)PF_6, Ni(NO_3)$_2$·6H_2O, a bioxazole ligand **1082**, 2,6-lutidine as a base, EtOAc as a solvent under irradiation with a 26 W CFL at room temperature for 5–8 hours. Aryl and heteroaryl bromides could accommodate a range of electron-withdrawing and electron-donating functional groups such as nitrile, amide, ester, aldehyde, phenol, ketone, sulfonamide, and trifluoromethyl groups, while the amino acid component included L-Ala, D-Ala, L-Val, and L-Ile, with retention of the chiral purity. As an example of complex heteroaryl bromide, caffeine was functionalized with the methyltrifluoroborate salts of both D- and L-Ala to give compounds **1084** and **1085** in good yields (Scheme 190).

5.2.6 Alkylation with boracene-based alkyl borates. An alternative strategy to achieve methylation and alkylation of aryl bromides relied on the formation of tertiary, secondary, and primary alkyl radicals upon direct visible light excitation of boracene-based alkylborates **1086** (Scheme 191).[259] This catalytic system, based on the photophysical properties of the organoboron molecule, did not require an external photoredeox catalyst. It was applicable to the introduction of a variety of C(sp^3) fragments *via* decyanoalkylation, Giese addition, and alkyl–aryl cross-coupling or three-component vicinal alkylarylation of alkenes. The alkyl radical precursors, that were stable to air/moisture, were readily synthesized from boracene and alkyllithium reagents and, remarkably, the boracene could be recovered at the end of the reaction and reused. Experimentally, the transformation required Ni(TMHD)$_2$ or Ni(acac)$_2$ as the nickel source in DMA as a solvent under blue LEDs irradiation. The aryl bromides/chlorides scope embodied both electron-rich and electron-poor substrates, as well as π-conjugated β-bromostyrene. Upon modification of the standard conditions, methylation of complex bioactive substrates such as indomethacin was achieved in a good 80% yield (**1087**, Scheme 191).

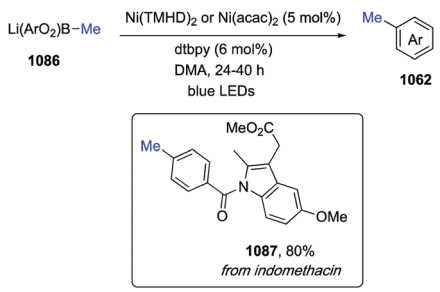

Scheme 191 Alkylation with boracene-based alkyl borates.

5.2.7 Alkylation with cyclic alcohols. Recently, L. Huang *et al.* developed a metallaphotoredox protocol to activate cyclic alcohols (**1088**) for the formation of remote carbon-centered radicals upon C–C cleavage, and to promote a further nickel catalyzed cross-coupling with aryl bromides (Scheme 192).[260]

More in detail, the reaction proceeded in DCE, with Mes-Acr-Me$^+$ as the photosensitizer, $NiCl_2$·glyme as the nickel source and dtbbpy as the ligand, and 2,4,6-collidine as a base under blue LEDs irradiation at room temperature for 48 hours. Evaluation of a range of electrophilic coupling partners led to a wide substrate scope including both electron-rich and electron-poor aryl bromides, as well as a variety of heteroaromatic motifs. Scope of the tertiary alcohols included from 3- to 15-membered cycles, bridged rings, and linear alcohols. Late-stage functionalization of a celecoxib derivative led to **1090** in a good 71% yield (Scheme 192).

5.2.8 Synthesis of cyclobutanes. Functionalization of electrophilic aryl iodides (**1092**) with a cyclobutyl ring could be accomplished through a strain-release-driven methodology starting from bicyclo[1.1.0]butanes (**1091**, BCBs, Scheme 193).[261] The protocol developed by M. Ociepa *et al.* relied on a polarity-reversal strategy, where a nucleophilic C-centered BCB radical formed under light-driven cobalt catalysis. Besides Co/Nickel catalyzed cross coupling, the authors also explored Giese-type addition of such radicals with alkenes. After extensive optimization by using heptamethyl cobyrinate (hydrophobic vitamin B_{12}) as a cobalt-based catalyst, Ni(DME)Cl_2 along with dtbbpy as a ligand, Zn, ammonium chloride in acetone under blue LEDs irradiation, a wide number of functionalized aryl iodides were chemoselectively cyclobutylated in good to excellent yields. The potential of this method as a tool for the late-stage cyclobutylation of complex bioactive molecules was investigated by using dehydrocholic acid, the NSAID indomethacin, the uricosuric probenecid, and the antibiotic fluoroquinolone (**1094–1097**, Scheme 193).

5.2.9 Alkylation with epoxides. Hetero(aryl)iodides (**1092**) could undergo a regioselective cross coupling reaction with epoxides (**1098**) catalyzed by a triple catalytic system involving a nickel- and a titanium-based catalyst, and an organic photosensitizer (Scheme 194).[262] The mild devised conditions consisted of 4CzIPN as the photocatalyst, Cp_2TiCl_2 and $NiBr_2$•diglyme as the titanium and the nickel source, respectively, Et_3N as a sacrificial electron

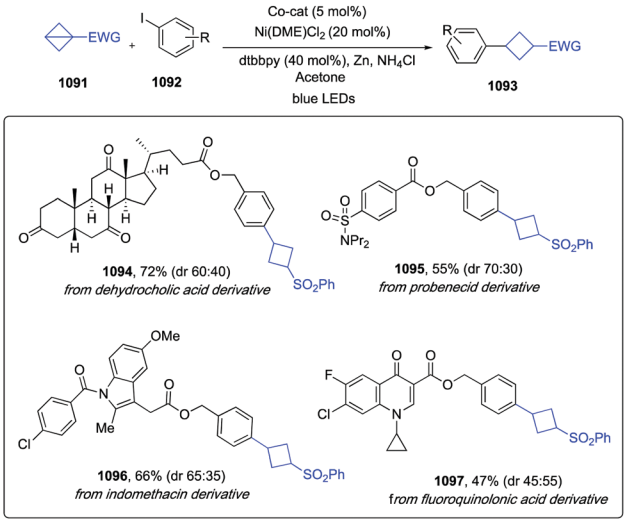

Scheme 193 Synthesis of cyclobutanes.

donor in DMF under irradiation with 34 W blue LEDs at room temperature for 24–60 hours. Three different classes of epoxides. *i.e.* styrene oxides, cyclic epoxides, and aliphatic epoxides showed to be amenable to the transformation by selecting the proper ligand, *i.e.* piperidyl amidine, BPhen, and *t*-Bu-terpy, respectively. The scope was broad, with tolerated functional groups including ethers, esters, double bonds, imides, halogens, and ketones as exemplified in the late-stage derivatization of estrone-derived epoxide to **1100** (Scheme 194).

5.2.10 Synthesis of cyclopentanes. (Hetero)aryl bromides and chlorides (**623**) could be harnessed, in a three-component photoinduced cross-coupling and in combination with radical precursors and dienes (**1101**), to achieve saturated carbocycles such as cyclopentanes **1103** (Scheme 195).[263] Thoroughly, a sodium sulfinate salt **1102** was exploited as sulfonyl radical precursor ($PhSO_2^{\bullet}$); once formed, the S-centered radical added to the diene triggering a 5-*exo-trig* cyclization forming a C-centered radical. Interception of the latter by Ni^0 and subsequent oxidative addition of an aryl halide yielded a Ni^{III} complex, which delivered the final product *via* reductive elimination. The transformation was promoted by $[Ir(dtbpy)(bpy)_2]PF_6$ as a photoredox catalyst, $NiCl_2{\cdot}6H_2O$ as a nickel source, 4,4′-di-*tert*-butyl-2,2′-bipyridine (dtbbpy) as a ligand in MeCN under blue LEDs irradiation at room

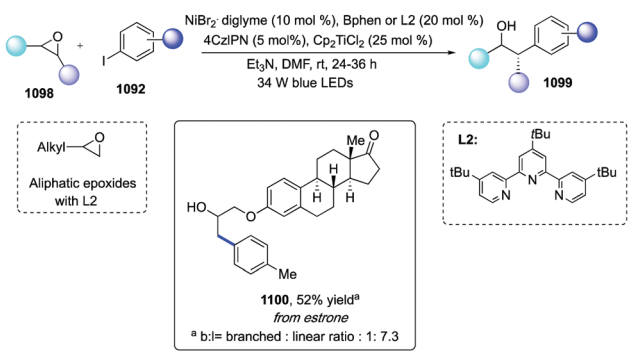

Scheme 194 Alkylation with epoxides.

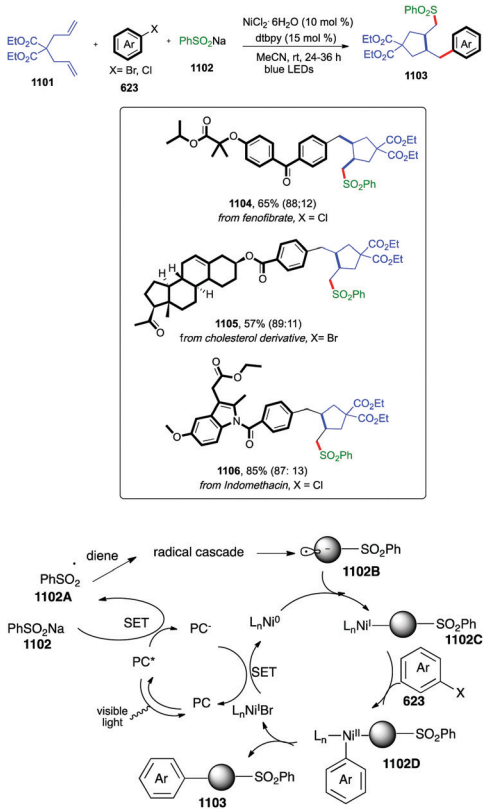

Scheme 195 Synthesis of cyclopentanes.

temperature for 20 hours. By applying these conditions, a number of functionalized aryl- and heteroaryl-bromides underwent the metallaphotoredox conversion to cyclopentane derivatives in good to excellent yields and with diastereoselectivities consistent with previous reports on the stereochemistry of radical cyclizations. As for the radical acceptors, the reaction was not limited to 1,6-dienes, being amenable to more challenging substrates such as 2,5-norbornadiene and 1,5-cyclooctadiene. The exquisite functional group tolerance was further showcased with fenofibrate, cholesterol, and indomethacin **1104–1106** (Scheme 195).

5.2.11 Activation of alkyl and aryl halides *via* halogen-atom transfer (XAT). Recently, the groups of D. Leonori and F. Juliá reported the exploitation of aminoalkyl radicals, easily accessible from simple amines, as halogen-atom transfer agents for the homolytic activation of both alkyl and aryl halides.[264] The latter could be engaged in a wide range of redox transformations such as deuteration, alkylation, allylation, olefination, and arylation (Scheme 196).

Notably, the method relied on the ability of nucleophilic α-aminoalkyl radicals to abstract halogen atoms through polarized transition states, in analogy to the classical tin and silicon radicals. The thermodynamic driving force was provided by the conversion of a resulting α-haloamine into an iminium salt. Standard experimental conditions featured 4CzIPN as an organic photocatalyst, a tertiary amine (changing on the basis of the starting organic halides; *e.g.* triethylamine for alkyl iodides and tribenzylamine for alkyl bromides) in a 10 : 1 mixture of MeCN/H_2O as a solvent system at room temperature for 16 hours under blue LEDs

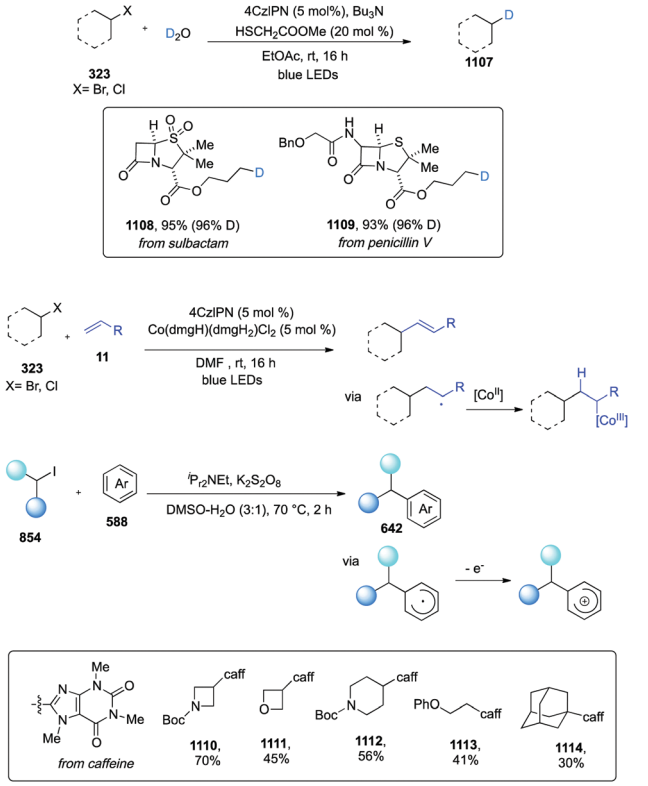

Scheme 196 Activation of alkyl and aryl halides *via* halogen-atom transfer (XAT).

irradiation (Scheme 196). Such conditions were applied to a wide range of organic halides (**323**) in order to accomplish dehalogenation and deuteration reactions as well as hydroalkylation, allylation, olefination (metallaphotoredox conditions), and (hetero)arylations. Representative biorelevant scaffolds included sulbactam and penicillin V, that were deuterated into **1108** and **1109**, while caffeine was alkylated into different derivatives **1110–1114** (Scheme 196).

5.2.12 Trifluoromethylation of (hetero)aryl bromides. Bromoarenes (**12**) could be trifluoromethylated, by exploiting a dual photoredox/copper catalysis able to promote the formation of an aryl radical through a silyl radical halogen abstraction, and to subsequently trigger an aryl radical-capture mechanism with a Cu(II)–CF_3 adduct (Scheme 197).[265] This metallaphotoredox catalytic platform required the supersilanol **1116** as silyl radical precursor, an electrophilic CF_3 reagent **1115** (dMesSCF$_3$, dimesityl sulfonium triflate salt), Ir(dFFppy)$_2$(4,4′-dCF$_3$bpy)PF$_6$ as the photoredox catalyst, and $CuBr_2$·2LiBr in acetone as the solvent at room temperature and under blue LEDs irradiation. A wide range of aryl and heteroaryl bromides was successfully trifluoromethylated in good to excellent yields, sometimes with slight variations to the above cited standard conditions. As a further evidence of the reaction efficiency, marketed drugs such as celecoxib, gemfibrozil ethyl ester derivative, metaxalone, and rupatadine were efficiently functionalized to **1118–1121** (Scheme 197).

5.2.13 Difluoromethylation of (hetero)aryl bromides. Aryl and heteroaryl bromides (**12**) can undergo a silane-mediated

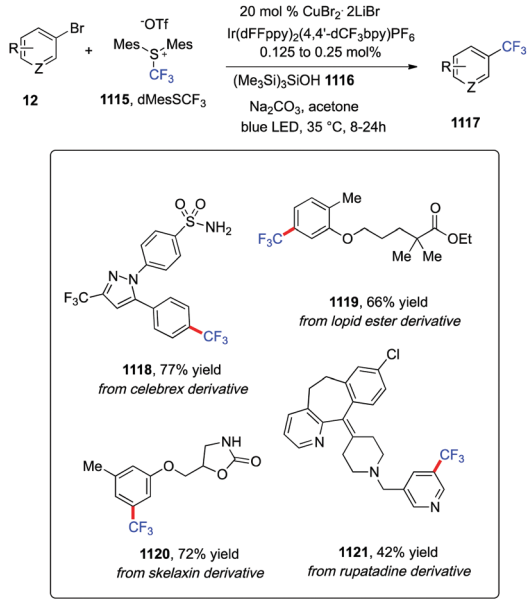

Scheme 197 Trifluoromethylation of (hetero)aryl bromides.

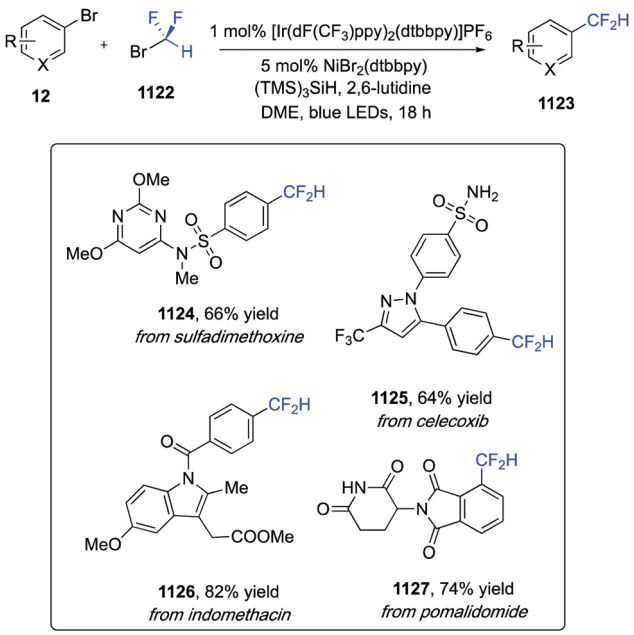

Scheme 198 Difluoromethylation of (hetero)aryl bromides.

difluoromethylation under dual photoredox/nickel catalysis (Scheme 198).[266]

Commercially available bromodifluoromethane **1122** was harnessed as an effective source of difluoromethyl radical *via* open-shell silyl-radical-mediated halogen abstraction. The reaction was promoted by [Ir(dF(CF$_3$)ppy)$_2$(dtbbpy)]PF$_6$, NiBr$_2$(dtbbpy), (TMS)$_3$SiH and 2,6-lutidine in DME under blue LEDs irradiation for 18 h at room temperature. For electron-deficient heteroaryl bromides, optimum yields were obtained using 4 equiv. of CF_2HBr, while electron-neutral and electron-rich aryls gave a better outcome with less equiv. (1–2). Tolerated functional

groups included esters, ketones, nitriles, and sulfones; heteroarenes and 5-membered bromoarenes were also found suitable electrophiles. Late-stage difluoromethylation was reported for sulfadimethoxine, celecoxib, indomethacin, and pomalidomide from the corresponding aryl bromide precursors in good yields (64–82% for **1124–1127**, Scheme 198).

5.2.14 Formylation of aryl chlorides. M. K. Nielsen *et al.* investigated the formylation of aryl chlorides (**1060**) *via* selective 2-functionalization of 1,3-dioxolane **1128** with dual photoredox-nickel catalysis (Scheme 199).[267] If compared to other traditional approaches for the introduction of a carbonyl functional groups into aromatic systems, this protocol was endowed with some key advantages as no carbon monoxide, pressurized gas, nor stoichiometric reductant was requested. The transformation was indeed promoted by an iridium photocatalyst, $NiCl_2$ DME and dtbbpy as cocatalyst, K_3PO_4, under 34 W blue LEDs irradiation for 72 h. 1,3-Dioxolane **1128** was used as both formyl precursor and solvent, at 0.05 M concentration. A subsequent mild acidic workup with 1 M HCl in acetone at room temperature, gave the desired aryl and heteroaryl aldehydes (**341**). Biologically relevant substrates involved (±)-chlormezanone, fenofibrate, procymidone, (±)-cyproconazole, monalide, (±)-hexythiazox, loratadine, diazepam, zomepirac, and salmon-gal to afford derivatives **1130–1139** (Scheme 199).

One more protocol to achieve formylation of aryl chlorides based on a dual nickel/photoredox catalytic system was reported by H. Huang *et al.* (Scheme 200).[268] The developed method harnessed 4CzIPN as organic dye photocatalyst and diethoxyacetic acid **1140** as precursor of a formyl-radical equivalent. The mild conditions identified allowed a broad reaction scope and a wide functional group tolerance as exemplified in the late-stage elaboration of fenofibrate and indomethacin methyl ester into the aldehyde derivatives **1141** and **1142**, respectively (Scheme 200).

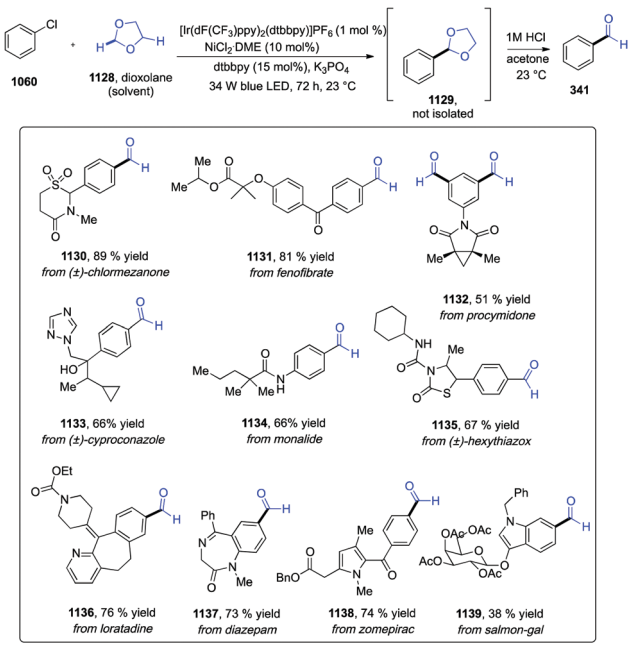

Scheme 199 Formylation of aryl chlorides.

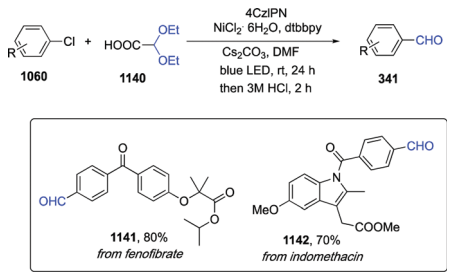

Scheme 200 Formylation of aryl chlorides.

5.2.15 Carbonylation reactions. (Hetero)aryl bromides (**12**) could be converted into amide derivatives (**1143**) starting from cheap and stable 4-carbamoyl-1,4-dihydropyridine **1143** as carbamoyl radical precursors by merging photoredox and nickel catalysis (Scheme 201).[269] The method required 4CzIPN as an organic photosensitizer, $NiCl_2$·glyme and 4,4′-dMeObpy as a ligand, Na_2CO_3 as a base in THF, while irradiating with a 460 nm HP single LED at room temperature for 16 hours. The broad scope, along with the functional group tolerance including unprotected alcohols, ethers, amides, esters, ketones, and sulfonamides, provided a valuable alternative approach to synthesize functionalized (hetero)aryl amides with respect to "classical" procedures requiring stoichiometric coupling agents and dehydrating agents. Additionally, this metallaphotoredox approach enabled the installation of amides bearing either electron-poor or sterically hindered substituents otherwise difficult to prepare. Functionalized aryl bromides bearing L-menthol and 2′,3′-*O*-isopropylideneuridine were used as examples of complex bioactive scaffolds to prove the synthetic potential of this method in the late-stage modification of medicinally relevant compounds (derivatives **1145** and **1146**, Scheme 201).

A more general approach to achieve conversion of both alkyl and aryl halides to acid chlorides, esters, amides, and ketones was developed by G. M. Torres and Y. Liu by exploiting a palladium catalytic-based system where concurrent excitation of palladium(0) and palladium(II) intermediates played key roles for the success of the target carbonylations (Scheme 202).[270]

Carboxylic acid chlorides could be formed by reacting aryl or alkyl bromides/iodides in the presence of carbon monoxide as the carbonyl source, [Pd(allyl)Cl_2]/DPE-Phos as a photoactive catalytic system, in the presence of Bu_4NCl and collidine, in toluene as a solvent under irradiation with a 40 W blue LED

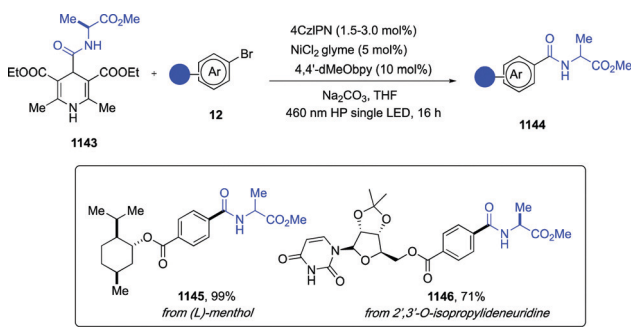

Scheme 201 Carbamoylation of (hetero)aryl bromides.

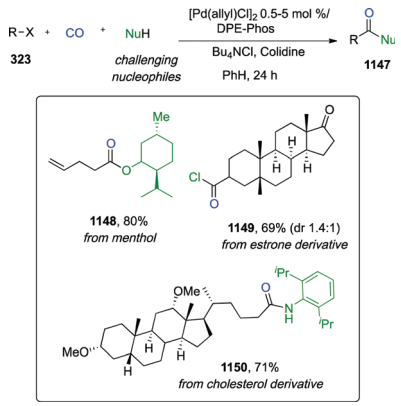

Scheme 202 Carbonylation of (hetero)aryl bromides.

for 24 hours. The presence in the reaction mixture of an additional nucleophile orthogonal to reaction conditions such as anilines, alcohols, or thiols provided amide, ester, and thioester adducts in good to excellent yields. Examples of complex bioactive substrates were also provided (**1148–1150**, Scheme 202).

5.2.16 Formation of benzylic ethers. B. J. Shields and A. G. Doyle reported the development of a C(sp^3)–H cross coupling of aryl chlorides and both cyclic and acyclic ethers enabled by the merging of iridium photoredox and nickel catalysis (Scheme 203).[271]

Interestingly, this process featured the generation of an intermediate chlorine radical, which acted as hydrogen atom abstractor from the ether in order to form the key alkyl radical intermediate finally undergoing the nickel assisted cross-coupling to give the benzyl ether derivatives. As a catalytic system, the iridium catalyst Ir[dF(CF_3)ppy]$_2$(dtbbpy)PF_6 was used, in combination with Ni(cod)$_2$ (cod = 1,5-cyclooctadiene), dtbbpy, and potassium phosphate under 34 W blue LEDs irradiation at room temperature. The ether selected as the coupling partner was also used as the reaction solvent. The scope of the transformation included a broad range of diversely functionalized aryl chlorides and both secondary and primary, cyclic or acyclic, ethers. Functional groups such as nitrile, ketone, aldehyde, amide, and alkene were well tolerated. As example of complex medicinally relevant scaffold, loratadine was converted into **1152** in an excellent 93% yield (Scheme 203).

A similar dual iridium photoredox and nickel catalytic system was used by I. Karakaya *et al.* to synthesize a diverse

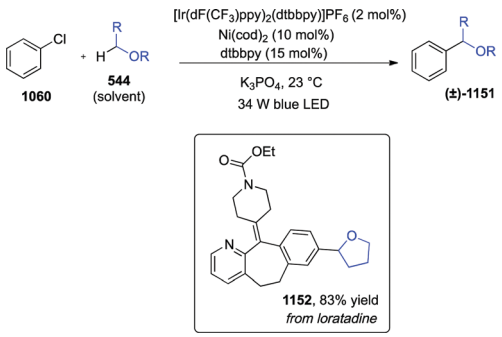

Scheme 203 Formation of benzylic ethers.

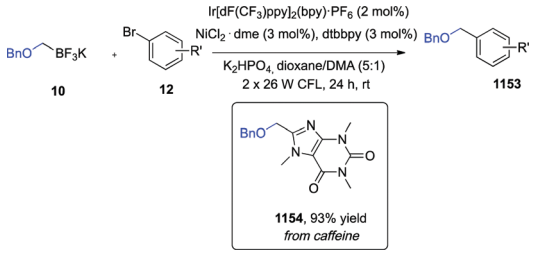

Scheme 204 Formation of benzylic ethers.

set of benzylic ethers (**1153**, Scheme 204) from α-alkoxymethyltrifluoroborate salts (**10**) and aryl and heteroaryl bromides.[272] The use of these salts, enabled a wide variability in the final ethers, as exemplified in the synthesis of allylic, dibenzylic, and tertiary benzylic ethers. The bromoarenes and heteroarenes scope included nitrogen-, oxygen, and sulfur containing 6-membered, or 5,6- and 6,6-membered fused rings. Among them, caffeine was functionalized to **1154** with an excellent 93% yield (Scheme 204).

5.2.17 Synthesis of phenols. Hydroxylation of aryl halides with water could be carried out *via* the merging of photoredox and nickel catalysis (Scheme 205).[273]

Both aryl bromides and less reactive aryl chlorides were effective substrates, while the OH group was generated from water, upon coordination with the nickel/ligand complex and subsequent deprotonation by an intramolecular base group on the ligand. Accordingly, no strong organic base or expensive noble-metal catalyst were required, with the reaction proceeding in a MeCN/DMF 1 : 1 mixture, in the presence of water and DIPEA, at 50 °C (for aryl bromides) or 120 °C (for aryl chlorides) under blue LEDs irradiation for 24 h. The hydroxylation scope tolerated a broad array of functional groups such as ketones, esters, nitriles, and ethers, and both aryl and heteroaryl halides reacted efficiently. Interestingly, the developed protocol enabled late-stage hydroxylation of fenofibrate, indomethacin, flumazenil, and a key intermediate in the synthesis of elbasvir in excellent yields (**1157–1160**, Scheme 205).

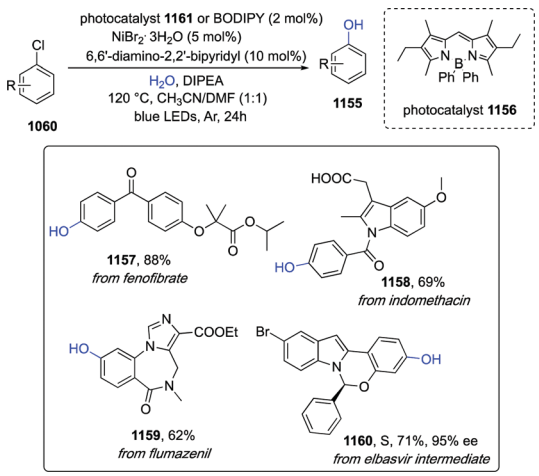

Scheme 205 Synthesis of phenols.

5.2.18 Thiolation of aryl iodides and bromides. A transition-metal-free C(sp^2)–S bond formation methodology to afford aromatic thioethers was established by B. Liu *et al.* (Scheme 206).[274] The reaction required Cs_2CO_3 as a base and proceeded in DMSO at room temperature under white LEDs irradiation. As for the reaction scope, a number of electron-rich and electron-poor aryl iodides and bromides were competent substrates, although longer irradiation times and electron-rich thiophenols were required to retain efficient yields with electron-rich or electron-neutral aryl iodides. In addition, aryl thiols bearing free hydroxy-, amine-, or carboxyl-groups did not necessitate protecting groups; likewise, thiols bearing fluoro-, chloro-, or bromo-substituents successfully afforded adducts suitable for further modifications. Late-stage thiolation of pharmaceuticals was exemplified for indomethacin, fenofibrate, moclobemide, and hydrochlorothiazide (**1163–1168**, Scheme 206).

Conversion of (hetero)aryl bromides (**12**, Scheme 207) to aliphatic thioethers (**1170**) could be accomplished by using hypervalent alkylsilicates.[275] The latter, indeed, are readily accessible precursors of alkyl radicals, which could act as hydrogen atom abstractors from thiols affording thiyl radicals. M. Jouffroy *et al.* reported that this reactive sulfur species could be exploited in a nickel-mediated cross coupling with bromoarenes and bromoheteroarenes to give thioethers. Optimum yields were obtained by employing $[Ru(bpy)_3](PF_6)_2$ as the photocatalyst, $NiCl_2$(dme), and dtbbpy as a ligand, in DMF as a solvent under blue LEDs irradiation at room temperature. Remarkably, the thiol selective hydrogen atom abstraction enabled a wide functional group tolerance, thus conferring the transformation a broad scope. Examples of compatible groups involved ketones, free alcohols, nitriles, free carboxylic acids, carbamates, and ethers. Cysteine was also efficiently used as starting thiol, providing thioether-derivatized heterocycles in good to excellent yields. As example of complex biorelevant substrate caffeine underwent thioetherification in a good 70% (**1171**, Scheme 207).

5.2.19 Synthesis of sulfones and sulfonamides. Heteroaryl halides could be converted into their corresponding sulfones (**1173**, Scheme 208) and sulfonamides by exploiting thiourea dioxide **1172** as the source for sulfonyl groups under visible-light photoredox catalytic conditions.[276] The transformation proceeded *via* a radical coupling of a heteroaryl radical and sulfur dioxide radical anion, thereby forming a heteroaryl sulfinate intermediate, which can be trapped *in situ* by different electrophiles such as alkyl bromides/iodides. Either fluorescein or *fac*-Ir(ppy)$_3$ proved to be effective catalysts with heteroaryl iodides and bromides, respectively. Sodium hydroxide was required as a base and DMSO as a solvent, with a 35 W CFL as photon source. These mild conditions enabled a wide functional group tolerance as shown for adenosine (Scheme 208).

5.2.20 Synthesis of arylboronates, arylstannanes, and biaryl products. T. H. Lambert, S. Lin, and coworkers recently reported a reductive electrophotocatalytic strategy enabling the generation of excited radical anions, which could activate substrates with high reduction potentials, *i.e.* from −1.9 to −2.9 V, such as aryl halides (Scheme 209).[277] Thoroughly, the cathodic reduction of dicyanoanthracene (DCA) resulted in the corresponding photoactive radical anion DCA$^{\bullet}$-, whose excited state DCA$^{\bullet}$-* possessed an exceptionally high reducing potential of −3.2 V *vs.* SCE and an estimated lifetime of 13.5 ns. The tandem electrochemical and photochemical activation circumvented chemoselectivity issues usually associated with the use of strongly reducing conditions. Electrolysis of DCA, along with borylation of aryl bromides/chlorides, occurred at a constant cell voltage using a porous

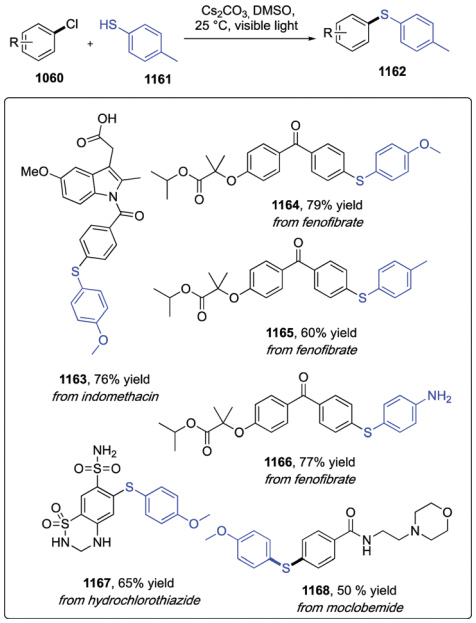

Scheme 206 Thiolation of aryl iodides and bromides.

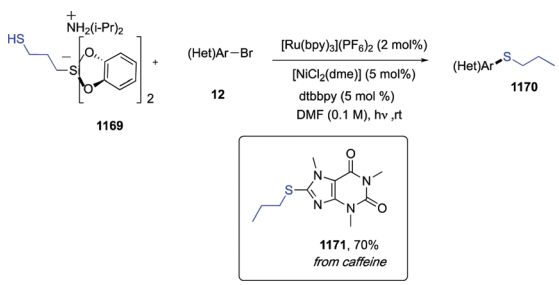

Scheme 207 Thiolation of aryl iodides and bromides.

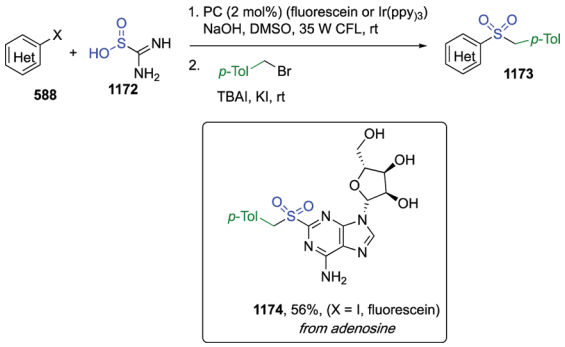

Scheme 208 Synthesis of sulfones and sulfonamides.

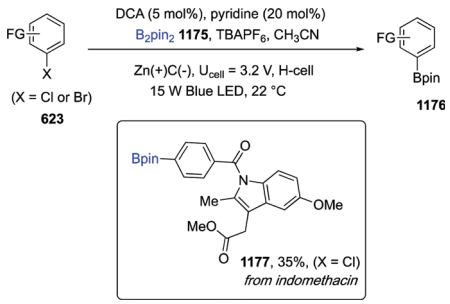

Scheme 209 Synthesis of arylboronates, arylstannanes, and biaryl products.

carbon cathode and a zinc plate sacrificial anode in an H-type divided cell, with $TBAPF_6$ as the electrolyte, catalytic amounts of pyridine, B_2Pin_2, in MeCN under blue LEDs irradiation. This protocol could be extended to the formation of C–Sn and C–C bonds by using hexamethylditin and *N*-methylpyrrole or 1,4-difluorobenzene as trapping agents, respectively. Application to indomethacin methyl ester, a substrate bearing multiple Lewis basic coordinating groups led to 35% of the borylated adduct **1177** (Scheme 209).

5.2.21 Synthesis of non-classical arylated C-saccharides. A. Dumoulin *et al.* reported a photoredox/nickel dual catalytic protocol to introduce saccharide derivatives into multifunctionalized complex scaffolds (Scheme 210).[278] Here, a photoredox-generated saccharyl radical underwent a nickel promoted cross-coupling with aryl- and heteroaryl-bromides. Remarkably, the anomeric carbon was left available, thereby providing the access to an unconventional class of arylated glycosides. Optimized reaction conditions required 4CzIPN as an organic photocatalyst, $NiBr_2$·dme as metal cocatalyst, dMeObpy as a ligand, in acetone and under blue LEDs irradiation at room temperature for 24 h. The scope of the carbohydrate embodied

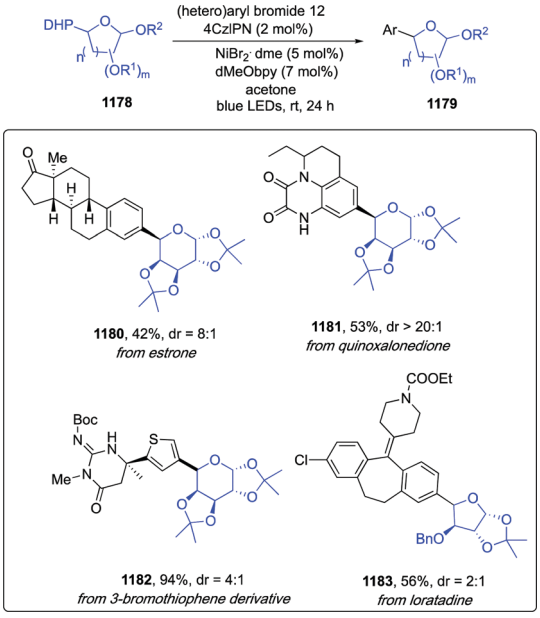

Scheme 210 Synthesis of non-classical arylated *C*-saccharides.

furanosyl units such as L-arabinofuranose and D-xylofuranose, as well as pyranose; in most cases excellent diastereoselectivities were observed. Likely, electron-poor (hetero)aryl bromides exhibited optimum reactivity, while electron-neutral and electron-rich substrates led to lower yields. To further explore the potential of this protocol in the late-stage diversification of complex biorelevant scaffolds a steroid derivative, together with aryl bromides from the Merck's chemistry informer library were selected as starting materials. In particular, estrone, a quinoxalonedione derivative (ionotropic glutamate receptor antagonist) and a 3-bromothiophene derivative with a guanidine moiety (aspartic protease inhibitors) smoothly afforded pyranose products **1180–1182**, respectively. In addition, loratadine was converted into furanosyl derivative **1183** (Scheme 210).

6. Chemical modification of alcohols, ethers and related analogues

Alcohols found plenty of applications as radical precursors in visible light photoinduced transformations. To cite a few, α-functionalizations of alcohols and ethers such as alkylation, diarylamination, and acetalization have been reported thanks to the development of synergic photoredox/HAT catalytic systems. *O*-Alkylation of aliphatic and aromatic alcohols has been accomplished *via* palladium or copper catalysis, while Giese-type addition of C-centered radicals derived from alcohols derivatives including mesylates, oxalate salts, and aryl triflates have shown efficiency and generality. Conversion of alcohols into C–N, C–O, C–S, and C–B bonds either *via* an iodination/S_N2 sequence or photocalytic Barton–McCombie reaction have also been highlighted in the following paragraphs, along with oxidative transformations such as conversion to carbonyl compounds and to benzoates. Interestingly, remote C(sp^3)–H functionalization of linear and cyclic alcohols enabled the site-selective introduction of new useful moieties into unactivated aliphatic bonds.

6.1 α-Alkylation/lactonization

In 2015 D. W. C. MacMillan and coworkers described an efficient and selective HAT catalytic system to accomplish photoredox α-alkylation/lactonization of alcohols with methyl acrylate (Scheme 211).[279] Interestingly, tetra-*n*-butylammonium phosphate (TBAP) showed as a key additive to enhance the selectivity for α-hydroxy-C–H bonds in the presence of allylic, benzylic, α-C=O, and α-ether C–H bonds, *via* formation of a hydrogen bond between the phosphate acceptor and the hydroxyl group of the alcohol. Formation of such a complex increased n–σ* delocalization of the oxygen lone pair, thus enhancing the polarization of the α-C–H bond, that becoming more hydridic was more susceptible to HAT by an electrophilic radical species. The developed system relied on the cooperation of an iridium-based photoredox catalyst, a HAT catalyst such as quinuclidine, and TBAP as a hydrogen-bonding catalyst. The efficacy and the selectivity of the developed protocol for strong C–H bond was

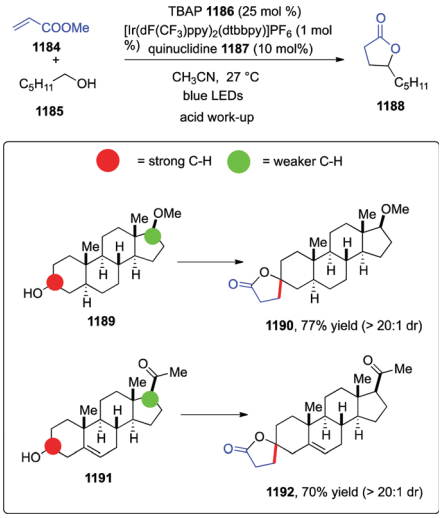

Scheme 211 α-Alkylation/lactonization.

showcased with a number of alcohols containing weaker C–H bonds, such as steroid derivatives **1189** and **1191** (Scheme 211).

6.2 Alkylation with dienes and alkyl bromides

The group of F. Glorius developed a three-component palladium catalyzed radical three-component coupling of dienes, unactivated alkyl bromides, and N-, O-, S-, or C-based nucleophiles proceeding *via* an interrupted Heck/allylic substitution sequence mediated by visible light (Scheme 212).[280] The method featured the use of $Pd(PPh_3)$, BINAP as a ligand, KOAc in DMA under 5 W blue LEDs irradiation for 24 hours at room temperature. These optimized conditions proved to be scalable to a multigram scale and quite general, as a wide range of acyclic and cyclic primary and secondary amines, phthalimide, activated methylenes, phenols, and sulfonates proved to be competent nucleophiles affording more than 130 examples. The broad functional group tolerance was also probed in the late-stage derivatization of estrone, ethynylestradiol, umbelliferone, the antiseptic chloroxylenol, the NSAIDS diflunisal, paracetamol, the antipsychotic norquetiapine and the H1-antagonist desloratadine (**1194–1204**, Scheme 212).

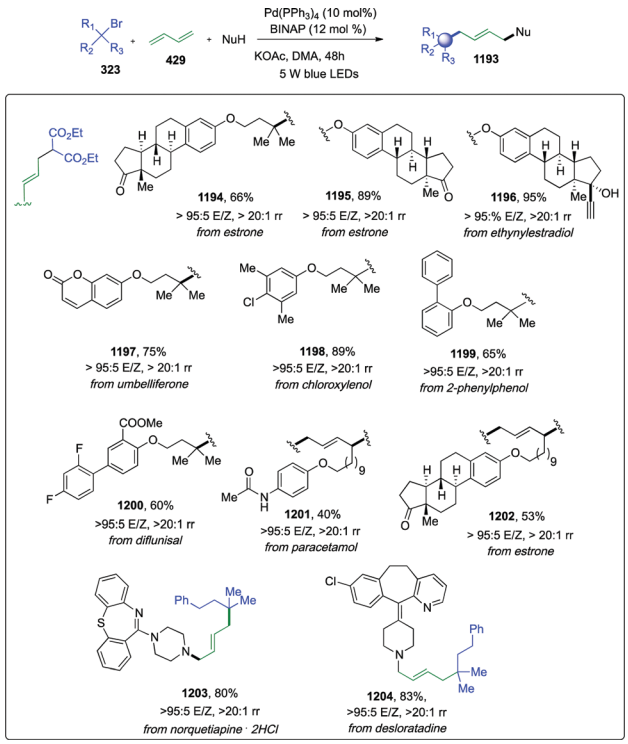

Scheme 212 α-Alkylation/lactonization.

6.3 Alkylation of unreactive alcohols with aryl diazoacetates

S. Jana *et al.* recently reported the use of hexafluoroisopropanol (**1206**, Scheme 213) as a regent to achieve the synthesis of fluorinated ethers.[281] The reaction mechanism relied on the formation of a hydrogen bonding complex between the alcohol and the diazoacetate, which upon visible light excitation was able to promote a proton transfer, with concomitant formation of an ion pair where the aryl diazoacetate underwent a rapid nucleophilic substitution with the alkoxide and loss of nitrogen gas. Besides hexafluoroisopropanol, the exceptionally mild reaction conditions were successfully applied to trifluoro- and difluoro-ethanol, perfluoroalkyl and diversely substituted α-branched halogenated alcohols, and phenols. Late-stage etherification of estrone was carried out in 76% and 1 : 1 dr (**1208**, Scheme 213).

6.4 Alkylation of phenols

Recently, the group of J.-R. Chen devised a visible light-driven copper-catalyzed synthesis of cyanoalkylated aryl ethers *via* $C(sp^3)$–O coupling of redox active oxime-ester derived benzylic radicals with phenols (Scheme 214).[282] Remarkably, the copper catalyst acted both as photosensitizer and cross coupling catalyst, avoiding the need for additional photocatalysts and/or external additives (for a recent review about copper-based photocatalysts see ref. 283). Copper indeed, was known to be a good trapping agent for aliphatic open-shell intermediates, thereby forming a high-valent copper(III) complex with the C-centered radical generated upon ring-opening of an amidyl radical intermediate. Final reductive elimination of the Cu(III) species provided the cross-coupled product. The mild conditions were applied to a range of diverse oxime esters and phenols providing the target compounds in moderate to good

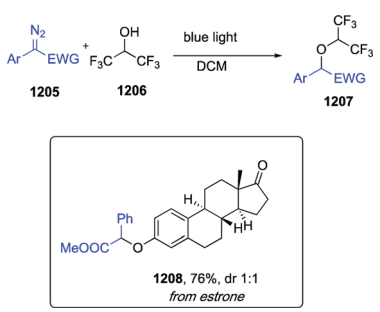

Scheme 213 Alkylation of unreactive alcohols with aryl diazoacetates.

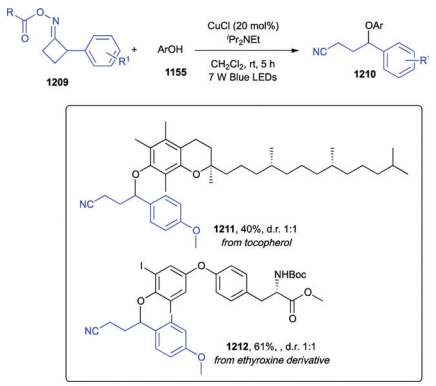

Scheme 214 Alkylation of phenols.

yields and thus highlighting a good functional group tolerance. Biologically relevant molecules such as vitamin E and an ethyroxine derivative were smoothly converted into cyanoalkylated derivatives **1211** and **1212** (Scheme 214).

6.5 Giese-type reaction of mesylates

Aliphatic mesylates (as well as alkyl chlorides and bromides, trifluoroacetates, and Katritzky salts) could be used as competent and readily available starting materials to generate alkyl radical intermediates, which could then add to alkenes, under very mild reaction conditions (Scheme 215).[284] In a very elegant strategy reported by Melchiorre group a nucleophilic dithiocarbamate anion catalyst **1216**, bearing a tailored chromophoric unit, was shown to activate alkyl electrophiles *via* an S_N2 pathway. The resulting photoactive intermediate underwent homolytic cleavage of the weak C–S bond, upon visible-light irradiation, to generate carbon radicals. After extensive optimization, reaction conditions featured the use of the thiocarbamate catalyst **1216**, γ-terpinene as cheap and stable donor of both hydrogen atoms and electrons, 2,6-lutidine or NaOAc as a basic additive, in MeCN or in DCE as a solvent. Remarkably, the reaction employed inexpensive reagents, did not require absence of oxygen, and tolerated the presence of some amounts of water. Additionally, it proved to be well-suited for a multi-gram scale. Its synthetic potential was shown with a broad range of both electron-rich and electron-poor benzylic electrophiles, providing compatibility with ethers, alkenes, aminomethylation reagents (*e.g.* oxazolidinone and phthalimide), N-, O-, and S-heterocycles, unprotected carboxylic acids and alcohols, as well as ketones, aldehydes, nitriles, and esters. Competent olefin substrates involved activating functional groups such as esters, nitriles, and amides. Uracyl chloride and adenine derived-chloride were transformed into **1217** and **1218** in 44 and 55% yields, while a cortisone-derived mesylate was functionalized in moderate to high yields giving **1221** and **1222** (Scheme 215).

Shortly after, W. Zheng *et al.* reported a green synthetic approach based on visible light induced disproportionation of pyrroles to carry out reductive functionalization of mesylates as well as aryl bromides and chlorides (Scheme 216).[285] Differently from alkyl halides, which could be used as alkyl radical precursors, aryl halides exhibited higher bond dissociation energies, falling

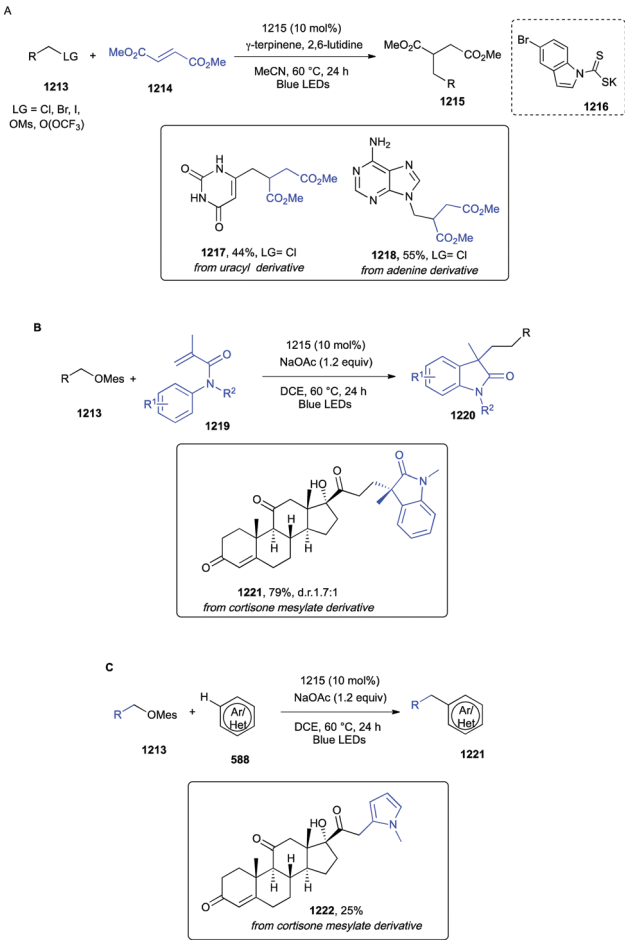

Scheme 215 Giese-type reaction of mesylates.

out of the range of a visible light photon. Accordingly, this protocol relied on the formation of a key pyrrole radical anion intermediate acting as the strong reduction species, *via* a photoinduced disproportionation occurring without the addition of any photocatalysts or additives. The pyrrole radical anion indeed was able to reduce the aryl halide, thus generating the corresponding aryl radical intermediate and eventually forming the heterocyclic adduct. Hence, the reaction proceeded in DMSO as a solvent at 25 °C under air and irradiation with blue LEDs. Aryl halides bearing cyano, esters, and ketone functional groups as well as heteroaromatic substrates such as substituted quinolines, and benzothiazoles smoothly underwent the derivatization with NH-, *N*-Me, *N*-aryl pyrroles and indole. Late-stage modification of cortisone, albeit activated as OMs, yielded with moderate efficiency compound **1224** (Scheme 216).

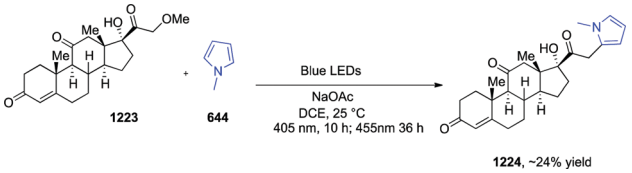

Scheme 216 Pyrrolation of mesylates.

6.6 Conversion of alcohols to C–heteroatom bonds

Blue-light promoted iodination of alcohols enabled a scalable and phosphine-free conversion of alcohols into C–N, C–O, C–S, and C–C derivatives *via* an S_N2 pathway (Scheme 217).[286]

This straightforward methodology avoided stoichiometric waste usually associated with the need of activating alcohols as good leaving groups, *e.g.* in Mitsunobu reactions. To this end, iodoform was used as iodinating agent in the presence of DMF as solvent and blue LEDs irradiation; after 20 h at room temperature a nucleophile is added, together with K_2CO_3 as base and the reaction was heated at 100 °C for additional 20 h. A variety of alcohols were efficiently reacted under standard conditions, including cyclopentanol, indole ethanol, primary alcohols bearing alkenes and terminal alkynes, and even a substrate containing a phosphine-sensitive alkyl azide. As pronucleophiles 4-bromobenzoic acid, a range of thiols, primary and secondary amines, phthalimide, phenols, and carboxylic acids, all afforded the desired alkylated adducts. Late-stage modification of fluoxetine, indomethacin, and a ketoprofen derived alcohol afforded the corresponding adducts **1227–1232** in good yields (Scheme 217).

6.7 Synthesis of enantioenriched α-trifluoromethyl ethers *via* enantioselective Hiyama cross-coupling

The use of bisfunctionalized electrophiles such as α-chloro-α-trifluoromethyl ethers, bearing both a trifluoromethyl and a functional group as direct substituents of the reactive center, could be employed in a Hiyama enatioselective cross-coupling reaction by using (hetero)aryltrimethoxy sylanes, TBAT, the methylene bisooxazoline ligand (**1234**, Scheme 218) in combination with $NiCl_2$·glyme, in DMA as a solvent at room temperature and under 10 W blue LEDs irradiation.[287]

Although essential to achieve optimum yields, the precise mechanism of the photoinduction was not clarified by the authors. The scope of the aryl trimethoxy silanes included electron-rich and electron-poor, *ortho*-, *meta*-, and *para*-substituted substrates, as well as alkenyl and heterocyclic silanes. Besides the trifluoromethyl group, perfluoroalkyl motifs such as $-C_4F_9$ and $-C_8F_{17}$ could be successfully introduced. Hydrogenolysis of some benzylic ether derivatives was also accomplished in both excellent yields and enantiomeric excesses, thus providing valuable α-trifluoromethylated alcohols. Likewise, various primary and secondary α-chloroethers containing ether, ester, protected amine, benzyl, and an unfunctionalized alkyl moiety afforded the corresponding α-trifluoromethyl ethers in superb yields and exquisite enantiomeric excesses. On the other hand, tertiary ethers showed to be not suitable, affording only traces of the target compounds. A cholesterol-derived α-chloroether was efficiently converted into **1236** in 88% yield and 96% ee (Scheme 218).

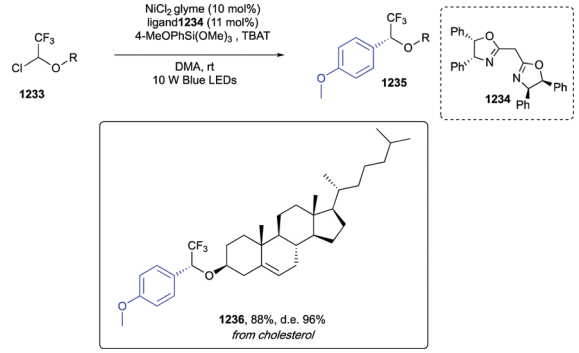

Scheme 218 Synthesis of enantioenriched α-trifluoromethyl ethers.

6.8 Deoxygenation of secondary and tertiary alcohols

Secondary and tertiary alcohols could be deoxygenated, upon prior conversion into thiocarbamates, under visible light photoredox catalytic conditions (Scheme 219).[288,289] This photocatalytic Barton–McCombie deoxygenation was promoted by the iridium complex *fac*-Ir(ppy)$_3$, in the presence of Hünig's base, (*i*-Pr)$_2$NEt, as sacrificial electron donor in MeCN as a solvent under blue LEDs irradiation for 24 hours at room temperature. The reaction scope was robust as shown in the LSF of lithocholic acid- and quinic acid-derived *O*-thiocarbamates to compounds **1239** and **1240** (Scheme 219).

6.9 Deoxyalkylation and deoxyfluorination of alcohols oxalate salts

In 2015, the group of D. W. C. MacMillan in collaboration with L. E. Overman from the University of California, showed that

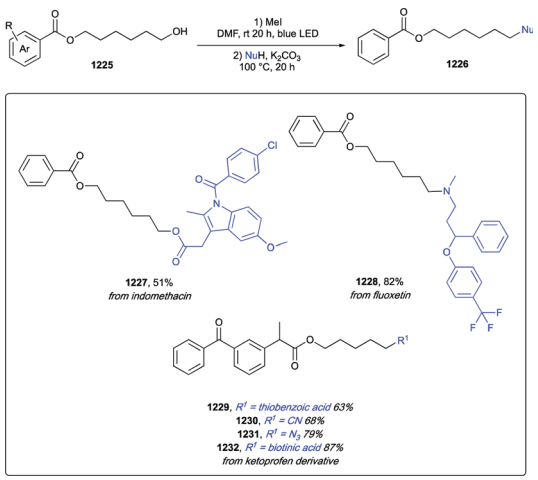

Scheme 217 Conversion of alcohols to C–heteroatom bonds.

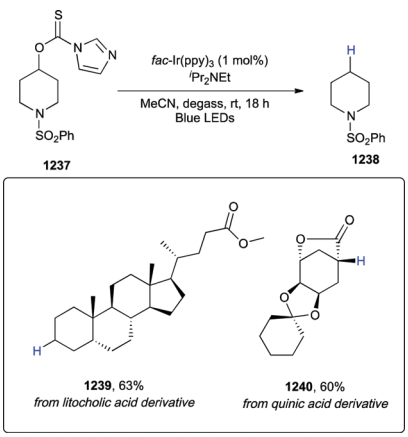

Scheme 219 Deoxygenation of secondary and tertiary alcohols.

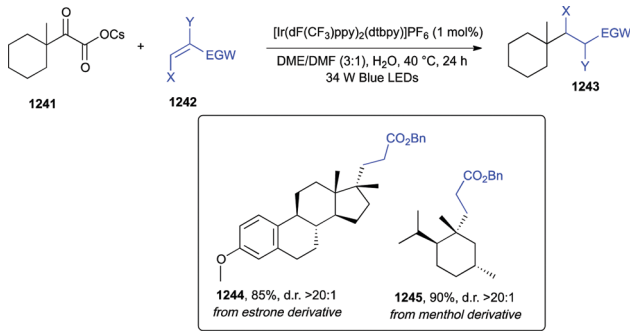

Scheme 220 Deoxyalkylation of alcohols oxalate salts.

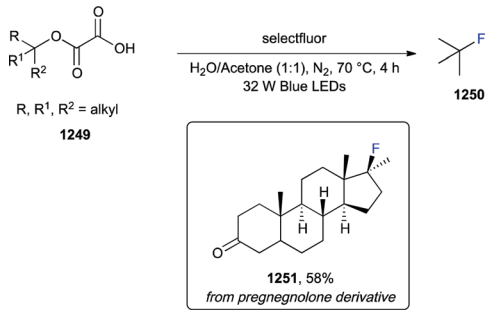

Scheme 222 Deoxyfluorination of alcohols oxalate salts.

alkyl oxalates could behave as bench-stable alcohol-activating group to generate alkyl radical intermediates under photoredox conditions (Scheme 220).[290] By using these precursors, under exceptionally mild reactions involving an iridium photocatalyst in a 3 : 1 DME/DMF mixture as a solvent system, in the presence of water at 40 °C and under 34 W blue LEDs irradiation, a number of suitable Michael acceptors (**1242**) afforded the corresponding 1,4-addition products in good to excellent yields. The alcohol scope included sterically hindered substrates, cyclic and heterocyclic substrates, with good diastereoselectivities in the formation of quaternary centers observed with chiral alcohols as in the case of the steroid- and menthol-derived compounds **1244** and **1245**, respectively (Scheme 220).

More or less at the same time, the group of D. W. C. MacMillan reported a C(sp^3)–C(sp^2) cross-coupling of oxalates with aryl halides *via* a metallaphotoredox catalytic approach (Scheme 221).[291] More in detail, the combination of [Ir(dFppy]$_2$(dtbbpy)PF_6, $NiBr_2$·glyme, and dtbbpy in the presence of $CsHCO_3$ in a 5 : 1 mixture of THP/DMSO as a solvent system, at room temperature and under blue LEDs irradiation, readily afforded the arylation products. Both aryl and heteroaryl bromides showed a good functional group tolerance including ester, aldehyde, sulfonyl, sulfonamide, trifluoromethyl, and nitrile. A wide range of tertiary, secondary, and primary alcohols gave the corresponding adducts in moderate to good yields. The conversion of the pregnenolone-derived oxalate into arylated adduct **1248** was carried out in a good 51% yield (Scheme 221).

A few years later, F. J. Aguilar Troyano *et al.* reported that tertiary alcohols, if converted to their corresponding cesium oxalate derivatives, could be deoxyfluorinated to afford tertiary alkyl fluorides (**1250**, Scheme 222) through selective SET oxidation with TEDA$^{2+\bullet}$, a radical cation derived from Selectfluor®, under blue LEDs irradiation.[292] The reaction proceeded in a mixture of acetone/water at room temperature and displayed a wide scope covering tertiary aliphatic, (hetero)benzylic, and propargylic alcohols containing functional groups such as amides, sulfonamides, carbamates, ethers, alkynes, and ketones, as in the case of estrone derivative **1251** (Scheme 222). Conversely, secondary and primary alcohols were not efficient substrates.

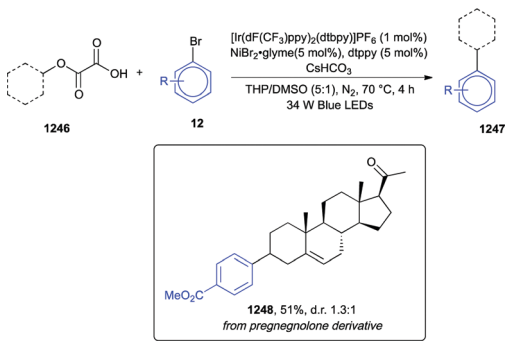

Scheme 221 C(sp^3)–C(sp^2) cross-coupling of oxalates with aryl halides.

6.10 Deoxygenative borylation of aliphatic alcohols

Aliphatic alcohols can be converted into boronic esters upon pre-activation as 2-iodophenyl-thionocarbonates (**1252**, Scheme 223) triggering a Barton–McCombie-type radical deoxygenation under visible-light irradiation.[293] The reaction did not require a photocatalyst, a radical initiator, nor tin or silicon hydrides. The resulting alkyl radicals were intercepted by bis(catecholato)diboron (**334**, B_2cat_2) to afford a wide range of structurally complex boronic esters. The reaction proceeded under blue LEDs irradiation in DMF for 18 h; then, addition of pinacol and triethylamine promoted a transesterification of the initially formed catechol boronic esters to pinacol. Reaction scope proved to be wide and biorelevant substrates such as menthol, borneol, epiandrosterone, rockogenin, tigogenin, hecogenin, and glycyrrhetinic acid were readily converted into boronic esters with high stereoselectivity (**1254–1261**, Scheme 223).

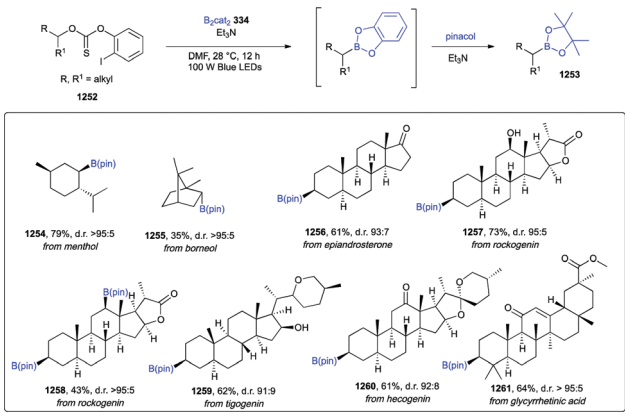

Scheme 223 Deoxygenative borylation of aliphatic alcohols.

6.11 Phenols *ortho*-diarylamination

Phenols can undergo a cross-dehydrogenative coupling with acyclic diaryl amines promoted by a non-metallic oxidative system based on an organic dye photocatalyst and a stoichiometric amount of persulfate (Scheme 224).[294] This metal-free approach showed exclusive *ortho*-selectivity with respect to the phenolic –OH functional group, as it occurred *via* a radical cross-coupling between an N-centered radical intermediate and a phenoxonium radical derived from phenol oxidation. The reaction scope was widely investigated: as for the amines, the reaction efficiency was strictly related to electronic effects, with electron-donating groups giving the best yields in shorter times. On the hand, sterically hindered amines underwent the transformation with moderate yields, and partial recovery of the starting materials. Several phenols showed to be competent substrates, with a good functional group tolerance including ethers and alkenyl- or alkynyl-moieties. Late-stage functionalization of (+)-δ-tocopherol to **1265** and **1266** under standard conditions was accomplished in 82% yield (Scheme 224).

6.12 Phenols as amides and ureas α-C(sp^3)–H arylating agents

The arylation of α-C(sp^3)–H bonds of amides and ureas was realized by combining photoredox catalysis, hydrogen atom transfer (HAT), and nickel catalysis (Scheme 225).[295] Aryl tosylates were generated *in situ* with TsCl; sequential filtration and 30 W blue LEDs irradiation with catalytic [Ir(dF(CF_3)ppy)$_2$(dtbbpy)]PF_6 and $NiBr_2$·glyme as catalysts and a stoichiometric amount of 3-acetoxyquinuclidine **1268** gave the desired arylated derivatives. A variety of amides and ureas, including DMF, *N*,*N*-dimethylacetamide, 1,1,3,3-tetramethylurea, and *N*-methylpyrrolidin-2-one were competent substrates. When unsymmetrical amides were used, arylation at methylene C–H bonds was favored over methyl C–H, with reasonable to excellent regioselectivity. As for the phenols, electron-withdrawing or electron-donating groups did not affect the reaction outcome, and good yields were generally obtained. Natural products estrone and 7-hydroxyflavone were smoothly coupled in NMP with 60 and 52% yields, respectively (**1270** and **1271**, Scheme 225).

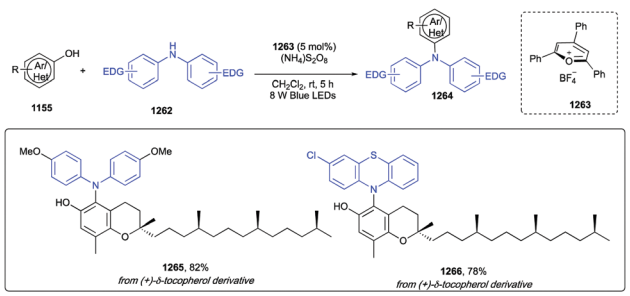

Scheme 224 Phenols *ortho*-diarylamination.

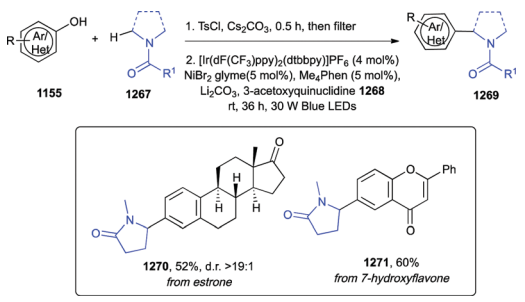

Scheme 225 Phenols as amides and ureas α-C(sp^3)–H arylating agents.

6.13 Synthesis of 2-deoxyglycosides from glycals

G. Zhao and T. Wang developed a stereoselective synthetic approach to 2-deoxyglycosides starting from glycals (**1273**, Scheme 226) and alcohols.[296] This transformation was promoted by a photoactive acid such as eosin Y, under blue LEDs irradiation in CH_2Cl_2 at room temperature. PhSSPh **42** was also essential to achieve optimum yields. To explore the scope of this photocatalytic glycosylation ten different alcohols and two glycal donors such as perbenzyl galactal and peracetyl galactal were probed as starting materials. Their successful combination highlighted the functional group tolerance (acetal, ether, ester, carbamate), and the high α-selectivities observed. Moreover, cholesterol and a protected nucleoside were smoothly glycosylated in **1275** and **1276** in 91% and 80% yields, respectively (Scheme 226).

A few years before B. Wang *et al.* reported a photoredox catalytic protocol to carry out trifluoromethylation of hexose-derived glycals (Scheme 227).[297] By employing the Umemoto's reagent **187**, *fac*-Ir(ppy)$_3$ as the photocatalyst, in DMA as a solvent at room temperature under visible light irradiation diversely protected substrates, such as acetylated, methylated, benzylated, or *p*-methoxybenzylated 3,4-dideoxy-glycals, were smoothly trifluoromethylated. Remarkably, as example of biorelevant scaffold, the electron-deficient 2,3-unsaturated *N*-acetylneuraminic acid (Neu2en) derivatives were converted into derivatives **1279** and **1280** (Scheme 227).

6.14 Acetalization of cyclic ethers

B. Ye *et al.* reported the stereoselective functionalization of C(sp^3)–H bonds of cyclic ethers by using a photochemically active diaryliodonium salt in combination with an anionic phase-transfer catalyst under CFL irradiation (Scheme 228).[298] Thoroughly, upon irradiation, the diaryliodonium salt underwent a homolytic fragmentation to give an iodonium cation radical and an aryl radical, which participated in HAT event to

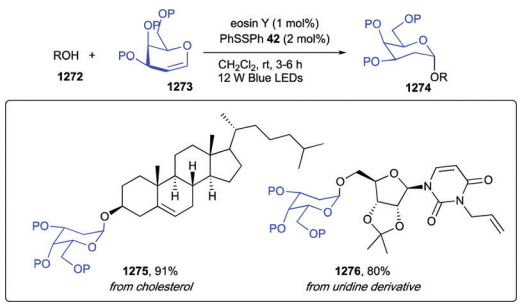

Scheme 226 Synthesis of 2-deoxyglycosides from glycals.

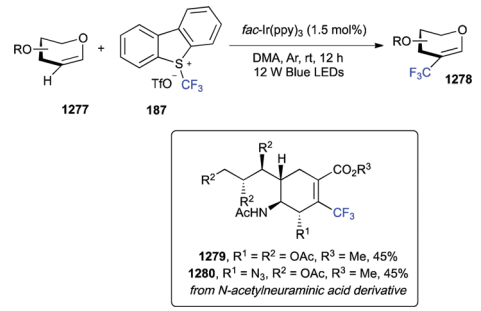

Scheme 227 Trifluoromethylation of hexose-derived glycals.

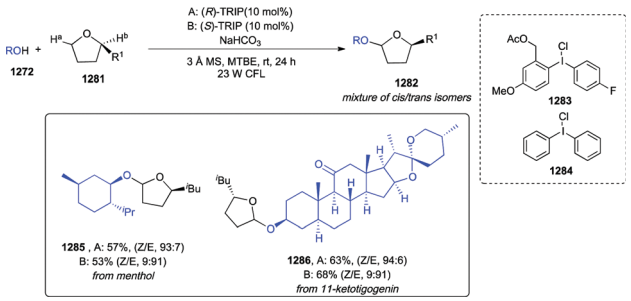

Scheme 228 Acetalization of cyclic ethers.

afford an α-oxy-alkyl radical, thus being responsible of the regioselectivity of the transformation. On the other hand, control of stereoselectivity was achieved by using a chiral phosphoric acid as the anionic partner of the iodonium salt. Thus, a wide range of achiral primary and secondary alcohols, as well as optically pure alcohols reacted in the presence of this dual catalytic system, $NaHCO_3$ as a base, MTBE as a solvent, and 3 Å MS to give acetal derivatives in good yields and diastereomeric ratios. Carbohydrates, nucleosides, naturally occurring alcohols such as menthol, and a steroid derivative were converted into **1285** and **1286** under standard reaction conditions (Scheme 228).

6.15 Oxidation to aldehydes and ketones

Primary and secondary alcohols could be oxidated to aldehydes and ketones, respectively, by using 9-fluorenone as a photocatalyst under visible-light irradiation (Scheme 229).[299] This metal- and additive-free protocol required DMSO as a solvent, air/oxygen as an oxidant and blue LEDs as the light source at room temperature. The reaction scope embodied aliphatic, heteroaromatic, aromatic, and alicyclic substrates as competent alcohols, including several steroids such as testosterone, stanolone, and androsterone (**1292** and **1293**, Scheme 229). Later on, the scope of this oxidative protocol was extended to benzyl alcohols, with slight variations of the reaction conditions (*i.e.* under air and two 80 W CFL lamps in place of blue LEDs).[300]

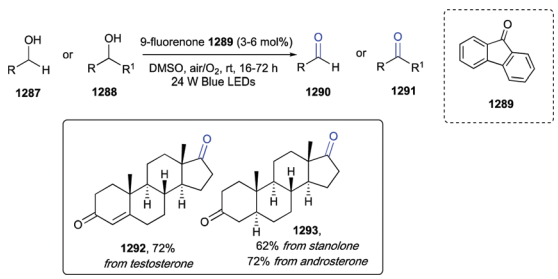

Scheme 229 Oxidation to aldehydes and ketones.

More recently, H. Fuse *et al.* developed a ternary hybrid catalytic acceptorless system based on a photoredox catalyst, a thiophosphate (TPA) organocatalyst, and a nickel catalyst to carry out dehydrogenation of aliphatic secondary alcohols to ketones under visible light irradiation (Scheme 230).[301] The reaction mechanism proceeded through hydrogen atom transfer from the α-C–H bond of the alcohol to the thiyl radical generated upon SET reduction of the thiol mediated by the excited state Mes-Acr^+*. Interception of the C-centered radical with $Ni(NTf)_2{\cdot}xH_2O$ was eventually followed by β-hydride elimination. The optimized conditions were applied to various alcohols in good to excellent yields, including sterically hindered substrates and pharmaceutical derivatives such as epiandrosterone (β-OH) and oxaprozin (**1293** and **1294**, Scheme 230). Additionally, performing the reaction in the presence of an aldehyde led to ester derivatives.

More strategies to achieve selective oxidation of alcohols to aldehydes or ketones are available in literature. L.-M. Zhao *et al.* exploited 3-mercaptopropionic acid (MPA)-capped CdSe quantum dot (MPA-CdSe QD), where visible light promoted a SET generating a thiyl radical able to abstract the α-hydrogen atom from the C–H bond of the alcohol, thus forming a C-centered radical (Scheme 231).[302]

The catalytic system was efficient and site-selective in case of polyhydroxy compound, as showcased for 6β-hydroxy-17β-estradiol, whose oxidation was successfully performed also on a multigram scale. More recently, W. Zhang *et al.* described a

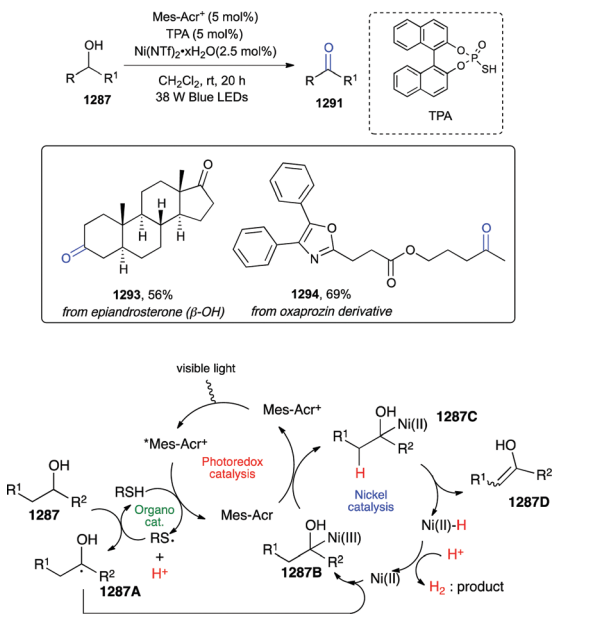

Scheme 230 Oxidation to ketones.

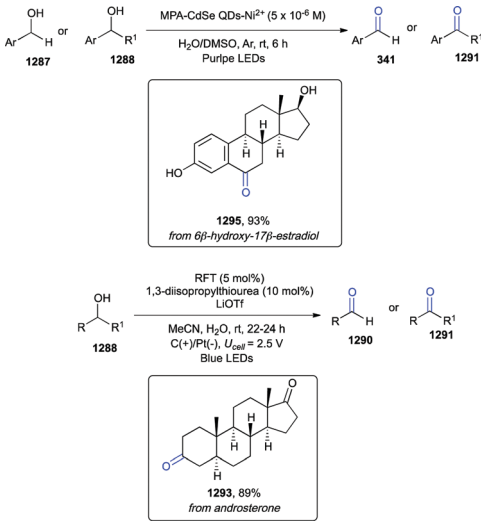

Scheme 231 Oxidation to ketones.

photoelectrocatalytic system based on riboflavin-derived photocatalysts, while a thiourea cocatalyst was harnessed as a thiyl radical source acting as HAT agent.[303] The broad scope and the functional group tolerance were further witnessed by the late-stage oxidation of steroids **1295** and **1293** (Scheme 231).

6.16 Formation of benzoates

Alcohols could be converted into benzoates by using aryldiazonium salts and CO gas under visible light photoredox catalytic conditions (Scheme 232).[304] The procedure was metal-free and employed the organic dye fluorescein as photoactive catalyst, 16 W white LEDs as the photon source, 80 atm CO in methanol as the solvent at room temperature for 10 hours. By applying optimized reaction conditions, a library of diverse aromatic esters was synthesized, with variation of the electronic properties of aryldiazonium salts showing little influence on the outcome. Tolerated functional groups included ethers, free alcohols, bromo, sulfonate anion, nitrile, nitro, and ester. Likewise, a broad range of aliphatic alcohols took part to the transformation, regardless the steric bulk around the hydroxy function, such as in the case of hindered isopropyl-, cyclohexyl-, and *tert*-butyl-alcohols. As example of biorelevant substrate (−)-menthol was converted into **1297** both on 0.4 and 6 mmol scale, with good yields of 72 and 73% (Scheme 232).

Alternatively, benzoates could be obtained from benzyl ethers *via* a photocatalytic oxidation promoted by dye-sensitized semiconductors under visible-light irradiation (Scheme 233).[305]

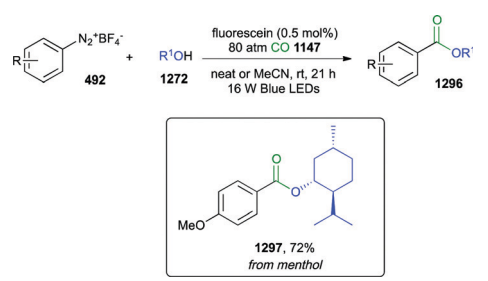

Scheme 232 Formation of benzoates.

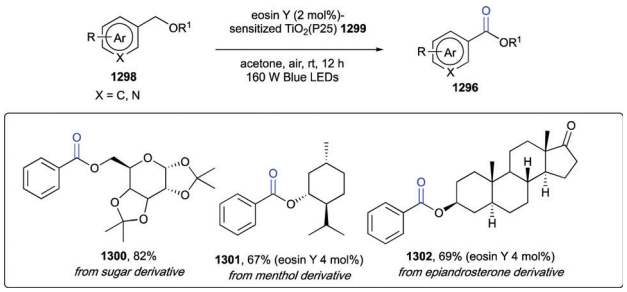

Scheme 233 Formation of benzoates.

Notably, catalytic eosin Y-sensitized titanium dioxide enabled an efficient aerobic photooxidation, with low-cost, high atom-economy, and user-friendly setup. The reaction proceeded with reagent-grade acetone as solvent and balloon-pressure air as the oxidant. Mechanistic studies suggested a radical two-step process *via* an isolable peroxide intermediate. The authors described 32 examples with high selectivity and broad substrate scope: regardless the steric effects of the alkyl groups, primary, secondary, and tertiary alkyl benzoates were smoothly obtained in good yields. Functional groups tolerance included bromo-, nitriles, cyclopropropyl-, pyridyl-, epoxides, aldehydes, and nitro-, to cite a few. As examples of more complex substrates, a monosaccharide-derivative, benzyl-protected menthol, and epiandrosterone were converted into their corresponding benzoates (**1300–1302**, Scheme 233).

On the other hand, phenolic esters could be achieved *via* a site-selective phenol acylation mediated by thioacids (**1303**, Scheme 234) under visible light photoredox catalytic conditions.[306] More in detail, the formation of this class of ester derivatives was carried out with a one-pot-two-steps protocol: by using $Ru(bpy)_3Cl_2$ as a photosensitizer, K_2CO_3 as a basic additive in MeCN under air and irradiation with a 45 W CFL, a diacyl sulfide intermediate was formed, while addition of DMAP as a transacylation agent and a base such as triethylamine to provide a nucleophilic phenate anion provided the final target compounds. The reaction scope proved to be wide, including both aromatic and aliphatic thioesters as well as a wide range of substituted phenols, tolerating functional groups such as halogens, ethers, alkynes, and ketones. LSF of estradiol provided the benzoate derivative **1304** (Scheme 234).

6.17 Trifluoromethylthiolation of tertiary ethers

$C(sp^3)$–SCF_3 coupling of tertiary alkyl ethers was achieved by W. Xu *et al.* by exploiting 4CzIPN as an organic photocatalyst

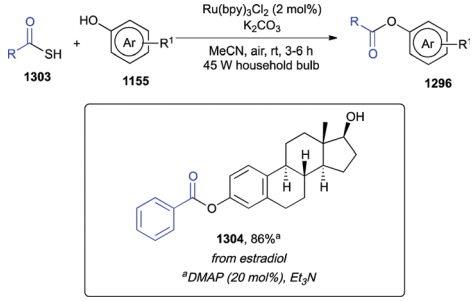

Scheme 234 Formation of benzoates.

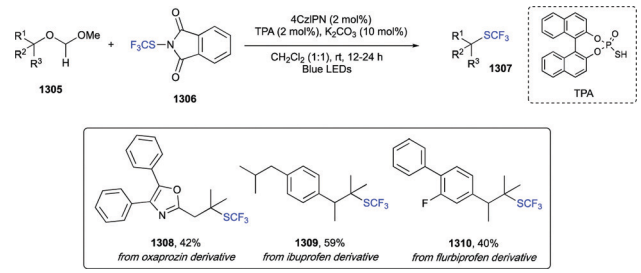

Scheme 235 Trifluoromethylthiolation of tertiary ethers.

and BINOL-based phosphorothiols (Scheme 235).[307] The process was initiated by polarity-matching HAT event, which produced a site-selective cleavage of tertiary C(sp^3)–O ether bond. Electrophilic Phth-SCF_3 reagent was used as CF_3 source, or, alternatively, difluoromethylation could be carried out with the analogue Phth-SCF_2H. Suitable tertiary alkyl ethers included MOM-type substrates (MOM = methoxy methyl), with exquisite selectivity even in the presence of competing cleavable C–H bonds such as hydridic and weak benzylic ones. Electron-withdrawing and -donating substituents in *ortho*-, *meta*-, and *para*-positions of aryl rings, as well as heteroaromatic rings were well tolerated. Late-stage trifluoromethylthiolation of complex bioactive ethers such as oxaprozin, ibuprofen, and flurbiprofen was achieved in good yields (**1308–1310**, Scheme 235).

6.18 Carboxylation of aryl triflates

The introduction of a carboxylic acid functional group onto aryl triflates and both aliphatic and aromatic bromides was accomplished by Q.-Y. Meng *et al. via* a dual organic photoredox-nickel catalysis (Scheme 236).[308]

Remarkably, K_2CO_3 was used as a source of CO_2. More in detail, optimized reaction conditions required 4CzlPN as organic photosensitizer, $NiBr_2$·glyme combined with neocuproine as cocatalyst, Hantzsch ester (HEH) as the reductant, K_2CO_3, DMF as solvent, and blue LEDs irradiation for 24 h at room temperature. A CO_2 balloon was also beneficial, as CO_2 generated *in situ* from K_2CO_3 partially escaped from the solution into the gas phase, thus decreasing its concentration. Under these reaction conditions, several *para*- and *meta*-substituted bromoarenes were smoothly carboxylated in moderate to excellent yields (47–93%). Tolerated functional groups involved ethers, alcohols, fluoro- and chloro-, nitriles, esters, ketones, trifluoromethyl-, and Boc-protected amines. Disubstituted aryl bromides, and naphthalene and heteroaromatic systems were also suitable substrates. The scope of the alkyl bromides covered primary alkyl-, secondary and tertiary cyclic ones. On the other hand, aryl triflates showed an opposite trend with respect to bromides, as electron-rich substrates showed a better reactivity. As example of LSF, bioactivate estrone was carboxylated in 48% yield (**1313**, Scheme 236).

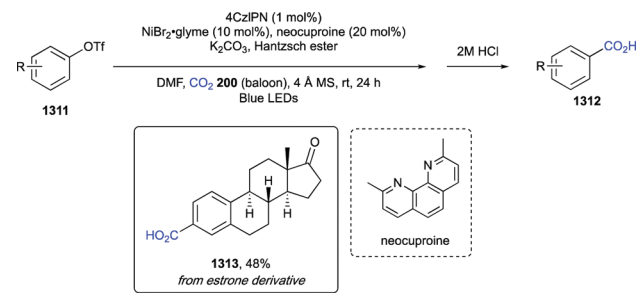

Scheme 236 Carboxylation of aryl triflates.

6.19 Functionalization of alcohols as α-bromoalkyl ester derivatives

Esterification of alcohols as α-bromoalkyl ester derivatives can unlock further modification with arene motifs *via* a visible-light ruthenium catalysis (metallaphotocatalysis) (Scheme 237).[309] This transformation was characterized by a high *meta*-regioselectivity with respect to the substituted aryl ring and did not require any exogenous photosensitizer. Standard reaction conditions employed $[RuCl_2(p\text{-cymene})]_2$ as the catalyst, diphenylphosphoric acid as the ligand, K_2CO_3 as a base, and 1,4-dioxane as the solvent under blue LEDs irradiation at room temperature for 24 h. A variety of both tertiary and secondary unactivated alkyl bromides provided the desired products in excellent yields, and functional groups such as imide, enone, piperidyl, and ester were well tolerated. The compatibility with α-bromoesters enabled the late-stage functionalization of complex substrates such as sugar **1316**, estrone **1317**, and menthol **1318** (Scheme 237).

6.20 Ring-opening of cycloalkanols and remote functionalization of linear alkanols

Cleavage and subsequent amination of the C–C bond of cycloalkanols could be achieved by using a dialkylazodicarboxylate reagent **1320** (Scheme 238), in the presence of cerium(III) chloride ($CeCl_3$), *tert*-butylammonium chloride (TBACl) in MeCN as a solvent and under blue LEDs irradiation at room temperature.[310] The reaction mechanism exploited the formation of a photoactive cerium(III) complex with the starting alcohol, which was oxidized to a Ce(IV) species upon photoexcitation, thus promoting a β-scission cleavage to generate a carbon-centered radical.

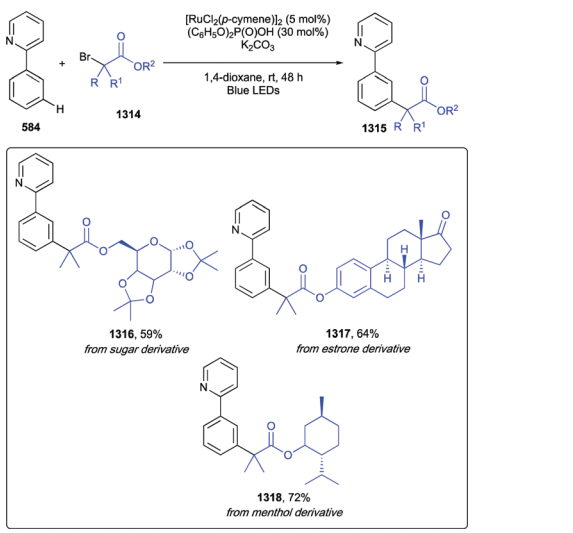

Scheme 237 Functionalization of alcohols as α-bromoalkyl ester derivatives.

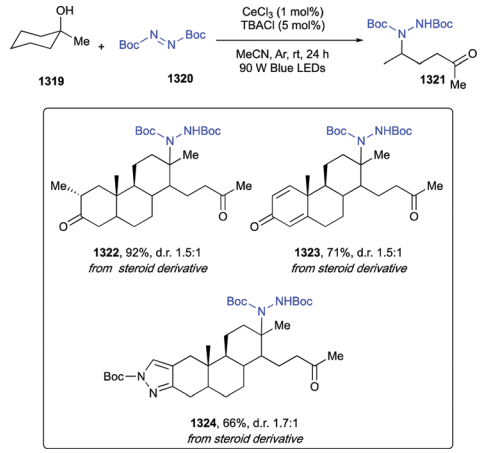

Scheme 238 Ring-opening of cycloalkanols.

The authors showed that interception of the latter with an azadicarboxylate radical acceptor led to synthesis of hydrazine derivatives. The transformation demonstrated a wide scope and a good functional group tolerance as exemplified in the conversion of sterically congested steroid-derived cycloalkanols (**1322–1324**, Scheme 238).

A few years later, the same group demonstrated that the formation of a photoactive complex between a cerium(III) catalyst and an aliphatic linear alcohol could trigger the formation of an alkoxy radical, followed by a 1,5-HAT, thus enabling a site-selective remote C(sp^3)–H functionalization of linear aliphatic alcohols (Scheme 239).[311] In analogy with the cyclic alkanols, the functionalization was accomplished with DBAD (**1320**, di-*tert*-butyl azodiformate) as exemplified for lithocolanyl alcohol (**1327**, Scheme 239).

The regiospecific introduction of an allyl group into cycloalkanols or simply their ring-opening to formyl-derivatives was later reported by J. Wang *et al.* (Scheme 240).[312] The process relied on the formation of a key O-centered radical, which mediated the sequential ring-opening and allylation/formylation. Thoroughly, the use of acrylate derivatives, $[Ir(dF(CF_3)ppy)_2(dCF_3bpy)]PF_6$ as a photocatalyst, collidine as a base, in CH_2Cl_2 and under irradiation with a 20 W white LED afforded vinyl adducts in good to high yields. Conversely, the same reaction conditions, in the absence of the alkene partner, and with a solvent switch to CF_3CH_2OH under air, allowed the obtainment of the formylated adducts. As example of complex bioactive alcohols, diosgenin was converted into derivative **1331** in a good 68% yield (Scheme 240).

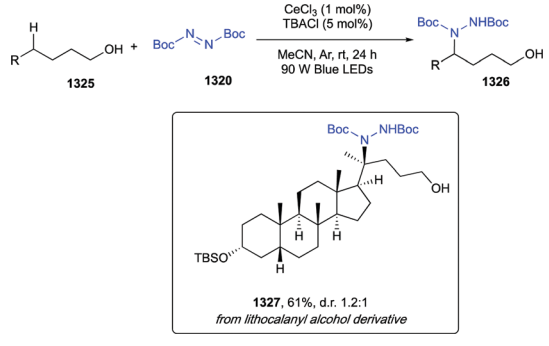

Scheme 239 Remote C(sp^3)–H functionalization of linear aliphatic alcohols.

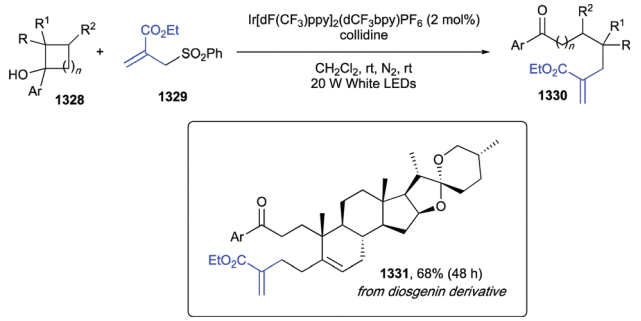

Scheme 240 Functionalization of cycloalkanols.

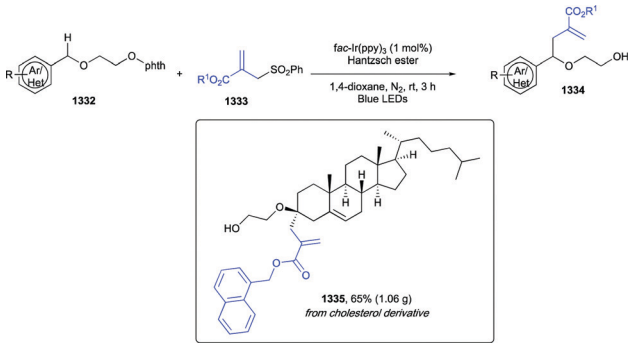

Scheme 241 Remote C(sp^3)–H functionalization of linear aliphatic alcohols.

Remote C(sp^3)–H allylation and alkenylation of linear aliphatic alcohols was reported by J. Zhang *et al.* (Scheme 241).[313] The authors reported for the first time the formation of alkoxy radicals starting from *N*-alkoxyphthalimides under photoredox catalytic conditions. The alkoxy radical, once generated, triggered a 1,5-HAT to form a C-centered radical, which was intercepted by either aryl–allyl or vinyl sulfones. The scope of the radical acceptor was good, with electron-deficient aryl vinyl sulfones giving higher yields. The regioselectivity for δ-C(sp^3)–H bond was shown to be exclusive, also in the presence of ε-C(sp^3)–H bonds. Remarkably, late-stage allylation of a cholesterol-derived *N*-alkoxyphthalimide was performed on a gram scale affording derivative **1335** in 65% with complete stereoretention (Scheme 241).

6.21 Synthesis of urethanes

Alcohols could be used as trapping agents for isocyanates, generated *in situ* from oxamic acids, to afford urethanes (**1337**, Scheme 242).[314] This transformation was promoted by an organic dye photocatalyst, a hypervalent iodine reagent and a light source. Likewise, the authors showed that interception of isocyanates with amines was also feasible, thus enabling the synthesis of ureidic derivatives. This approach, by offering compatibility with free alcohols and amines, was endowed with the great advantage of avoiding the isolation, purification, and storage of carcinogenic isocyanates. The scope

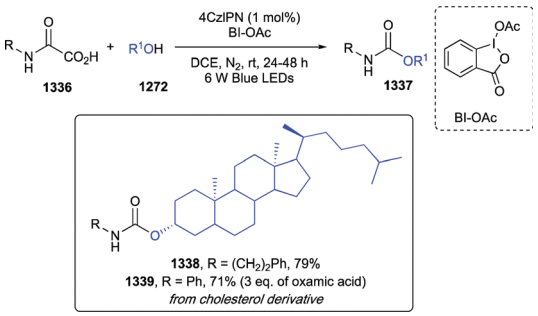

Scheme 242 Synthesis of urethanes.

of the oxamic acid was wide, including both linear and bulky cyclic aliphatic amines, benzylic amines, as well as anilines and naphthylamine. Alike, the alcohols partners included both linear and bulky cyclic aliphatic substrates, such as cholesterol (**1338** and **1339**, Scheme 242). The presence of double and triple bonds, albeit leading to moderate yields, was tolerated.

6.22 Heck-type arylation of vinylphenols

Recently, the group of C. Xia disclosed a protocol to achieve a photochemical Heck-type arylation of vinylphenols with non-activated (hetero)aryl halides (Scheme 243).[315]

Interestingly, the vinylphenolate anions generated *in situ* upon Cs_2CO_3-mediated deprotonation in DMSO were photoactive, and under blue LEDs irradiation, in their excited-state, were able to generate an aryl radical upon SET reduction of the (hetero)aryl halide. The aryl radical added to the double bond with regio- and stereo-selectivity, to afford a benzylic radical, which underwent a further hydrogen atom transfer to finally yield the arylated vinylphenol. The mild reaction conditions enabled an exquisite functional group tolerance, as mirrored by the late-stage modification of representative bioactive natural compounds such as chlorogenic acid, esculin, and scutellarin (**1343–1345**, Scheme 243).

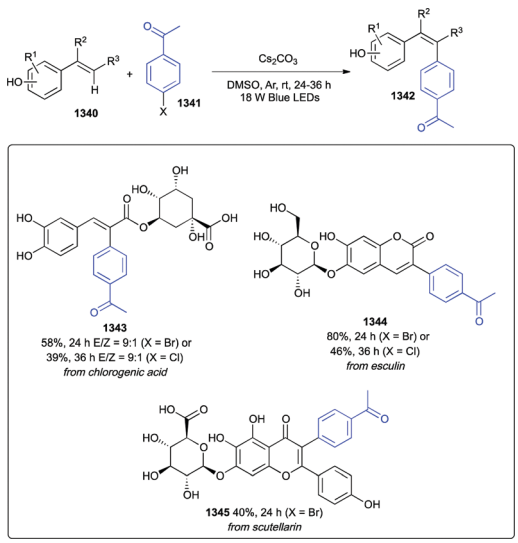

Scheme 243 Heck-type arylation of vinylphenols.

7. Chemical modification of amines, amides, carbamates, and related analogues

Amines are highly useful reagents in radical chemistry thanks to the possibility to tune their reactivity towards the formation of α-amino radicals, iminium ions, or distonic ions, by simply changing the reaction conditions.[316,317] Additionally, tertiary aliphatic amines, owing to their redox potentials (*e.g.* triethylamine $E^{red}_{1/2}$ = +1.0 V *vs.* SCE) are widely used as sacrificial electron donors to promote reductive catalytic cycles of ruthenium- or iridium-based polypyridyl complexes, or as reductant to regenerate the oxidized photocatalyst when oxidative catalytic cycles prevail. The following paragraph will deal with functionalizations at the N-atom of aliphatic and aromatic amines, such as *N*-arylation, *N*-alkylation, and *N*-cyanoalkylation as well as some recent developments in the derivatization of the C(sp^3)–H at the *alpha* position to the amine, such as α-oxygenation to amides, α-cyanation, and α-alkenylation. While Xiao investigated the involvement of primary amines in a three-component reaction leading to cyanoalkylcarboxylated adducts, Aggarwal and Glorius focused on deaminative processes such as borylation, alkylation, and alkynylation by taking advantage of Katriztky salts.[318] C(sp^2)–H functionalization of anilines with trifluoromethyl or sulfonyl groups can also be achieved under mild conditions as well as remote C(sp^3)–H functionalization. Valued protocols to carry out deuteration and tritiation of nitrogen-containing pharmaceuticals have also been highlighted hereafter.

7.1 Alkylation of secondary amines

Secondary amines could be alkylated in a three-component photoredox process involving ketones or aldehydes, and alkenes (Scheme 244).[319] The protocol required an iridium-photocatalyst, a Hantzsch ester, propionic acid, 4 Å molecular sieves in CH_2Cl_2 at room temperature, and under blue LEDs irradiation for 2 h.

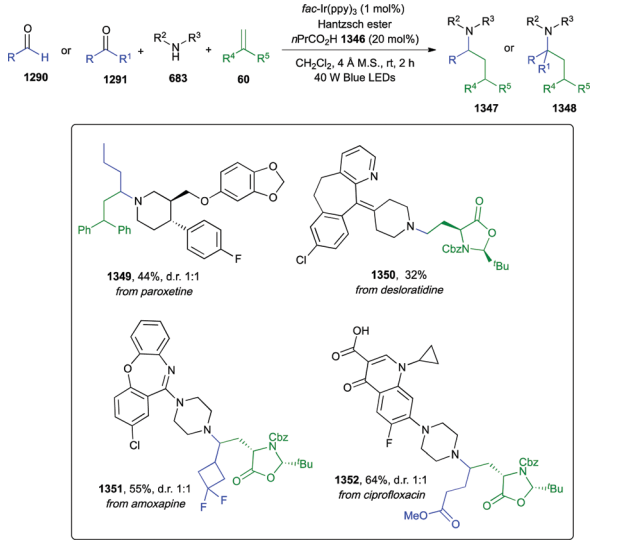

Scheme 244 Alkylation of secondary amines.

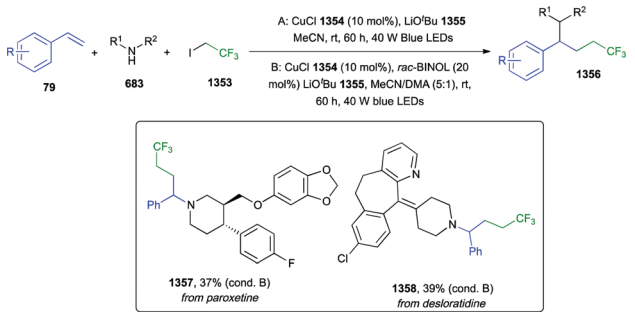

Scheme 245 Alkylation of secondary amines.

The design of this synthetic strategy relied on the condensation to iminium ion of the amine and the carbonyl compound, and on its conversion, upon a SET event, to an α-aminoalkyl radical, able to add onto the olefin. The alkyl radical thus formed underwent a hydrogen atom transfer to give the final tertiary amine. Formaldehyde, linear and α-branched aldehydes were all competent substrates, while benzaldehyde failed to react. Benzylamine derivatives, as well as linear or branched amines, along with several electron-deficient alkenes proved as suitable coupling partners. Late-stage alkylation of paroxetine, desloratadine, amoxapine, and ciprofloxacin proceeded smoothly under standard reaction conditions (**1349–1352**, Scheme 244).

One-more multicomponent protocol to realize alkylation of secondary amines was recently reported by Y. Xiong *et al.* (Scheme 245).[320] This convergent approach involved both secondary alkyl and aryl amines, activated and non-activated alkenes, and alkyl halides, including perfluoroalkyl-derivatives. CuCl was used as dual photo- and coupling catalyst, LiO^{t}Bu as a base, and MeCN as the solvent under 40 W blue LEDs irradiation at room temperature for 60 h. Depending on the starting amine, *rac*-BINOL as a ligand was required to achieve efficient trifluoromethyl alkylation. The reaction scope was wide with respect to both the alkenes and the alkyl halides, and competent amines included, among others, 9*H*-carbazoles, indoles, and indazoles. Paroxetine and desloratadine smoothly underwent late-stage alkylation under standard reaction conditions (**1357** and **1358**, Scheme 245).

Recently, K. P. S. Cheung *et al.* reported a photoinduced palladium-catalyzed alkylation of amines starting from conjugated dienes and alkyl iodides (Scheme 246).[321] The reaction mechanism was based on a radical-polar crossover event of a putative π-allyl hybrid palladium radical intermediate, to a "traditional" π-allyl palladium intermediate, which was eventually trapped by the amine to deliver the final product. In order to achieve optimum yields, the three-component reaction required $PdCl_2$ as the catalyst, Xantphos as the ligand, silver triflimide ($AgNTf_2$) as an additive to decrease the formation of radical dimerization adducts, Cs_2CO_3 as a base, in THF under blue LEDs irradiation at room temperature for 15 hours. Electron-rich dienes proved to be more efficient than electron-deficient analogues, which afforded the expected products in moderate to good yields. A number of alkyl iodides smoothly underwent the allylamination, albeit bulky substrates such as *tert*-butyl iodide produced a mixture of 1,2- and 1,4-adducts. On the other hand, standard reaction conditions proved to be quite general with respect to the amines, enabling the LSF of complex bioactive settings such as ciprofloxacin and desloratadine (**1362–1363**, Scheme 246).

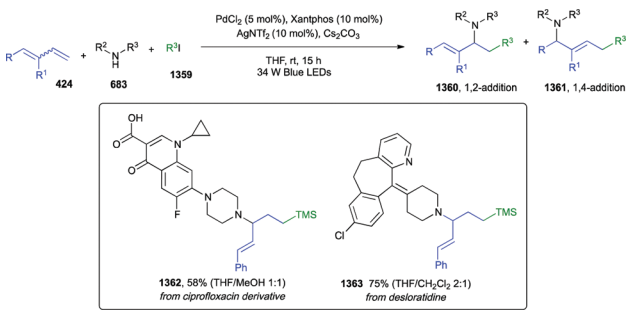

Scheme 246 Alkylation of secondary amines.

7.2 α-Oxygenation of tertiary amines to amides

Y. Zhang *et al.* developed a metal-free system to convert tertiary amines into amides using oxygen as an oxidant, rose bengal as an organic photocatalyst, 1,5-diazabicyclo[4.3.0]non-5-ene (DBN) as a base, in DMF as a solvent and under 12 W blue LEDs irradiation at room temperature for 16–48 hours (Scheme 247).[322] The reaction mechanism relied on the formation of a N-centered cation radical intermediate **1364A**, which upon base-mediated deprotonation afforded a carbon radical **1364B.** At the same time the photocatalyst radical anion, formed in the SET oxidation of the starting amine, reacted with molecular oxygen O_2 to provide the superoxide radical anion ($O_2^{\bullet -}$), which protonated to peroxide radical HOO$^\bullet$. The latter quenched the carbon centered radical, affording, after loss of a molecule of water, the final amide **1365.** The reaction scope was mainly investigated with cyclic amines, while a sole example with *N*,*N*-dimethylbenzylamine was reported. Functional groups such as ethers, alkyls, alkenes, fluoro, and nitro were well tolerated. Interestingly, the standard reaction conditions proved to be amenable also in the synthesis of phthalimide and maleimide derivatives. Late-stage

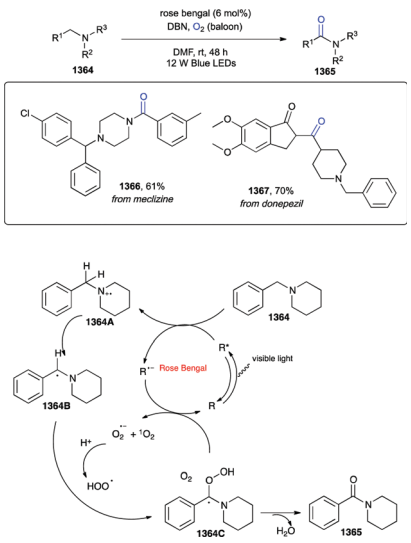

Scheme 247 α-Oxygenation of tertiary amines to amides.

oxidation of meclizine and donezepil was achieved in 61 and 70% yields, respectively (**1366** and **1367**, Scheme 247).

7.3 Cyanation of aliphatic amines α-C(sp^3) carbons

C_α–H cyanation of unactivated secondary and tertiary aliphatic amines can be realized under photoredox conditions to yield valuable α-aminonitriles using NaCN as inexpensive cyanide source (Scheme 248).[323]

The reaction was carried out in mild conditions, with air as the external oxidant, $[Ir(dF(CF_3)ppy)_2(dtbpy)]PF_6$ as photocatalyst, in MeCN as solvent under 72 W blue LEDs irradiation for 24 h. The synthetic utility of this protocol was demonstrated on a wide range of amines; with volatile secondary amines the reaction was performed in MeCN-d_3 and yields measured by quantitative ^{1}H-NMR. Secondary amines with little steric hindrance, such as diethylamine, provided a mixture of mono- and dicyanated products, while bulkier amines afforded mono-substituted adducts. Cyclic secondary amines, dibenzylamine, and a wide range of tertiary aliphatic amines were efficiently converted into the corresponding α-aminonitriles, with a preference for ring C_α–H amination observed. Tolerated functional groups included ketones, tertiary alcohols, cyano-, ester-, and pyridine, to cite a few. Late-stage derivatization of complex substrates such as nicotine, gramine, and known drugs such as lidocaine, imipramine, gefitinib, (*R*)-(−)-phenylefrine, and chantix, a therapeutic agent for nicotine addiction, was successfully performed (**1369–1377**, Scheme 248).

One more protocol to achieve cyanation of C(sp^3)–H bonds at the α-position with respect to amines was reported by T. Wakaki et coauthors (Scheme 249).[324]

The reaction was promoted by visible-light photoredox/phosphate hybrid catalysis, where phosphate radicals, generated by SET oxidation of a phosphate salt, acted as HAT catalysts to provide nucleophilic carbon radicals. The latter were trapped by a cyano radical source, such as TsCN, to give, eventually, the cyanation products. The mild reaction conditions, involving $[Ir(dFCF_3ppy)_2(5,5'\text{-}dCF_3bpy)](PF_6)$ as photoredox catalyst, 1,1′-binaphthyl-2,2′-diyl hydrogen phosphate (BINOL-phosphate) as HAT agent, K_2CO_3 as a base in MeCN and under blue LEDs light irradiation, allowed a broad scope and high functional group tolerance. Boc-protected amines such as piperidine, azepane, morpholine, and dibutyl amine

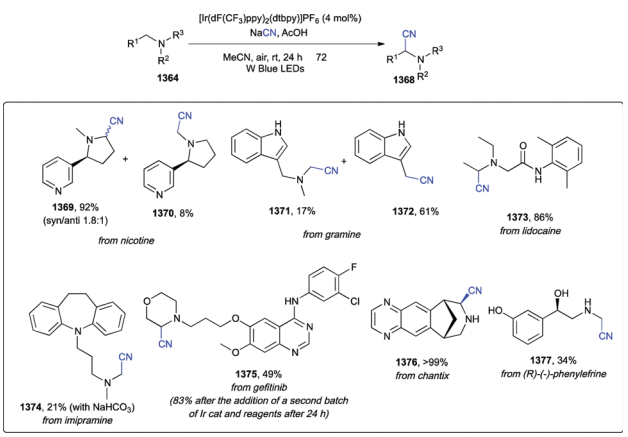

Scheme 248 Cyanation of aliphatic amines α-C(sp^3) carbons.

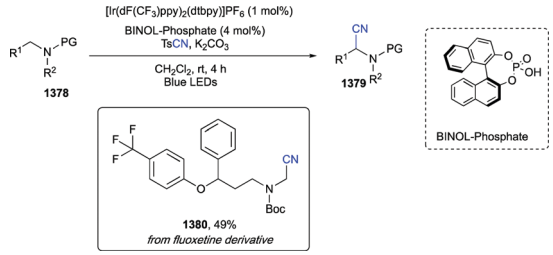

Scheme 249 Cyanation of aliphatic amines α-C(sp^3) carbons.

gave excellent yields, while secondary amines with methyl and phenylpropyl substituents at the nitrogen atom provided methyl C–H cyanation adducts with excellent selectivity. Remarkably, cyanation of α-C–H bonds bound to an oxygen or a sulfur atom (*e.g.* in isochromane, tetrahydrothiophene, and thiane) cleanly underwent cyanation under standard reaction conditions). Late-stage cyanation of *N*-Boc-fluoxetine to **1380** was regioselectively accomplished in a medium 38% (Scheme 249).

7.4 Cyanoalkylcarboxylation of aliphatic and (hetero)aromatic amines

A three-component variation of the above depicted cyanoalkylation protocol was reported by B. Lu *et al.* (Scheme 250).[325] Actually, both alkyl- and hetero(aryl)-amines can be reacted with cycloketone oxime esters (**1386**) in the presence of CO gas to afford cyanoalkylated amides. The transformation was catalyzed by CuI, in the presence of the tridentate ligand **1387** and CF_3Ph as the solvent and 2 × 3 W blue LEDs irradiation. As above, it's worth noting that the reaction proceeded without requiring any exogenous photosensitizer. A range of cyclobutanone oxime esters bearing methyl, propargyl, substituted benzyl groups, along with 3-monosubstituted substrates with phenyl-, fused aromatic rings, or esters was efficiently reacted under standard conditions. Likewise, substituted alkyl amines, and both electron-rich and electron-poor anilines, with *ortho*-, *meta*-, and *para*-substitution patterns, as well as fused (hetero)aromatic groups smoothly afforded the three-component products. To further prove the robustness of the synthetic approach, (±)-mexiletine was derivatized to **1385** in 50% and with 1.1 : 1 d.r. (Scheme 250)

7.5 Cyanoalkylation of aliphatic and (hetero)aromatic amines

C(sp^3)–N bond coupling of cycloketone oxime esters with amines allowed the incorporation of cyanoalkyl moieties into

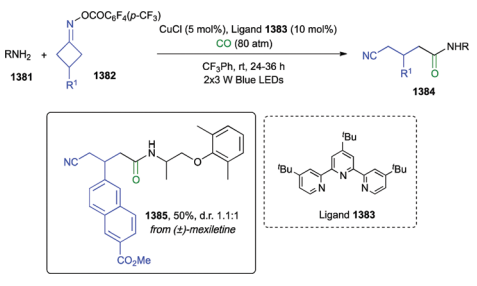

Scheme 250 Cyanoalkylcarboxylation of aliphatic and (hetero)aromatic amines.

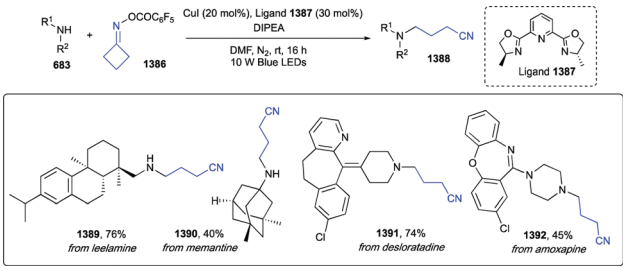

Scheme 251 Cyanoalkylation of aliphatic and (hetero)aromatic amines.

a wide range of nitrogen-containing scaffolds (Scheme 251).[326] This transformation was catalyzed by CuI and performed in DMF at room temperature for 16 h. Albeit visible-light was not necessary to promote the transformation, depending on the substrates, its use was often required to achieve high yields. The protocol proved to be robust with (hetero)aromatic amines and aromatic *N*-heterocycles, as well as with aliphatic amines with a good functional group tolerance including, for example, Br, I, CN, SO_2Me, and Bpin groups. Likely, a wide variety of cyclobutanone oxime esters allowed a rich structural diversification of aniline. Leelamine, memantine, desloratadine, and amoxapine further highlighted the potential of this synthetic approach for LSF of drugs (**1389–1392**, Scheme 251).

7.6 Arylation

Primary and secondary aliphatic amines could react with simple nonactivated arenes to afford *syn*-1,4-diaminated products (Scheme 252).

Thoroughly, arene–arenophile *para*-cycloadducts, formed *in situ* upon visible-light mediated [4+2]-photocycloaddition, underwent a formal allylic substitution with amines under Pd catalysis.[327] As arenophile, *N*-methyl-1,2,4-triazoline-3,5-dione (MTAD) was employed. The dearomative 1,4-diamination was accomplished in a one-pot two-step procedure, by reacting the arene and MTAD **1395** in EtOAc under visible light irradiation and at −50 °C for 12 h, followed by addition of the amine and the Pd catalyst in THF at −20 °C for 20 h. Secondary amines required $Pd(PPh_3)_4$ as catalyst, while primary amines showed better results with $Pd_2(dba)_3$/dppf. Both acyclic and cyclic secondary amines, and linear- or branched primary amines, smoothly afforded 1,4-diaminated naphthalenes and benzenes. Tolerated functional groups involved alkenes, silyl-protected alcohols, and esters. Remarkably, with benzene and naphthalene, disubstituted products formed as single diastereo- and constitutional isomers. Diversely, substituted benzenes were unreactive, while polynuclear arenes led in some cases to a lack in regioselectivity, along with the formation of mixtures of constitutional isomers. Memantine, an anti-Alzheimer drug, was converted into derivative **1396** under standard conditions in 66%.

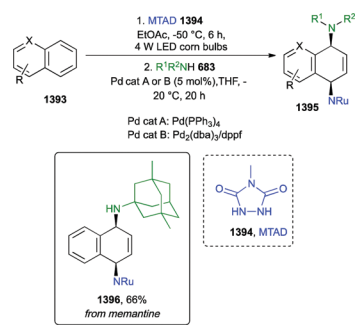

Scheme 252 Arylation of primary and secondary aliphatic amines.

7.7 Deaminative borylation of aliphatic amines

The groups of V. K. Aggarwal and F. Glorius concurrently reported a mild and general protocol to achieve deaminative borylation of aliphatic amines (Scheme 253A and B).[328,329]

The two laboratories, indeed, independently reported that aliphatic primary amines could be (either prior or *in situ*) converted into their corresponding redox-active pyridinium salts (**1397**, Katritzky salts) to generate alkyl radicals. The latter, in the presence of bis(catecholate)diboron **334**, afforded the corresponding alkyl borylated adducts (**1398**). The reaction mechanistically relied on the formation of an electron donor–acceptor (EDA) complex, thus avoiding the need for an additional photocatalyst. Standard reaction conditions indeed required DMA as solvent, blue LEDs irradiation, at room temperature or 60 °C for 6–24 h. Treatment of the crude reaction mixture with pinacol and triethylamine at room temperature for 1 h afforded the pinacol esters (**1399**) in good to excellent yields and with a wide reaction scope. The robustness of this protocol was further tested on complex biorelevant substrates such as hecogenin and tigogenin

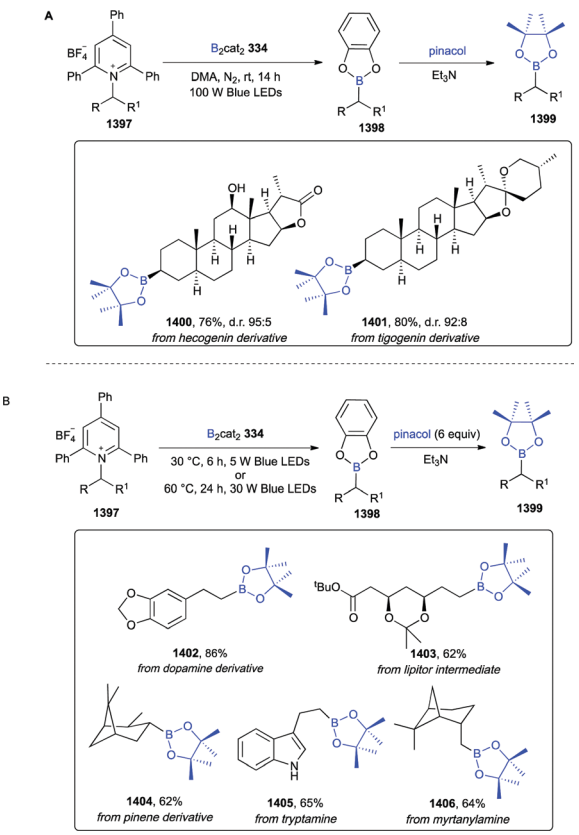

Scheme 253 Deaminative borylation of aliphatic amines.

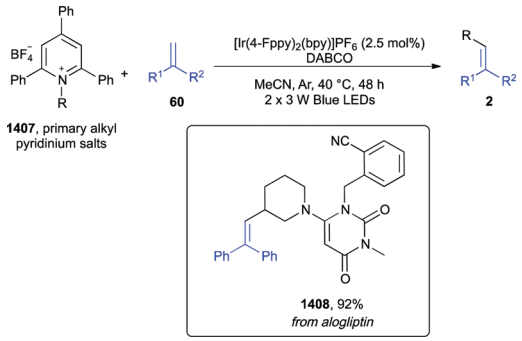

Scheme 254 Deaminative Heck-type reaction.

(**1400** and **1401**, Scheme 253A), as well as dopamine, a Lipitor intermediate, pinanamine, myrtanylamine, and tryptamine (**1402–1406**, Scheme 253B).

7.8 Deaminative Heck-type reaction

As reported by W. Xiao and coworkers, primary aliphatic amines, when converted into their corresponding Katrizky salts (**1407**, Scheme 254), can undergo either a deaminative or a carbonylative Heck-type reaction with alkenes under photoredox conditions.[330] In order to carry out the first transformation, $[Ir(4\text{-}Fppy)_2(bpy)]PF_6$ as the photocatalyst, DABCO as the base, MeCN as the solvent and 2×3 W blue LEDs irradiation were required, while performing the reaction in the presence of carbon monoxide (80 atm) led to carbonylated three-component adducts. The scope of Katrizky salts was broad, as both cyclic and acyclic amines were efficiently alkenylated, and F-, endocyclic O- and N-heteroatoms, nitriles, and esters were well tolerated. As for the alkenes, substrates with weakly electron-withdrawing groups (F-, Cl-) or electron-donating groups (Me-) were more efficient than electron-rich substrates (MeO-, Me_2N-); yet, cyclic aryl alkenes, cinnamylic acid, α-aryl and α-heteroaryl silyl enol ethers, as well as amide-derived enamines were all competent starting materials. As example of bioactive complex amine, the antidiabetic drug alogliptin was converted into derivative **1408** with an excellent 92% (Scheme 254).

7.9 Deaminative alkylation and alkynylation

Functionalization of 2,4,6-triphenylpyridinium salts (**1407**, Katritzsky salts, Scheme 255) derived from primary amines with alkynes (**88**) was shown to be promoted by eosin Y as a photocatalyst, in the presence of DIPEA and in a 3 : 1 mixture of MeOH/DCE under green LEDs irradiation.[331]

The use of Katritzsky salts offered multiple advantages as this prefunctionalization was chemoselective, required one reaction step, and did not need chromatographic purification. A wide range of pyridinium salts were reacted under the standard conditions, showing compatibility with carbamates, unprotected hydroxyl, sulfide, halogens, ester, basic nitrogen atom, and alkene. Likewise, as the alkyne partner, several alkynyl *p*-tolylsulfones proved to be competent substrates. The generality of the protocol was successfully tested on complex bioactive scaffolds such as mexiletine, metaraminol, dehydrocholic acid, and indomethacin (**1410–1413**, Scheme 255).

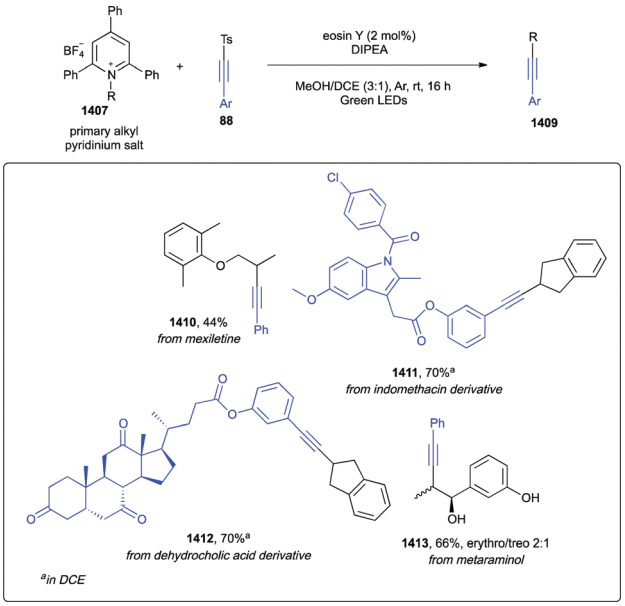

Scheme 255 Deaminative alkynylation.

Shortly after, the group of V. K. Aggarwal described that the reaction between Katriztky salts (**1397**, Scheme 256) and Michael acceptors (**168** or **488**) with a Hantzsch ester as a dual electron-donor and stoichiometric reductant in DMA and under blue LEDs irradiation led to alkylated Giese adducts, along with allylated, vinylated, alkynylated, thioether-, and hydrodeaminated derivatives.[332]

In contrast to the above reported protocol, here the authors reported catalyst-free conditions. Accordingly, Katrizky pyridinium salts and either Hantzsch ester or Et_3N formed electron donor–acceptor (EDA) complex, able to trigger a SET event, upon visible-light absorption, thus generating non-stabilized alkyl radicals intermediate. The latter added to a broad range of Michael acceptors to afford Giese products. Competent alkenes enclosed acrylates, acrylonitriles, methyl vinyl ketone, *N*-phenylacrylamide, phenyl vinyl sulfone, vinyl silanes and boronic esters, among others. As for the amines, a variety of cyclic and acyclic secondary alkyl substrates reacted cleanly. Late-stage modification of amine containing drugs such as norephedrine, mexiletine, tigogenin, baclofen, and leelamine was smoothly achieved in good yields under standard conditions (**1416–1422**, Scheme 256).

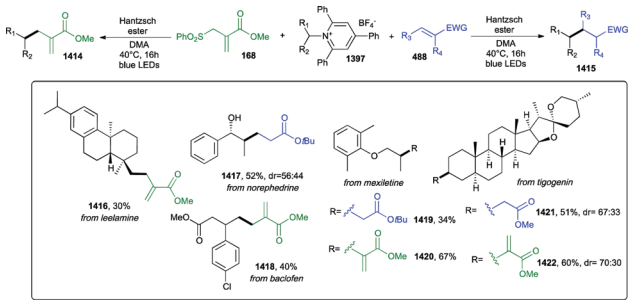

Scheme 256 Deaminative alkylation and allylation.

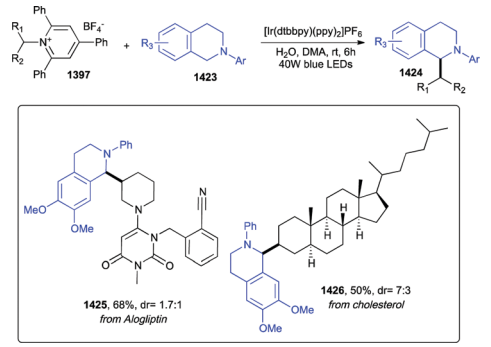

Scheme 257 α-Alkylation of *N*-arylamines.

Additionally, Katritzsky salts (**1397**) have been recently exploited in the α-alkylation of *N*-arylamines (**1423**) *via* either an iridium-complex photocatalyzed protocol or metal-free conditions (Scheme 257).[333] In both cases the reaction proceeded in DMA and in the presence of water, under irradiation with a 10 W or a 40 W blue LED light at room temperature. The scope of the Katrizsky salts (**1397**) included a variety of electron-rich and electron-deficient benzyl substrates, bearing functional groups such as methoxy, alkyl, halogen, and ester groups, as well as secondary alkyl amines. As α-amino-alkyl substrates, besides a wide range of substituted *N*-phenyltetrahydroisoquinolines, complex substrates such as the antidiabetic alogliptin and cholesterol gave the target derivatives **1425** and **1426** in moderate yields (Scheme 257). The method was further exploited also in the derivatization of peptides.

7.10 Trifluoromethylation of free anilines

J. Xie *et al.* developed a visible light induced radical trifluoromethylation of free anilines by using Togni's reagent **76** (Scheme 258) as CF_3 radical source, *fac*-Ir(ppy)$_3$ in DMF under 7 W blue LEDs irradiation at room temperature.[334] The protocol was endowed with a wide scope and an exceptional functional group tolerance, which enabled the synthesis of densely functionalized anilines bearing for example halogens, ethers, ketones, amides, nitriles, primary aliphatic amines, free alcohols, alkynyl, and Bpin groups. LSF of tocopherol 4-aminobenzoate provided product **1429** in 43% yield, with good regioselectivity (Scheme 258).

7.11 Sulfonylation of anilines

Aniline derivatives can be sulfonylated to aryl sulfones (**1431**, Scheme 259) with bench-stable sulfinate salts (**173**) under

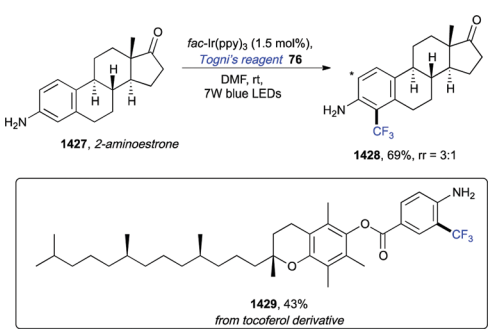

Scheme 258 Trifluoromethylation of free anilines.

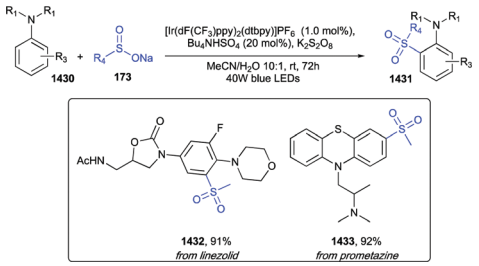

Scheme 259 Sulfonylation of anilines.

visible-light photoredox catalytic conditions.[335] [Ir(dF(CF$_3$)ppy)$_2$-(dtbpy)]PF$_6$ was identified as the most efficient catalyst, while potassium persulfate served as the oxidant; TFA as an additive was also necessary to achieve high yields and a mixture of 10 : 1 MeCN/water as the solvent system and blue LEDs irradiation provided optimized reaction conditions. As for the anilines both alkyl and aryl substituents were tolerated, as well as electron-donor methoxy- and unprotected hydroxyl groups, and electron-withdrawing halogens. Elseways, alkyl groups at the nitrogen atom of anilines underwent competing dealkylation processes, resulting in lower yields. Worth of note, a good regioselectivity was observed, with *ortho*- and *para*-substitution being generally predictable. Drugs such as linezolid and promethazine were methylsulfonylated with excellent 91% and 92% yields, respectively (**1432** and **1433**, Scheme 259).

7.12 C–H arylation of benzylamines

A mild protocol to accomplish regio- and chemo-selective C(sp^3)–H arylation of benzylamines was reported by T. Ide *et al.* (Scheme 260).[336] The mechanism underpinning this transformation relied on both single-electron transfer (SET) and hydrogen atom transfer (HAT) events. More in detail, PhC(O)SH acted as HAT agent enabling the selective generation of a sulfur-centered radical and favoring *N*-benzyl selectivity as opposite to *N*-methyl and *N*-methylene selectivity generally observed under exclusive SET conditions. The reaction showed excellent regioselectivity and required *fac*-Ir(ppy)$_3$ as the photocatalyst, the HAT agent, terephthalonitrile as an additive, K_2HPO_4 as a base, in DMA as solvent under blue LEDs irradiation at room temperature. Several *N*,*N*-dimethylbenzylamines (**683**) were tested as substrates, with strongly electron-poor derivatives showing as unsuitable

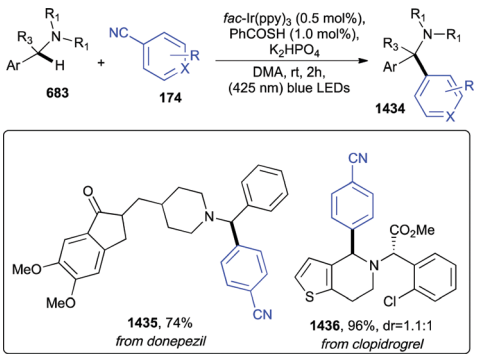

Scheme 260 C–H arylation of benzylamines.

starting materials. Contrarily, the reaction tolerated steric hindrance and unprotected primary and secondary amines, together with heterocyclic aromatic derivatives. As examples of drugs compounds, donezepil and clopidogrel underwent late-stage functionalization in 74% and 96% yields, respectively (**1435** and **1436**, Scheme 260).

7.13 Alkylation of α-amino C(sp^3)–H bonds

C(sp^3)–H bonds adjacent to amides, carbamates, ethers, and thioethers can be efficiently alkylated with a dual photoredox-nickel catalytic system, using quinuclidine **1187** (Scheme 261) as HAT agent and K_2CO_3 as a base, in a MeCN/H_2O solvent mixture, under blue LEDs irradiation at room temperature.[337] A wide array of alkyl bromides showed efficient as alkyl radical precursors, and nitriles, heteroaromatics, esters, ethers, phosphonates and acetals were all compatible with standard reaction conditions. α-Branched and sterically demanding alkyl fragments gave moderate yields, but still proved to be suitable substrates. As example of regio- and chemo-selective late-stage functionalization of a therapeutically relevant compound, *N*-Boc-fluoxetine was converted into three different alkylated adducts **1440–1442** (Scheme 261).

Recently, D. A. Nicewicz and coworkers described a site-selective C–H alkylation of piperazine derivatives under photoredox catalytic conditions (Scheme 262).[338] Interestingly, the site-selectivity arose from the electronically distinct properties of the two nitrogen centers of the piperazine scaffold as predictable by means of DFT natural population analysis (NPA), which measured the relative electron density at both nitrogen centers in the neutral and in the oxidized form as cation radical.

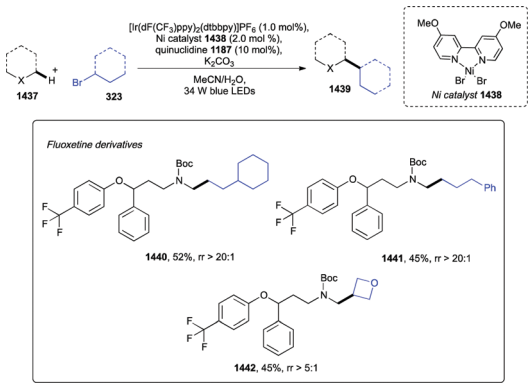

Scheme 261 Alkylation of α-amino C(sp^3)–H bonds.

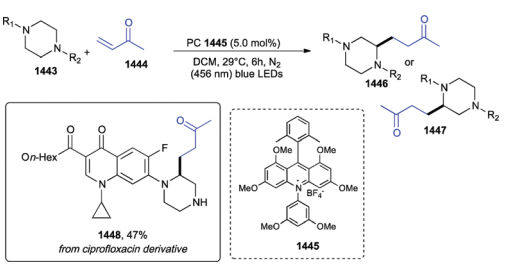

Scheme 262 Alkylation of α-amino C(sp^3)–H bonds.

According to the computational support, the nitrogen atom undergoing the major change in electron density would be the preferred site for alkylation. The protocol required the acridinium catalyst **1445** in CH_2Cl_2 at 29 °C under irradiation with 456 nm LEDs. Piperazine scope included a range of Boc- and/or CBz-arylpiperazines, as well as benzamide and trimethylacetamide substrates. Suitable electron-acceptors were identified as methyl vinyl ketones (MVK), and other Michael acceptors bearing sulfones, amides, and nitriles. The method was successfully applied to the late-stage alkylation of ciprofloxacin in 47% as a single regioisomer (**1448**, Scheme 262).

7.14 Monofluoroalkenylation of dimethylamino compounds

A radical–radical cross-coupling of α-aminoalkyl radicals and monofluoroalkenyl radicals derived from *gem*-difluoroalkenes under visible-light photoredox catalysis was reported by J. Xie *et al.* (Scheme 263).[339] This tandem C(sp^3)–H and C(sp^2)–F bonds functionalization provided the access to tetrasubstituted monofluoroalkenes, and in order to achieve optimum yields [Ir(dF(CF_3)ppy)$_2$(dtbbpy)]PF_6 as the photocatalyst and Na_2CO_3 as a base, in DMF as solvent, and under blue LEDs irradiation, were essentials. The wide reaction scope and the exquisite functional group tolerance were proven, in addition to the synthesis of more than 40 diverse products, by the late-stage functionalization of 7 different complex bioactive substrates such as (+)-diltiazem, citalopram, rosiglitazone, venlafaxine, dihydroartemisinin, oleanic acid, and androsterone (**1452–1459**, Scheme 263).

7.15 Hydroamination and *N*-arylation

Aryloxy-amides, thanks to their propensity to undergo SET readuction, could be valuable precursors for the generation of amidyl radicals. This inclination has been exploited by the group of D. Leonori for the synthesis of *N*-containing compounds through a transition metal-free photoredox hydroamination–cyclization

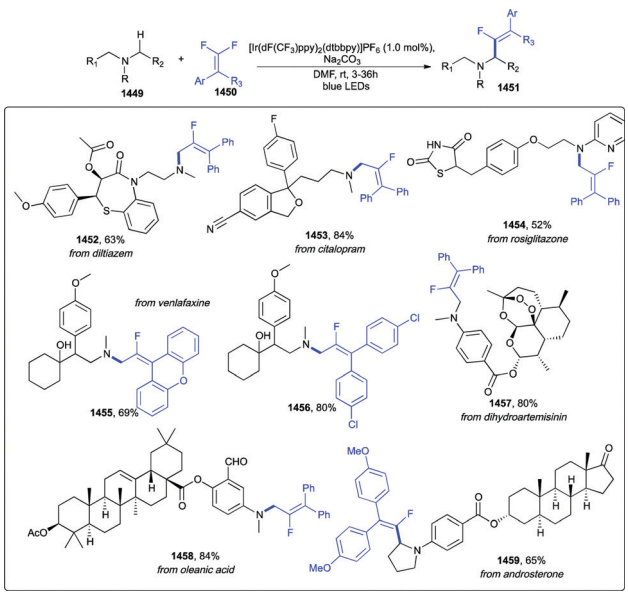

Scheme 263 Monofluoroalkenylation of dimethylamino compounds.

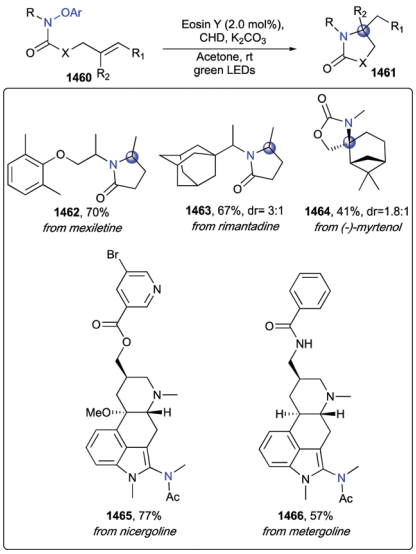

Scheme 264 Hydroamination and *N*-arylation.

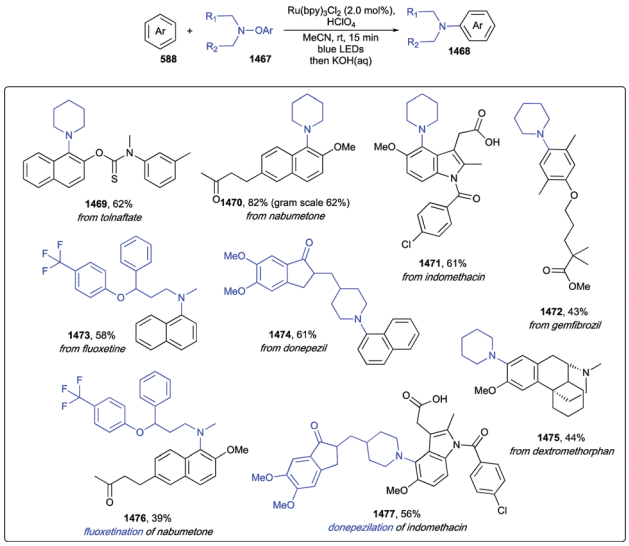

Scheme 265 Hydroamination and *N*-arylation.

and *N*-arylation (Scheme 264).[340] Thoroughly, the developed protocol featured eosin Y as the photocatalyst, 1,4-cyclohexadiene (CHD) as both a hydrogen atom donor and SET reductant, K_2CO_3 as a base in acetone under green LEDs irradiation at room temperature. These optimized reaction conditions enabled the generation of amidyl radicals with broad substitution patterns, including primary and secondary alkyl groups, as well as redox-active sulfone containing heterocycles and *N*-Boc and *N*-Cbz protection. As examples of complex bioactive scaffolds, the anti-inflammatory (−)-myrtenol, and two blockbuster drugs mexiletine and rimantadine were converted into derivatives **1462–1464** in high yields (Scheme 264). Additionally, the authors reported that the same method could be used to carry out intermolecular *N*-arylation and heteroarylation. The robustness of this transformation was excellently showcased in the LSF of ergot derivatives nicergoline and metergoline (**1465** and **1466**, Scheme 264).

Shortly afterwards, the same group reported that protonated electron-poor *O*-aryl hydroxylamines could give aminium radicals in the presence of $Ru(bpy)_3Cl_2$ under visible-light irradiation (Scheme 265).[341] These species are isoelectronic to alkyl radicals, but the formal positive charge make them highly electrophilic enabling a polarized radical addition to aromatic compounds with high yields and regioselectivity. This direct aromatic amination smoothly progressed in the presence of the above-mentioned ruthenium photocatalyst, $HClO_4$ as a Brønsted acid, in MeCN as the solvent and blue LEDs irradiation at room temperature.

Control experiments revealed that irradiation was not necessary to promote the transformation, but still, it enabled higher yields suggesting a complex interplay between "dark" and photochemical pathways. The reaction showed a broad applicability to both weakly and strongly electron-rich aromatic partners, with monosubstituted benzenes preferentially derivatized at the *para*-position. Complex polycyclic aromatic compounds were competent substrates and late-stage amination of a wide number of pharmaceutical agents was efficiently accomplished with good yields and regioselectivity (**1469–1477**, Scheme 265).

7.16 Remote C(sp^3)–H functionalization of *N*-chlorosulfonamides

N-Chlorosulfonamides (NCSs) could undergo remote intramolecular C(sp^3)–H amidation and chlorination by using $[Ir(ppy)_2(dtbbpy)]PF_6$ as a photocatalyst, Na_2HPO_4 as a base in MeCN and under white LEDs irradiation (Scheme 266).[342] During the exploration of the substrate scope, it was found that the electronic properties exerted by the nitrogen protecting groups could dramatically influence the reaction outcome. Actually, electron-rich NCSs reacted more efficiently than electron-deficient substrates. Still, a number of diversely functionalized pyrrolidines were successfully synthesized, along with oxazolidines and cyclic benzosulfonamides in moderate to good yields. In order to demonstrate the practicability of the method, a gram scale reaction was also performed decreasing the photocatalyst loading to 0.05% so that the isolated yield of 87% indicated a turnover number of 1740. Additionally, standard conditions were applied to the late-stage functionalization of matrix-2 protein inhibitor (−)-*cis*-myrtanylamine-derived NCS **1478** and (+)-dehydroabietylamine-derived NCS **1479**, providing derivatives **1480** and **1481** in excellent yields (Scheme 266).

7.17 Deuteration and tritiation of nitrogen containing pharmaceuticals

Y. Y. Loh reported a photoredox-mediated hydrogen atom transfer protocol efficiently and selectively installing deuterium (D) and

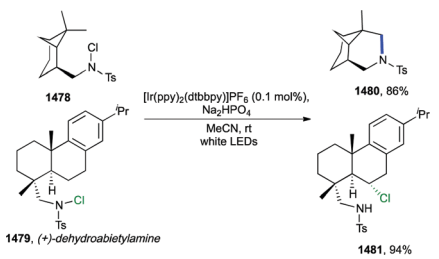

Scheme 266 Remote C(sp^3)–H functionalization of *N*-chlorosulfonamides.

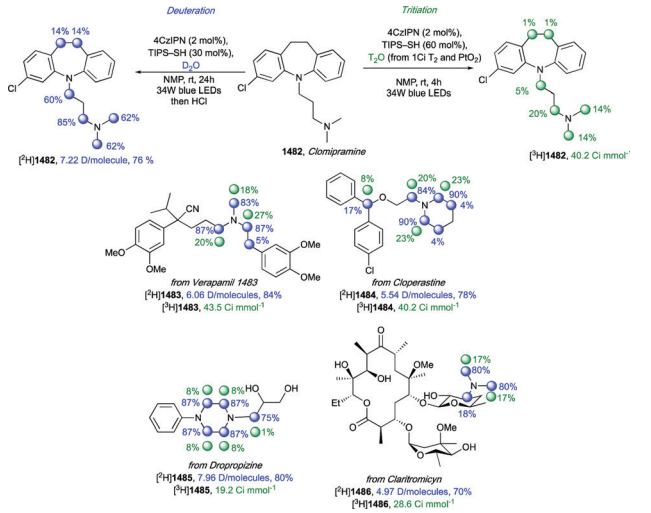

Scheme 267 Deuteration and tritiation of nitrogen containing pharmaceuticals.

tritium (T) at α-amino sp^3 carbon–hydrogen bonds in a single step, using isotopically labeled water (D_2O or T_2O) as the source of hydrogen isotope (Scheme 267).[343] This mild protocol provided valuable deuterium- and tritium-labeled pharmaceutical compounds, which could meet the needs of drug discovery research as useful diagnostic tools. Here, merger of photoredox and hydrogen atom transfer (HAT) catalysis enabled the generation of α-amino alkyl radicals and their subsequent incorporation of D or T mediated by a thiol-based *in situ* generated D/T donor. By changing reaction conditions, different protocols were optimized to efficiently convert 18 drug molecules into D- or T-labeled derivatives.

8. Chemical modification of carboxylic acid and ester derivatives

Readily available and bench-stable carboxylic acids have been deeply explored as both acyl- and alkyl-radical precursors. Accordingly, a wide range of aliphatic and aromatic carboxylic acids can be engaged in deoxygenative or decarboxylative processes. Representative transformations preserving the C=O functionality include conversion to aldehydes and ketones, and deuteration, while decarboxylative pathways are more common and consist of alkylation, trifluoromethylation, arylation, alkynylation, formation of carbocycles such cyclopropanes and cyclobutanes as well as C–N coupling to form amines, hydrazines, and imines, and conversion to functional groups such as ethers, esters, and thioesters, to cite a few.[344] Interestingly, carboxylic acids can be used as such or as Redox-Active Esters (RAEs), for instance NHPI (*N*-HydroxyPhthalimide) esters or oxime esters, or as α-imino-oxy acids, in order to achieve modulation of the redox potential, and be able to generate, under a vast selection of reaction conditions, a wide array of structurally diverse C-centered radical intermediates. The recent developments reported further corroborate the central role of this class of functional groups as versatile and convenient radical precursors.

8.1 Hydrodecarboxylation

Primary, secondary, and tertiary carboxylic acids (**1487**, Scheme 268) could undergo a hydrodecarboxylation reaction to alkanes (**1488**) by using a Fukuzumi acridinium photooxidant, phenyldisulfide as a redox-active cocatalyst, and substoichiometric quantities of Hünig's base in trifluoroethanol as a solvent and under blue LEDs irradiation.[345]

Thiophenol, formed *in situ* upon homolytic scission of the disulfide precursor, SET reduction, and subsequent protonation, acted as hydrogen atom transfer reagent for the alkyl radical intermediate generated from SET oxidation/fragmentation of the carboxylic acids. The reaction scope was good, and the generality of the protocol was further tested in the late-stage dehydrocarboxylation of enoxolone (**1489**, Scheme 268).

8.2 Dehydrodecarboxylation to alkenes

A dual catalytic system to achieve dehydrodecarboxylation of primary, secondary, and tertiary aliphatic carboxylic acids was developed by V. T. Nguyen *et al.* (Scheme 269).[346] The protocol relied on the exploitation of a photoinduced acridine catalyzed O–H hydrogen atom transfer (HAT, **1492a–d**) and cobaloxime-catalyzed C–H HAT (**1491**) (for a recent review see: J. A. Tunge[347]). Remarkably, this cooperative chemoenzymatic procedure could be amenable for a triple catalytic cooperative lipase–acridine–cobaloxime process enabling direct conversion of plant oils and biomass to long-chain terminal alkenes. The conversion of carboxylic acids to alkenes was performed as shown in Scheme 269, starting from a broad array of carboxylic acids including complex biorelevant scaffolds such as biotin, dihydromycophenolic acid, chlorambucil, deoxycholic acid, cholic acid, sulfisoxazole, sulfamerazine, glycyrrhetinic acid, and gemfibrozil (**1493–1502**, Scheme 269).

A protocol for the decarboxylative desaturation of aliphatic carboxylic acids, was also developed by W.-M. Cheng *et al.*

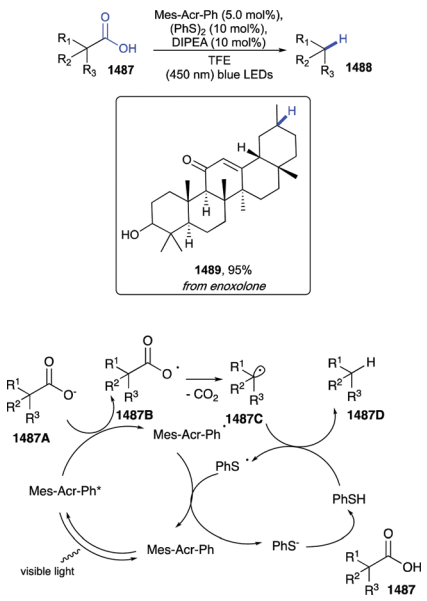

Scheme 268 Hydrodecarboxylation.

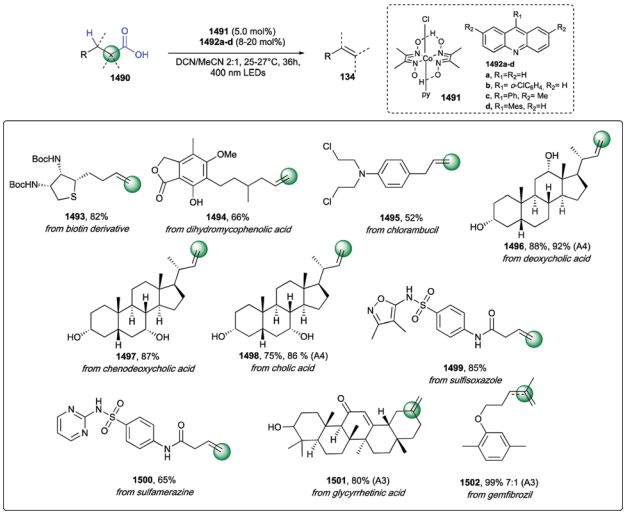

Scheme 269 Dehydrodecarboxylation to alkenes.

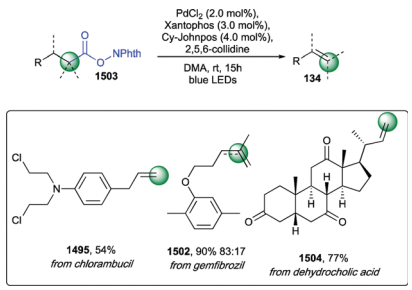

Scheme 270 Dehydrodecarboxylation to alkenes.

(Scheme 270).[348] Opposite to the previous catalytic system, here carboxylic acids needed to be derivatized as *N*-hydroxyphthalimide (NHPI) esters (**1503**). The transformation required $PdCl_2$, Xantphos and Cy-Johnphos as ligands, 2,4,6-collidine in DMA under blue LEDs irradiation at room temperature for 15 h. Interestingly, by using α-hydroxy- and α-amino carboxylates, the scope of the reaction was further extended to enol ethers, enamides, and peptides. LSF of pharmaceutical compounds such as chlorambucil, gemfibrozil, and dehydrocholic acid (**1495**, **1502**, and **1504**) proved the utility of this synthetic approach to achieve an easy diversification of complex substrates.

8.3 Decarboxylative Heck-type coupling

An alternative and general approach to access exclusively (*E*)-substituted olefins (**1507**, Scheme 271) from NHPI esters (**1506**) and styrenes (**1505**) was reported by the group of F. Glorius.[349] Thoroughly, the reaction proceeded *via* photoexcitation of $Pd(PPh_3)_4$ and subsequent SET reduction of the redox active ester, which after fragmentation, delivered an alkyl radical intermediate. Addition of the latter to styrene, followed by β-hydride elimination afforded the final alkene. The mild conditions identified, as shown in Scheme 271, provided a wide scope for styrenes, primary, secondary, and tertiary carboxylic acids, along with a good functional group tolerance, including double and triple bonds, halogens, ethers, esters, carbamates, halogens, and heteroarenes

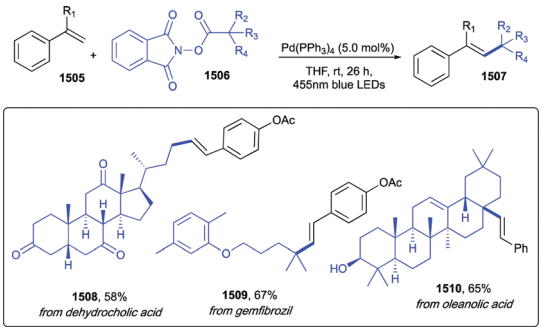

Scheme 271 Decarboxylative Heck-type coupling.

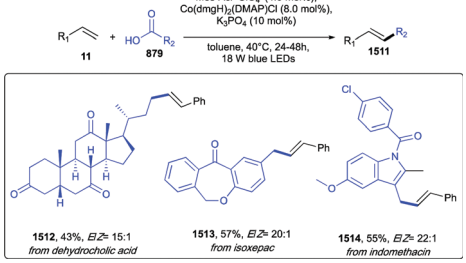

Scheme 272 Decarboxylative Heck-type coupling.

such as pyridine, to cite a few. Late-stage Heck-type coupling of gemfibrozil, dehydrocholic acid and oleanolic acid provided derivatives **1508–1510** in good yields.

Shortly after, J. Wu and coworkers developed a protocol to achieve alkylation of vinyl arenes, vinyl silanes, and vinyl boronates through a photoinduced decarboxylative Heck-type coupling starting from alkyl carboxylic acids (Scheme 272).[350] In contrast to the Glorius protocol, this transformation did not require acid activation as NHPI esters. Added values are the use of an organic photosensitizer, the absence of an external oxidant, the broad substrate scope along with the excellent functional groups compatibility as shown by more than 90 examples, and the scalability to gram quantity. Experimentally, the Heck-type coupling was run in toluene, in the presence of $Mes\text{-}Acr^{+}ClO_4^{-}$, $Co(dmgH)_2(DMAP)Cl$ as cobaloxime cocatalyst, K_3PO_4 as a base, under 18 W blue LEDs irradiation at 40 °C for 24–48 hours. These conditions proved to be effective also in the late-stage conversion of carboxylic acid-containing drugs such as indomethacin, isoxepac, and dehydrocholic acid into derivatives **1512–1514** (Scheme 272).

More recently, J.-L. Tu *et al.* reported that α-imino-oxy acids could be involved in a radical aza-cyclization to afford *N*-heterocycles *via* a dual photoredox/cobaloxime catalytic system (Scheme 273).[351] The method was endowed with excellent functional group compatibility and avoided the use of noble-metal catalysts and external oxidants. Remarkably the reaction worked either in the presence or in the absence of an additional alkene, affording a variety of alkene-containing dihydropyrroles in both cases, albeit, in the presence of external alkenes, *E*-selective coupling adducts were generated with excellent chemo- and stereo-selectivity. The wide scope was also demonstrated

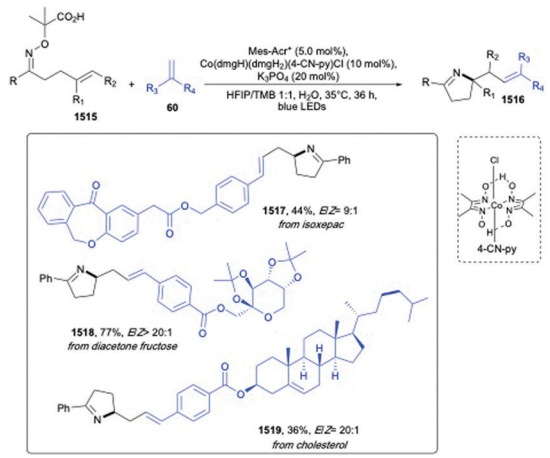

Scheme 273 Decarboxylative Heck-type coupling.

by selecting complex bioactive alkene-containing scaffolds such as isoxepac, diacetone fructose, and cholesterol (**1517–1519**, Scheme 273).

8.4 Decarboxylative alkynylation

As shown by Q.-Q. Zhou *et al.*, a wide range of aliphatic carboxylic acids, α-keto, and α-amino acids could be converted into their corresponding decarboxylated alkynyl-derivatives under photoredox catalytic conditions (Scheme 274).[352,353] Thoroughly, this transformation was promoted by $[Ir(dF(CF_3)ppy)_2(dtbbpy)]PF_6$, Cs_2CO_3 in CH_2Cl_2 as a solvent in the presence of 4 Å MS, and 8 W blue LEDs irradiation. Interestingly, when the reaction was performed in the presence of carbon monoxide (60 bar) and irradiated with two bulbs of 7 W blue LEDs, a carbonylative alkynylation occurred to give ynone products. Tolerated functional groups embodied Boc- and Fmoc-protected amines, ethers, free hydroxy groups as shown in the late-stage modification of ursolic acid (**1522**, Scheme 274).

More recently, Y. Mao *et al.* reported a decarboxylative cross-coupling method to obtain substituted alkynes (**463**, Scheme 275) from redox active esters as alkyl radical precursors and by exploiting copper catalysts CuCl and $Cu(acac)_2$.[354] The protocol did not require any additional photocatalyst, as the photoexcitation of copper acetylides with Et_3N as a ligand enabled the generation of alkyl radicals. The scope of the reaction was further extended to aliphatic alkynes and alkynyl silanes by using catalytic amounts of preformed copper-phenylacetanilide. DFT-based mechanistic investigations revealed that the acetylacetonate ligand of the copper catalyst was necessary to avoid the homo-coupling of the alkyne. The substrate scope was wide for both the redox active esters and the alkynes, including representative complex biorelevant scaffolds such as arachidonic acid, pinonic acid,

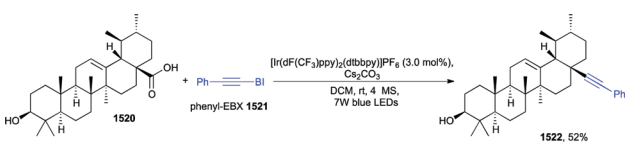

Scheme 274 Decarboxylative alkynylation.

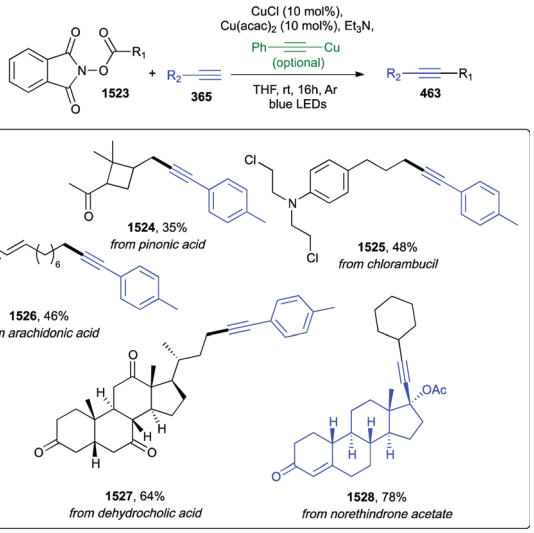

Scheme 275 Decarboxylative alkynylation.

chlorambucil, dehydrocholic acid, and 19-norethindrone acetate (**1524–1528**, Scheme 275).

8.5 Decarboxylative arylation and alkylation of α-fluorocarboxylic acids

α-Fluorocarboxylic acids (**1529**, Scheme 276) could be engaged in a decarboxylative $C(sp^3)$–$C(sp^2)$ and $C(sp^3)$–$C(sp^3)$ bond formation with organic halides to afford fluorinated products.[355] The cross coupling was efficiently promoted by a dual catalytic system based on an iridium-photocatalyst and a bipyridine–Ni complex. Extensive optimization of reaction conditions, computationally driven by DFT calculations, allowed to increase the efficiency of metallaphotoredox decarboxylative cross coupling catalytic system, whereas the presence of the fluorine atom led to low yields by applying methods previously reported for phenylacetic acid derivatives. Accordingly, $[Ir(dF(CF_3)ppy)_2(dtbbpy)]PF_6$, $NiBr_2{\bullet}DME$, 4,4′-dimethoxy-2,2′-bipyridine as a ligand, 1,1,3,3-tetramethylguanidine as the base, and stoichiometric potassium triflate (KOTf) as an additive in DMA as a solvent under blue LEDs irradiation were identified as optimum conditions. The scope of α-fluoro acids was demonstrated with a wide range of substituted inputs, leading to medium to good yields. Likewise, both aryl and alkyl

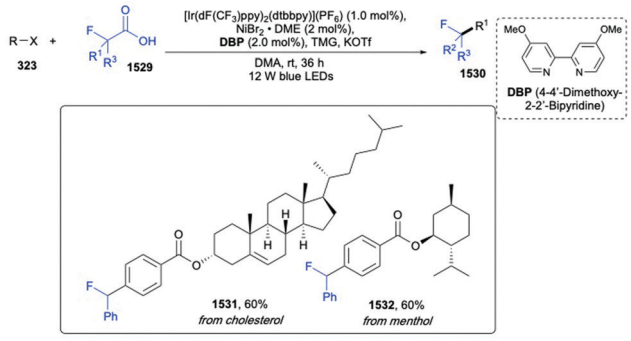

Scheme 276 Decarboxylative arylation and alkylation of α-fluorocarboxylic acids.

halides provided a large library of fluorinated adducts, including heterocycles such as pyridines, pyrimidines, and indoles, and tolerating double bonds, esters, ethers, aldehydes, cyano-, sulfonamides, and ketones functional groups as showcased with the ester- and alkene-containing cholesterol and with menthol (**1531** and **1532**, Scheme 276).

8.6 Decarboxylative *N*-alkylation

Recently, V. T. Nguyen *et al.* reported a direct conversion of carboxylic acids into *N*-alkylated aromatic carbocyclic and heterocyclic amines by exploiting a dual catalytic system consisting of an acridine photocatalyst (**1492b** or **1492e**, Scheme 277), $Cu(hfac)_2$ (hfac = hexafluoroacetylacetonate), and di-*tert*-butyl peroxide (DTBP) as an oxidant.[356] The reaction proceeded in EtOAc as a solvent under 400 nm LEDs irradiation at room temperature for 12 hours. The carboxylic acids scope covered primary, secondary, and tertiary hindered aliphatic inputs, while both *N*-alkylanilines and diarylamines were smoothly alkylated under the standard conditions. Primary anilines led to dual alkylated derivatives, and remarkably nitrogen-containing heterocycles such as indoles and carbazoles, as well as heterocyclic aromatic amines gave the alkylated product in good to excellent yields. Late-stage alkylation of amine-containing bioactive compounds, including the aromatase inhibitor aminoglutethimide (**1543–1545**, Scheme 277) was accomplished in 54–67% yields. Likewise, naturally occurring aleuritic, oleic acid, cholic, deoxycholic, and chenodeoxycholic acids were cleanly converted into the corresponding *N*-alkyl anilines **1535–1542**.

8.7 Decarboxylative C–N coupling to protected amines

W. Zhao *et al.* reported a photoinduced rearrangement of *N*-hydroxyphthalimide (NHPI) esters to phthalimide protected amines, as an alternative to the Curtius reaction (Scheme 278).[357]

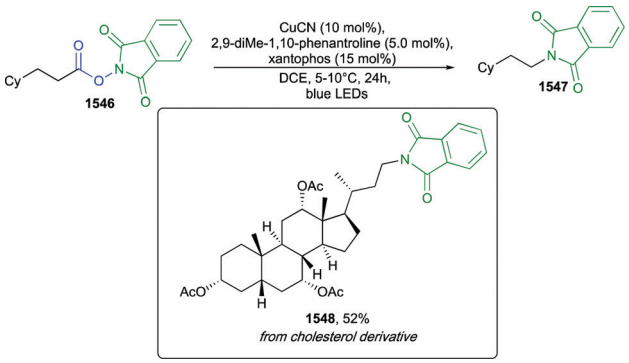

Scheme 278 Decarboxylative C–N coupling to protected amines.

The decarboxylative amination was achieved by using CuCN as a copper catalyst, 2,9-dimethyl-1,10-phenanthroline (dmp or neocuproine), and Xantphos in DCE at 5–10 °C and under blue LEDs irradiation. The reaction scope was wide, with tolerated functional groups including alcohol, aldehyde, epoxide, indole, nitroalkane, and sulfide. Late-stage modification of a steroid derivative gave further evidence of the generality of the developed protocol (**1548**, Scheme 278).

Shortly after, the group of X. Hu developed a general strategy for amination of alkyl electrophiles *via* a dual photoredox/copper catalysis (Scheme 279).[358] The design of the reaction relied on the exploitation of alkyl redox active esters as readily available alkyl radical precursors, which, once formed, could be trapped by a low-valent metal amido complex, formed by the primary amine and the copper catalyst. Optimized reaction conditions featured $Ru(bpy)_3(PF_6)$ as the photoredox catalyst, CuBr as the copper source, 2-(2,6-dimethoxylphenylamino)-2-oxoacetic acid **1549** as a ligand, Et_3N as a base, in MeCN under blue LEDs irradiation at room temperature. By applying these conditions, a wide range of anilines, and acyclic primary-alkyl and secondary-alkyl carboxylic acids underwent the metallaphotoredox cross-coupling to afford a library of secondary amines. Besides anilines, other competent nitrogen heterocycles included pyridines, quinolines, sulfonamides, amides, and ureas. Functional groups

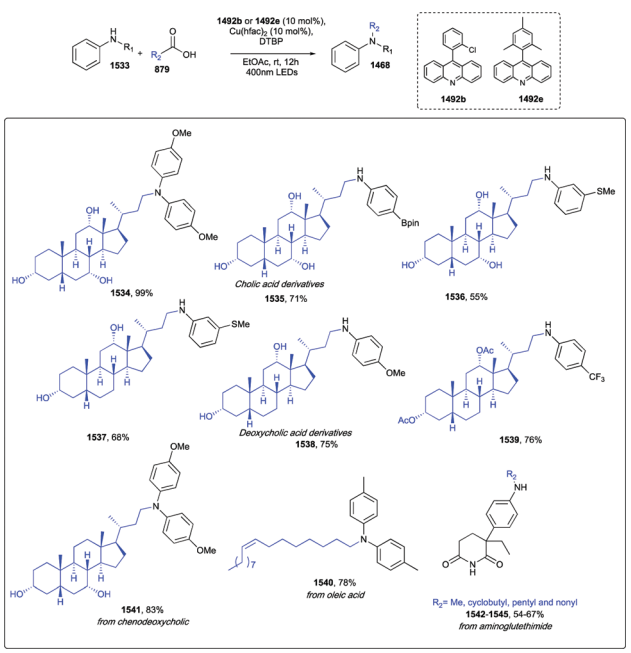

Scheme 277 Decarboxylative *N*-alkylation.

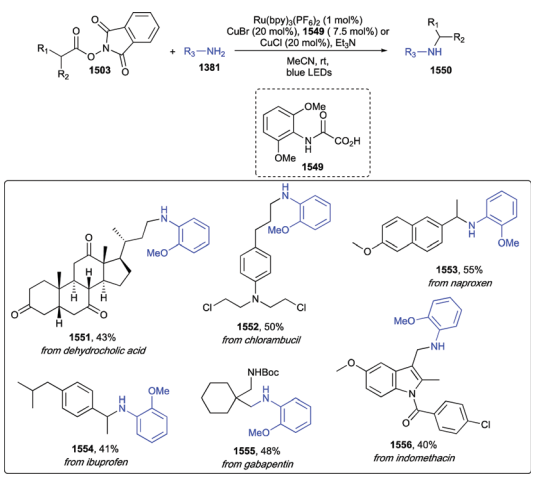

Scheme 279 Decarboxylative C–N coupling to protected amines.

such as ethers, halogens, cyano, ester, and ketone were well tolerated, while the presence of double and triple bonds led to decreased yields. LSF of carboxylic acid-containing drugs was showcased for dehydrocholic acid, chlorambucil, naproxen, gabapentin, indomethacin, and ibuprofen (**1551–1556**, Scheme 279).

In parallel, the same group developed a protocol to achieve the cross-coupling of alkyl *N*-hydroxyphthalimide esters with benzophenone-derived imines by employing an iridium photocatalyst and $Cu(MeCN)_4PF_6$ as the copper source (Scheme 280).[359] Secondary and tertiary NHPI esters (**1523**) reacted efficiently in DMA and with Cs_2CO_3 as a base, while primary NHPI esters required an organic base, such as diisopropylamine in MeCN. A range of amines protected as benzophenone imine was readily synthesized. Cyclic alkyl groups up to 12-membered rings, as well as heterocyclic alkyl and perfluoroalkyl derivatives proved to be competent substrates, with tolerated functional groups including sulfonamides, ethers, and alkenes. Late-stage amination of complex bioactive scaffolds such as dehydrocholic acid, chlorambucil, abietic acid, and gemfibrozil was reported in good yields (**1559–1562**, Scheme 280). Importantly, these drugs presented bromo, chloro, and keto groups, which are incompatible with classical alternative methodologies such as direct alkylation and reductive amination, respectively.

Recently, a further advancement was reported by F. Glorius and coworkers, who developed a method for the intermolecular carboimination of alkenes starting from benzophenone oxime esters of aliphatic carboxylic acids (**1563**, Scheme 281).[360] Upon irradiation with blue LEDs and in the presence of $[Ir(dF(CF_3)ppy)_2(dtbbpy)]PF_6$ as a photosensitizer, the oxime esters underwent a homolytic scission to generate both an alkyl **1563B** and an iminyl radical **1563A**. Addition of the alkyl radical **1563B** to the alkene **11** led to a transient radical **1563C** prone to undergo selective radical–radical cross coupling with the persistent iminyl radical **1563A**. Experimental observations supported the mechanistic hypothesis of a triplet–triplet energy transfer event between the oxime ester **1563** and the excited state photocatalyst. The generality of the transformation was investigated with a range of alkenes with different electronic and steric properties. On the other hand, cyclic alkenes and alkynes proved

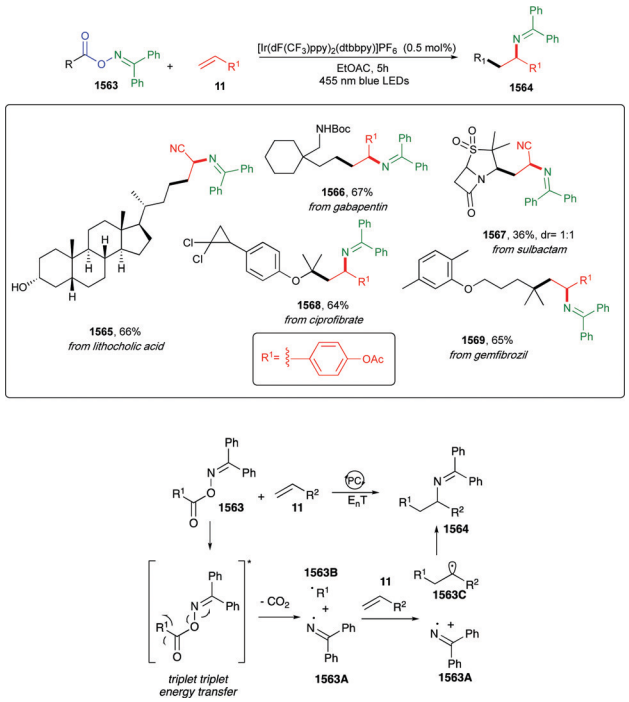

Scheme 281 Decarboxylative C–N coupling to protected amines.

to be unreactive under the developed conditions. The carboxylic acid scope involving a plethora of diversely functionalized primary, secondary, and tertiary substrates, bearing linear, carbo-, and heterocycles inputs. Oxime esters derived from pharmaceuticals such as gabapentin, sulbactam, ciprofibrate, gemfibrozil, and lithocholic acid were carboiminated in good yields (**1565–1569**, Scheme 281). Additionally, the method proved to be effective also with amino acids, and by simple hydrolysis, it was possible to isolate primary ammonium chloride salts.

8.8 Dehydrodecarboxylative synthesis of imines

The homolytic N–O bond cleavage of oxime esters induced by an excited state iridium photocatalyst afforded acyloxy and iminyl radicals (Scheme 282).[361]

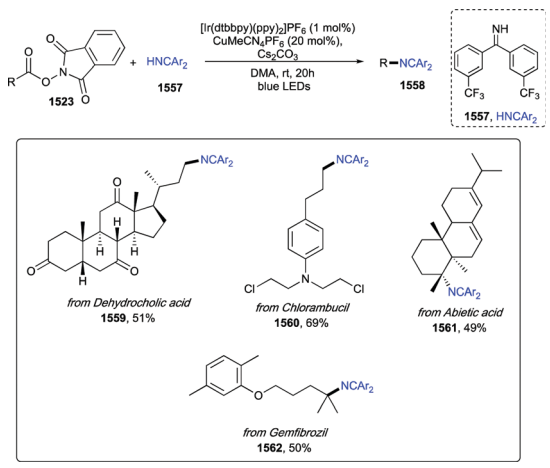

Scheme 280 Decarboxylative C–N coupling to protected amines.

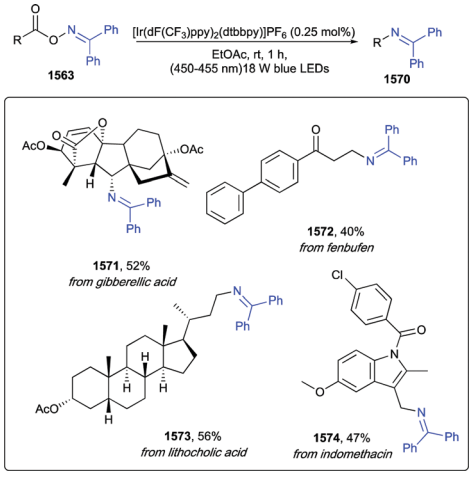

Scheme 282 Dehydrodecarboxylative synthesis of imines.

Decarboxylation of the iminyl radical led to alkyl radical intermediates, which underwent a cross-coupling with the iminyl radicals to afford, with high atom economy, imine derivatives (**1570**). Short reaction times (typically 1 h) and 0.25 mol% loading of the photocatalyst were sufficient to afford in high yields imine adducts. The use of EtOAc as a solvent also proved to be essential to achieve selectivity. The reaction proceeded through an exclusive energy transfer mechanism enabling this challenging radical–radical C(sp^3)–N cross-coupling. The reaction scope covered primary alkyl, benzylic, and secondary alkyl carboxylic acids, while the iminyl moiety tolerated alkyl, halogens, heterocyclic, and cyano-functional groups. The generality of this synthetic protocol was further demonstrated with bioactive fenbufen, lithocholic acid, indomethacin, and gibberellic acid (**1571–1574**, Scheme 282).

8.9 Decarboxylative hydrazination

Carboxylic acids could undergo a radical decarboxylative hydrazination by reacting with di-*tert*-butylazodicarboxylate (DBAD) in the presence of $CeCl_3 \cdot 7H_2O$, a catalytic amount of Cs_2CO_3, in MeCN as a solvent under blue LEDs irradiation at room temperature for 24 hours (Scheme 283).[362] Interestingly, this protocol exploited a Ligand to Metal Charge Transfer (LMCT) event to generate a radical species upon homolysis of the metal–ligand bond **879A** (*i.e.* Cerium and the carboxylic acid functional group), thus being a valuable alternative to the SET events initiated from a Metal to Ligand Charge Transfer (MLCT) as in the case of the photoredox catalysts based on ruthenium and iridium complexes.

The reaction scope was wide including primary, secondary, and tertiary bulky carboxylic acids, with functional groups such as ethers, alkynes, alkenes, bromo, esters, cyano, and Boc-protected amines affording the desired hydrazines in medium to high yields. The protocol was also successfully tested in the LSF of drugs such as gabapentin, fenclozic acid, tolmetin, isoxepac, gemfibrozil, and the biorelevant TBS-protected lithocholic acid (**1576–1581**, Scheme 283).

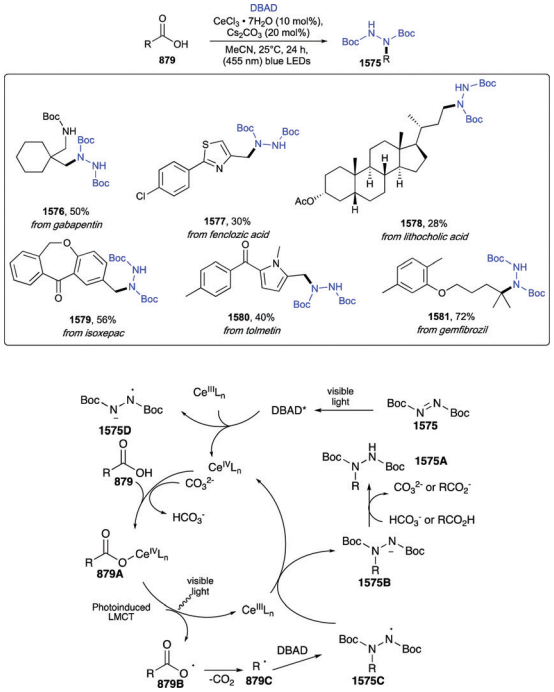

Scheme 283 Decarboxylative hydrazination.

8.10 Enantioselective decarboxylative cyanation

The merger of photoredox catalysis and asymmetric copper catalysis enabled the conversion of achiral carboxylic acids into enantio-enriched alkyl nitriles, *via* prior derivatization of carboxylic acids as *N*-hydroxyphthalimide esters (*e.g.* **1582**, Scheme 284).[363] Experimentally, in order to achieve optimum yields, the reaction required *fac*-Ir(ppy)$_3$ as the photocatalyst, CuBr as the copper catalyst, along with the chiral (1*R*, 2*S*)-**1583**, while TMSCN was employed as –CN source, and a 4 : 6 mixture of DMF/*p*-xylene as solvent system, under blue light irradiation, at room temperature for 24 h. The broad substrate scope was exemplified with complex bioactive (±)-ketoprofen, (±)-flurbiprofen, (±)-loxoprofen, (±)-pranoprofen, (±)-carprofen, and (±)-zaltoprofen (**1585–1591**, Scheme 284).

8.11 Conversion to aldehydes

The group of A. G. Doyle reported a synthetic strategy to access aldehydes from carboxylic acids and alkanes from alcohols, by exploiting the ability of phosphoranyl radicals, generated *in situ* upon a polar/SET crossover between a phosphine radical cation and an oxygen-centered nucleophile, to undergo a β-scission, forming an acyl (or an alkyl) radical along with triphenylphosphine oxide (Scheme 285).[364] A number of aromatic and heteroaromatic carboxylic acids were converted into the corresponding reduced aldehydes (**341**) with yields ranging from 38% to 94%. Tolerated functional groups included ethers, aldehyde, amide, ester, free hydroxy, and cyano. Worthy of note, two marketed drugs such as probenecid and telmisartan afforded the aldehyde derivatives **1592** and **1593** in 68% and 80% yields, respectively (Scheme 285).

8.12 Deoxygenative deuteration

Deuterated aldehydes could be conveniently prepared from both aliphatic and aromatic carboxylic acids with D_2O as an inexpensive deuterium source (Scheme 286).[365]

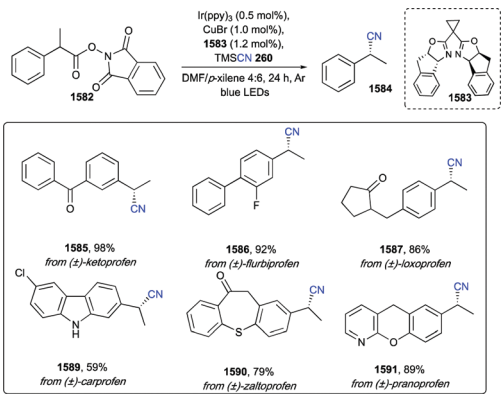

Scheme 284 Enantioselective decarboxylative cyanation.

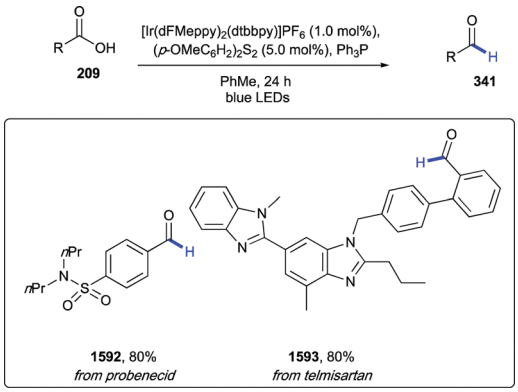

Scheme 285 Conversion to aldehydes.

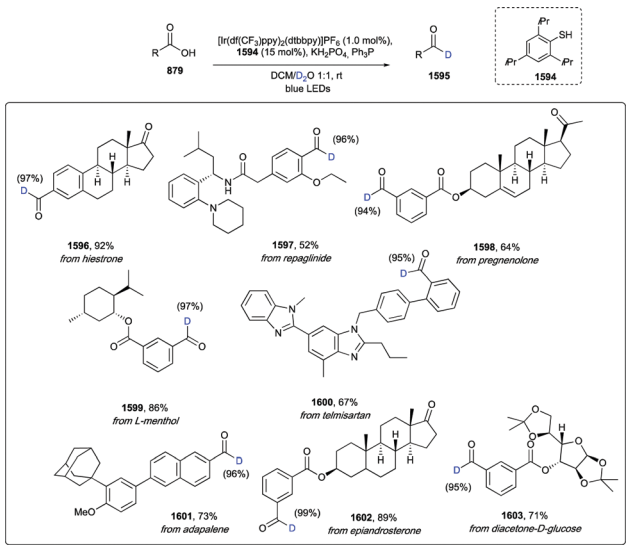

Scheme 286 Deoxygenative deuteration.

Triphenyl phosphine (PPh_3) and its analogue PPh_2OEt acted as *O*-atom transfer reagent for aromatic and aliphatic acids, respectively. 2,4,6-Triisopropylbenzenethiol, after exchanging with excess D_2O, afforded a deuterium labeled thiol, able to act as the HAT and deuterium source. An iridium catalyst as shown in Scheme 286 and a 1 : 1 solvent mixture of CH_2Cl_2/D_2O were also essential to achieve high yields. Deoxygenative deuterium incorporation was achieved for a wide range of both electron-rich and electron-poor aromatic carboxylic acids, no matter the substitution pattern (*ortho*-, *meta*-, and *para*-). Tolerated functional groups included free hydroxyls and amines, boronic esters, ketones, aldehydes, alkenes, and alkynes. On the other hand, aliphatic carboxylic acids gave moderate yields, along with a decreased D incorporation. The potential for the LSF of pharmaceuticals was shown for hiestrone, telmisartan, adapalene, repaglinide (a visible light induced HIE at the α-C(sp^3)–H positions of tertiary amine was also observed), epiandrosterone, pregnenolone, diacetone-D-glucose, and L-menthol (**1596–1603**, Scheme 286).

8.13 Conversion to alkyl ketones

C. L. Joe and A. G. Doyle developed a metallaphotoredox protocol to achieve C(sp^3)–H functionalization of *N*-aryl amines

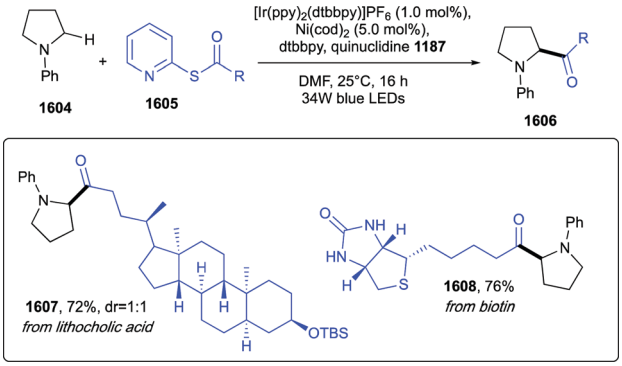

Scheme 287 Conversion to alkyl ketones.

with acyl electrophiles, generated *in situ* carboxylic acid anhydrides or thioesters (Scheme 287).[366] The reaction was promoted by $[Ir(ppy)_2(dtbbpy)]PF_6$, $Ni(cod)_2$ and dtbbpy as a ligand, quinuclidine, in DMF as a solvent under irradiation with 34 W blue LEDs at 25 °C for 16 hours. A variety of symmetric and nonsymmetric acyclic *N*-aryl amines, as well as indolines, tetrahydroisoquinolines, and morpholines afforded the α-amino carbonylated adducts in good to high yields. As for the carboxylic acid partner, thioesters derived from TBS-lithocholic acid and from biotin were reacted with *N*-phenylpyrrolidine to afford compounds **1607** and **1608** in 72% and 76%, respectively (Scheme 287).

Shortly after J. Amani and G. A. Molander exploited a metallaphotoredox catalytic system to achieve the direct conversion of carboxylic acids to alkyl ketones (**1610**, Scheme 288) *via* the generation of alkyl radical intermediates from potassium alkyltrifluoroborates, and subsequent nickel mediated acyl-sp^3 coupling.[367] More in detail, dimethyl dicarbonate (DMDC) was used as activator of the carboxylic acids, by converting them into an activated carbonic anhydride *in situ*. Its subsequent cross-coupling with an alkyl radical, generated upon SET oxidation of the alkyltrifluoroborate, led to the desired acyl derivative with loss of CO_2 and two equivalents of methanol. Optimized reaction conditions employed both an iridium photocatalyst, $[Ni(dttbbpy)(H_2O)_4]Cl_2$ as the nickel source, DMDC, ammonium chloride as an additive, and a 2 : 1 mixture of ^{i}PrOAc/THF as solvent system, under blue LEDs irradiation at room

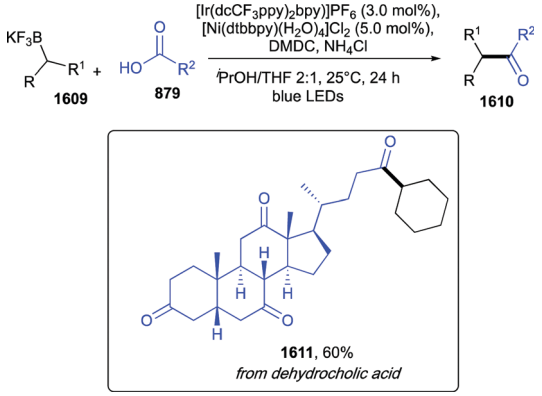

Scheme 288 Conversion to alkyl ketones.

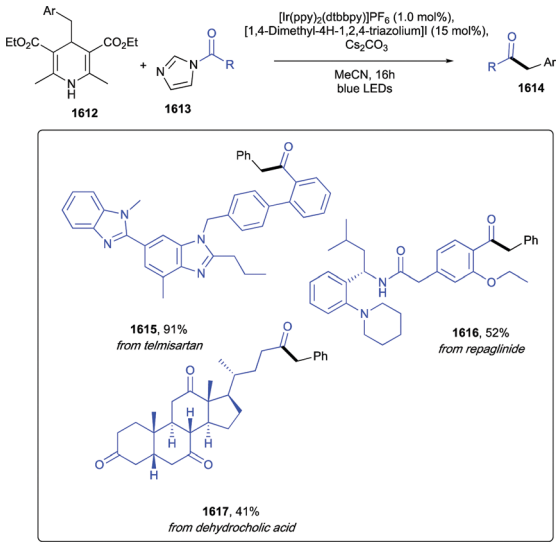

Scheme 289 Conversion to alkyl ketones.

temperature for 24 h. Reaction scope was wide for both the potassium alkyltrifluoroborates and the carboxylic acids, including dehydrocholic acid (**1611**, Scheme 288).

More recently, A. V. Davies *et al.* reported a new protocol based on the merging of *N*-heterocyclic carbene (NHC) and photoredox catalysis (Scheme 289).[368] Carboxylic acids were converted into acyl azolium salts, which underwent a SET reduction to form an azolium radical ion. Eventually, the latter coupled with an alkyl radical generated *in situ* from easily prepared Hantzsch esters. Optimum yields were achieved with $[Ir(dFCF_3ppy)_2(dtbpy)]PF_6$ as the photocatalyst, dimethyltriazolium as the NHC precursor, and Cs_2CO_3 in MeCN as solvent under blue LEDs irradiation at room temperature for 16 h. The scope of acyl imidazoles (**1613**) was wide, tolerating both electron-withdrawing and electron-donor substituents, along with heteroaromatic substrates. On the other hand, aliphatic substrates gave moderate yields. As for the alkyl radical precursors, benzyl- and cyclohexyl-Hantzsch esters and Meyer nitriles proved to be competent substrates. Additionally, LSF of telmisartan, repaglinide, and dehydrocholic acid was accomplished in excellent to medium yields, directly from carboxylic acids, by forming *in situ* their acyl imidazole equivalents (**1615–1617**, Scheme 289).

8.14 Deoxygenative synthesis of γ,γ-difluoroallylic ketones

Aromatic carboxylic acids, if reacted with α-trifluoromethyl alkenes (**1618**, Scheme 290), in the presence of triphenylphosphine, an iridium photocatalyst, $NaHCO_3$ as a base, in DMF, under blue LEDs irradiation could afford γ,γ-difluoroallylic ketones in good to excellent yields.[369] Unfortunately, the protocol was not effective with aliphatic- or with α,β-unsaturated carboxylic acids, albeit functional groups tolerance was good, including, among others, alkenes, alkynes, halogens, ethers, *N*-Boc protected amines, and esters. LSF of dicamba, adapalene, and indomethacin with α-trifluoromethyl alkene **1618** was reported in medium to high yields (**1620–1622**, Scheme 290).

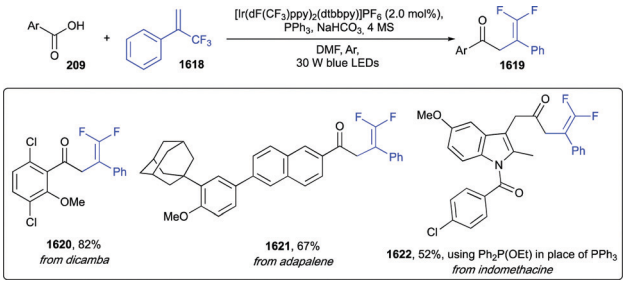

Scheme 290 Deoxygenative synthesis of γ,γ-difluoroallylic ketones.

8.15 Synthesis of reversed *C*-acyl glycosides

The group of G. A. Molander reported an unprecedented synthesis of non-anomeric *C*-acyl glycosides through a dual nickel/photoredox catalytic system using highly functionalized carboxylic acids as acyl source (Scheme 291).[370] Thoroughly, the authors exploited 1,4-dihydropyridines (**1623**) as glycosyl-based radical precursors, as their low oxidation potentials enabled fragmentation by using inexpensive photocatalysts in lieu of stoichiometric oxidants. After exploration of different conditions, 4CzIPN resulted the photocatalyst of choice, $NiCl_2(dtbbpy)\cdot 6H_2O$ was selected as the nickel source, dimethyldicarbonate (DMDC) as an activator, in a 2 : 1 mixture of acetone/*i*-PrOAc at room temperature under blue LEDs irradiation for 24 hours. By applying this protocol, various functionalized glycosidic scaffolds were coupled with primary, secondary, and tertiary carboxylic acids bearing functional groups such as cyano, esters, free hydroxy, Fmoc-protected amines, ethers, and ketone. LSF of biorelevant compounds such as dehydrocholic acid, indomethacin, and naproxen was reported with yields ranging from 51% to 77% (**1625–1627**, Scheme 291). Interestingly, *C*-acyl-glycosylation of dehydrocholic acid was scaled up without loss in efficiency. The feasibility of using non-glycosyl-based DHPs was also evaluated, as shown in the synthesis of dialkyl ketones **1628–1630** derived from flurbiprofen and naproxen (Scheme 291).

8.16 Decarboxylative trifluoromethylation

The merger of photoredox and copper catalysis enabled the conversion of carboxylic acids to trifluoromethyl derivatives

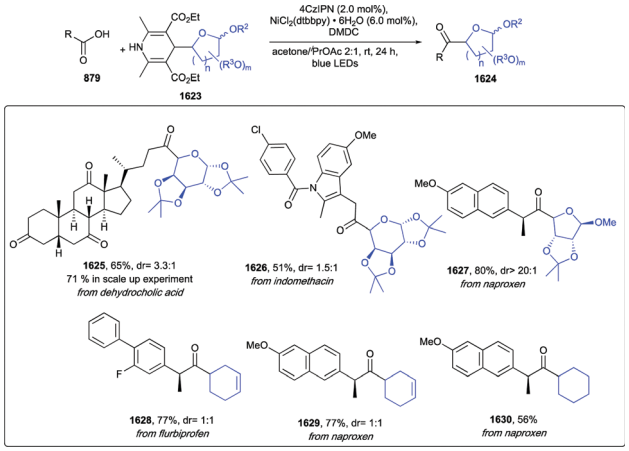

Scheme 291 Synthesis of reversed *C*-acyl glycosides.

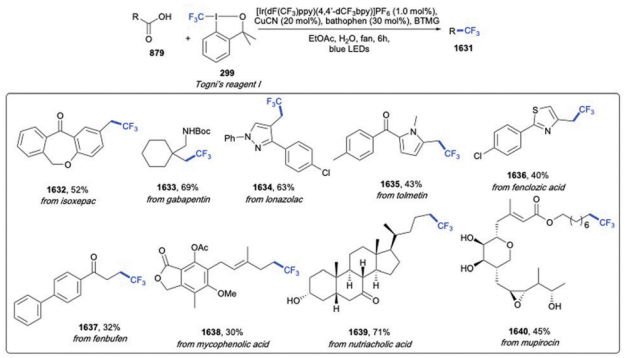

Scheme 292 Decarboxylative trifluoromethylation.

(Scheme 292).[371] Togni's reagent I was employed as CF_3 source, $Ir[dF(CF_3)ppy]_2(4,4'\text{-}dCF_3bpy)PF_6$ as a highly oxidizing excited state photocatalyst, CuCN as the copper catalyst, and bathophenanthroline as the ligand. Also, the addition of 30 equiv. of water proved to be essential to achieve optimum yields. The reaction scope ranged from substituted aryl and heteroaryl carboxylic acids to secondary and tertiary cyclic carboxylic acids. LSF of medicinal agents such as gabapentin, lonazolac, isoxepac, tolmetin, fenclozic acid, fenbufen, mycophenolic acid, nutriacholic acid and mupirocin was reported in good to moderate yields (**1632–1640**, Scheme 292).

8.17 Decarboxylative trifluoromethylselenolation

A protocol for the oxidative decarboxylation and subsequent trifluoromethylselenolation of aliphatic carboxylic acids with $(Me_4N)(SeCF_3)$ salt **1641** (Scheme 293) and Mes-Acr-PhBF$_4$ (9-mesityl-10-methylacridinium tetrafluoroborate) as organic photocatalyst was reported by Q.-Y. Han *et al.*[372] During the optimization of reaction conditions, it was observed that NFSI (*N*-fluorobenezenesulfonimide) acted as the most efficient

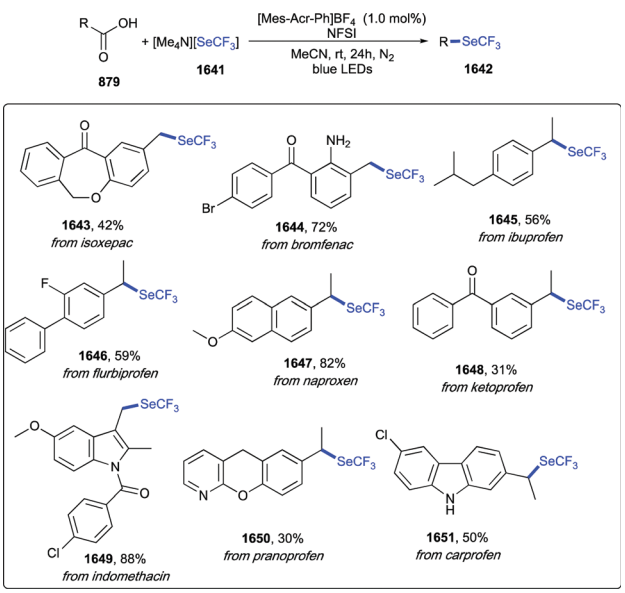

Scheme 293 Decarboxylative trifluoromethylselenolation.

oxidant, while the solvent of choice was MeCN. These mild conditions enabled a smooth conversion, without the need for preactivating the carboxylic acid functional group, of a range of NSAIDs including isoxepac, bromfenac, indomethacin, ibuprofen, flurbiprofen, naproxen, ketoprofen, pranoprofen, and carprofen into their corresponding trifluoromethyl selenoethers in medium to high yields (**1643–1651**, Scheme 293).

8.18 Decarboxylative borylation

The group of V. K. Aggarwal reported that carboxylic acids, upon conversion into NHPI ester derivatives (**1503**, Scheme 294), could undergo a decarboxylative borylation with the diboron reagent bis(catecholato)diboron **334** under blue LEDs light irradiation without the requirement of any photocatalyst or additive.[373] A simple work up with pinacol and triethylamine allowed the isolation of the pinacol boronic ester derivatives. This procedure was endowed with some key advantages such as easy of performance, scalability, transition-metal and additive free conditions, and broad functional group tolerance. In addition, primary, secondary, and tertiary carboxylic acids, including perfluoroalkyl, chiral, and strained cyclic scaffolds, were all competent substrates. Remarkably, it was applied to the LSF of complex carboxylic acids such as lithocholic acid, stearic acid, arachidonic acid, fenbufen, gibberellic acid, and indomethacin (**1652–1658**, Scheme 294).

A similar transformation, but still requiring an iridium photoredox catalyst, was reported more or less at the same time by D. Hu *et al.* (Scheme 295). Their report described that NHPI ester derivatives of aliphatic carboxylic acids could generate organoboron compounds under visible-light photoredox conditions with tetrahydroxydiboron $B_2(OH)_4$ as the borylating agent.[374] $[Ir(ppy)_2(dtbpy)]PF_6$ was found to be the most effective photocatalyst, DMF the solvent of choice, and a compact fluorescent lamp (CFL) the appropriate light source. The boronic acids, once formed in the reaction mixture, were isolated as alkyltetrafluoroborates after treatment with aqueous KHF_2. Interestingly, no sacrificial additives were needed to regenerate the active catalyst. The reaction scope was limited to aliphatic carboxylic acid derived NHPI esters, albeit high functional group tolerance was verified

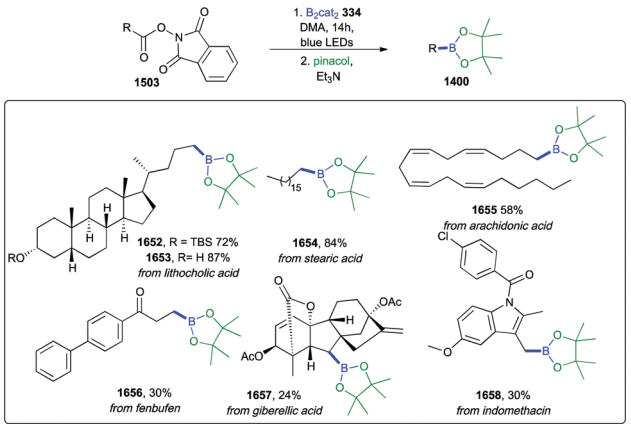

Scheme 294 Decarboxylative borylation.

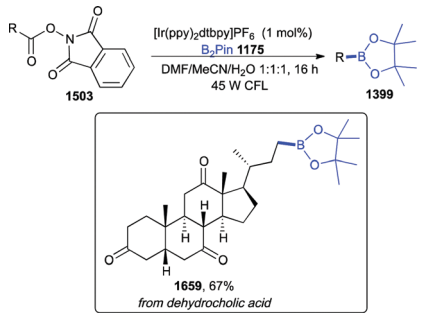

Scheme 295 Decarboxylative borylation.

with halogens, ketones, alkenes, alkynes, ethers, and esters. Late-stage borylation of dehydrocholic acid was achieved in a good 67% yield (**1659**, Scheme 295).

8.19 Decarboxylative radical addition to vinyl boronic esters

A diverse range of substrates such as α-amino, α-oxy, and alkyl carboxylic acids could undergo decarboxylative radical addition to vinyl boronic esters (**1660**, Scheme 296) under mild photoredox catalytic conditions.[375] The reaction mechanism relied on a SET reduction of an α-boryl radical intermediate to the corresponding anion, and subsequent protonation to boronic acid derivative. When 5- and 6-membered cyclic amino acids possessing different carbamoyl protecting groups and *N*-methyl or *N*-benzyl Boc protected amino acids were employed as substrates, optimum yields were obtained by using $[Ir(ppy)_2(dtbbpy)]PF_6$, C_2CO_3 in DMF at 35 °C under blue LEDs irradiation. On the other hand, substrates bearing free NH groups, such as simple *N*-Boc protected amino acids, required slight modification of the reaction conditions to photocatalyst $[Ir(dF(CF_3)ppy)_2(dtbbpy)]PF_6$ and DMA as a solvent. These latter conditions were also applied to alkyl carboxylic acids, providing alkyl boronic esters, as exemplified with bezafibrate, trolox, dehydroabietic acid, and gemfibrozil (**1662–1666**, Scheme 296).

8.20 Decarboxylative cyclopropanation

Aliphatic carboxylic acids could be engaged in a photoredox catalyzed decarboxylative radical addition to haloalkyl alkenyl boronic esters, or carboxylic acid esters, followed by reduction to carbanion and intramolecular cyclization with the tethered alkyl chloride (Scheme 297).[376]

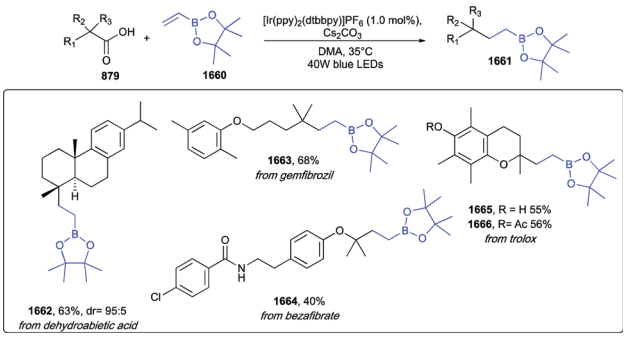

Scheme 296 Decarboxylative radical addition to vinyl boronic esters.

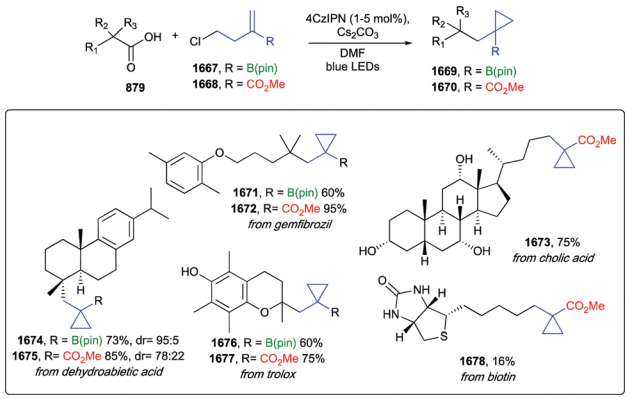

Scheme 297 Decarboxylative cyclopropanation.

The developed procedure made use of 4CzIPN as an organic photocatalyst, Cs_2CO_3 as a base in either DMF or CH_2Cl_2 as a solvent under blue LEDs irradiation. The heat generated by the LEDs resulted in reaction temperatures of *ca.* 50 °C. Cyclopropanation of homoallyl chlorides bearing electron-withdrawing groups such as carboxylate esters, nitriles, primary amides, sulfones, and phosphonate esters was carried out in excellent yields. Less electron-poor styrene derivatives afforded cyclopropanes containing phenyl and naphthyl groups in high yields, while homoallyl chlorides functionalized with electron rich benzofurans gave good yields. The carboxylic acid substrates included cyclic and acyclic α-amino acids, γ-amino butyric acid, Cbz-protected dipeptides, and α-oxy acids. More complex carboxylic acids-containing drugs such as dehydroabietic acid, the vitamin E analogue trolox, the fibrate gemfibrozil, cholic acid, and biotin were cyclopropanated to give densely functionalized derivatives **1671–1678** (Scheme 297).

8.21 Decarboxylative cyclobutylation

A Giese-type addition of C(sp^3)-centered radicals, generated from α-amino and α-oxy carboxylic acid derivatives, to highly strained bicyclo[1.10]butanes (BCBs) was developed by G. Ernouf *et al.* (Scheme 298).[377] The mild photoredox conditions exploited $[Ir(dF(CF_3)ppy)_2(dtbbpy)]PF_6$ as the photocatalyst, phenyl sulfonyl bicyclo[1.1.0]butane as a bench stable acceptor of α-amino and α-oxy alkyl radicals, Cs_2CO_3 as a base, MeCN as the solvent, and a 40 W blue LED lamp as the light source. Also, the addition of water (10 equiv.) was essential to achieve

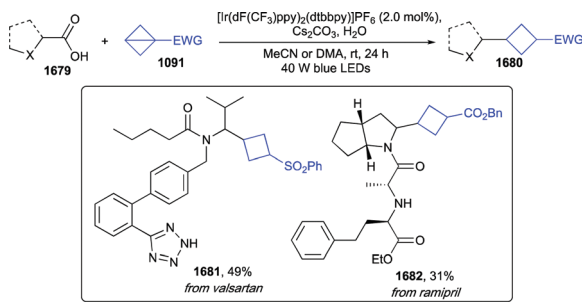

Scheme 298 Decarboxylative cyclobutylation.

optimum yields. As for the reaction scope, electron-donating substituents on the BCB moiety reacted less efficiency than their electron-poor analogues, while α-carbamoyl radicals from *N*-Boc protected proline, piperidine, azetidine, morpholine, and piperazine were smoothly generated under standard reaction conditions. With slight modifications of reaction conditions, the scope was extended to *N*-Boc protected amino acids and oxo-heterocycles such as tetrahydrofuran and tetrahydropyran. Pharmaceutically relevant and more complex radical precursors involved valsartan and ramipril, which were cyclobutylated to **1681** and **1682** in moderate yields of 49 and 31%, respectively (Scheme 298).

8.22 Decarboxylative spirocyclization of oxalates to lactones

Tertiary alcohol derived homoallylic oxalates could generate, under photoredox catalytic conditions, alkoxycarbonyl radicals, which are prone to undergo a tandem 5-*exo*-cyclization-cross coupling cascade to afford γ-butyrolactones in one step (Scheme 299).[378] In order to be successful, the protocol required cesium salts of oxalate derivatives, an iridium photocatalyst and a nickel catalyst, and it was run in a 1 : 1 mixture of benzene and 1,4-dioxane as the solvent system, at 60 °C and under irradiation with two 34 W blue LED lamps. A wide variety of spirocyclic lactones could be obtained from both oxygen and nitrogen containing 4,5, and 6-membered rings, as well as more complex heterocycles such as an estrone-derived oxalate as shown in Scheme 299 (**1686**).

8.23 Synthesis of benzo[*b*]phosphole oxides

L. Liu *et al.* reported a cascade reaction relying on decarboxylation of NHPI esters, alkyl radical addition to alkynyldiphenylphosphine oxides, followed by aryl C–H cyclization to benzo[*b*]phosphole oxides (Scheme 300).[379] The developed protocol is metal- and oxidant-free, requiring eosin B as a photocatalyst, *i*-Pr_2NEt as a sacrificial electron donor, H_2O, DMSO as a solvent and blue LEDs as the light source at room temperature. The reaction scope was wide, highlighting orthogonality towards a number of functional groups such as Boc-protected amines, ethers, alkenes, alkynes, esters, halogens, cyano, and alkyls, with both primary and secondary carboxylic acids affording from moderate to good yields. Additionally, heterocyclic diphenylphosphine oxides bearing a pyridine or a thiazole ring showed a good reactivity. As an example of bioactive carboxylic acid, the gemfibrozil-derived NHPI ester was converted into **1689** in a medium 40% yield (Scheme 300).

8.24 Synthesis of polycyclic quinoxalines

Carboxylic acids, upon *in situ* conversion into phenyliodine(III) dicarboxylate reagents, could generate, under photoredox catalytic conditions, alkyl radical intermediates, which are prone to react with *ortho*-substituted arylisocyanides to afford polycyclic quinoxaline derivatives (Scheme 301).[380]

More in detail, the reaction required $PhI(OAc)_2$, *fac*-$Ir(ppy)_3$ as a photocatalyst and proceeded in DMF as a solvent under irradiation with a 26 W fluorescent bulb at 25 °C for 5–24 hours. The isocyanide scope was wide, tolerating functional groups such as halogens, ethers, and ketone, and including nitrogen-rich heterocycles such as imidazole, benzoimidazole, pyrazole, 1,2,4-triazole, 1,2,3-triazole, and tetrazole. Likewise, a wide array of carboxylic acids bearing esters, halogens, amides, double and triple bonds were readily converted into their corresponding annulated products. Late stage modification of litocholic acid and cholic acid was successfully carried out, albeit in moderate yields, thus proving orthogonality with respect to free hydroxy groups (**1692** and **1693**, Scheme 301).

8.25 Esterification of carboxylic acids with aryl halides

B. Pieber *et al.* developed a dual nickel/photocatalytic protocol to induce selective C–O cross-coupling of carboxylic acids (**879**) with aryl halides (**1092**, Scheme 302).[381]

Here, graphitic carbon nitrides, a class of metal-free polymers employed as heterogeneous semiconductors were employed as photocatalysts, exhibiting a broad substrate scope and the possibility to be recycled multiple times. In order to be successful, the reaction required $NiCl_2$·glyme or $Ni(OAc)_2·4H_2O$ as the nickel

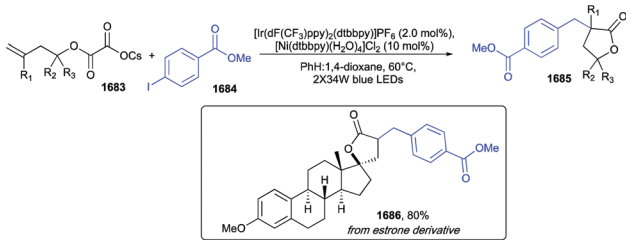

Scheme 299 Decarboxylative spirocyclization of oxalates to lactones.

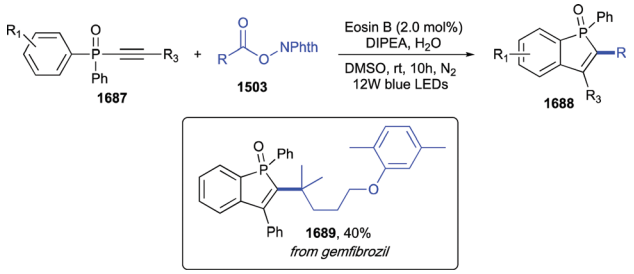

Scheme 300 Synthesis of benzo[*b*]phosphole oxides.

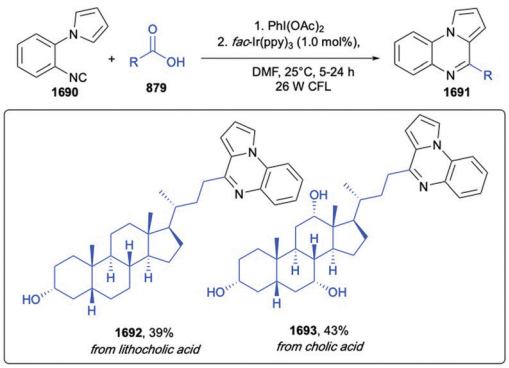

Scheme 301 Synthesis of polycyclic quinoxalines.

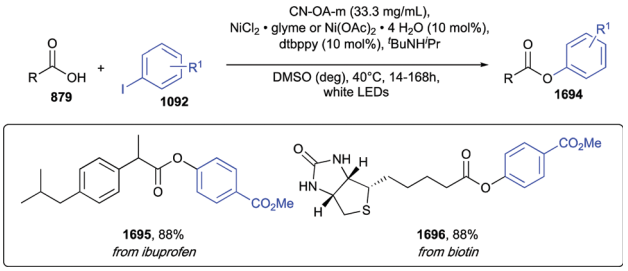

Scheme 302 Esterification of carboxylic acids with aryl halides.

source, dtbbpy as a ligand, and *N-tert*-butylisopropylamine (BIPA) as an organic base in DMSO as solvent under white LEDs irradiation at 40 °C. Suitable aryl iodides tolerated a wide range of functional groups such as esters, ketones, aldehydes, cyano-, and halogens, while competent carboxylic acids included, as examples of complex substrates, ibuprofen and biotin (**1695** and **1696**, Scheme 302).

8.26 Synthesis of ethers

Phenols could be converted into alkyl aryl ethers *via* decarboxylative C(sp^3)–*O* cross-coupling by merging photoredox and copper catalysis starting from alkyl NHPI esters (**1503**, Scheme 303). Optimum yields were achieved when $[Ir(dtbbpy)(ppy)_2]PF_6$ was used as the photocatalyst, $(CuOTf)_2{\cdot}C_6H_6$ as the copper catalyst, triethylamine as the base, CH_2Cl_2 as the solvent, and blue LEDs as the light source.[382] Both electron-rich and electron-poor phenols successfully provided the corresponding ethers in moderate to good yields, while tolerated functional groups included halogens, boronic ester, ketone, cyano, trifluoromethoxyl, and polycyclic aromatic rings. Likewise, various secondary acyclic, cyclic, and heterocyclic aliphatic NHPI esters, as well as tertiary substrates, could be coupled in good to excellent yields. On the other hand, primary alkyl NHPI esters required slight modification of reaction conditions, with $Cu(MeCN)_4OTf$ as copper source and *N*-isopropyl-*N*-methyl-*tert*-butylamine as the base. Remarkably, this protocol was applied to the late-stage modification of a number of carboxylic acid-containing drugs such as chlorambucil, indomethacin, isoxepac, zaltoprofen, ketoprofen, naproxen, and ibuprofen (**1697–1703**, Scheme 303).

More recently, the group of H. Ohmiya reported the synthesis of aliphatic ethers starting from aliphatic alcohols and secondary or tertiary alkyl carboxylic acid-derived NHPI esters (**1503**, Scheme 304).[383] The reaction was promoted by a

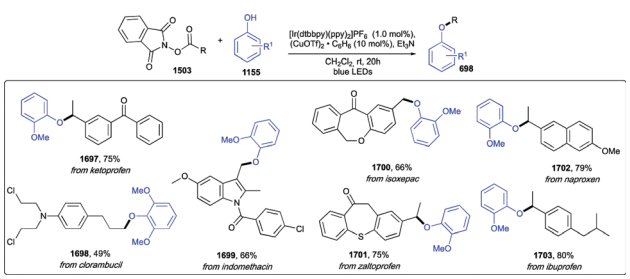

Scheme 303 Synthesis of ethers.

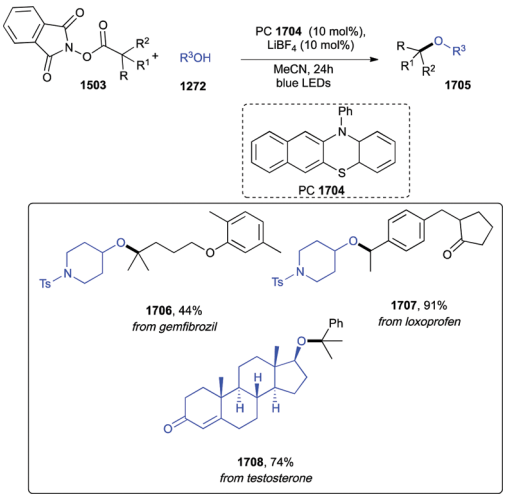

Scheme 304 Synthesis of ethers.

benzo[*b*]phenothiazine organic photocatalyst (PTH), in the presence of $LiBF_4$ as an additive under irradiation with blue LEDs at room temperature for 24 hours. The scope of the redox active esters was explored by selecting tertiary, secondary benzylic, and α-heteroatom (*O*-, *N*Boc-) containing carboxylic acids, and remarkably, complex scaffolds such as the medicinal agents gemfibrozil and loxoprofen underwent the decarboxylative etherification in moderate to good yields (**1706** and **1707**, Scheme 304). As for the alcohol partners, the authors showed that a variety of functional groups, including halogens and double bonds, was well tolerated as, for example, in the etherification of testosterone (**1708**, Scheme 304).

8.27 Synthesis of thioesters

Redox-active esters derived from aliphatic carboxylic acids could be converted into thioester derivatives *via* a dual photoredox/copper catalyzed cross coupling with thiobenzoic acid.[384] The method required $[Ru(bpy)_3]Cl_2{\cdot}6H_2O$ as the photoredox catalyst, CuBr as the copper source, bpy and triphenylphosphine as the ligands, and Et_3N in MeCN under 6 W blue LEDs irradiation at room temperature for 18 hours. The substrate scope covered secondary, tertiary, and primary acids, albeit sterically hindered inputs led to moderate yields. On the other hand, the developed conditions provided orthogonality with respect to a wide array of functional groups, as further experimented in the late-stage thioesterification of oleic acid, gemfibrozil, fenbufen, abietic acid, and indomethacin (**1711–1715**, Scheme 305).

8.28 Aryl and alkyl decarboxylative functionalizations

A general strategy to access both aryl and alkyl radicals from carboxylic acids esters was reported by T. Patra *et al. via* photosensitized decarboxylation (Scheme 306).[385] Such radicals, generated upon an energy transfer mediated homolysis of unsymmetrical N–O σ-bonds, followed by radical fragmentation with concomitant release of CO_2, could then be used in carbon–carbon and carbon–heteroatom bond forming reactions. $[Ir(dF(CF_3)ppy)_2(dtbbpy)]PF_6$, thanks to its long excited-state

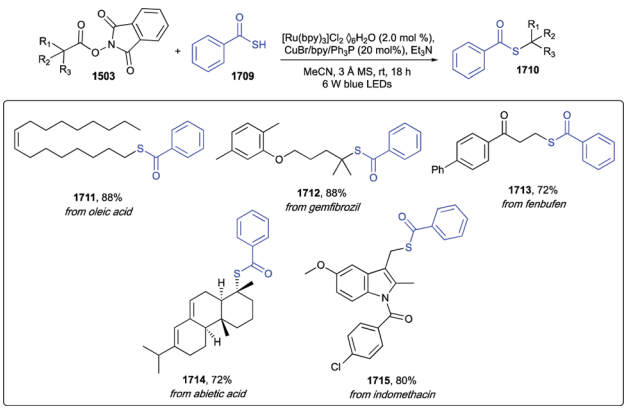

Scheme 305 Synthesis of thioesters.

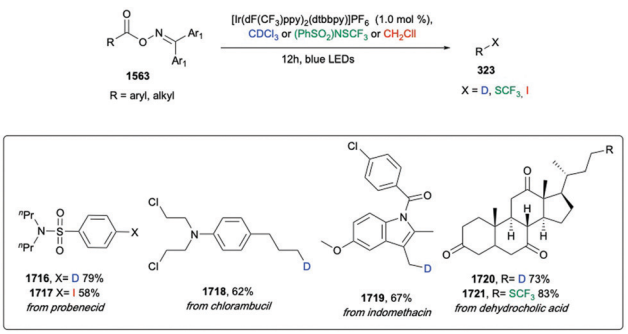

Scheme 306 Aryl and alkyl decarboxylative functionalizations.

lifetime and high triplet energy, was selected as competent catalyst, able to avoid competing SET events. This approach enabled deuteration of aryl-, heteroaryl-, and alkyl-substrates by using $CDCl_3$ as the solvent under blue LEDs irradiation. Drugs such as probenecid, chlorambucil, and indomethacin, as well as dehydrocholic acid were labeled with deuterium, chemoselectively and in high yields (**1716**, **1718–1720**, Scheme 306). Other suitable trapping agents were: $(PhSO_2)NSCF_3$ to accomplish trifluoromethylthiolation (**1721**, Scheme 306, from dehydrocholic acid); CH_2ClI, CCl_3Br, and B_2pin_2, to get iodination, bromination, and borylation, respectively (**1717**, Scheme 306, iodination of probenecid).

8.29 Functionalization of aryl acetic acids

Aryl acetic acids, key structural frameworks in a number of bioactive compounds, could underwent a photoredox catalyzed decarboxylation to benzyl radicals, which were prone to give a radical–radical coupling with N-, O-, and Cl-based partners (Scheme 307).[386]

The use of $[Ru(bpy)_3]Cl_2{\cdot}6H_2O$ as the photocatalyst, and 1-butoxy-1λ^3-benzo[*d*][1,2]iodaoxol-3(1*H*)-one (IBB) as hypervalent iodine-based oxidant under blue LEDs irradiation in CH_2Cl_2 at 40 °C enabled the decarboxylative imidation with $HN(SO_2Ph)_2$ of a broad array of aryl acetic acid derivatives. Tolerated functional groups embodied methyl-, methoxy-, halogens-, while strong electron-withdrawing substituents such as the nitro-group led to a drop in the yields. α-Branched aryl acetic acids tolerated small

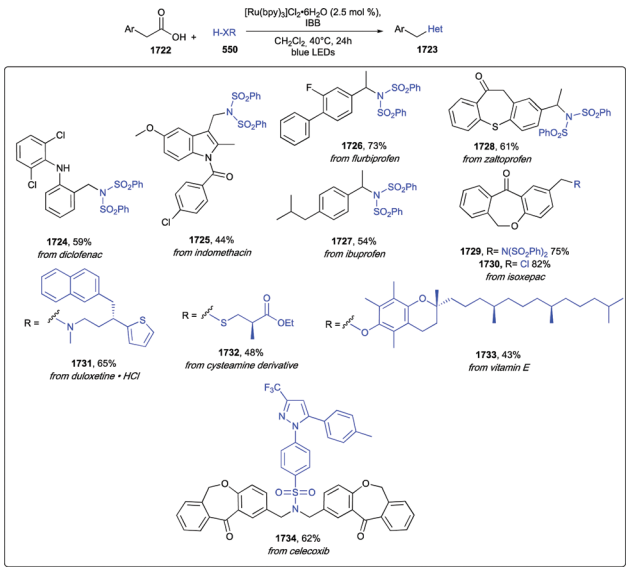

Scheme 307 Functionalization of aryl acetic acids.

aliphatic groups such a methyl-, whereas a bulkier phenyl group completely inhibited the reaction. Likely, the scope of the imide substrate was good, with both alkyl and aryl-substituted sulfonimide, along with cyclic sulfonimide and saccharin, a cyclic imide, leading to the desired adducts with high to moderate yields. Nucleophiles other than imides, such as trifluoroacetic acid and dibutylphosphonic acid also showed to be suitable substrates. LSF of complex bioactive compounds such as diclofenac, indomethacin, flurbiprofen, ibuprofen, zaltoprofen, and isoxepac was efficiently accomplished as shown in Scheme 307 (**1724–1734**). It is worth of note that the formation of diclofenac derivative **1724** was also performed on a gram scale.

8.30 Use of α-diazo carboxylic esters

Aryl azides and α-diazo carboxylic esters (**589**, Scheme 308) could be used to perform α-amination and α-alkylation of 2-acyl imidazoles in the presence of chiral-at-metal rhodium-based

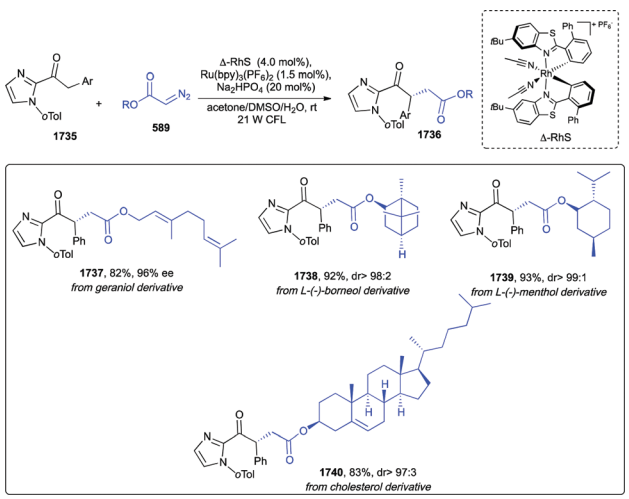

Scheme 308 Use of α-diazo carboxylic esters.

Lewis acid (**Λ-RhS**) in combination with a ruthenium photoredox catalyst.[387]

The protocol, besides the chiral catalyst and the photosensitizer, required Na_2HPO_4 as a base and a mixture of acetone/DMSO/H_2O as a solvent system under 21 W CFL irradiation at room temperature. Worthy of note, molecular nitrogen is the leaving group and the sole byproduct of the reaction, while the wide scope provided yields up to 99% and excellent enantioselectivities of up to 99% ee. The exquisite functional group tolerance was further showcased in the late-stage functionalization of esters derived from the mosquitoes repellent geraniol, L-(−)-borneol, L-(−)-menthol, and cholesterol (**1737–1740**, Scheme 308).

9. Functionalization of carbonyl compounds and derivatives

The open-shell chemistry promoted by visible light photocatalysis of aldehydes and ketones has been offering in recent years plenty of opportunities to achieve aldehydes, ketones, and imines functionalization to ketones, alcohols, and amines, whereas irradiation of aldehydes and ketones with UV light usually enables their use as photosensitizers mainly *via* triplet state energy transfer processes (EnT) thanks to small triplet-singlet energy gap (20–70 kJ mol^{-1}) and high intersystem crossing rates.[388,389] By harnessing organic or metal-based photoredox catalysts, efficient and general protocols to achieve α-alkylation and α-acylation as well as aminothiocyanation of ketones have been reported. Aldehydes, on the other hand, provide even more opportunities to explore a far-ranging chemical space since they can be involved in hydrogen atom transfer (HAT) catalytic pathways, by means of either photoactive HAT catalysts or HAT agents generated *in situ* such as O-, N-, S-, or halogen radicals. Representative transformations involving HAT events include alkynylation, arylation, pyridinylation, formation of thioesters, and remote functionalization. Additionally, aldehydes can behave as suitable precursors of ketyl radicals, which can add to a radical acceptor such as olefins or undergo cross radical/radical pathways to afford alcohols.[390] Enantioselective approaches capitalizing asymmetric photoactive catalysts will also be discussed further on. Imines' potentialities, albeit less explored so far, have been showcased in the synthesis of amines and hydroboration adducts.[391]

9.1 Formation of $C_{sp^2}(O)$–$C(sp^2)$, $C_{sp^2}(O)$–C(sp), and $C_{sp^2}(O)$–$C(sp^3)$ bonds

9.1.1 Acylation of ketones. α-Diazoketones can be used as acylating agents of β-ketoesters to accomplish either a *C*- or an *O*-acylation depending on the reaction conditions (Scheme 309).[392] More in detail, *C*-acylated products were exclusively obtained by employing a $NiCl_2$·glyme complex with a bis(oxazoline)ligand as a Lewis acid catalyst, while the use of a Lewis base such as pyridine or DABCO afforded regioselectively *O*-acylated adducts. Mechanistically, the reaction proceeded *via* a visible-light-induced Wolff rearrangement. A wide range of diversely functionalized β-ketoesters cleanly reacted under optimized reaction conditions, in $CHCl_3$ as solvent and 2 × 3 W blue LEDs irradiation, at room temperature, for 12 h. Modification of a β-ketoester estrone derivative afforded both *C*-acylated **1747** and *O*-acylated **1744** with good 78 and 89% yields, respectively (Scheme 309).

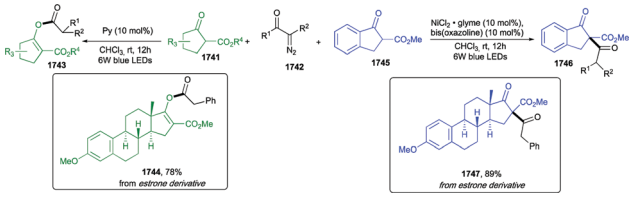

Scheme 309 Acylation of ketones.

9.1.2 Alkynylation of aldehydes. Aldehydes could be converted into ynones, ynamides, and ynoates with high regio- and chemoselectivity *via* a photoredox catalytic reaction with electrophilic ethynylbenziodoxolone (EBX) reagents (Scheme 310).[393] This method relied on a HAT strategy, by exploiting the ability of $[Ir(dF(CF_3)ppy)_2(dtbbpy)]PF_6$, sodium 2-iodobenzoate as sacrificial electron donor and HAT agent, and BIOAc (BI = benziodoxolone) as a sacrificial electron-acceptor, to efficiently promote the formation of an acyl radical intermediate from the aldehyde, which finally added onto the EBX reagent. The protocol proved to be quite general, with both aliphatic and aromatic aldehydes, and various aryl substituted EBX reagents reacting cleanly under standard conditions. Biorelevant cholesterol-, lithocholic acid-, probenecid-, and adapalene-derivatives demonstrated the potential of the developed protocol as a tool for LSF of drugs (**1750–1753**, Scheme 310).

9.1.3 Aldehydes arylation. Recently, the merging of HAT catalysis and palladium catalysis, has been shown to promote direct C–H arylation and alkenylation of aldehydes thus providing an easy access to ketones (Scheme 311).[394] More in detail, tetrabutylammonium decatungstate (TBADT) or anthraquinone (AQ) acted as synergistic HAT photocatalyst with $Pd(OAc)_2$, while DFT calculations suggested that regeneration of the Pd^0 catalyst and the photocatalyst occurred simultaneously in the presence of $KHCO_3$, therefore resulting in an efficient coupling of the palladium cycle with the photocatalytic cycle. TBADT required irradiation with 390 nm LEDs (conditions A), whereas the use of AQ

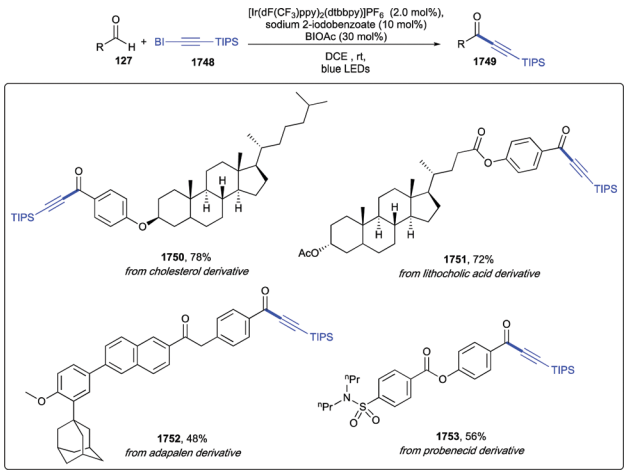

Scheme 310 Alkynylation of aldehydes.

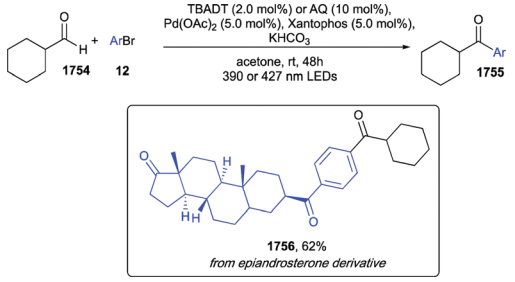

Scheme 311 Aldehydes arylation.

(conditions B) enabled a visible light induced C (sp^2)–H arylation (427 nm light). The aldehyde and the (hetero)aryl bromide scope was investigated in both conditions A and B, and in most cases conditions B provided the target ketones in higher yields. Representative complex bioactive substrates included epiandrosterone derivative **1756** obtained in 62% by applying conditions B (Scheme 311).

9.1.4 Aldehydes pyridinylation. Formation of either 2- or 4-acylated pyridines from aldehydes and pyridinium salts under visible-light photocatalytic conditions was reported by S. Jung *et al.* (Scheme 312).[395] Thoroughly, a methoxy- or an amidyl-radical, photocatalytically generated from the pyridinium salts, provided hydrogen atom abstraction from the aldehydes to form an acyl radical intermediate. The latter further engaged in addition to pyridinium salts. Notably, *N*-methoxypyridinium salts enabled the regioselective formation of *C*2-acylated pyridines, whereas *N*-aminopyridium equivalents afforded exclusively *C*4-acylated derivatives. The transformation proceeded efficiently by using $[Ir(dF(CF_3)ppy)_2bpy]PF_6$ as photoredox catalyst, sodium acetate as a base in DCE, under blue LEDs irradiation at room temperature. Reaction scope was wide, including both aliphatic and aromatic aldehydes, while pyridyl salts with methyl, methoxy-, ketone, ester-, cyano-, and trifluoromethyl substituents were all competent substrates. LSF of adapalene and vismodegib afforded derivatives **1759–1762** in good yields (Scheme 312).

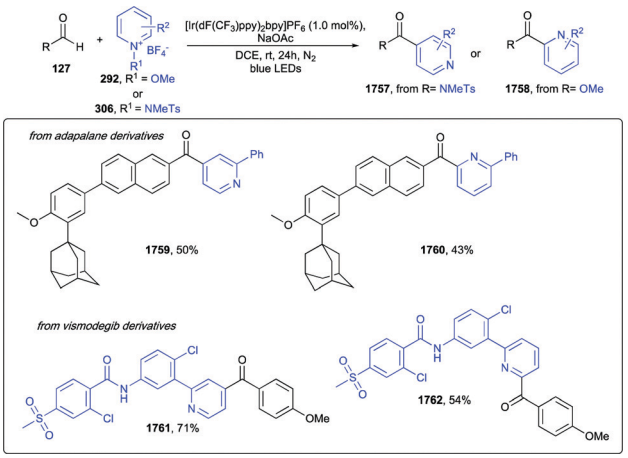

Scheme 312 Aldehydes pyridinylation.

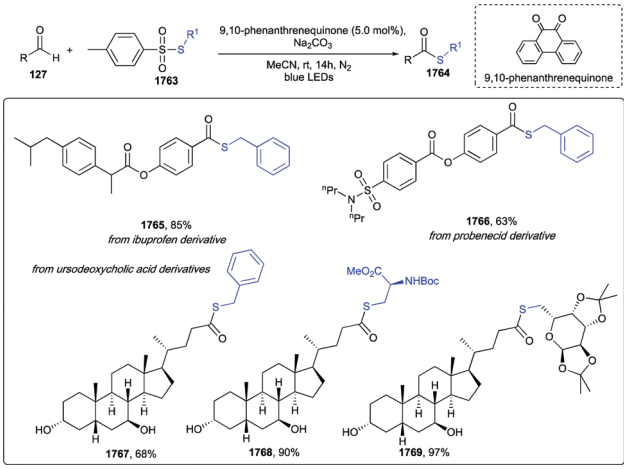

Scheme 313 Synthesis of thioesters from aldehydes.

9.2 Formation of C_{sp^2}(O)–X bonds

9.2.1 Synthesis of thioesters from aldehydes. Y. Zhang and coworkers provided a metal- and oxidant-free protocol to access thioesters from readily available carbonyl compounds and thiosulfonate *S*-esters (**1763**, Scheme 313).[396] The transformation was promoted by the excited state 9,10-phenanthrenequinone as HAT agent, which was able to generate acyl radicals *via* hydrogen abstraction from aldehydes, without inducing crossover reactivity of the thioester products. Standard reaction conditions required Na_2CO_3 as a base, MeCN as the solvent, and blue LEDs irradiation at room temperature under a nitrogen atmosphere. Aldehydes scope was shown to be wide, encompassing electron-poor and electron-rich aromatic-, heteroaromatic-, and aliphatic-aldehydes. Marketed drugs such as ibuprofen and probenecid aldehyde precursors were also readily converted into thioesters **1765** and **1766** with 85% and 63% yield, respectively (Scheme 313). Additionally, ursodeoxycholic acid derived aldehyde was subjected to thioesterification with benzyl, amino acid, and monosaccharide derived thiosulfonate *S*-esters to afford **1767–1769** (Scheme 313).

9.2.2 Synthesis of trifluoromethylthioesters from aldehydes. A powerful strategy enabling the synthesis of trifluoromethylthioesters from aldehydes was reported by S. Mukherjee *et al.* (Scheme 314).[397] The procedure did not require an external oxidant and capitalized $[Ir(dF(CF_3)ppy)_2(dtbbpy)]PF_6$ as a photocatalyst, sodium benzoate as both sacrificial electron donor to quench the excited state photocatalyst and HAT catalyst in its

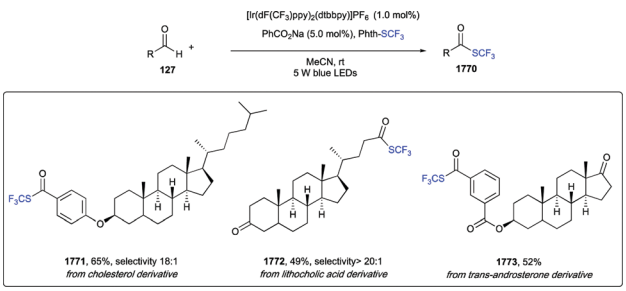

Scheme 314 Synthesis of trifluoromethylthioesters from aldehydes.

oxidized form benzoyloxy radical PhCOO•. The acyl radical intermediate thus generated reacted then with the electrophilic *N*-(trifluoromethylthio)phthalimide (Phth-SCF_3) to give the desired product, along with a phthalimide radical, responsible for the oxidation of the intermediate Ir^{II} species, thereby regenerating the Ir^{III} species and forming a phthalimide anion ($Phth^-$), which served as internal base. The reaction was performed in MeCN under 5 W blue LEDs irradiation at room temperature. The mild conditions allowed a high functional group tolerance, resulting in a wide scope as exemplified by the trifluoromethylthiolation of complex molecules such as cholesterol derivative **1771**, lithocholic acid derivative **1771**, and *trans*-androsterone **1773** (Scheme 314).

9.2.3 Aminothiocyanation of activated ketones. Ketones could be converted into multisubstituted olefins upon reaction with inexpensive ammonium thiocyanate **484**, in the presence of fluorescein as an organic photocatalyst, in MeCN as solvent at room temperature under air and blue LEDs irradiation (Scheme 315).[398] This metal-free aerobic method was endowed with *E*-selectivity, exceptionally mild conditions and high atom economy as water was the only by-product. In order to evaluate the reaction scope, a number of β-ketoesters including DL-menthyl esters, as well as cholesterol- and dehydroepiandrosterone derivatives as shown in Scheme 315, were converted into their corresponding aminothiocyanated olefins **1776–1778** with good to excellent yields (Scheme 315).

9.3 Formation of $C(sp^3)$–$C(sp^3)$ bonds

9.3.1 Reaction of aldehydes and alkenylpyridines. K. N. Lee *et al.* discovered that aldehydes and imines could underwent, under photoredox catalytic conditions a SET reduction to ketyl or α-aminoalkyl radical, which are prone to add to Lewis acid-activated alkenylpyridines (Scheme 316).[399] Experimentally, such a transformation required a ruthenium photocatalyst, $La(OTf)_3$ as the Lewis acid, bpy as a ligand to solubilize $La(OTf)_3$, and Hantzsch ester as a reductant in MeCN under 30 W blue LEDs irradiation at 23 °C for 18 h. Both electron-rich and electron-poor alkenyl pyridines reacted cleanly. Likewise, a wide range of aldehydes took part to the transformation giving up to quantitative yields and tolerating functional groups such as ester, ketone, amide, nitrile, and ether. Selected examples with amines as coupling partners were also reported. Additionally, LSF of an estrone-derived aldehyde was accomplished in a medium 45% yield (**1781**, Scheme 316).

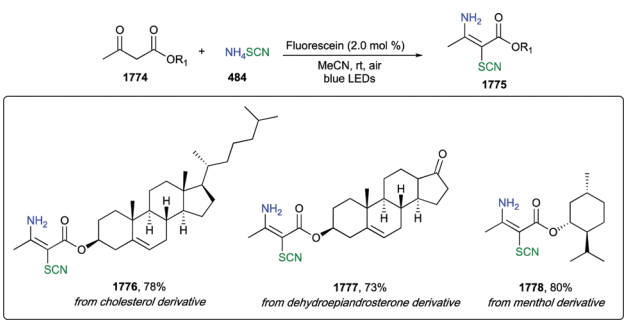

Scheme 315 Aminothiocyanation of activated ketones.

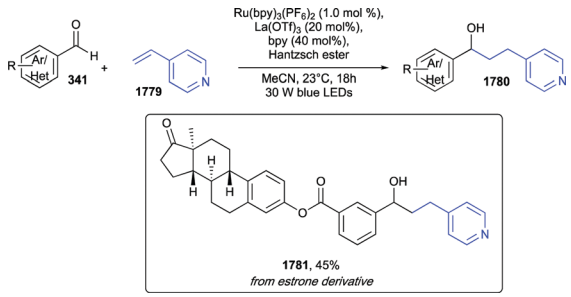

Scheme 316 Reaction of aldehydes and alkenylpyridines.

9.3.2 α-Alkylation of ketones. The group of P. Melchiorre reported the first asymmetric catalytic alkylation of cyclic ketones by using alkyl halides and an easily available cinchona-based primary amine catalyst **1784** (Scheme 317), which, besides driving the stereoselectivity of the process, was able to form a photoactive electron donor–acceptor complex with the ketone substrates.[400] Accordingly, the transformation did not require any additional metal catalyst, while TFA was employed as an acid co-catalyst, in the presence of NaOAc in toluene under irradiation with a 23 W CFL at 0 °C for 45 hours. A number of functionalized ketones, including 6- and 7-membered rings, were α-alkylated in good yields and with good to excellent enantiomeric excesses. As alkylated agents both electron-poor benzyl bromides and phenacyl bromides showed to be competent substrates. The potentiality of this protocol was further demonstrated in the late-stage alkylation of 5α-cholestan-3-one with 2-bromo acetophenone, affording derivative **1785** in 47% yield and a d.r. > 20 : 1 (Scheme 317).

Alternatively, ketones, under photoredox catalytic conditions, could undergo a SET reduction to ketyl radicals mediated by an excited state photocatalyst (Scheme 318).[401] The simultaneous presence of a HAT agent, able to abstract an allylic or benzylic $C(sp^3)$–H hydrogen atom, afforded a transient allylic or benzylic radical, which eventually underwent cross radical–radical coupling

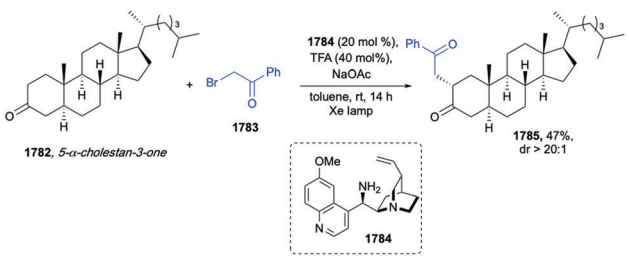

Scheme 317 α-Alkylation of cyclic ketones.

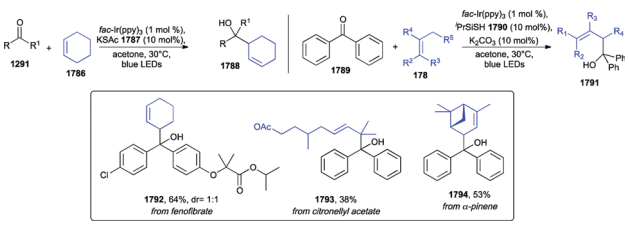

Scheme 318 α-Alkylation of ketones.

with the ketyl radical thereby forming tertiary alcohols. Optimization of the reaction conditions suggested *fac*-Ir(ppy)$_3$ as the photocatalyst, either KSAc or triisopropylsilanethiol as HAT agents, K_2CO_3 as a base, in acetone as solvent, under blue LEDs irradiation at room temperature. The reaction scope was limited to aromatic and heteroaromatic ketones, as aliphatic ones were not good quenchers of the excited state iridium-based photocatalyst. On the other hand, suitable allylic/benzylic systems were extended to cycloalkenes in various ring sizes, heterocyclic alkenes with a polarized double bond (*e.g.* dihydropyran and dihydrofuran), and even to free-hydroxyl-containing olefins. Application of the protocol to complex ketone drugs such as fenofibrate, or naturally occurring allylic systems such as citronellyl acetate and α-pinene led to derivatives **1792–1794** in moderate to good yields (Scheme 318).

1,2-Dicarbonyl compounds (typically α-ketoesters) can be reacted with 2-acyl imidazoles (**1795**, Scheme 319) and 2-acyl pyridines to afford an asymmetric β-C(sp^3)–H functionalization of the latter.[402] To this end, the authors employed a tailored stereogenic-at-rhodium Lewis acid catalyst (**Δ-RhS**, Scheme 319), which enabled high yields (up to 99%) and excellent stereoselectivities (up to >20 : 1 dr and up to >99% ee). The protocol required blue LEDs irradiation, DABCO as an additive, in acetone, at room temperature. Substrate scope with respect to the ketones showed good tolerance for functional groups such as alkyls-, ethers-, thiother-, hydroxyl-, bromine, olefin-, and indole. With strongly electron-withdrawing groups, a temperature increase to 50 °C assured satisfactory yields. Likely, the scope of the 1,2-dicarbonyl compounds was shown to be broad, and, remarkably, an α-ketoester cholesterol derivative was converted into **1799** in a good 82% yield, and excellent diastereoselectivity of 99 : 30 : 1 : 1 (Scheme 319).

Recently, P. Melchiorre and coworkers reported a visible-light promoted method relying on the ability of a nucleophilic organocatalyst to generate alkyl radicals from alkyl halides and mesylates *via* S_N2 activation (Scheme 320).[403] Accordingly, a dithiocarbonyl anion organocatalyst attacked the alkyl halide to form a photon-absorbing intermediate, which upon blue LEDs irradiation underwent a C–S bond cleavage to generate a carbon- and a sulfur-centered radical. The silyl enol ether intercepted the alkyl radical to form an α-oxo-stabilized radical, which after SET and hydrolysis afforded the functionalized ketone. Remarkably, this approach enabled to circumvent the

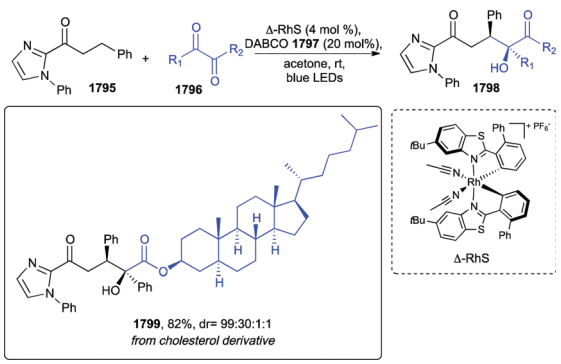

Scheme 319 α-Alkylation of ketones.

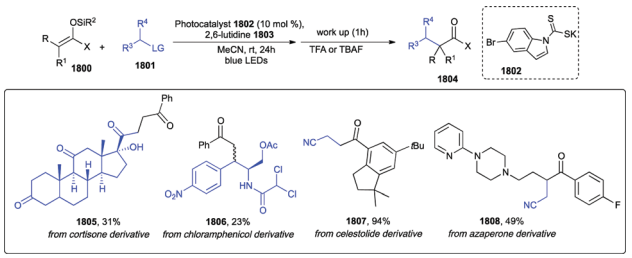

Scheme 320 α-Alkylation of ketones.

issues associated with the redox properties of the substrates, thus providing a general and mild protocol to achieve α-alkylated ketones even in the presence of functional groups not compatible with classical anionic strategies. To highlight the synthetic potential in the diversification of complex substrates, cortisone and chloramphenicol derivatives were successfully used as radical precursors (**1805** and **1806**, Scheme 320), while celestolide and azaperone were selected as examples of (hetero)aromatic ketone substrates (**1807** and **1808**, Scheme 320).

9.3.3 Allylation of aldehydes. The combination of photoredox and chromium catalysis enabled the formation of homoallylic alcohols *via* allylation of aldehydes with electron-rich (hetero)arenes, β-alkyl styrenes, and allyl diarylamines (Scheme 321).[404]

The developed protocol showed high levels of selectivity for the *anti* diastereomer and required [Ir(dF(CF$_3$)ppy)$_2$(dtbbpy)]PF$_6$ as the photoredox catalyst, $CrCl_2$ as the chromium source, Li_2CO_3 as a base in DMF under blue LEDs irradiation at room temperature for 24 hours. The generality of this allylation protocol was demonstrated with diverse simple allyl benzenes, as well as heterocyclic scaffolds such as allyl indoles and *N*-allylcarbazole. More complex substrates were also tested as in the case of estragole, which therefore required a more oxidizing catalyst [Ir(dF(CF$_3$)ppy)$_2$(bpy)]PF$_6$ to afford the desired product **1811** in 27% as a single diastereomer. The aldehyde scope included epiandrosterone derivative **1812**, that was obtained in a good 68% yield and >19 : 1 d.r. (Scheme 321).

Homoallylic alcohols could be also obtained *via* a nickel-catalyzed reductive coupling of aldehydes with 1,3-dienes under visible light photoredox catalytic conditions (Scheme 322).[405] The reaction mechanism relied on SET events to generate a key π-allylnickel intermediate *via* Ni–H insertion of 1,3-diene. Experimentally it proceeded in THF and in the presence of

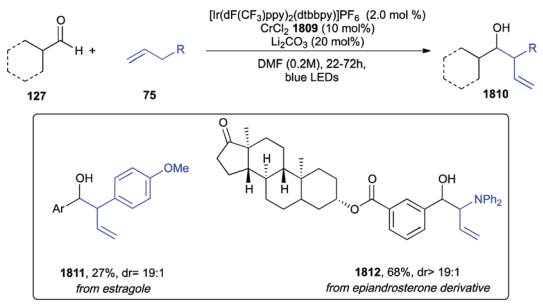

Scheme 321 Allylation of aldehydes.

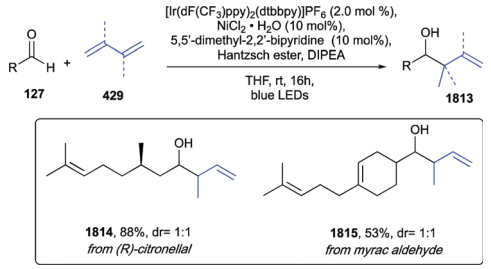

Scheme 322 Allylation of aldehydes.

$[Ir(dF(CF_3)ppy)_2(dtbbpy)]PF_6$, $NiCl_2{\cdot}6H_2O$, 5,5′-dimethyl-2,2′-bipyridine as a ligand, Hantzsch ester, and $^{i}Pr_2Net$, under blue LEDs irradiation at room temperature for 16 hours. By applying these conditions a wide number of diverse aromatic and aliphatic aldehydes were allylated in yields up to 99% and with complete branched regioselectivity, while the scope of dienes was shown with isoprene and 2,3-dimethyl-1,3-butadiene, and with representative complex natural compounds such as (*R*)-citronellal and myrac aldehyde (**1814** and **1815**, Scheme 322).

9.4 Formation of C(sp^3)–X bonds

9.4.1 Acetalyzation of aldehydes. A visible-light induced acetalization of aldehydes with alcohols was developed by H. Yi *et al.* (Scheme 323).[406]

As the authors reported, a wide range of aliphatic and (hetero)-aromatic aldehydes **127** could be protected by using the organic dye eosin Y as the photocatalyst under green LEDs irradiation in a mixture of MeCN/ROH at room temperature for 12 h. These standard conditions were applied to 48 different aldehydes, with yields up to 99%. This protocol provided a valuable alternative to get acetalization of acid-sensitive aldehydes, and, notably, it proved to be orthogonal to ketones as shown in Scheme 323 for steroid **1817**.

9.4.2 Reaction of aldehydes with aza-*ortho*-quinone methides. D. Liang *et al.* reported a hetero-Diels–Alder between aza-*ortho*-quinone methides, generated *in situ via* the attack of a perfluoroalkyl radical to a 2-vinylaniline precursor **1818** (Scheme 324), and π-electron-poor systems such as aldehydes.[407] Optimum yields were obtained when $[Ir(ppy)_2(dtbbpy)]PF_6$ was employed as the photocatalyst, NaOAc as a base in CH_2Cl_2 at 5 °C and under 7 W blue LEDs irradiation. This three-component protocol was endowed with some key advantages such as easily accessible substrates, broad

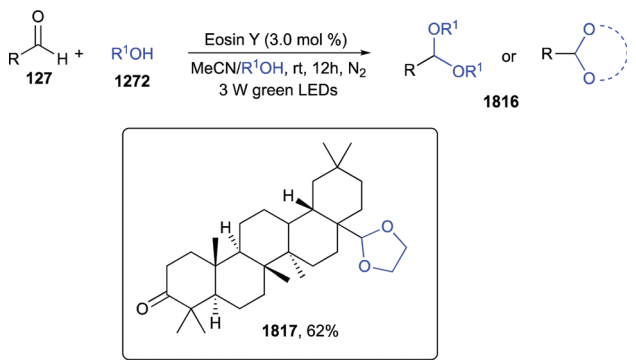

Scheme 323 Acetalyzation of aldehydes.

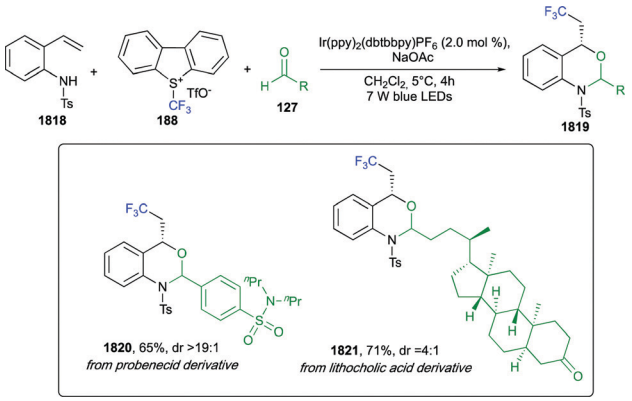

Scheme 324 Reaction of aldehydes with aza-*ortho*-quinone methides.

aldehyde scope, good yields, and high d.r. values. The functional group tolerance was showcased in the functionalization of two pharmaceutical-derived aldehydes such as probenecid and lithocholic acid, to give compounds **1820** and **1821** (Scheme 324).

9.4.3 Hydroboration of imines. By merging organocatalysis and photocatalysis, N. Zhou *et al.* achieved the first catalytic inverse hydroboration of imines with *N*-heterocyclic carbene (NHC) boranes affording a library of α-amino organoboron compounds (Scheme 325).[408] The exploitation of B-centered radical chemistry, starting from bench-stable, nontoxic, and easily available NHC boranes enabled the formation of a C–B bond, whereas traditional hydroboration resulted in nitrogen-bound boryl intermediates. The developed protocol featured $[Ir(ppy)_2(dtbbpy)]PF_6$ as the photoredox catalyst, phenylmethanethiol as the organocatalyst, 20 mol% NaH as the inorganic base in MeCN under irradiation with a 33 W CFL at room temperature. Investigation of the imine scope revealed excellent chemo- and regio-selectivities, together with good functional group compatibility as shown in the late-stage radical borylation of estrone and helicid (**1825** and **1826**, Scheme 325).

9.5 Remote functionalization of ketones

Ketones could undergo remote C(sp^3)–H functionalization, *via* their conversion to oxime derivatives, photoinduced generation of iminyl radicals, and radical transposition by C(sp^3)–C(sp^3) and C(sp^3)–H bond cleavage giving access to distal carbon

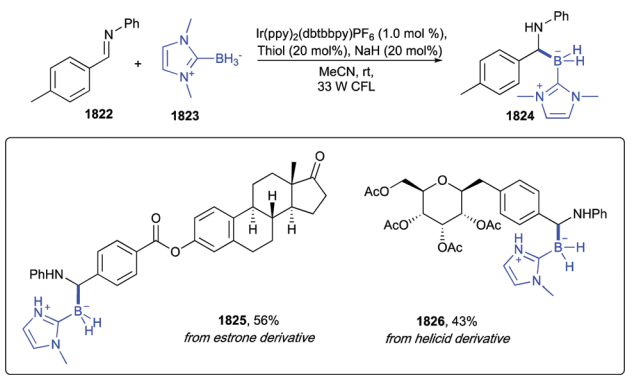

Scheme 325 Hydroboration of imines.

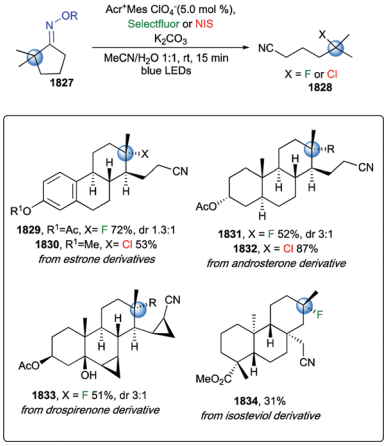

Scheme 326 Remote functionalization of ketones.

radicals (Scheme 326).[409] The latter, being nucleophilic, was prone to further react with a polarized SOMOphile (X–Y) where the X-atom has a partially positive character such as the fluorine atom in Selectfluor reagent, *via* a radical atom transfer (S_H2). Optimum yields were obtained by employing Fukuzumi's acridinium salt (Acr-Mes$^+$ClO$_4^-$) as the photoredox catalyst, K_2CO_3 as a base, in a 1 : 1 MeCN–H_2O mixture as the reaction medium under blue LEDs irradiation at room temperature for short times (15 minutes). Additionally, the replacement of Selectfluor with *N*-chlorosuccinimide (NCS) and triisopropylsulfonyl azide enabled the synthesis of chlorinated and azidated nitriles, respectively.

10. Functionalization of C(sp^3)–H bonds

The progress of photocatalytic HAT catalysis for the late-stage functionalization of complex molecular architectures, *via* homolytic cleavage of C(sp^3)–H bonds has been recently reviewed by D. Ravelli and coworkers.[410] According to the accurate classification reported by Ravelli *et al.* and based on mechanistic considerations, the formation of C-centered radicals can occur *via* different classes of HAT processes: direct processes (d-HAT), indirect processes (i-HAT), and remote processes (r-HAT). In d-HAT reactions the photocatalyst is able to directly abstract a hydrogen atom from a suitable substrate, while i-HAT pathways featured the formation of intermediate radical species such as N$^\bullet$, O$^\bullet$, S$^\bullet$, or halogens able to act as the effective hydrogen atom abstractors. The third class, the r-HAT can be considered as an intramolecular i-HAT catalysis where the generation of a hydrogen atom abstractor *via* a SET event enables a site-selective functionalization of unactivated C(sp^3)–H bonds.[410] Differently from the above cited overview focused on HAT catalytic approaches which include UV light promoted transformations, the following paragraph strictly pinpoints C(sp^3)–H functionalizations promoted by visible light irradiation.

10.1 Formation of C(sp^3)–C(sp^3) bonds

10.1.1 Alkylation. Selective alkylation of unactivated C(sp^3)–H bonds could be accomplished by installing either a

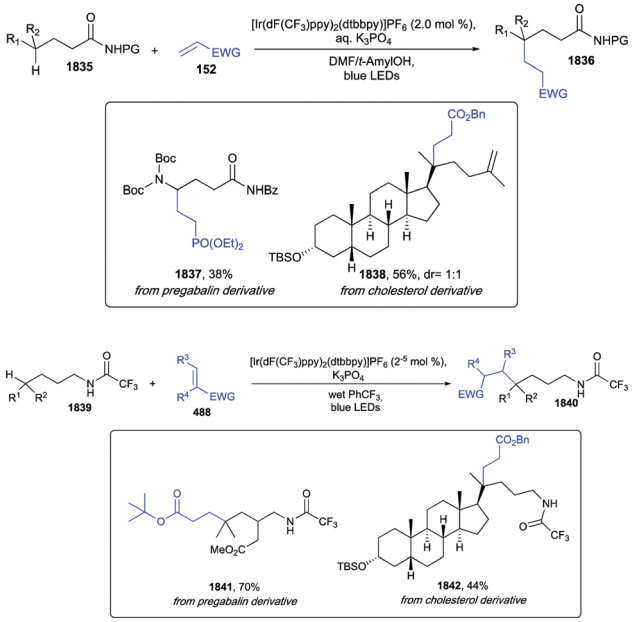

Scheme 327 Alkylation of C(sp^3)–H bonds.

trifluoroacetamide or an ethoxycarbonyl protected amide at the γ-position as reported by T. Rovis and coworkers (Scheme 327).[411,412]

Actually, this kind of functionalization enabled the formation *in situ* of an amidyl radical, able to promote a selective 1,5-HAT thus activating a remote site. The protocol required [Ir(dF(CF$_3$)ppy)$_2$(dtbbpy)]PF$_6$ as the photosensitizer, K_3PO_4 in wet PhCF$_3$[411] or saturated aq. K_3PO_4 in a mixture of DMF/*t*-AmylOH[412] under blue LEDs irradiation. The alkenes scope included both unsubstituted acrylates and those bearing α-substituents, as well as allyl acrylate, methacrylonitrile, and other electron-deficient alkenes such as methyl vinyl ketone, acrylamide, vinyl sulfone and vinyl phosphonate. As for the amide, substrates with tertiary γ-C–H bonds were well tolerated, while secondary C–H bonds can afford either mono- or dialkylated adducts by simply changing the ratio between the amide and the alkene. Worthy of note, in case of two different tertiary C–H bonds, the 1,5-HAT occurred with high regioselectivity. As examples of complex biorelevant substrates, a γ-aminobutyric acid derivative (pregabalin), and a steroidal compound gave monoalkylated products **1837** and **1838** in moderate yields (Scheme 327).

Later on, the group of P. Melchiorre reported a visible-light-mediated organocatalytic C–H functionalization of toluene

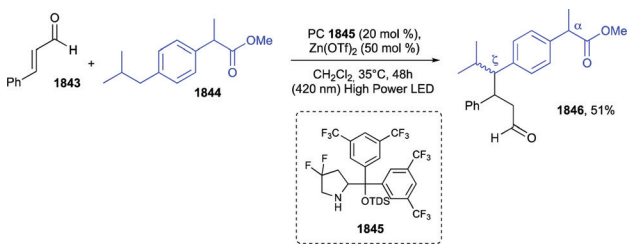

Scheme 328 Alkylation of C(sp^3)–H bonds.

derivatives with enals (**1843**, Scheme 328) to afford enantio-enriched β-benzylated aldehydes (*e.g.* **1846**). The reaction design relied on a sequential MultiSite Proton-Coupled Electron Transfer (MS-PCET) where an *in situ* formed photoactive iminium ion between the enal and the organocatalyst, generated, upon visible light excitation and through SET oxidation of toluene, a radical cation, along with a β-enaminyl radical.[413] The radical cation was then deprotonated by the counteranion of the iminium ion to deliver a benzyl radical intermediate, which was eventually intercepted by the chiral β-enaminyl radical to provide β-alkylated aldehydes. Experimentally, the method required $Zn(OTf)_2$ to promote the formation of the iminium ion and irradiation with a HP single Led (420 nm-violet light) in CH_2Cl_2 at 35 °C for 48 hours. The substrate scope included cinnamaldehydes bearing on the aromatic ring halogens, trimethylsilyl-, trifluoromethyl-, and even methyl-groups, while an exquisite functional groups tolerance was also shown with a wide range of toluene, benzylic, and xylene derivatives. The selective functionalization of (*S*)-ibuprofen Me-ester afforded derivative **1846** in 51% yield and moderate diastereoselectivity (Scheme 328).

More or less at the same time, R. Martin and coworkers reported a protocol to achieve C(sp^3)–H alkylation and arylation by exploiting triplet excited ketones as photocatalysts and nickel catalysts (Scheme 329).[414] Starting from both aryl and heteroaryl bromides, and using a bench stable diarylketone **1847**, $Ni(acac)_2$ as a nickel source, 5,5′-dimethyl-2,2′-bipyridine as a ligand, and Na_2CO_3 as a base under CFL irradiation at room temperature in THF **540** as both the solvent and the starting C(sp^3)–H partner, a number of multifunctionalized arylated ethers were obtained in medium to excellent yields. The protocol was endowed with an exceptional functional group tolerance, as further shown in the late-stage modification of cholesterol-, L-methol-, and D-allofuranose (**1849–1851**, Scheme 329).

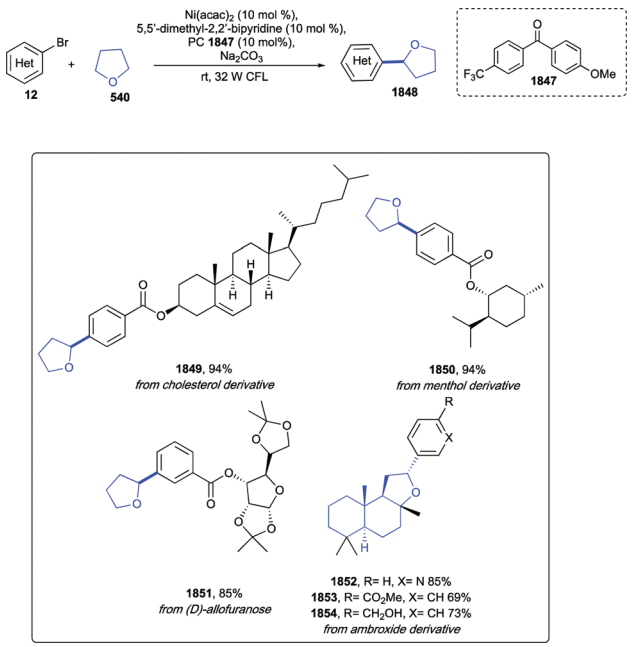

Scheme 329 Alkylation of C(sp^3)–H bonds.

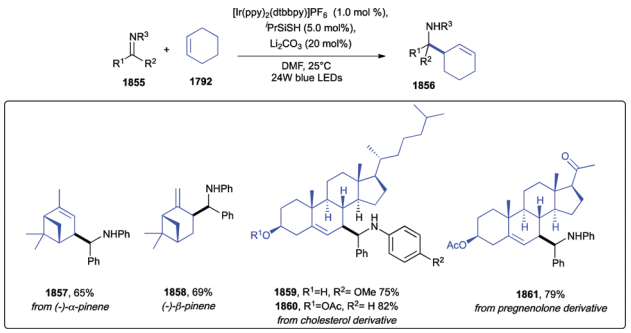

Scheme 330 Alkylation of C(sp^3)–H bonds.

Likewise, the scope of the C(sp^3)–H partner included ambroxide, which could be either arylated or heteroarylated by performing the reaction in benzene as a solvent (**1852–1854**, Scheme 329).

Recently, M. Rueping and L. Huang identified a synergistic organo- and photoredox catalytic system to promote alkylation of allylic C(sp^3)–H bonds from unactivated alkenes and imines (Scheme 330).[415]

The reaction design hinged on the formation of an N-centered radical intermediate formed upon addition of an allylic radical to the imine. Experimentally, the method required $[Ir(ppy)_2(dtbbpy)]PF_6$ as the photoredox catalyst, $^iPr_3SiSH$ as the oganocatalyst, and Li_2CO_3 in DMF under irradiation with 24 W blue LEDs at 25 °C. By applying these conditions, a wide range of *N*-aryl imines as well as more challenging ketimine substrates underwent allylic alkylation in good to excellent yields. Alike, the scope of the allylic radical included a variety of cyclic and acyclic alkenes, whereas the latter reacted less efficiently, leading to moderate to medium yields. Late-stage diversification of complex biorelevant scaffolds such as (−)-α- and (−)-β-pinene, cholesterol, and pregnenolone highlighted the excellent functional group compatibility (**1857–1861**, Scheme 330).

According to Z. Xu and coworkers, alkylation, carboamination, amination of remote C(sp^3)–H bonds could be accomplished *via* a C–C or a C–N cross coupling reaction (Scheme 331).[416] Thoroughly, while carboamination was achieved *via* the generation of *N*-centered radicals undergoing 1,5-HAT to afford C-centered radicals eventually trapped by α-aminoalkyl radicals, the alkylation required the use of Hantzsch ester derivatives generating alkyl radicals *via* 1,2-SET of *N*-centered radicals. Likewise, the use of primary and secondary anilines as coupling partners provided functionalized tertiary anilines *via* a direct cross coupling of an

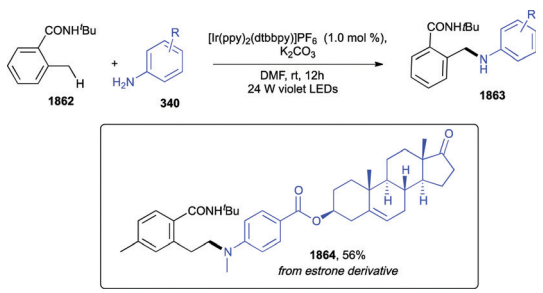

Scheme 331 Alkylation of C(sp^3)–H bonds.

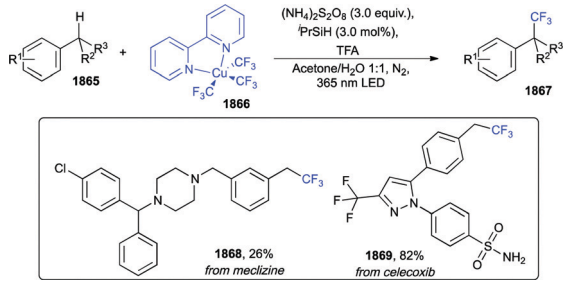

Scheme 332 Benzylic C(sp^3)–H trifluoromethylation.

N-centered radical and an alkyl radical. The amination and carboamination could be performed by using $[Ir(ppy)_2(dtbpy)]PF_6$ as a photocatalyst, K_2CO_3 as a base in DMF under violet LED irradiation (390–410 nm) at room temperature, while slight variations of reaction conditions were required to accomplish the alkylation with Hatzsch esters. Representative carboamination of an estrone derivative was carried out in 56% yield (**1864**, Scheme 331), to witness the robustness of the developed protocol.

10.1.2 Benzylic C(sp^3)–H trifluoromethylation. The reaction proceeded in the presence of Grushin's reagent 1866, ammonium persulfate, $^iPr_3SiH$, TFA in a 1:1 mixture of acetone/H_2O, and under irradiation with a 365 nm LED bulb.[417] Interestingly, $^iPr_3SiH$ was efficiently employed as a mild radical quenching agent able to suppress competitive aromatic trifluoromethylation. Benzylic trifluoromethyl groups were successfully installed on a number of substrates, showing tolerance for halides, ketones, esters, amides, nitriles, pyridines, pyrimidines, and silanes, and retaining high regioselectivity. Late-stage trifluoromethylation of meclizine and celecoxib was achieved in 26 and 82% yields, respectively (**1868** and **1869**, Scheme 332).

10.1.3 C(sp^3)–H trifluoromethylation. Recently, it was shown that the merger of light-driven decatungstate HAT (NaDT, Scheme 333) and copper catalysis enabled trifluoromethylation of both strong aliphatic and benzylic C–H bonds.[418] This metallaphotoredox protocol proceeded with excellent selectivity for positions distal to unprotected amines. Togni's reagent II (**76**) was used as a bench-stable and readily available trifluoromethylating agent, sodium decatungstate (NaDT) and $CuCl_2$ as catalysts, in a 9:1 H_2O/MeCN mixture under black light irradiation (390 nm Kessil lamp) at room temperature. This methodology was applied to a range of medicinally relevant amines, such as nortropinone, proline, and the neurotransmitter γ-aminobutyric acid (GABA). Remarkably, a number of non-amine-bearing compounds were also engaged in this trifluoromethylation strategy, thus demonstrating that the protocol is suitable for a broad range of organic substrates. Applicability in the late-stage functionalization of pharmaceuticals was showcased for celecoxib, nicotine, scareolide, lidocaine, torsemide, and prilocaine (**1869–1874**, Scheme 333).

10.1.4 Alkylation with α-carbonyl imines. The group of L. Gong developed a photocatalytic system to functionalize hydrocarbons lacking directing groups into chiral molecules (Scheme 334).[419]

Thoroughly, the authors exploited a hydrogen atom transfer organophotocatalyst, such as 5,7,12,14-pentacenetetrone **1877** and a BOX copper complex, generated *in situ* from $Cu(BF_4)\cdot H_2O$ and the chiral ligand **1876**, as a chiral catalyst. The reaction proceeded in CH_2Cl_2 under 24 W blue LEDs irradiation at −20 °C. By applying these conditions, a wide array of benzylic hydrocarbons was functionalized with α-carbonyl imine derivatives, providing the target compounds in excellent yields and ee up to 99%. Tolerated functional groups included halogens, ketones, esters, and boron esters. Late-stage diversification of medicinal agents such as celebrex, lopid, and skelaxin was carried out in good yields (**1879–1881**, Scheme 334).

10.1.5 Allylation. The introduction of an allyl group onto non-acidic C(sp^3)–H could be accomplished by using 5,7,12,14-pentacenetetrone **1877** (Scheme 335) as an organic photocatalyst, 1,2-bis(phenylsulfonyl)-2-propene **442** as allyl source, K_2CO_3 as a base, in CH_2Cl_2, and a 425 nm LED lamp at room temperature for 24 hours.[420]

Allylation of cyclic alkanes was achieved in medium to good yields, while moderate reactivity was observed for linear unactivated alkanes. On the other hand, allylation of heteroatom-containing

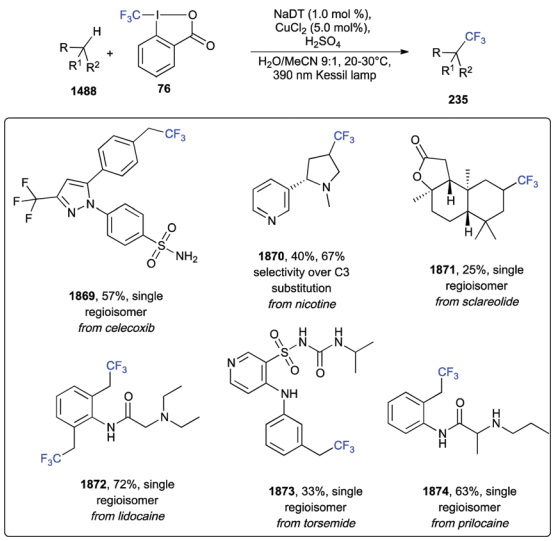

Scheme 333 C(sp^3)–H trifluoromethylation.

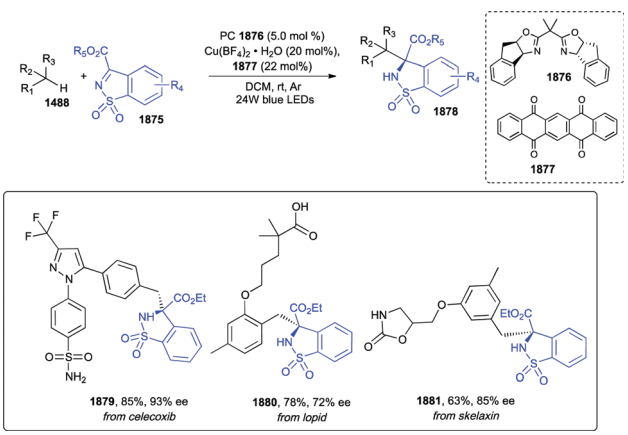

Scheme 334 Alkylation with α-carbonyl imines.

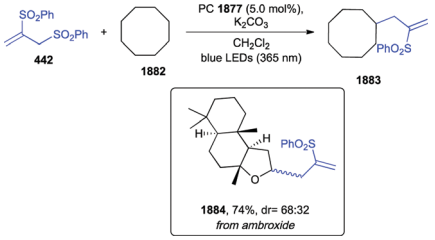

Scheme 335 Allylation of non-acidic C(sp^3)–H.

substrates demonstrated a good functional group tolerance, including ethers, Boc-protected aliphatic amines, and unprotected alcohols. Remarkably, allylation of a complex bioactive scaffold such as ambroxide was carried out with a high degree of chemoselectivity without affecting the potentially reactive methane C–H bonds (**1884**, Scheme 335).

10.2 Formation of C(sp^3)–C(sp^2) bonds

10.2.1 α-Monofluoroalkenylation. Heteroatomic alkanes can be directly α-monofluoroalkenylated *via* a combination of visible light photoredox catalysis and hydrogen-atom-transfer catalysis (Scheme 336).[421] Suitable heteroatomic alkanes involved amine derivatives such as carbamates, amides, and ureas as well as ethers, thioethers, and methyl-substituted benzenes. Remarkably, the reaction showed high regioselectivity for the C(sp^3)–H bond at the α-position with respect to the heteroatom (N-, O-, and S-). Optimized reaction conditions required [Ir(dF(CF_3)ppy)$_2$(dtbbpy)]PF_6 as photoredox catalyst, quinuclidine **1187** as HAT agent, and K_3PO_4 as a base in a 10 : 1 MeCN/H_2O mixture under blue LEDs irradiation at room temperature for 24 h. The high functional group tolerance of the reaction enabled the synthesis of diverse functionalized monofluoroalkenes including **1885** and **1886**, obtained from a precursor of tylocrebine and from linezolid (Scheme 336).

10.2.2 Arylation. A groundbreaking report from the D. W. C. MacMillan group appeared in 2015 provided a protocol to achieve the direct arylation of non-functionalized allylic C–H bonds (*i.e.* C–H bonds with an adjacent carbon involved in a C=C bond, *e.g.* **2**, Scheme 337).[422] The method exploited *fac*-Ir(ppy)$_3$ as a photoredox catalyst, triisopropylsilanethiol as organic catalyst, which delivered a thiyl radical responsible for the allylic hydrogen atom abstraction to **2A**, K_2CO_3 as a base in acetone under irradiation with a 26 W CFL at room temperature. These conditions enabled the direct coupling of electron-deficient arenes with a wide range of functionalized cyclic and acyclic

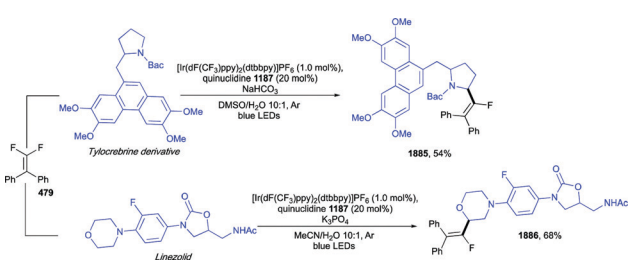

Scheme 336 α-Monofluoroalkenylation.

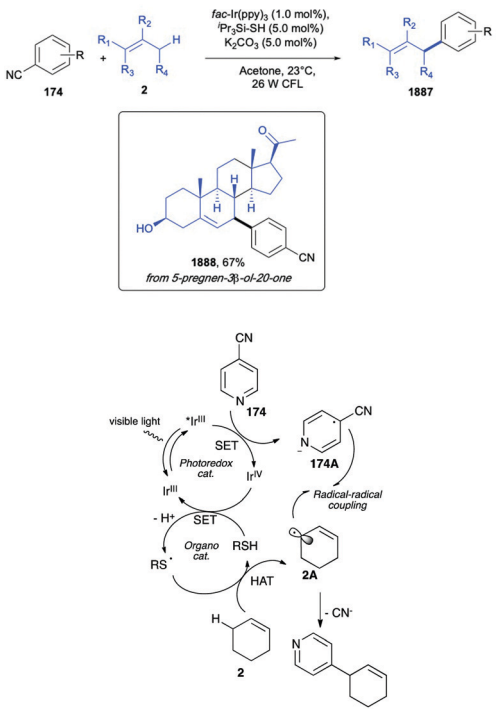

Scheme 337 Arylation of C(sp^3)–H bonds.

olefins. The potential for the late-stage diversification of complex bioactive substrates was illustrated with 5-pregnen-3β-ol-20-one (**1888**, Scheme 337).

A few years later, it was shown that allylic and benzylic sp^3-hybridized carbon could be arylated by using 1,4-dicyanobenzene and sterically and electronically tuned diarylsulfonamides (**1889**, Scheme 338), which upon visible light photoredox catalytic conditions, generated a sulfonamidyl radical behaving as a hydrogen atom transfer (HAT) agent.[423] It followed the formation of an alkyl radical intermediate, which reacted with the reduced radical anion of the starting 1,4-dicyanobenzene, to eventually afford, after elimination of a cyanide ion, the arylated alkane. The protocol featured Ir(Fppy)$_3$, HAT catalyst **1889**, K_2CO_3 as a base, in acetone at 40 °C under blue LEDs irradiation for 34 hours. These conditions proved to be effective with cycloalkenes, cyclic and acyclic benzylic ethers, and even unprotected benzyl alcohols. This photoredox/HAT dual catalytic system was applied to the LSF of prasterone, giving the arylated adduct in

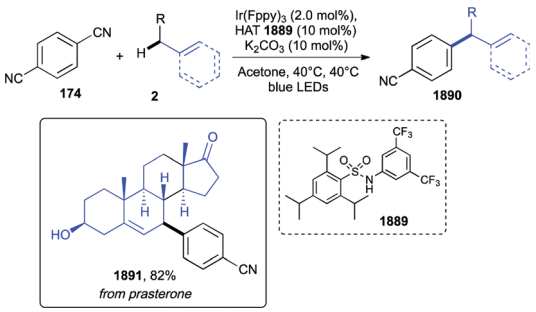

Scheme 338 Arylation of C(sp^3)–H bonds.

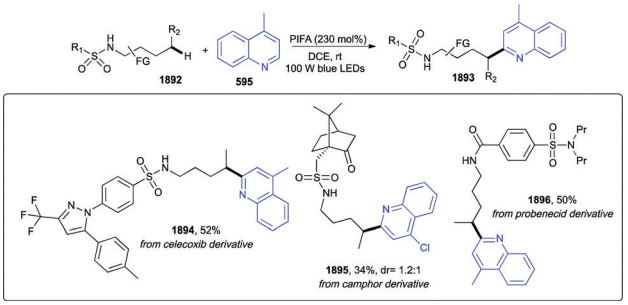

Scheme 339 Heteroarylation of C(sp^3)–H bonds.

high yield and good regioselectivity (**1891**, Scheme 338, 82%, >10 : 1), albeit as a mixture of uncharacterized isomers.

10.2.3 Heteroarylation. Aliphatic amides such as carboxamides, sulfonamides, and phosphoramides can undergo a site-selective remote C(sp^3)–H heteroarylation *via* a direct generation of amidyl radicals from the amide N–H bonds, which triggered a subsequent 1,5-HAT to form a challenging alkyl radical (Scheme 339).[424]

The transformation required the hypervalent iodine reagent PIFA (phenyliodine bis(trifluoroacetate)), in DCE as the solvent and under blue LEDs irradiation at room temperature. It is worth noting that PIFA acted as both the initiator of amidyl radical and the oxidant. The scope of the heteroarene included a variety of five- and six-membered-nitrogen-containing heteroarenes, *e.g.* isoquinolines, phenathridine, acridine, quinoxaline, thiazoles, and benzothiazoles, to cite a few, while both linear and cyclic, primary and secondary, sulfonamides, along with electron-rich or deficient benzamides, phosphoramidate and phosphinamide, were all competent substrates. Celecoxib, camphor, and probenecid were selected as example of complex bioactive scaffolds and converted into derivatives **1894–1896** (Scheme 339).

10.2.4 Pyridylation. Remote C(sp^3)–H bonds can be heteroarylated by exploiting the ability of *N*-alkoxyheteroarenium salts to serve as both alkoxy radical precursors and heteroaryl sources (Scheme 340).[425] The method developed by I. Kim *et al.* relied on the visible-light promoted SET reduction of an *N*-alkoxypyridinium salt by a photoexcited quinolinone catalyst. The alkoxy radical then translocated to form a nucleophilic alkyl radical, which underwent addition to the heteroaryl substrate, thereby enabling a remote C (sp^3)–H heteroarylation. The mild reaction conditions were applied to a wide range of *N*-alkoxypyridinium substrates, providing a library of 36 derivatives in good to high yields and, in some cases, with exclusive regioselectivity with respect to the heteroaryl ring positions. Late-stage functionalization of drugs such as pentoxifylline, pyriproxyfen, and vismodegib, along with cholesterol, proved to be viable (**1899–1902**, Scheme 340).

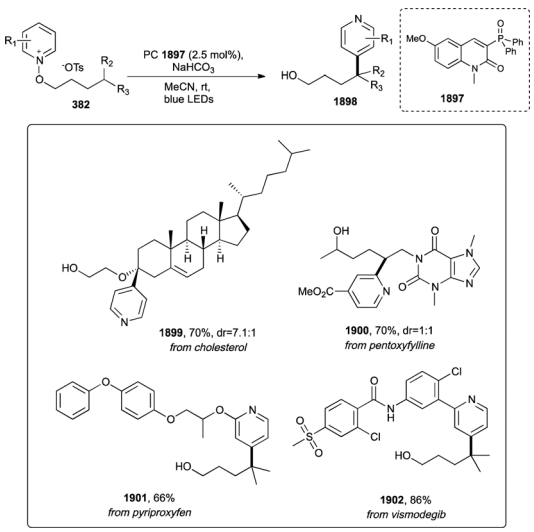

Scheme 340 Pyridylation of C(sp^3)–H bonds.

The same authors reported a similar visible-light induced site-selective C(sp^3)–H pyridylation of sulfonamides and carboxamides by using *N*-amidopyridinium salts (Scheme 341).[426] The reaction design was analogous to the one reported above with *N*-alkoxypyridinium salts: the nitrogen-centered radicals generated upon SET reduction of the pyridinium salts underwent 1,5-hydrogen atom transfer to form alkyl radical intermediates. Nevertheless, excellent C4-selectivity for the pyridine ring in the radical trapping was observed. Besides the substrate scope exploration with a number of both sulfonamide- and benzamide–pyridinium salts, late-stage functionalization of bisacodyl, abiraterone acetate, and pentoxifylline was achieved in good yields (**1905–1907**, Scheme 341).

10.2.5 Synthesis of esters. The merging of photoredox and nickel catalysis enabled the synthesis of esters from cyclic alkanes or toluenes, and chloroformates (Scheme 342).[427] This direct cross coupling relied on the formation of chlorine radical intermediate as HAT agent, responsible for the generation of an alkyl radical intermediate *via* hydrogen abstraction from the alkane. Hereinafter, the reaction proceeded *via* the addition of this alkyl radical to the nickel/formate complex and reductive elimination of the ester product. In order to achieve optimum yields, $[Ir(dF(CF_3)ppy)_2(dtbbpy)]PF_6$ was used as the photoredox catalyst, $Ni(cod)_2$ as the nickel source, dtbbpy as a ligand, K_3PO_4 and $Na_2WO_4{\cdot}2H_2O$ as bases, in toluene under 34 W blue LEDs irradiation at 34–40 °C for 48 hours. The substrate scope embodied both aromatic and aliphatic acyl derivatives, unactivated C(sp^3)–H partners, functionalized cyclic and acyclic alkanes bearing Boc-protected amines, ethers, ketones, cyano-, esters, amides, and imides, as well as benzylic C(sp^3)–H containg compounds. Application of this method to the LSF of sclareolide led to **1911**

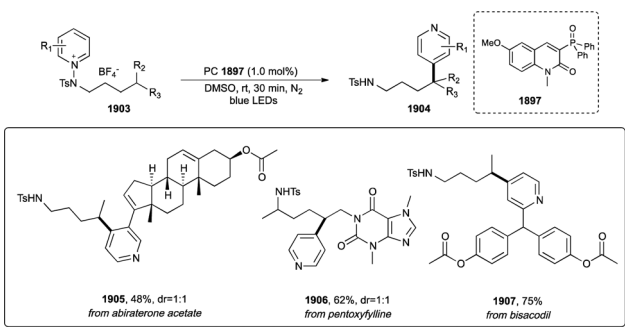

Scheme 341 Pyridylation of C(sp^3)–H bonds.

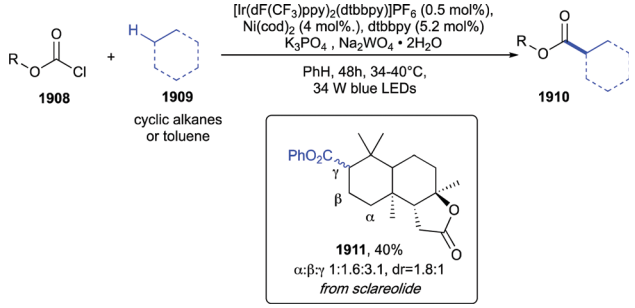

Scheme 342 Synthesis of esters.

in 40% combined yields at the most electron-rich and sterically accessible methylene sites (Scheme 342).

10.3 Formation of C(sp^3)–X bonds

10.3.1 Hydroxylation and amidation. Tertiary and benzylic C(sp^3)–H bonds could be either hydroxylated or amidated under photoredox catalytic conditions by exploiting hypervalent iodine(III) reagents such as hydroxyl perfluorobenziodoxole (PFBI-OH) or unmodified benzoiodoxole (BI-OH), respectively (Scheme 343).[428] The protocol required $Ru(bpy)_3Cl_2$ as the photocatalyst, a HFIP/H_2O (26 : 1, to achieve oxygenation) or HFIP/MeCN (for acetylated adducts following a Ritter-type mechanism) as solvent mixtures under 23 W CFL irradiation at 30 °C for 20 h. The process relied on a radical-polar crossover mechanism, where a carbocation intermediate was trapped by either water or acetonitrile. Both the scope of tertiary alkyls and benzyl-derivatives was wide, with a broad functional group tolerance. In order to showcase the potential of this synthetic methodology for late-stage modification of pharmaceutical compounds, sulbactam and thalidomide derivatives were hydroxylated in 65 and 62% yields (**1912** and **1913**, Scheme 343). Ibuprofen was converted into hydroxylated

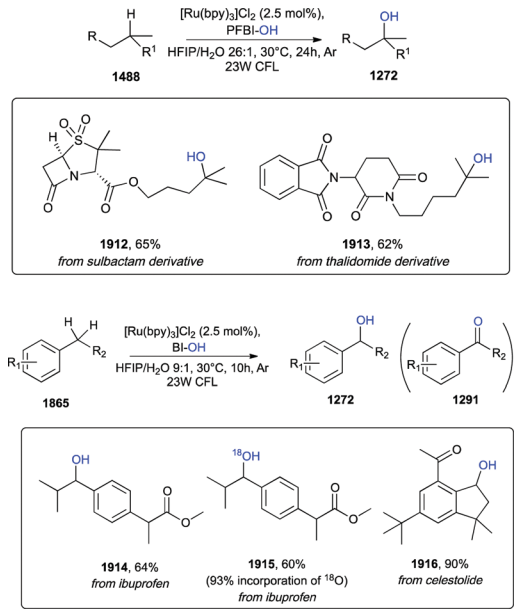

Scheme 343 Hydroxylation of C(sp^3)–H bonds.

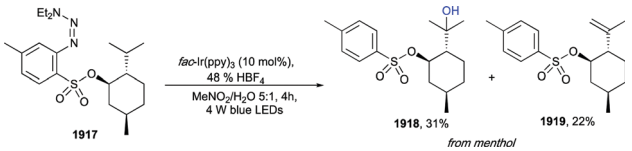

Scheme 344 Hydroxylation of C(sp^3)–H bonds.

derivative **1914** and ^{18}O-labelled ibuprofen **1915** by performing the reaction in $H_2{}^{18}O$. Reaction of natural product celestolide also proceeded smoothly to afford **1916** in excellent yield (Scheme 343).

An alternative approach to achieve hydroxylation of aliphatic C–H bonds employed Tz° sulfonate esters (**1917**, Scheme 344) and sulfonamides in the presence of *fac*-Ir(ppy)$_3$ as a photoredox catalyst.[429] The reaction mechanism relied on a radical translocation of an electron-poor aryl radical, which abstracted a hydrogen atom from a sp^3-hybridized carbon atom to generate an alkyl radical, followed by oxidation to carbocation and trapping with water, thus resulting in a radical-polar crossover process. Optimum yields were obtained by using 48% HBF_4 as an acidic additive for the liberation of an arenediazonium species from the Tz° ester, and a 5 : 1 mixture of CH_3NO_2/H_2O as a solvent system under 4 W blue LEDs irradiation for 18 hours. The substrate scope was good, showing tolerance towards functional groups such as alkenes and esters. Conversion of menthyl derivative **1917** gave the hydroxylated adduct **1918** in a moderate 31% yield, together with 22% of the elimination product **1919** (Scheme 344).

10.3.2 Amination. One of the rare examples about the use of halogen bond noncovalent interactions to induce and guide chemical reactions was reported by F. Wu *et al.*[430] Actually, the authors identified a HAT relay strategy to access pyrrolidines (**1922**, Scheme 345) from alkanes, based on a halogen bonding charge-transfer complex able to promote the formation of nitrogen radicals from sulfonamides thus initiating a HAT relay process. Radical hydrogen abstraction from the alkane, followed by iodination and substitution with sulfonamide **1920** led to the first C–N bond.

An ensuing nitrogen relay process occurring *via* visible light mediated Hofmann–Löffler–Freytag (HLF) reaction led to the formation of the target pyrrolidines (**1922**). The reaction proceeded in CH_2Cl_2 in the presence of *N*-iodosuccinimide (NIS); interestingly, by simply changing the amounts of NIS from 300 mol% to 500 mol% and the reaction times it was possible to achieve either benzylamines (**1921**) or pyrrolidines (**1922**), respectively. The generality of this method was explored with a number of aliphatic (hetero)aromatic sulfonamides as well as alkylbenzenes, providing the target compounds in moderate to good yields. LSF of estradiol, dehydro-abietylamine, and celecoxib was also successfully accomplished (**1923–1926**, Scheme 345).

10.3.3 Azidation and halogenation. Azidation of tertiary aliphatic C–H bonds could be accomplished by using the Zhdankin azidoiodane reagent **1927** (Scheme 346), $Ru(bpy)_3Cl_2$ as a photoredox catalyst in hexafluoroisopropanol (HFIP) under irradiation with a 12 W fluorescent light bulb.[431] Additionally, performing

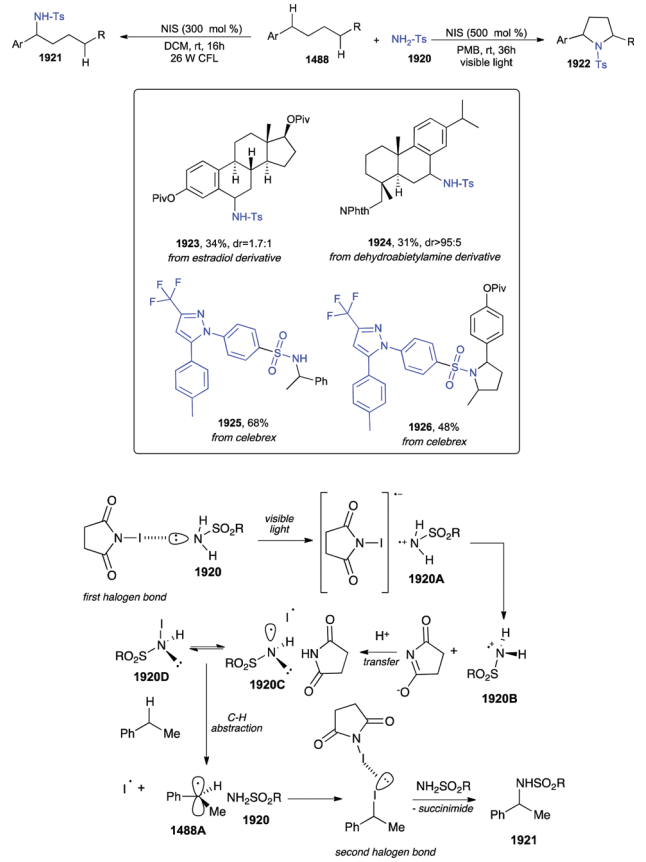

Scheme 345 Amination of C(sp^3)–H bonds.

the reaction in the presence of 4 equiv. of LiCl or 2 equiv. of nBu$_4$NBr provided chlorinated and brominated adducts, respectively. The developed azidation protocol showed excellent selectivity towards tertiary aliphatic sp^3-hybridized carbons and tolerated a wide range of functional groups such as Boc, Bn, TBS, ester, and amide. Selective azidation of the more distal tertiary C–H site of *N*-phthaloyl pregabalin methyl ester indicated that steric hindrance and electron-withdrawing groups decreased the reactivity of the neighboring C–H bonds, thus enabling regioselective functionalization. Late-stage azidation of menthol and estrone were also carried out, albeit with moderate yields (**1928** and **1929**, Scheme 346).

An alternative procedure for site-selective aliphatic bromination of unactivated alkenes was reported by V. A. Schmidt *et al.* and

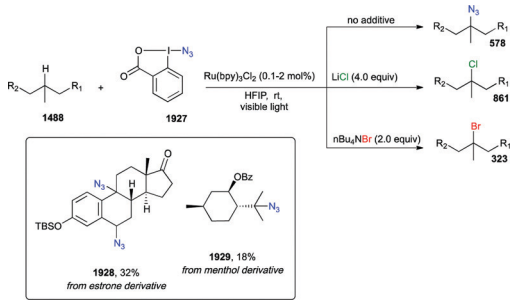

Scheme 346 Azidation and halogenation of C(sp^3)–H bonds.

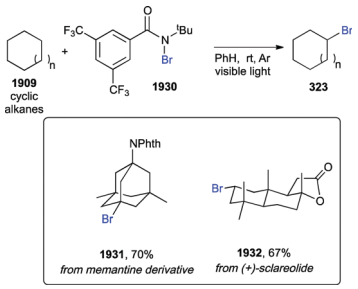

Scheme 347 Azidation and halogenation of C(sp^3)–H bonds.

foresaw *N*-bromoamide reagents and visible light (Scheme 347).[432] Optimization of reaction conditions required the identification of a competent *N*-bromoamide precursor, which would be bench stable, easily accessed from amides, with tunable steric and electronic properties, and unique selectivity profiles. Among the investigated *N*-bromoamides, reagent **1930** was shown to provide intermolecular aliphatic C–H bromination under mild conditions (toluene as a solvent and 100 W or 23 W CFL, 30 minutes) and in good yields. Remarkably, it was found that the *N*-substituent of the reagent could influence the site-selectivity of the process: while N–H and *N*-trifluoroethyl *N*-bromoamides favor the functionalization of weak tertiary C–H bond, *N*-*t*Bu reagents enabled the functionalization of less sterically hindered secondary sites. A survey of complex bioactive substrates such as *N*-Phth memantine and (+)-sclareolide afforded derivatives **1931** and **1932** in 70% and 67% isolated yields, respectively.

Site selective chlorination of unactivated C(sp^3)–H bonds of aliphatic amines and intramolecular/intermolecular chloroaminations of unactivated alkenes could be accomplished through a simple and efficient protocol exploiting the formation of amidyl radicals from amines (Scheme 348).[433] The reaction mechanism relied on a manganese-mediated atom-transfer event under visible light irradiation. Thoroughly, *N*-chlorination was performed by using *t*BuOCl in CH_2Cl_2 at room temperature, while the situ addition of $Mn_2(CO)_{10}$ under 6 W blue LEDs irradiation for 1 hour led to remote chlorination, *via* 1,5-HAT of the amidyl radical to form a *C*-centered radical. The latter eventually underwent a Cl-atom transfer from either the *N*-chlorosulfonamide or a Cl–Mn(CO)$_5$ formed *in situ*. The application of the mild developed reaction conditions provided access to alkyl chlorides, chlorinated pyrrolidines, and vicinal chloroamine adducts. Late-stage remote chlorination of NSAIDS celecoxib, valdecoxib, and zonisamide, as well as intermolecular chloroamination of alkene-containing complex scaffolds derived from fenofibric acid, ibuprofen, and isoxepac was accomplished in medium to good yields (**1935–1937** and **1940–1942**, Scheme 348). Additionally, gram scale reaction and diversification of a celecoxib derivative provided valuable products **1943–1946** in two reaction-steps (Scheme 348).

10.3.4 Alkoxylation of benzylic C(sp3)–H bonds. Most of the literature methods enabling direct C–H alkoxylation require the use of an alcohol component as a solvent or a cosolvent, thus limiting their scope to simple and inexpensive inputs. Recently, the group of T. P. Yoon reported a photocatalytic

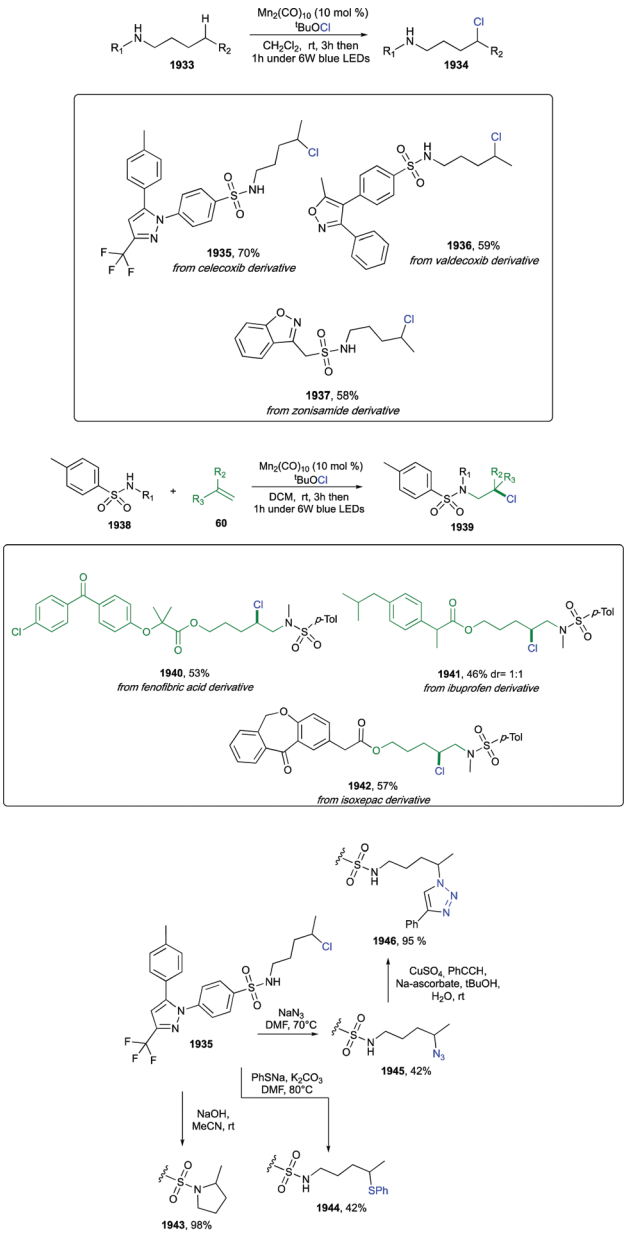

Scheme 348 Chlorination of C(sp^3)–H bonds.

approach for introducing benzylic C–O bonds with site- and chemo-selectivity (Scheme 349).[434]

A dual catalytic system, based on [Ir(dF(CF_3)ppy)$_2$(5,5′-dCF_3bpy)]PF_6 as a photoredox catalyst and Cu(TFA)$_2$·H_2O as a terminal oxidant, promoted the formation of benzylic radical intermediates, which were subsequently oxidized by the copper(II) species. A base, such as K_2HPO_4 was also necessary in order to obtain optimum yields, while the reaction proceeded in MeCN under irradiation with a 427 nm blue LED at room temperature for 6 hours. Methoxylation of a wide range of multifunctionalized benzyl derivatives was accomplished in medium to high yields. The alcohol scope embodied a plethora of aliphatic scaffolds substituted with double and triple bonds, aldehyde, ether, Boc-protected secondary amine, halogens, silyl,

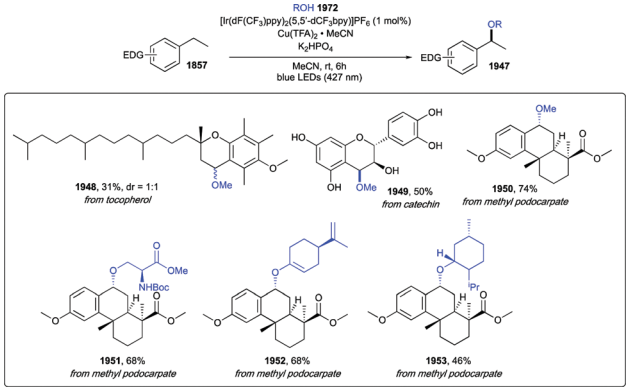

Scheme 349 Alkoxylation of benzylic C(sp^3)–H bonds.

cyano, unprotected alcohols, and sulfonyl, highlighting an extraordinary functional group tolerance. The site-selectivity was also investigated by selecting starting materials with multiple benzylic positions. Besides alcohols, other nucleophiles such as carboxylic acids and *N*-Boc carbamate were reactive under standard conditions, providing ester and carbamate derivatives, respectively. While heteroarene afforded the methoxylated adducts in medium yields, nucleophiles such as phenols and sulfonamides were not compatible. Awfully, application of the oxidative photoredox catalytic protocol to complex biorelevant compounds including tocopherol, catechin, and methyl podocarpate led to derivatives **1948–1953** with good efficiencies (Scheme 349).

10.3.5 Synthesis of β-chloroketones from aryl cyclopropanes. Aryl cyclopropanes can be converted into β-chloroketones by applying a visible-light mediated catalyst-free method requiring cheap standard laboratory reagents such as oxygen, hydrochloric acid, and nitric acid (Scheme 350).[435] The authors proposed a light-driven radical chain mechanism initiated by molecular chlorine generated upon reaction of diluted HCl with HNO_3. Investigation of the substrate scope revealed that electron-donating substituents gave better yields than electron-withdrawing ones, which sometimes suppressed the reaction completely. Interestingly, standard reaction conditions were successfully applied to bioactive ciprofibrate and tramadol, albeit derivative **1957** was obtained in low yield, probably due to a facile decarboxylation of the aliphatic carboxylic acid (Scheme 350). Indeed, the corresponding methyl ester **1958** gave the desired product in 65% yield.

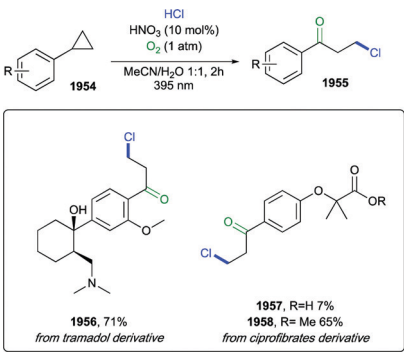

Scheme 350 Synthesis of β-chloroketones from aryl cyclopropanes.

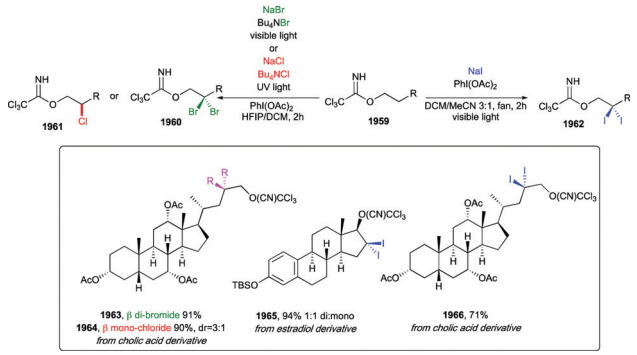

Scheme 351 β C–H di-halogenation of imidates.

10.3.6 β C–H di-halogenation of imidates. C(sp^3)–H bonds at the β-position of imidates could be di-halogenated *via* sequential iterative HAT events mediated by *in situ* generated imidate radicals, which promoted selective N$^\bullet$ to C$^\bullet$ radical translocations (Scheme 351).[436] Extensive optimization of reaction conditions revealed that the use of *N*-iodosuccinimide (NIS) as an oxidant favored the formation of a β mono-iodide, while a combination of NaI and $PhI(OAc)_2$ provided the β di-halogenated congeners. The robustness of the protocol was displayed with imidates derived from primary and secondary alcohols. Steric congestion in primary inputs was tolerated, whereas cyclic secondary alcohols afforded a mixture of β-mono- and β-di-iodides thus indicating conformational constraints for the HAT process. Additionally, C–H di-bromination and mono-chlorination were also carried out by employing NaBr/Bu_4NBr or NaCl/Bu_4NCl, respectively, in the presence of $PhI(OAc)_2$ in a 3 : 1 HFIP:CH_2Cl_2 mixture. However, while bromination was efficiently promoted by visible light, chlorination required UV light (300 nm). Late-stage halogenation of estradiol and cholic acid was accomplished in excellent yields (**1963–1966**, Scheme 351).

10.3.7 Halogenation of 8-aminoquinoline-tethered C(sp^3)–H bonds. M. L. Czyz *et al.* recently reported a protocol to achieve iodination, bromination, and chlorination of C(sp^3)–H bonds in compounds bearing an 8-aminoquinoline moiety (Scheme 352).[437]

The latter indeed, in the presence of a palladium catalyst, enabled the formation of photoactive palladacycle complexes, whose photoinduced electron-transfer afforded C–H halogenation products rather than C–C bond adducts. Palladacycles were preformed by stirring the aliphatic amides with $Pd(OAc)_2$ in MeCN at room temperature, while as the halogenating reagents $F_3C(F_2C)_2$–CF_2I, EtO_2C–CBr_3, and NC–CCl_3 were used. Optimum yields were achieved by using oxone as the co-oxidant. A high selectivity was observed for the β-methyl C(sp^3)–H bonds in the presence of β-methylene C(sp^3)–H bonds and functional groups such as alkyl chains, ethers, halogens, arenes, and saturated carbo- and hetero-cycles were all found orthogonal. Application of the method to the late-stage iodination of a cholic acid derivative afforded **1969** in 84% yield, without epimerization, at the α-C–H bond.

10.3.8 Thiolation. The site-selective formation of C(sp^3)–S bonds could be accomplished *via* remote functionalization of aliphatic *N*-fluoroamides (Scheme 353).[438] The optimized catalytic system featured $Cu(acac)_2$ in combination with 1,10-phenanthroline as a ligand, indium powder, Na_2HPO_4 as a base in DCE at 40 °C and under 50 W blue LEDs irradiation for 9 hours. The reaction mechanism was based on the formation of a photoactive Cu(I) complex with a disulfide (**1970**, ArS–SAr), which upon excitation induced a reduction of the N–F amide to generate an *N*-centered radical. The latter underwent a 1,5-HAT to form a *C*-centered radical, which was intercepted by a high-valent Cu(III)–SAr species to give, after further reductive elimination the target thioether compound. The transformation proceeded efficiently with a broad range of aliphatic amides and aromatic disulfides, whereas also benzyl disulfide afforded the expected thioether, albeit with a medium yield. C(sp^3)–H thiolation of biologically active compounds was shown to be feasible with menthol and lithocholic acid derived *N*-fluoroamide substrates, and with estrone-derived disulfide (**1975–1978**, Scheme 353).

HAT catalysis has been recently harnessed to achieve direct allylic C(sp^3)–H thiolation with disulfides by S. H. Hong and coworkers (Scheme 353).[439]

The Hong protocol enabled the synthesis of allyl thioethers by employing $Ir(CF_3ppy)_3$ as a photoredox catalyst, NaOH as a base in DMA under 40 W blue LEDs irradiation at room temperature. The role of the base was shown to be critical to

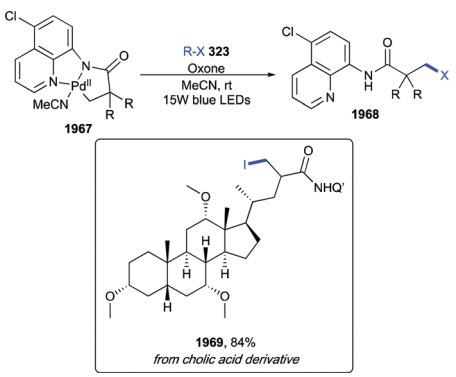

Scheme 352 Halogenation of 8-aminoquinoline-tethered C(sp^3)–H bonds.

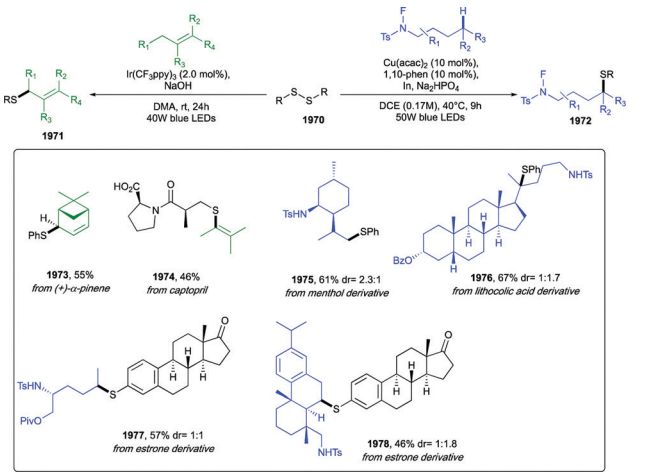

Scheme 353 Thiolation of C(sp^3)–H bonds.

route the reaction towards the formation of allylic thioethers circumventing undesired hydrothiolation occurring *via* thiyl radical addition to olefin. Thoroughly, the formation of such a radical was prevented by immediate deprotonation of thiol, which coupled to photocatalyst-mediated oxidation of allyl radical into an allyl cation, made the reaction pathway an ionic process. A wide range of diaryl sulfides (**1970**) and alkenes afforded the target allyl thioethers with high efficiency. The scope was further extended to unsymmetrical disulfide by synthesizing various alkyl 2-benzothiazolyl disulfides. Additionally, the authors demonstrated that the method was amenable to complex bioactive skeletons such as (+)-α-pinene and captopril (**1973** and **1974**, Scheme 353).

10.3.9 Trifluoromethylthiolation. Selective activation of unactivated C(sp^3)–H bonds and subsequent trifluoromethylthiolation was achieved by S. Mukherjee *et al.* by exploiting a photoredox-mediated HAT catalysis (Scheme 354).[440] More in detail, [Ir(dF(CF$_3$)ppy)$_2$(dtbbpy)]PF$_6$ (Ir–F) was selected as the photocatalyst, sodium benzoate was used as precursor of benzoyloxy radical (PhCO$_2^\bullet$), which acted as HAT agent, while the shelf-stable electrophilic trifluoromethylthiolating reagent Phth-SCF$_3$ gave the desired product R-SCF$_3$ along with a phthalimide radical (Phth$^\bullet$). The reaction proceeded in MeCN under blue LEDs irradiation at room temperature, showing high selectivity between methylene and methine C–H bonds, even on multiple methine C–H bond containing substrates. The robustness of the protocol was further proved on complex biorelevant scaffolds such as androsterone and cholesterol derivatives, and pregabalin (**1979–1981**, Scheme 354).

A more recent protocol to achieve trifluoromethylthiolation of benzylic C–H bonds was reported by W. Xu *et al.* (Scheme 355).[441] Here the authors described a metal-free and site-selective organophotoredox catalyzed functionalization of alkyl arenes and heteroarenes (**1865**). Remarkably, the observed regioselectivity originated from an inner-sphere benzylic radical initiation mechanism, thus avoiding the need of external oxidants or hydrogen atom abstractors. The reaction proceeded by using 4CzIPN as the organic photocatalyst, Phth-SCF$_3$ as trifluoromethylthiolating agent, K$_2$CO$_3$ as a base in MeCN and under blue LEDs irradiation at room temperature. The wide scope and the broad functional group tolerance, along with the exclusive selectivity were proven on a number of drugs and complex molecules, including pirfenidone, proxelpl, menthol, celestolide, triclosan, epiandrosterone, and D-δ-tocopherol (**1982–1988**, Scheme 355).

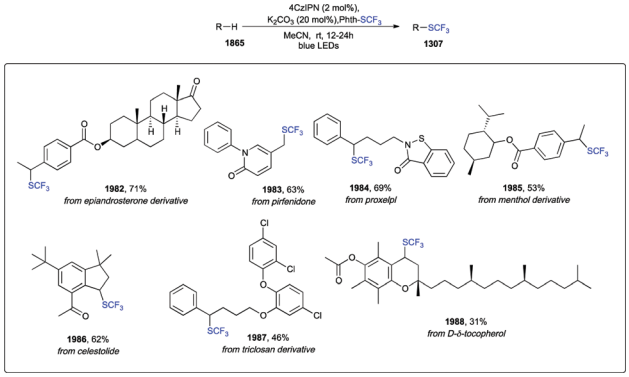

Scheme 355 Trifluoromethylthiolation of C(sp^3)–H bonds.

10.3.10 Alkane functionalization *via* xanthylated adducts. A general and mild protocol to achieve different chemotypes *via* C–H functionalization was reported by the group of E. J. Alexanian.[442] The use of an easily prepared and bench stable *N*-xanthylamide (**1989**, Scheme 356) under visible light irradiation in PhCF$_3$ as a solvent and at room temperature afforded C–H xanthylated products (**1990**), which could then be easily converted in a plethora of functional groups *via* both polar and radical manifolds. Representative transformations included C–H vinylation, C–H amination, C–H deuteration, C–H thiolation and thiol–ene glycoconjugation, C–H trifluoromethylthiolation, and C–H hydroxylation. The substrate scope was shown with both simple hydrocarbons and functionalized substrates, and the potential of this method was highlighted in the C–H xanthylation of complex biorelevant scaffolds such as (+)-sclareolide, (−)-ambroxide, 5α-cholestane, *trans*-androsterone acetate, and (+)-longifolene (**1991–1994**, Scheme 356). Additionally, late-stage diversification of (+)-sclareolide xanthate afforded a wide array of derivatives **1996–2002** in medium to good yields.

A few years later, the same group reported a site-selective aliphatic dithiocarbamylation of C(sp^3)–H bonds *via* the formation of stable and isolable *N*-dithiocarbamates, which, upon blue LEDs irradiation, delivered amidyl radical intermediates (Scheme 357).[443]

The latter, once formed, were prone to undergo an intramolecular hydrogen atom transfer, to afford dithiocarbamylation products (**2005**). The reaction proceeded in PhCF$_3$ at room

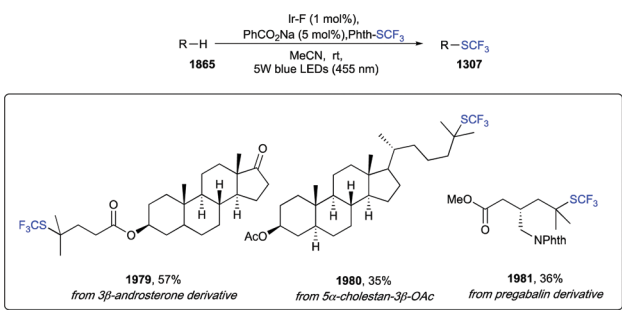

Scheme 354 Trifluoromethylthiolation of C(sp^3)–H bonds.

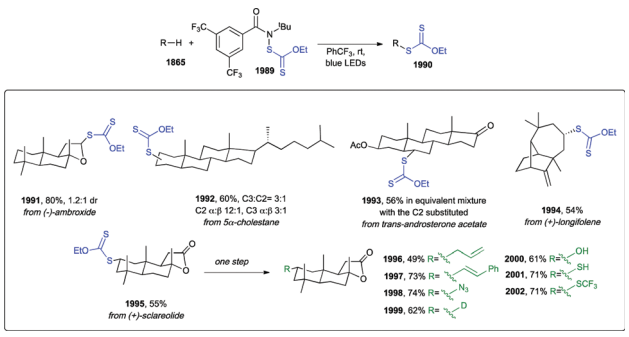

Scheme 356 Alexanian alkane functionalization.

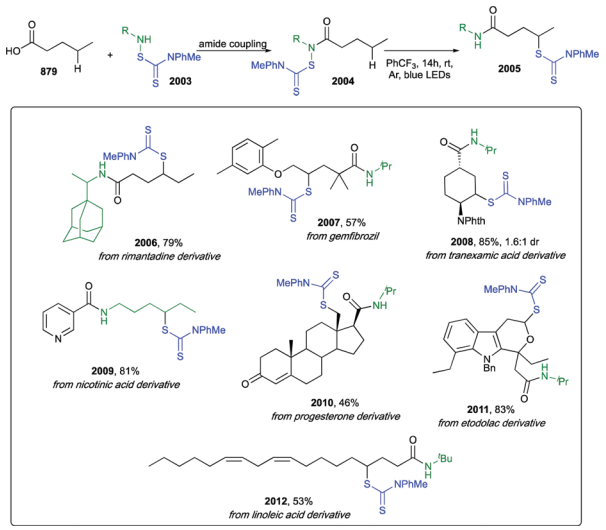

Scheme 357 Alkane functionalization *via* xanthylated adducts.

temperature for 14 hours, and proved to be quite general in the scope, as both methylene and primary C–H functionalization were successful. Likewise, cyclic substrates provided 1,2- or 1,3-substituted adducts in good yields. Additionally, to further prove the potential of this method, the authors performed site-specific C–H dithiocarbamylation of pharmaceutical derivatives such as rimantadine, gemfibrozil, tranexamic acid, nicotinic acid, progesterone, and linoleic acid as shown in Scheme 357 (**2006–2012**).

More or less at the same time the group of E. J. Alexanian, in collaboration with D. A. Nicewicz, developed a strategy enabling a direct one-step conversion of aliphatic C–H bonds into diverse functional groups (Scheme 358).

As opposite to the previous two-step approach, such a method relied on the decoupling of the C–H abstraction step from the radical trapping step, thus enabling diverse functionalization by simply changing the radical trapping agent.[444] Experimentally, an excited-state acridinium photoredox catalyst was responsible for the formation of heteroatom-centered radicals, which acted as HAT agents, thereby generating a carbon centered radical from the unactivated alkane. Mechanistic studies supported the hypothesis of a putative oxygen-centered radical as HAT agent, which generated upon SET oxidation of the phosphate salt mediated by an excited-state Mes-Acr^{+}*. As the radical trapping agent, sulfonyl azide **2015** provided azidated products, while *N*-fluorobenzene-sulfonimide (NFSI), diethyl bromomalonate, and *N*-chlorosuccinimide afforded fluoro-, bromo-, and chloro-derivatives, respectively. Likewise, with the judicious choice of the proper reagents, trifluoromethylthiolation and alkylation were successfully achieved. The protocol proved to be robust and showed good functional group tolerance as further demonstrated in the site-selective C–H functionalization of complex bioactive scaffolds such as (−)-menthol benzoate, *N*-Phth memantine, ibuprofen methyl ester, and 5α-cholestan-3-one (**2016–2020**, Scheme 358).

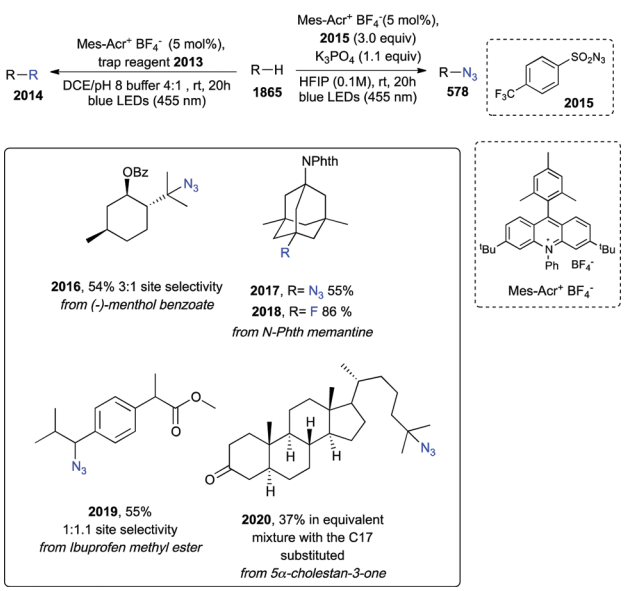

Scheme 358 Alexanian alkane functionalization.

11. Miscellaneous

11.1 Synthesis of aryl phosphonates from aryl iodonium salts

W. Lecroq *et al.* reported a metal-free synthesis of aryl phosphonates starting from diaryliodonium triflates (**763**, Scheme 359) and phosphites (**759**), in the presence of K_2CO_3 as a base and MeCN as solvent under blue LEDs irradiation.[445]

In particular, the authors exploited the ability of Ar_2I^{+} and phosphites to act as electron-acceptors and electron-donors, respectively, thus forming an EDA complex. The latter, upon blue light irradiation, generated a phosphorous radical cation along with an aryl radical, which underwent a cross-coupling to form the desired aryl phosphonate after a nucleophilic displacement from a phosphonium intermediate. The reaction proceeded smoothly with both electron-rich and electron-poor *ortho*-, *meta*-, and *para*-substituted diaryliodonium triflates. On the other hand, sterically hindered iodonium salts led to decreased yields. Remarkably, pyridine-derived iodonium salts also proved to be suitable substrates. As for the phosphites, triisopropyl, methyl, and phenyl phosphites were employed. The phosphonation of an iodonium-derived steroid smoothly afforded the organo-phosphorous compound **2021**, albeit in a moderate 28% yield.

11.2 Trifluoromethoxylation of arenediazonium salts

Dual photoredox and copper catalytic conditions were applied to the trifluoromethoxylation of arenediazonium tetrafluoroborates (**492**, Scheme 360), with trifluoromethyl arylsulfonate **2022** (TFMS)

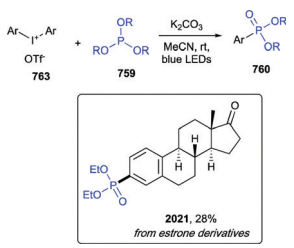

Scheme 359 Synthesis of aryl phosphonates from aryl iodonium salts.

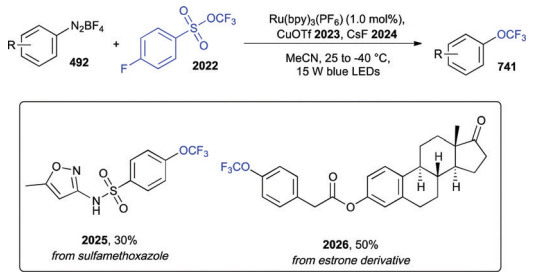

Scheme 360 Trifluoromethoxylation of arenediazonium salts.

as the trifluoromethoxylation agent.[446] The reaction proceeded regioselectively with $Ru(bpy)_3(PF_6)_2$ as the photocatalyst, CuOTf as the copper source, CsF as an additive in MeCN at temperatures ranging from 25 to −40 °C and using a 15 W white LED lamp as the photon source. These conditions provided compatibility with a wide range of functional groups including halogens, cyano-, amide-, nitro-, ketones, and tertiary amines. As example of complex substrates, sulfamethoxazole and estrone derivatives **2025** and **2026** were obtained in 30 and 50% yield, respectively.

11.3 Petasis reaction with alkyltrifluoroborates

J. Yi *et al.* developed an alkyl Petasis reaction proceeding *via* photoredox catalysis starting from (hetero)aromatic benzaldehydes (**341**, Scheme 361) and glyoxalate-derived aldehydes, (hetero)aromatic amines (**340**) and primary, secondary, and tertiary alkyltrifluoroborates (**2027**).[447]

In contrast to the traditional two-electron Petasis reaction, limited to unsaturated boronic acids, here, a single-electron transfer mechanism extended the scope of this key organic transformation to alkyl substituents. The reaction design harnessed the generation of an alkyl radical *via* SET oxidation mediated by an excited state photocatalyst. The alkyl radical could then add to the *in situ* condensed imine to form an amine radical cation, which was reduced by the reduced state photocatalyst to give the final functionalized amine. Experimentally, such a transformation was achieved with $[Ir\{dF(CF_3)ppy\}_2(bpy)]PF_6$ in the presence of sodium bisulfate in 1,4-dioxan as solvent under blue LEDs irradiation for 24 h at room temperature. Diverse alkyltrifluoroborates including heteroaromatic systems, sterically disfavored tertiary substrates, and primary aliphatic ones with high oxidation potentials proved to be amenable. As for the aldehyde scope, remarkably, halo-substituted benzaldehydes and dicarbonyl substrates provided the target compounds with high chemoselectivity and good yields. Likely, the aniline partner showed a high functional group tolerance, with poor or no electronic or steric effects. Late-stage modification of a set of drugs derived benzaldehydes prepared from indomethacin, fenofibrate, and sulfadimethoxine was accomplished in excellent to acceptable yields (**2029–2031**, Scheme 361).

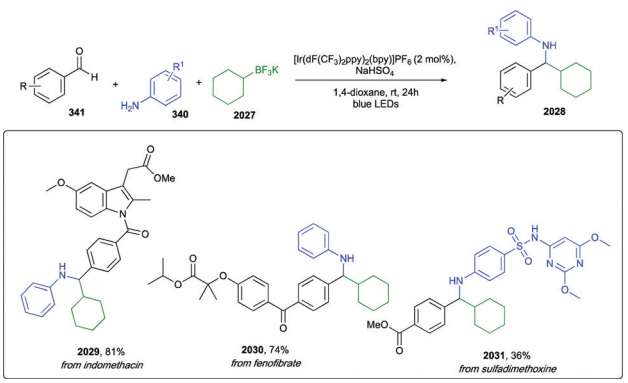

Scheme 361 Petasis reaction with alkyltrifluoroborates.

11.4 Multicomponent synthesis of α,α-difluoroketone hydrazones

Aldehydes, hydrazines, and bromodifluorinated reagents (*e.g.* **89**, Scheme 362) could be engaged in a one-pot three-component visible-light photocatalyzed reaction to afford α,α-difluoroketone hydrazine derivatives.[448] More in detail, the transformation was catalyzed by the organic dye 4CzIPN, in the presence of Na_2HPO_4 as a base, DMF as a solvent under 8 W blue LEDs irradiation at 23 °C for 12 h. Remarkably, the authors shown that the photocatalyst could be recycled in 95% in a large-scale synthesis. The broad substrate scope and the excellent functional group compatibility were also showcased in the LSF of estrone-derived aldehyde (**2034**, Scheme 362).

11.5 Photolysis of aryldiazoacetates

Aryldiazoacetates (**2035**, Scheme 363), when irradiated with blue LEDs, underwent photoexcitation to a higher energy singlet state, followed by loss of N_2 with concomitant formation of a singlet carbene.[449] The latter could be trapped by different partners such as styrene, carboxylic acids, amines, alkanes, and arenes thus

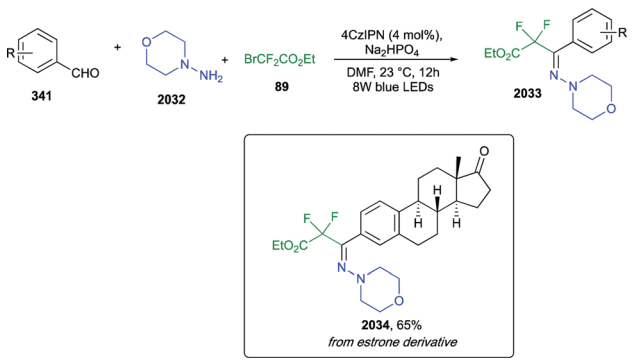

Scheme 362 Multicomponent synthesis of α,α-difluoroketone hydrazones.

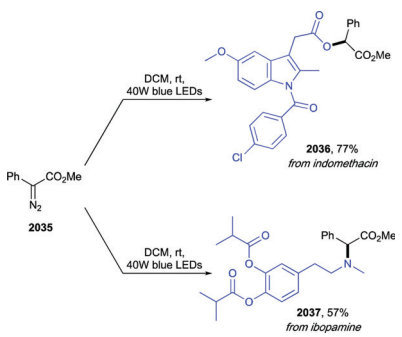

Scheme 363 Photolysis of aryldiazoacetates.

offering the possibility to functionalize a wide range of organic compounds. The reaction proceeded in the absence of any catalyst, in CH_2Cl_2 as the solvent, under air, and at room temperature. This mild protocol was also evaluated in the LSF of indomethacin and ibopamin, as shown in Scheme 363 (**2036** and **2037**, respectively).

11.6 Synthesis of cyclobutanes from alkyl boronic esters

Methylcyclobutanation of alkyl boronic esters could be achieved under photoredox catalytic conditions *via* a SET induced deboronative radical addition to an electron-deficient alkene (Scheme 364).[450]

A further SET reduction, together with a polar 4-*exo*-*tet* cyclization with a pendent alkyl halide afforded the final cyclic adducts. Nevertheless, this transformation was enabled by a prior conversion of the boronic esters (**1399**) into easily oxidizable aryl boronate complexes (**2038**), whose formation was achieved with phenyllithium in THF for 1 h. After evaporation of the solvent *in vacuo*, the addition of the haloalkyl alkene (*e.g.* **2039**), the organic photocatalyst 4CzIPN, and DMSO under blue LEDs irradiation, and the stirring of this mixture for 20 h afforded the desired cyclobutyl adducts (**2040**) in good to high yields. As examples of complex medicinal compounds menthol, gemfibrozil, cholesterol, and lithocholic acid were converted into derivatives **2041–2045** (Scheme 364).

11.7 *ipso*-Hydroxylation of boronic acids

Boronic acids (**2046**, Scheme 365) could be converted into their corresponding phenols (**1155**) *via* a metal-free and base-free method exploiting the formation of a key unstable Lewis adduct intermediate formed upon reaction with *tert*-butylhydroperoxide (TBHP) and trichloroacetonitrile (Cl_3CCN).[451] Both a radical and an ionic mechanism could in theory underly this transformation, albeit blue LEDs irradiation demonstrated to be essential to get high yields. The boronic acid scope was limited to aromatic substrates, albeit a wide range of functional groups such as methoxy-, bromo-, iodo-, and oxidation sensitive ones (*e.g.* ether and thioether) were tolerated. The boronic acid derivative of lithocholic acid was successfully converted into derivative **2047**,

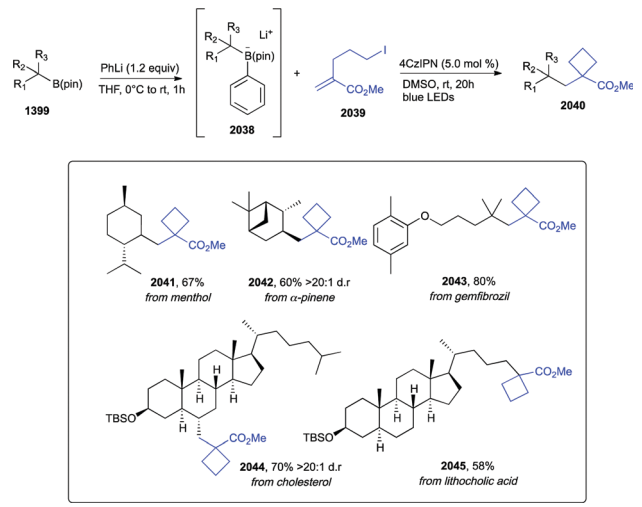

Scheme 364 Synthesis of cyclobutanes from alkyl boronic esters.

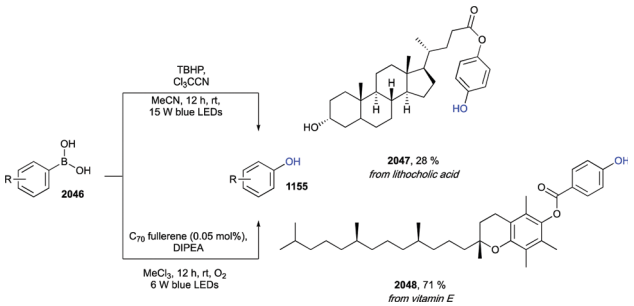

Scheme 365 *ipso*-Hydroxylation of boronic acids.

albeit with a moderate 28% yield. Alternatively, I. Kumar *et al.* reported a metal-free C_{70} fullerene-catalyzed method for the *ipso*-hydroxylation of aryl and heteroaryl boronic acids to afford the corresponding phenols (Scheme 365).[452] Mechanistic studies suggested that C_{70} played a crucial role in the generation of reactive oxygen species under blue LEDs irradiation. The reaction required DIPEA as an electron donor and $CHCl_3$ as a solvent. The wide scope was demonstrated in the formation of phenols bearing alkyl, esters, ethers, ketones, halogens, alkenes, and amides as functional groups. Vitamin E was hydroxylated in 71% yield under standard conditions (**2048**, Scheme 365).

11.8 *ipso*-Nucleophilic substitution of alkoxy arenes

N. E. S. Tay *et al.* developed a valuable protocol for a cation radical-accelerated nucleophilic aromatic substitution of arenes using methoxy- and benzyloxy-groups as nucleofuges (Scheme 366).[453] Imidazoles, pyrazoles, benzimidazoles, and triazoles were used as nucleophilic partners. Reaction conditions were exceptionally mild, as the organic dye acridinium salt Mes-Acr$^+$BF4$^-$ was employed as the photocatalyst and no external additives were needed. With multifunctionalized methoxy arenes, such as guaiacole and veratrole derivatives, a wide functional group tolerance was observed, along with good regioselectivities. Example of complex biorelevant arenes included protected L-dopa **2055**, and naproxen methyl ester **2052**, which sequentially underwent a C–H functionalization with a cyano group and then *ipso*-substituted with imidazole to give **2054** (Scheme 366).

11.9 Oxo-amination of aryl cyclopropanes

Arylcyclopropanes could be converted to radical cation intermediates *via* a single electron oxidation; a S_N2-like nucleophilic

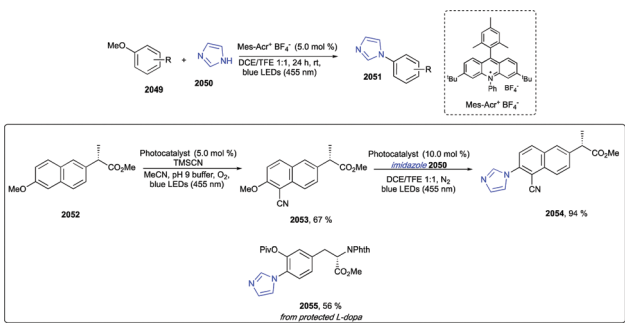

Scheme 366 *ipso*-Nucleophilic substitution of alkoxy arenes.

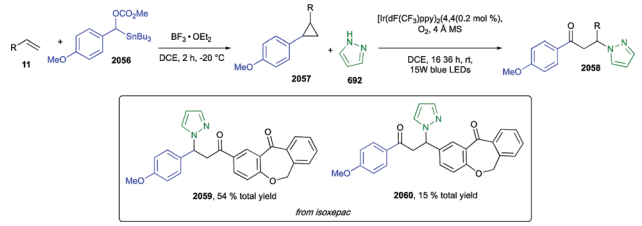

Scheme 367 Oxo-amination of aryl cyclopropanes.

attack/ring-opening oxo-amination provided β-amino ketone derivatives (Scheme 367).[454] The developed mild reaction conditions harnessed [Ir(dF(CF$_3$)ppy)$_2$(4,4′-dCF$_3$bpy)](PF$_6$) as the photoredox catalyst, DCE as the solvent, 4 Å molecular sieves in a dioxygen atmosphere under blue LEDs irradiation at room temperature. The scope of cyclopropanes was wide, including substrates bearing electron-donating as well as electron-withdrawing groups such as halogens, disubstituted aryl motifs, and heterocycles. Additionally, the cyclopropyl moiety could bear a *gem*-dialkyl group, or a single aliphatic substituent, or still, they can be spiro-fused. Remarkably, a one-pot procedure starting from alkenes was also developed, and applied, among other substrates, to the NSAIDs isoxepac to furnish a mixture of two regioisomers **2059** and **2060** in a good 69% yield.

11.10 Visible light enabled aza Paternò–Büchi reactions

M. R. Becker *et al.* developed a mild protocol to enable a smooth [2+2] cycloaddition between imine and alkene precursors to afford functionalized azetidines (Scheme 368).[455] The success of this transformation relied on the selective activation of the alkene, characterized by lower triplet energies, while avoiding excitation of the imine and subsequent competing reaction pathways. This aim was achieved by using [Ir(dF(CF$_3$)ppy)$_2$(dtbbpy)]PF$_6$ as the photocatalyst able to reach selectively the triplet state of the alkene, THF as the optimal solvent and a 40 W blue LEDs light. By applying these reaction conditions, a number of different oximes and hydrazones underwent the [2+2] cycloaddition in good to excellent yields. Notably, the observed diastereoselectivity of the azetidines **2062** was found to be independent from the *E*/*Z* ration of both oximes and hydrazones. The protocol was also applied to an isoxadifen-derived alkene to give **2063** in 87% yield and 4 : 1 d.r.

11.11 Generation of acyl radicals from 2-*S*-pyridyl thioesters

M. Ociepa *et al.* developed a visible light-driven cobalt-catalyzed method to generate acyl radicals from 2-*S*-pyridyl thioesters and

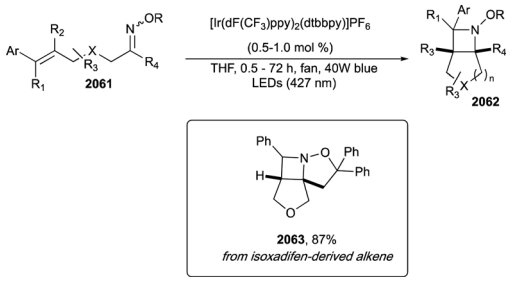

Scheme 368 Visible light enabled aza Paternò–Büchi reactions.

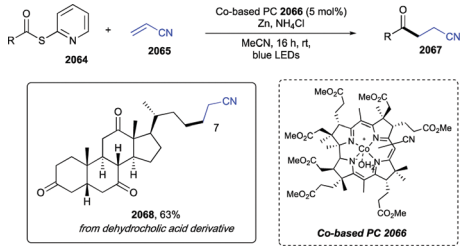

Scheme 369 Generation of acyl radicals from 2-*S*-pyridyl thioesters.

trap them with activated alkenes (Giese-type acylation, Scheme 369).[456] More in detail, the most efficient catalyst was found to be heptamethyl cobyrinate **2066**, a vitamin B$_{12}$ derivative, while Zn and NH$_4$Cl provided essential reductive conditions in MeCN and under blue LEDs irradiation at room temperature. Both alkene and thioester scopes were broad, tolerating functional groups such as ketones, cyano-, and esters. A dehydrocholic acid-derived thioester was converted under standard conditions into derivative **2068** in a good 63% yield (Scheme 369).

11.12 *ortho*-Alkylation of pyridine *N*-oxides

Pyridine *N*-oxides could afford *ortho*-alkylated pyridines by reacting with alkenes (*e.g.* **2070**, Scheme 370) under visible light photoredox catalytic conditions.[457] More in detail the reaction proceeded through the generation of cation radicals *via* SET oxidation of the alkene mediated by the excited state photocatalyst, followed by coupling with the pyridine *N*-oxide to afford a tethered radical intermediate, which underwent intra *ortho*-addition with a subsequent elimination of a carbonyl compound, thus promoting a tandem β-*N*–*O* and a β-*C*–*C* alkene cleavage. In order to achieve an efficient catalytic system 9-mesityl-10-phenylacridinium tetrafluoroborate (Mes-Acr$^+$ BF$_4^-$) and HBF$_4$ (42 wt% in H$_2$O) in CH$_2$Cl$_2$, together with blue LEDs irradiation were all indispensable. Besides diversely functionalized pyridine-*N*-oxides, other bi- and tri-cyclic *N*-oxides, such as quinolines, isoquinolines, phenanthridines, and 7,8-benzoquinolines smoothly underwent *ortho*-alkylation. Late-stage derivatization of a quinine *N*-oxide tetrafluoroboric acid complex **2069** afforded the *ortho*-benzylated adduct **2071** in 52% yield (Scheme 370).

11.13 *O*- and *N*-Nucleophiles alkylation

Recently, R. Zhu and coworkers developed a general protocol to accomplish a Markovnikov-selective intermolecular hydrofunctionalization of alkenes with different nucleophiles such as phenols, sulfonamides, and various *N*-heterocycles (Scheme 371).[458] The method exploited a dual Co/Ru catalysis, featuring a

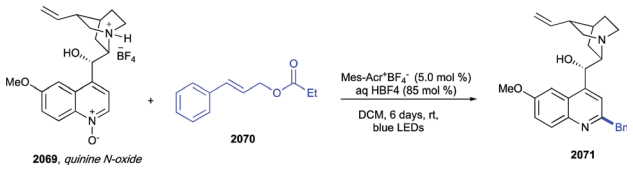

Scheme 370 *ortho*-Alkylation of pyridine *N*-oxides.

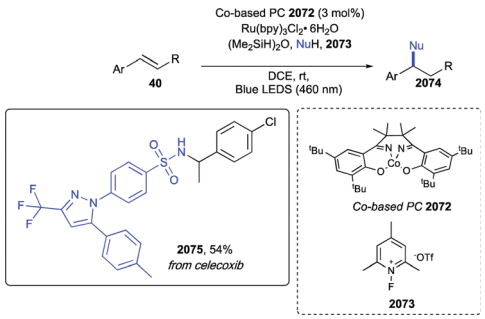

Scheme 371 *O*- and *N*-Nucleophiles alkylation.

photochemical oxidation of an organocobalt(III) intermediate derived from a HAT event. Experimentally, the reaction required the cobalt salen complex **2072**, $Ru(bpy)_3Cl_2{\cdot}6H_2O$ as a photocatalyst, $(Me_2SiH)_2O$ as hydrogen atom donor, and a hypervalent iodine reagent as the final oxidant in CH_2Cl_2 at room temperature under blue LEDs irradiation. Functionalization with the nitrogen nucleophiles required a switch from **2072** to *N*-fluorotrimethyl-pyridinium triflate **2073** as the stoichiometric oxidant to avoid the presence of a competing nucleophile. The scope included indazoles, imidazoles, carbazoles, pyrazole, and sulfonamides as exemplified in the derivatization of celecoxib (**2075**, Scheme 371).

11.14 Synthesis of carbonates, carbamates, and ureas

The group of B. König reported the photocatalytic *in situ* generation of fluorophosgene upon SET reduction and subsequent fragmentation of bench-stable and commercially available 4-(trifluoromethoxy)benzonitrile **2077** (Scheme 372).[459] This highly reactive intermediate could be intercepted by dinucleophilic species such as diamines, amino acids, and amino alcohols to afford carbonates, carbamates, and urea derivatives. The reaction was catalyzed by a phenoxazine based photosensitizer **2078** and DIPEA in MeCN at room temperature and under irradiation with a 400 nm light. The wide scope was also investigated with structurally complex bioactive compounds such as uridine, ribothymidine, the antiviral drug ribavirin, the β-blocker propranolol, and the sympathomimetic ephedrine, which afforded in good yields derivatives **2080–2083** (Scheme 372).

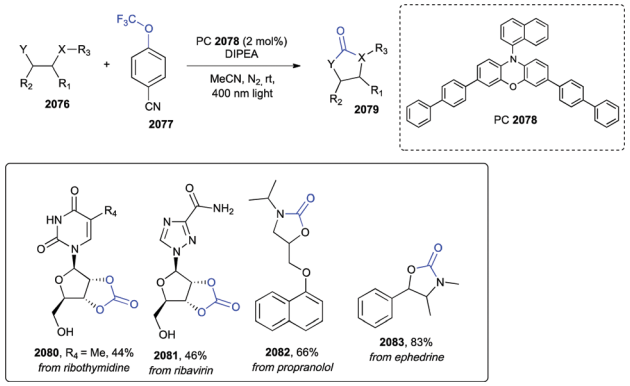

Scheme 372 Synthesis of carbonates, carbamates, and ureas.

11.15 Difunctionalization of carbonyls

Carbonyl compounds, upon conversion into *N*-sulfonylhydrazones, could be involved in a photoredox Wolff–Kishner reaction (Scheme 373).[460] The mechanistic design relied on a radical-carbanion relay sequence, where photogenerated radical intermediates, such as sulfur-centered radicals, added to the hydrazone, to trigger the release of a sulfonyl radical and molecular nitrogen, with the concomitant formation of a carboanion **2084C**. The latter could be intercepted by different electrophiles including CO_2 and aldehydes. Differently, the replacement of the S-radical with a $CF_3^{\bullet}$ led to *gem*-difluoroalkenes **479** *via* β-fluoride elimination from the α-CF_3 carbanion intermediates. The broad applicability of the reaction was demonstrated with more than 80 examples, including nabumetone, zingerone, and stanolone (**2085–2087**, Scheme 373).

11.16 Synthesis of 1,4-dienes from allylic carbonates

Allylic carbonates and vinyl triflates could undergo a stereodivergent reductive coupling to afford both *E*- and *Z*-1,4-dienes (**2090** and **2091**, Scheme 374) under visible-light-induced photoredox/nickel dual catalysis.

Interestingly, the stereoselectivity could be controlled *via* the triplet-state energy of the photoredox catalyst.[461] Thoroughly, the combination of $Ru(bpy)_3(PF_6)_2$ as the photoredox catalyst, $Ni(OAc)_2{\cdot}4H_2O$ as a nickel catalyst, 2,2′-bipyridine as a ligand, Hantzsch ester (HE) as a reductant, and 1,4-diazabicyclo-[2.2.2]octane (DABCO) as a base the 1,4-diene adducts were obtained with excellent *E*-selectivity. Conversely, the use of a photocatalyst of increased triplet energy such as $[Ir(ppy)_2(dtbbpy)]PF_6$ led to the almost exclusive formation of *Z*-1,4-dienes. The above cited conditions provided compatibility with many functional groups and promoted the metallaphotoredox cross coupling with good efficiencies and selectivities also in complex allylic carbonates

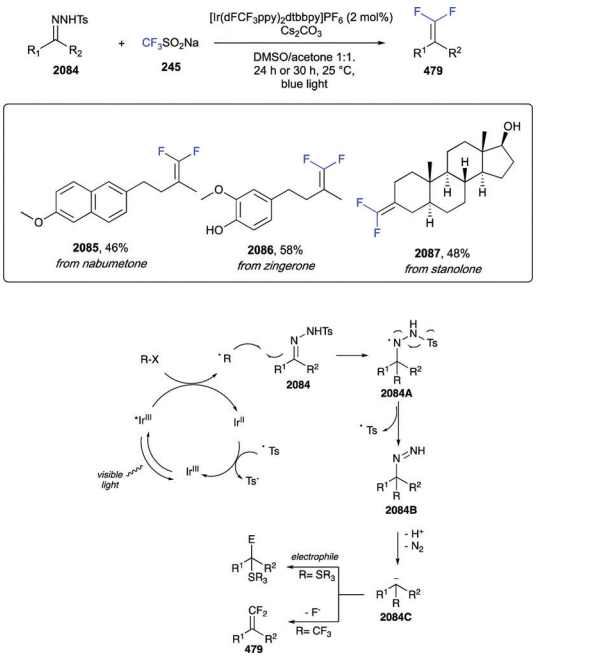

Scheme 373 Difunctionalization of carbonyls.

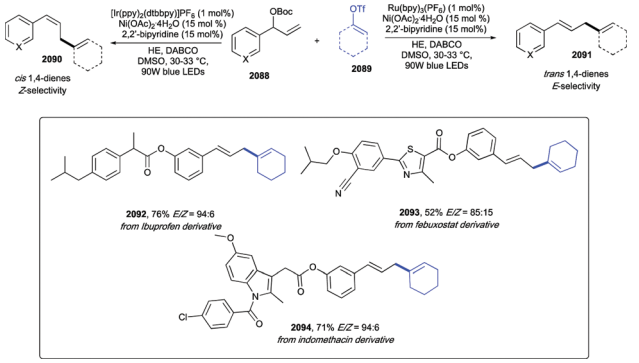

Scheme 374 Synthesis of 1,4-dienes from allylic carbonates.

derived from bioactive compounds such as ibuprofen, febuxostat, and indomethacin (**2092–2094**, Scheme 374).

11.17 Conversion of *O*-aryl carbamothioates to *S*-aryl carbamothioates

The conversion of *O*-arylcarbamothioates to *S*-aryl carbamothioates, known as the Newman–Kwart rearrangement, is one of the most used methods to synthesize thiophenols for the corresponding phenols.[462] Notwithstanding its synthetic utility, the highly thermal conditions required often manifested incompatibility with functional groups, leading to decomposition. D. A. Nicewicz and coworkers developed a photocatalytic mild protocol by using 2,4,6-tri(*p*-tolyl)pyrylium tetrafluoroborate as a commercially available organic single-electron photooxidant (Scheme 375). The reaction proceeded at room temperature under blue LEDs irradiation in MeCN. The substrate scope was broad, with exquisite functional group tolerance including aldehyde, double bonds, amides, carbamates, esters, to cite a few. Late-stage functionalization of sterically hindered (±)-α-tocopherol yielded compound **2097** in 99% yield (Scheme 375).

11.18 Thiolation of (multi)halogenated heteroarenes

F. Glorius and coworkers recently developed a general and simple strategy for the site-selective thiolation of electron-rich heteroarenes with thiols (Scheme 376).[463]

By using $[Ir(dF(CF_3)ppy)_2(dtbbpy)]PF_6$ as the photoredox catalyst in DMA under 30 W blue LEDs irradiation at room temperature for 16 hours a C–S coupling at the most electron-rich position of (multi)-halogenated substrates occurred. Mechanistic studies suggested the involvement of a radical chain pathway, with a homolytic aromatic substitution of the heteroaryl halide by an

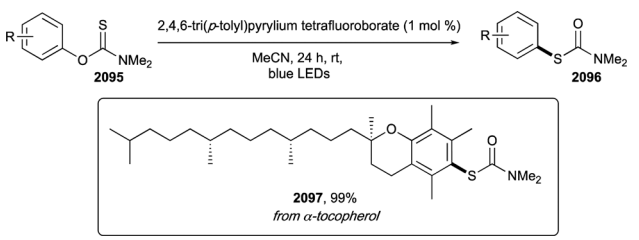

Scheme 375 Conversion of *O*-aryl carbamothioates to *S*-aryl carbamothioates.

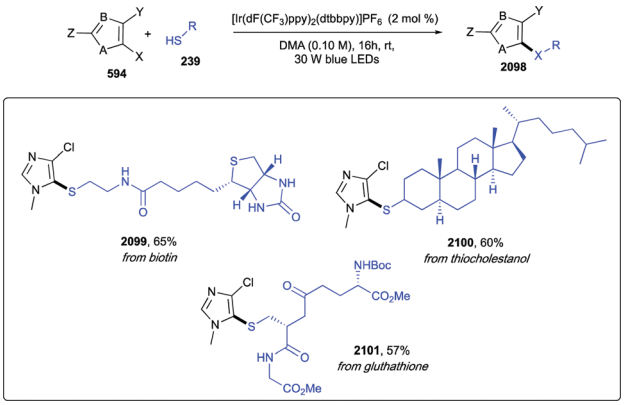

Scheme 376 Thiolation of (multi)halogenated heteroarenes.

electrophilic thiyl radical. The broad substrate scope embodied biotin, thiocholestanol, and glutathione (**2099–2101**, Scheme 376).

11.19 Desulfurilative site-specific deuteration of thiols

The Z. Sun lab recently reported a mild and efficient protocol to achieve deuterated compounds starting from readily available thiols (**239**, Scheme 377).[464] The metal-free method enabled deuterium incorporation by using D_2O as a deuterium source, DTBP (di-*tert*-butyl peroxide) and a phosphoric reagent such as Ph_2POEt in CH_2Cl_2 as a solvent under irradiation with a 36 W household CFL bulb on the two sides of the reaction flask. Remarkably, suitable starting thiols amino acids like cysteine and homocysteine as well as thiols containing a wide range of functional groups such as ketone, alkene, hydroxy, free amino, and sodium sulfonate, to cite a few. Peptides containing up to 16 amino acids units were converted into deuterated analogues in yields major than 95%, while drugs such as captopril, mesna, 3-azetidinthiol, and thiocholesterol were selected as representative bioactive scaffolds and efficiently deuterated (**2102–2105**, 75–97% yield, 90–96% D-incorporation, Scheme 377).

11.20 Formation of sulfur-containing spirocycles

The propensity of thiols to generate thiyl radicals under visible light photocatalytic conditions was recently exploited by

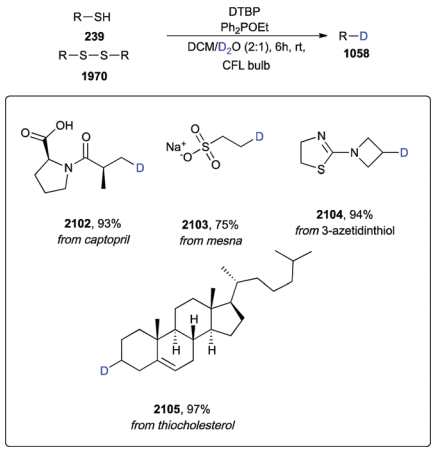

Scheme 377 Desulfurilative site-specific deuteration of thiols.

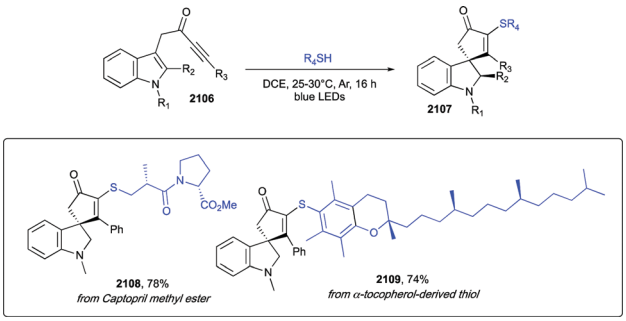

Scheme 378 Formation of sulfur-containing spirocycles.

H. E. Ho *et al.* to synthesize sulfur-containing spirocycles (**2107**) from indole-tethered ynones (**2106**, ITYs, Scheme 378).[465] Thoroughly, ITYs **2106** formed an intramolecular electron donor–acceptor complex undergoing photoinduced charge transfer to promote the formation of an *S*-centered radical. The latter triggered a radical chain sequence leading to dearomative spirocyclization with concomitant formation of a C–S bond. Awfully, this mechanistic pathway avoided the need for photocatalysts and/or transition metal catalysts, thus providing an extraordinarily mild protocol as witnessed by the broad scope of both ynones and thiols. As an extra evidence of the wide generality of the method, captopril methyl ester and an α-tocopherol-derived thiol were converted into derivatives **2108** and **2109** in 78% and 74% yields, respectively (Scheme 378).

11.21 Deoxygenation of sulfoxides

Photocatalytic deoxygenation of sulfoxides could be carried out by using either $[Ir(dF(CF_3)ppy)_2(dtbbpy)]PF_6$ or *fac*-$Ir(ppy)_3$ in the presence of triphenylphosphine in CH_2Cl_2 under irradiation with 60 W blue LEDs at room temperature (Scheme 379).[466]

The reaction pathway operated through a radical chain mechanism proceeding *via* a phosphoranyl radical generated from a radical/polar crossover process. Under the developed standard conditions, a wide range of aromatic and aliphatic functionalized sulfoxides was reduced to their corresponding sulfides in high to excellent yields and with exquisite functional group tolerance. Structurally complex biologically active sulfoxides such as fensulfothion and sulmazole were reduced in >99% and 67% yields, respectively (**2112** and **2113**, Scheme 379).

11.22 Synthesis of unsymmetrical ureas

Unsymmetrical ureas could be synthesized *via* an oxidative desulphurisation from isothiocyanates (**2114**) and amines

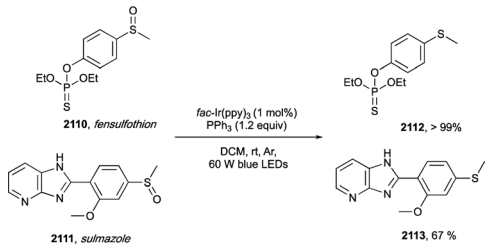

Scheme 379 Deoxygenation of sulfoxides.

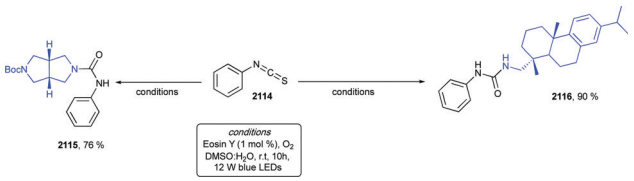

Scheme 380 Synthesis of unsymmetrical ureas.

without the addition of strong oxidants (Scheme 380).[467] Awfully, this transformation was accomplished by employing eosin Y as an organic photosensitizer in a $DMSO/H_2O$ solvent mixture under aerobic conditions and irradiation with a 12 W blue LED. The broad substrate scope was illustrated with the synthesis of more than 30 asymmetric ureas in high to excellent yields, bearing both aryl- and alkyl-substituents. Late-stage modification of antibacterial dehydroabietylamine (or leelamine) **2115** and **2116** was shown in Scheme 380.

11.23 Hydrodefluorination of trifluoromethylarenes

Recently, the group of V. Governeur disclosed a photoredox protocol for replacing a single fluorine atom with hydrogen in electron-poor trifluoromethylarenes (Scheme 381).[468]

The method required 2,4,5,6-tetrakis(diphenylamino)-isophthalonitrile (4-DPA-IPN) as an organic photocatalyst, a combination of 2,2,6,6-tetramethylpiperidine (TMP) and 1,2,2,6,6-pentamethylpiperidine (PMP), and 4-hydroxythiophenol (4-HTP) as hydrogen atom donor in DCE at room temperature for 12 hours under blue LEDs irradiation. The scope of the hydrodefluorination was investigated with a range of functionalized trifluoroarenes, including structurally complex pharmaceuticals such as bicalutamide and enzalutamide (used to treat prostate cancer), BAY 59-3074, a cannabinoid receptor agonist, the androgen receptor modulator enobosarm, and bendroflumethiazide used in mild heart failure. Medium to excellent chemoselectivities were observed (**2117–2121**, Scheme 381).

11.24 Late-stage functionalization of amino acids and peptides

A number of visible-light photoredox protocols to achieve late-stage functionalization of amino acids and peptides have been reported.[469,470] For example, S. P. Morcilli *et al.* reported a remote functionalization of amides and amines by exploiting electrophilic nitrogen radical reactivity.[471] Their protocol enabled the

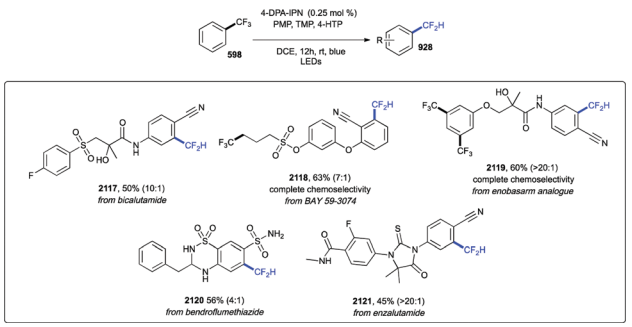

Scheme 381 Hydrodefluorination of trifluoromethylarenes.

introduction of fluorine and alkyne functional groups into L-isoleucine, L-lysine, and a glycine-L-leucine dipeptide. Other reports included but are not limited to the following transformations. C-terminus peptides could undergo a decarboxylative alkynylation with visible-light organic dye photocatalysts and hypervalent iodine reagents.[472] Functionalization of natural, unnatural α,β-dehydroamino acids and dipeptides with (fluorinated)alkyl halides, arylsulfonyl chlorides or *N*-(acyloxy)phthalimides (NHPI esters).[473] Site-selective C–H ^{18}F-fluorination of unprotected peptides for PET imaging has also be easily achieved.[474] Reductive amination by photoredox catalysis and polarity-matched HAT by using a ruthenium photocatalyst and ascorbic acid as the reducing agent was reported for L-tryptophan on a gram scale; notably this protocol was also applied for temporally and spatially controlled reactions on a solid support.[475] C. Wang *et al.* reported a visible-light induced copper-catalyzed decarboxylative alkylation of glycine and peptides to provide α-alkylated unnatural amino acids, along with late-stage α-alkylation of protected peptides.[476] A mild and general protocol to carry out a decarboxylative α-vinylation of *N*-Boc α-amino acids was reported by A. Noble and D. W. C. MacMillan.[477] Interestingly, the group of Y. Landais showed that α-amino acid-derived oxamic acids could generate carbamoyl radicals, which added to heteroarenes under metal-free photoredox catalytic conditions, to afford the corresponding amides without racemization.[478] Connection between serine/threonine and carbohydrates/amino acids could be built up *via* photoinduced decarboxylative radical reactions of serinyl and threoninyl acetic acids to electron deficient alkenes such as protected carbohydrate acrylates and acrylamides.[479] Decarboxylative cross-coupling of *N*-Boc protected proline and *N*-Me–*N*-Boc leucine to achieve vinylation products from diverse vinyl iodides and bromides was reported by A. Noble *et al.* by merging photoredox and nickel catalysis.[480] Indole-containing substrates such as tryptophan and related tryptamines could be cyclized into β-carboline and pyrroloindoline derivatives, respectively, under visible-light photocatalytic conditions as reported by N. Chalotra *et al.*[481] and by K. Liang *et al.*[482] More applications of photoredox catalytic conditions to modify peptidic scaffolds included the protocols by A. Dowine and G. Roelfes[483] exploiting the presence of dehydrated amino acids in natural antimicrobial peptides such as thiostrepton and nisin; the intramolecular thiol–yne hydrothiolation to afford stapled unprotected helical peptides described by Y. Tian *et al.*;[484] and the radical trifluoromethylation of fully unprotected peptides with up to 51 amino acids by S. W. Krska and coworkers.[485] Worthy of note is the photoredox catalytic protocol developed by H. Fu and coworkers to achieve chiral α-selenoamino acids.[486] Recently, the group of Z. Xu reported a visible light promoted deaminative C(sp^3)–H alkylation of glycine and peptides using Katritzsky salts as electrophiles to prepare unnatural α-amino acids and modification of peptides.[487] A pioneering report by D. W. C. MacMillan, A. G. Doyle, and coworkers merged photoredox and nickel catalysis to achieve decarboxylative sp^3-sp^2 cross coupling of α-amino acids with aryl and olefinic (sp^2) carbons providing a library of racemic benzylic amines in good to excellent yields.[488] Synthesis of enantioenriched α-deuterated α-amino acids under organophotoredox catalytic conditions and using D_2O as deuterium source was recently disclosed by W. Wang and coworkers.[489] Thiol-containing amino acids such as *N*-Boc-Cys-OMe and the tripeptide glutathione were shown to be competent thiol-partner in a radical cascade process with *ortho*-substituted arylisocyanides to access 2-sulfenylindoles.[490]

11.25 Photocatalytically cleavable protecting groups

E. Speckmeier and K. Zeitler reported a visible light photocatalytic strategy for the deprotection of classical phenacyl (Pac) and desyl (Dys) carboxylic acid esters (Scheme 382).[491] The cleavage was promoted by $[Ru(bpy)_3](PF_6)_2$ in combination with ascorbic acid as a reductive quencher, K_3PO_4 in a 4 : 1 mixture of MeCN/H_2O under blue LEDs irradiation. Both Pac and Dys could be easily introduced from commercially available reagents, and the possibility to remove them photocatalytically offered a valuable approach orthogonal to many other common protecting groups. The protocol showed high functional group tolerance and was also adapted to the requirements of the solid-phase synthesis.

Useful and general protocols for photoredox removal of *p*-methoxybenzyl ether and N-PMB-amide deprotection were reported by Z. Liu from Nanjing University, China, and N. Iqbal from Hanyang University, Republic of Korea.[492,493] Photoinduced S–N bond cleavage of tosyl-protecting group was reported by under continuous-flow conditions, where a better surface-to-volume ratio enabled an enhancement of the light source and a shortening of the reaction times.[494] *N*-methylpyridinium iodide esters were reported as photo-releasable groups to afford free carboxylic acids; the reaction proceeded *via* charge-transfer excitation and did not require additional photocatalyst.[495]

11.26 Late-stage modification of nucleosides and DEL platforms

A number of visible-light photoredox protocols to achieve late-stage functionalization of nucleosides is also available in literature. Representative examples include the stereoselective synthesis of aryl and heteroaryl *C*-nucleosides, promoted by a dual photoredox/nickel catalytic system reported by Y. Ma *et al.*;[496] A. Rentmeister and coworkers reported that aryl ketones such as benzophenone and α-hydroxyalkyl ketones were photolabile caging groups if installed at the N7 position of guanosine or the N1 position of adenosine thus enabling selective modification of such nucleobases.[497] A radical strategy for the fluorination of alkyl bromides exploiting the merging of halogen-atom abstraction and benzophenone photosensitization was reported for the late-stage modification of uridine.[498] The combination of *N*-alkoxypyridinium salts and phosphites under very mild photoredox catalytic conditions was reported to afford phosphate esters in good to high yields, and such a protocol was applied to the

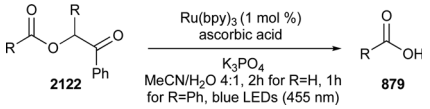

Scheme 382 Hydrodefluorination of trifluoromethylarenes.

synthesis of 5′-phosphate uridine in a good 78% yield.[499] DNA-encoded library (DEL) technology has been emerging as a novel approach to ligand discovery. Hence, mild and chemoselective protocols to increase chemical diversity and enabling the exploration of a wider chemical space are of utmost interest. In the realm of photocatalytic mediated transformations, the possibility to introduce C(sp^3)-hybridized centers without requiring amines protecting groups has been recently explored by G. A. Molander and coworkers.[500] D. K. Kölmel *et al.*, on the other hand, reported the formation of [2+2] cycloaddition product from DNA-tagged styrene and a wide variety of structurally diverse cinnamates.[501]

12. Conclusions

The emergence of visible light photocatalysis, besides injecting new life into the realm of radical chemistry, has further strengthened the long-standing intimate connection between synthetic organic chemistry advancements and medicinal chemistry progresses. The collection of photosynthetic approaches here reported calls attention to the importance of including examples of bioactive complex scaffolds, during the evaluation of the scope of new synthetic protocols, in an ever-increasing number of articles. Major future perspectives undoubtedly include the increase of site-selectivity along with its predictability, the investment of resources to identify effective and general protocols circumventing the use of precious metal complexes, and the implementation of flow techniques, which, by providing high illuminated surface-to-volume ratios, holds promise for the inclusion of photochemical processes in industrial settings. Likewise, the merging of photo- and micellar catalysis, albeit poorly investigated so far, could land new efficient green methodologies associated with optimum mass-based metrics (*e.g.* E factor and PMI) thanks for example to the possibility of recycling aqueous solutions of the photocatalyst while extracting the products with organic immiscible solvents.[502,503] Up-and-coming alliances come from photochemistry and electrochemistry as well as biocatalysis giving birth to research areas such as synthetic photoelectrochemistry and photobiocatalysis.[504,505] Light-driven synthetic applications keep becoming more and more exciting and we are confident that the late-stage functionalization of pharmaceuticals will mirror such a glowing future.

Conflicts of interest

There are no conflicts to declare.

Notes and references

1 C. R. McConnell and S. Y. Liu, *Chem. Soc. Rev.*, 2019, **48**, 3436–3453.
2 T. Cernak, K. D. Dykstra, S. Tyagarajan, P. Vachal and S. W. Krska, *Chem. Soc. Rev.*, 2016, **45**, 546–576.
3 M. Moir, J. J. Danon, T. A. Reekie and M. Kassiou, *Expert Opin. Drug Discovery*, 2019, **14**, 1137–1149.
4 M. C. White and J. Zhao, *J. Am. Chem. Soc.*, 2018, **140**(43), 13988–14009.
5 S. Govaerts, A. Nyuchev and T. Noel, *J. Flow Chem.*, 2020, **10**, 13–71.
6 H. Schönherr and T. Cernak, *Angew. Chem., Int. Ed.*, 2013, **52**, 12256–12267.
7 Y. Fujiwara, J. A. Dixon, F. O'hara, E. D. Funder, D. D. Dixon, R. A. Rodriguez, R. D. Baxter, B. Herlé, N. Sach, M. R. Collins, Y. Ishihara and P. S. Baran, *Nature*, 2012, **492**, 95–99.
8 Z. Liu, J. Li, S. Li, G. Li, K. B. Sharpless and P. Wu, *J. Am. Chem. Soc.*, 2018, **140**, 2919–2925.
9 C. Stephenson, T. Yoon and D. W. C. MacMillan, *Visible Light Photocatalysis in Organic Chemistry*, Wiley-VCH Verlag GmbH & Co. KGaA, Weinheim, Germany, 2018.
10 M. Yan, J. C. Lo, J. T. Edwards and P. S. Baran, *J. Am. Chem. Soc.*, 2016, **138**, 12692–12714.
11 F. Dénès, *Chimia*, 2020, **74**, 23–32.
12 R. Ciriminna, R. Delisi, Y. J. Xu and M. Pagliaro, *Org. Process Res. Dev.*, 2016, **20**, 403–408.
13 J. J. Douglas, M. J. Sevrin and C. R. J. Stephenson, *Org. Process Res. Dev.*, 2016, **20**, 1134–1147.
14 M. A. Miranda and M. L. Marin, *Curr. Opin. Green Sustainable Chem.*, 2017, **6**, 139–149.
15 D. Petzold, M. Giedyk, A. Chatterjee and B. König, *Eur. J. Org. Chem.*, 2020, 1193–1244.
16 T. P. Yoon, M. A. Ischay and J. Du, *Nat. Chem.*, 2010, **2**, 527–532.
17 D. Ravelli, S. Protti, M. Fagnoni and A. Albini, *Curr. Org. Chem.*, 2013, **17**, 2366–2373.
18 G. E. M. Crisenza and P. Melchiorre, *Nat. Commun.*, 2020, **11**, 803.
19 D. A. DiRocco and D. M. Schultz, in *Photocatalysis in Organic Synthesis*, ed. König, Georg Thieme Verlag, Stuttgart, 2019th edn, 2019, vol. 6, pp. 611–635.
20 L. Marzo, S. K. Pagire, O. Reiser and B. König, *Angew. Chem., Int. Ed.*, 2018, **57**, 10034–10072.
21 C. Wang and Z. Lu, *Org. Chem. Front.*, 2015, **2**, 179–190.
22 X. Lang, X. Chen and J. Zhao, *Chem. Soc. Rev.*, 2014, **43**, 473–486.
23 T. P. Yoon, *ACS Catal.*, 2013, **3**, 895–902.
24 D. M. Schultz and T. P. Yoon, *Science*, 2014, 343.
25 C. S. Wang, P. H. Dixneuf and J. F. Soulé, *Chem. Rev.*, 2018, **118**, 7532–7585.
26 J. Twilton, C. C. Le, P. Zhang, M. H. Shaw, R. W. Evans and D. W. C. MacMillan, *Nat. Rev. Chem.*, 2017, **1**, 1–19.
27 C. B. Larsen and O. S. Wenger, *Chem. – Eur. J.*, 2018, **24**, 2039–2058.
28 J. Xie, H. Jin and A. S. K. Hashmi, *Chem. Soc. Rev.*, 2017, **46**, 5193–5203.
29 D. M. Arias-Rotondo and J. K. McCusker, *Chem. Soc. Rev.*, 2016, **45**, 5803–5820.
30 D. Staveness, I. Bosque and C. R. J. Stephenson, *Acc. Chem. Res.*, 2016, **49**, 2295–2306.
31 T. P. Yoon, *Acc. Chem. Res.*, 2016, **49**, 2307–2315.
32 M. H. Shaw, J. Twilton and D. W. C. MacMillan, *J. Org. Chem.*, 2016, **81**, 6898–6926.
33 N. A. Romero and D. A. Nicewicz, *Chem. Rev.*, 2016, **116**, 10075–10166.

34 X. Lang, J. Zhao and X. Chen, *Chem. Soc. Rev.*, 2016, **45**, 3026–3038.
35 D. A. Nicewicz and T. M. Nguyen, *ACS Catal.*, 2014, **4**, 355–360.
36 C. K. Prier, D. A. Rankic and D. W. C. MacMillan, *Chem. Rev.*, 2013, **113**, 5322–5363.
37 J. M. R. Narayanam and C. R. J. Stephenson, *Chem. Soc. Rev.*, 2011, **40**, 102–113.
38 B. Giese and W. Zwick, *Angew. Chem., Int. Ed. Engl.*, 1978, **17**, 66–67.
39 C. Walling and E. S. Huyser, *Organic Reactions*, John Wiley & Sons, Inc., Hoboken, NJ, USA, 2011, pp. 91–149.
40 B. Giese, *Angew. Chem., Int. Ed. Engl.*, 1983, **22**, 753–764.
41 T. Koike, *Asian J. Org. Chem.*, 2020, **9**, 529–537.
42 F. Lima, U. K. Sharma, L. Grunenberg, D. Saha, S. Johannsen, J. Sedelmeier, E. V. Van der Eycken and S. V. Ley, *Angew. Chem., Int. Ed.*, 2017, **56**, 15136–15140.
43 X. L. Lv, C. Wang, Q. L. Wang and W. Shu, *Org. Lett.*, 2019, **21**, 56–59.
44 M. W. Campbell, J. S. Compton, C. B. Kelly and G. A. Molander, *J. Am. Chem. Soc.*, 2019, **141**, 20069–20078.
45 J. Liu, S. Wu, J. Yu, C. Lu, Z. Wu, X. Wu, X. Xue and C. Zhu, *Angew. Chem., Int. Ed.*, 2020, **59**, 8195–8202.
46 F. Wu, L. Wang, J. Chen, D. A. Nicewicz and Y. Huang, *Angew. Chem., Int. Ed.*, 2018, **57**, 2174–2178.
47 X. Yu, Q. Zhao, J. Chen, J. Chen and W. Xiao, *Angew. Chem., Int. Ed.*, 2018, **57**, 15505–15509.
48 J. Ma, J. Lin, L. Zhao, K. Harms, M. Marsch, X. Xie and E. Meggers, *Angew. Chem., Int. Ed.*, 2018, **57**, 11193–11197.
49 T. Miura, Y. Funakoshi, J. Nakahashi, D. Moriyama and M. Murakami, *Angew. Chem., Int. Ed.*, 2018, **57**, 15455–15459.
50 C. F. Meyer, S. M. Hell, A. Misale, A. A. Trabanco and V. Gouverneur, *Angew. Chem., Int. Ed.*, 2019, **58**, 8829–8833.
51 Q. Y. Lin, X. H. Xu, K. Zhang and F. L. Qing, *Angew. Chem., Int. Ed.*, 2016, **55**, 1479–1483.
52 S. P. Pitre, C. D. McTiernan, H. Ismaili and J. C. Scaiano, *ACS Catal.*, 2014, **4**, 2530–2535.
53 N. J. W. Straathof, S. E. Cramer, V. Hessel and T. Noël, *Angew. Chem., Int. Ed.*, 2016, **55**, 15549–15553.
54 W. Yu, X. H. Xu and F. L. Qing, *Org. Lett.*, 2016, **18**, 5130–5133.
55 W. Jin, M. Wu, Z. Xiong and G. Zhu, *Chem. Commun.*, 2018, **54**, 7924–7927.
56 B. Q. He, X. Y. Yu, P. Z. Wang, J. R. Chen and W. J. Xiao, *Chem. Commun.*, 2018, **54**, 12262–12265.
57 S. Zhou, D. Zhang, Y. Sun, R. Li, W. Zhang and A. Li, *Adv. Synth. Catal.*, 2014, **356**, 2867–2872.
58 E. Arceo, E. Montroni and P. Melchiorre, *Angew. Chem., Int. Ed.*, 2014, **53**, 12064–12068.
59 S. H. Oh, Y. R. Malpani, N. Ha, Y. S. Jung and S. B. Han, *Org. Lett.*, 2014, **16**, 1310–1313.
60 Q. Y. Lin, Y. Ran, X. H. Xu and F. L. Qing, *Org. Lett.*, 2016, **18**, 2419–2422.
61 H. Huang, C. Yu, Y. Zhang, Y. Zhang, P. S. Mariano and W. Wang, *J. Am. Chem. Soc.*, 2017, **139**, 9799–9802.
62 E. Voutyritsa and C. G. Kokotos, *Angew. Chem., Int. Ed.*, 2020, **59**, 1735–1741.
63 H. Jiang and A. Studer, *Chem. – Eur. J.*, 2019, **25**, 7105–7109.
64 Q. Qin, Y. Y. Han, Y. Y. Jiao, Y. He and S. Yu, *Org. Lett.*, 2017, **19**, 2909–2912.
65 S. M. Hell, C. F. Meyer, G. Laudadio, A. Misale, M. C. Willis, T. Noël, A. A. Trabanco and V. Gouverneur, *J. Am. Chem. Soc.*, 2020, **142**, 720–725.
66 Q. Zhu, D. E. Graff and R. R. Knowles, *J. Am. Chem. Soc.*, 2018, **140**, 741–747.
67 C. B. Roos, J. Demaerel, D. E. Graff and R. R. Knowles, *J. Am. Chem. Soc.*, 2020, **142**, 5974–5979.
68 Q. Zhao, J. Chen, X. Zhou, X. Yu, J. Chen and W. Xiao, *Chem. – Eur. J.*, 2019, **25**, 8024–8029.
69 B. Lipp, L. M. Kammer, M. Kücükdisli, A. Luque, J. Kühlborn, S. Pusch, G. Matulevičiūtė, D. Schollmeyer, A. Šačkus and T. Opatz, *Chem. – Eur. J.*, 2019, **25**, 8965–8969.
70 Y. D. Du, C. Y. Zhou, W. P. To, H. X. Wang and C. M. Che, *Chem. Sci.*, 2020, **11**, 4680–4686.
71 G. Dagousset, A. Carboni, E. Magnier and G. Masson, *Org. Lett.*, 2014, **16**, 4340–4343.
72 X. Geng, F. Lin, X. Wang and N. Jiao, *Org. Lett.*, 2017, **19**, 4738–4741.
73 B. Yang and Z. Lu, *ACS Catal.*, 2017, **7**, 8362–8365.
74 J. Chen, S. Zhu, J. Qin and L. Chu, *Chem. Commun.*, 2019, **55**, 2336–2339.
75 Q. Y. Meng, S. Wang, G. S. Huff and B. Konig, *J. Am. Chem. Soc.*, 2018, **140**, 3198–3201.
76 J. Hou, A. Ee, H. Cao, H.-W. Ong, J.-H. Xu and J. Wu, *Angew. Chem., Int. Ed.*, 2018, **57**, 17220–17224.
77 M. Zhang, J. Xie and C. Zhu, *Nat. Commun.*, 2018, **9**, 3517.
78 A. Barthelemy, B. Tuccio, E. Magnier and G. Dagousset, *Angew. Chem., Int. Ed.*, 2018, **57**, 13790–13794.
79 A. L. Barthelemy, B. Tuccio, E. Magnier and G. Dagousset, *Synlett*, 2019, 1489–1495.
80 B. Yang and Z. Lu, *Chem. Commun.*, 2017, **53**, 12634–12637.
81 Z.-Y. Ma, L.-N. Guo, Y.-R. Gu, L. Chen and X.-H. Duan, *Adv. Synth. Catal.*, 2018, **360**, 4341–4347.
82 N. Noto, T. Koike and M. Akita, *ACS Catal.*, 2019, **9**, 4382–4387.
83 W. Zhang, Z. Zou, Y. Wang, Y. Wang, Y. Liang, Z. Wu, Y. Zheng and Y. Pan, *Angew. Chem., Int. Ed.*, 2019, **58**, 624–627.
84 Y. Yasu, T. Koike and M. Akita, *Org. Lett.*, 2013, **15**, 2136–2139.
85 T. Koike and M. Akita, *Acc. Chem. Res.*, 2016, **49**, 1937–1945.
86 O. O. Fadeyi, J. J. Mousseau, Y. Feng, C. Allais, P. Nuhant, M. Z. Chen, B. Pierce and R. Robinson, *Org. Lett.*, 2015, **17**, 5756–5759.
87 W. Kong, H. An and Q. Song, *Chem. Commun.*, 2017, **53**, 8968–8971.
88 J. He, C. Chen, G. C. Fu and J. C. Peters, *ACS Catal.*, 2018, **8**, 11741–11748.
89 W. Huang, J. Chen, D. Hong, W. Chen, X. Cheng, Y. Tian and G. Li, *J. Org. Chem.*, 2018, **83**, 578–587.
90 M. Zhang, J. Lin and J. Xiao, *Angew. Chem., Int. Ed.*, 2019, **58**, 6079–6083.
91 Q. Guo, M. Wang, Q. Peng, Y. Huo, Q. Liu, R. Wang and Z. Xu, *ACS Catal.*, 2019, **9**, 4470–4476.
92 J. Chen, W. Huang, Y. Li and X. Cheng, *Adv. Synth. Catal.*, 2018, **360**, 1466–1472.

93 J. Yu, Z. Wu and C. Zhu, *Angew. Chem., Int. Ed.*, 2018, **57**, 17156–17160.
94 G. R. Mathi, Y. Jeong, Y. Moon and S. Hong, *Angew. Chem., Int. Ed.*, 2020, **59**, 2049–2054.
95 J. Jeon, Y. He, S. Shin and S. Hong, *Angew. Chem., Int. Ed.*, 2020, **59**, 281–285.
96 Y. T. He, D. Kang, I. Kim and S. Hong, *Green Chem.*, 2018, **20**, 5209–5214.
97 D. Chen, L. Xu, T. Long, S. Zhu, J. Yang and L. Chu, *Chem. Sci.*, 2018, **9**, 9012–9017.
98 Y. Moon, B. Park, I. Kim, G. Kang, S. Shin, D. Kang, M. H. Baik and S. Hong, *Nat. Commun.*, 2019, **10**, 4117.
99 A. Arora, K. A. Teegardin and J. D. Weaver, *Org. Lett.*, 2015, **17**, 3722–3725.
100 Y. H. Li, C. H. Wang, S. Q. Gao, F. M. Qi and S. D. Yang, *Chem. Commun.*, 2019, **55**, 11888–11891.
101 B. Zhao, Z. Li, Y. Wu, Y. Wang, J. Qian, Y. Yuan and Z. Shi, *Angew. Chem., Int. Ed.*, 2019, **58**, 9448–9452.
102 W. Zhang, Z. Zou, W. Zhao, S. Lu, Z. Wu, M. Huang, X. Wang, Y. Wang, Y. Liang, Y. Zhu, Y. Zheng and Y. Pan, *Nat. Commun.*, 2020, **11**, 2572.
103 L. M. Kammer, M. Krumb, B. Spitzbarth, B. Lipp, J. Kühlborn, J. Busold, O. M. Mulina, A. O. Terentev and T. Opatz, *Org. Lett.*, 2020, **22**, 3318–3322.
104 J. P. Phelan, S. B. Lang, J. S. Compton, C. B. Kelly, R. Dykstra, O. Gutierrez and G. A. Molander, *J. Am. Chem. Soc.*, 2018, **140**, 8037–8047.
105 T. Guo, L. Zhang, X. Liu, Y. Fang, X. Jin, Y. Yang, Y. Li, B. Chen and M. Ouyang, *Adv. Synth. Catal.*, 2018, **360**, 4459–4463.
106 A. G. Herraiz and M. G. Suero, *Chem. Sci.*, 2019, **10**, 9374–9379.
107 X. Huang, T. R. Quinn, K. Harms, R. D. Webster, L. Zhang, O. Wiest and E. Meggers, *J. Am. Chem. Soc.*, 2017, **139**, 9120–9123.
108 M. Claros, F. Ungeheuer, F. Franco, V. Martin-Diaconescu, A. Casitas and J. Lloret-Fillol, *Angew. Chem., Int. Ed.*, 2019, **58**, 4869–4874.
109 X. Huang, J. Lin, T. Shen, K. Harms, M. Marchini, P. Ceroni and E. Meggers, *Angew. Chem., Int. Ed.*, 2018, **57**, 5454–5458.
110 D. F. Chen, C. H. Chrisman and G. M. Miyake, *ACS Catal.*, 2020, **10**, 2609–2614.
111 Q. Q. Zhao, X. S. Zhou, S. H. Xu, Y. L. Wu, W. J. Xiao and J. R. Chen, *Org. Lett.*, 2020, **22**, 2470–2475.
112 Y. Kim, K. Lee, G. R. Mathi, I. Kim and S. Hong, *Green Chem.*, 2019, **21**, 2082–2087.
113 S. T. Nguyen, Q. Zhu and R. R. Knowles, *ACS Catal.*, 2019, **9**, 4502–4507.
114 D. C. Miller, G. J. Choi, H. S. Orbe and R. R. Knowles, *J. Am. Chem. Soc.*, 2015, **137**, 13492–13495.
115 L. Q. Nguyen and R. R. Knowles, *ACS Catal.*, 2016, **6**, 2894–2903.
116 J. Davies, N. S. Sheikh and D. Leonori, *Angew. Chem., Int. Ed.*, 2017, **56**, 13361–13365.
117 J. Cheng, Y. Cheng, J. Xie and C. Zhu, *Org. Lett.*, 2017, **19**, 6452–6455.
118 M.-Q. Zhang, T.-X. Wang, R. Li, Z.-L. Huang, W.-J. Han, X.-C. Dai and Y.-Q. Wang, *J. Sleep Res.*, 2017, **26**, 386–393.
119 D. Kurandina, M. Parasram and V. Gevorgyan, *Angew. Chem., Int. Ed.*, 2017, **56**, 14212–14216.
120 G. Z. Wang, R. Shang, W. M. Cheng and Y. Fu, *J. Am. Chem. Soc.*, 2017, **139**, 18307–18312.
121 D. P. Tiwari, S. Dabral, J. Wen, J. Wiesenthal, S. Terhorst and C. Bolm, *Org. Lett.*, 2017, **19**, 4295–4298.
122 S. M. Thullen and T. Rovis, *J. Am. Chem. Soc.*, 2017, **139**, 15504–15508.
123 J. L. Schwarz, H. M. Huang, T. O. Paulisch and F. Glorius, *ACS Catal.*, 2020, **10**, 1621–1627.
124 Z. Lei, A. Banerjee, E. Kusevska, E. Rizzo, P. Liu and M. Ngai, *Angew. Chem., Int. Ed.*, 2019, **58**, 7318–7323.
125 K. Wu, L. Wang, S. Colón-Rodríguez, G. U. Flechsig and T. Wang, *Angew. Chem., Int. Ed.*, 2019, **58**, 1774–1778.
126 W. Yu, Y. Luo, L. Yan, D. Liu, Z. Wang and P. Xu, *Angew. Chem., Int. Ed.*, 2019, **58**, 10941–10945.
127 S. Zhu, J. Qin, F. Wang, H. Li and L. Chu, *Nat. Commun.*, 2019, **10**, 749.
128 M. Ratushnyy, M. Kamenova and V. Gevorgyan, *Chem. Sci.*, 2018, **9**, 7193–7197.
129 P. Rai, K. Maji and B. Maji, *Org. Lett.*, 2019, **21**, 3755–3759.
130 S. B. Lang, R. J. Wiles, C. B. Kelly and G. A. Molander, *Angew. Chem., Int. Ed.*, 2017, **56**, 15073–15077.
131 H. Liu, L. Ge, D. Wang, N. Chen and C. Feng, *Angew. Chem., Int. Ed.*, 2019, **58**, 3918–3922.
132 J. Wang, B. Huang, C. Yang and W. Xia, *Chem. Commun.*, 2019, **55**, 11103–11106.
133 W. L. Lei, T. Wang, K. W. Feng, L. Z. Wu and Q. Liu, *ACS Catal.*, 2017, **7**, 7941–7945.
134 K. Ohmatsu, T. Nakashima, M. Sato and T. Ooi, *Nat. Commun.*, 2019, **10**, 2706.
135 H. Tang, X. Zhang, Y. Zhang and C. Feng, *Angew. Chem., Int. Ed.*, 2020, **59**, 5242–5247.
136 Q. Y. Meng, T. E. Schirmer, K. Katou and B. König, *Angew. Chem., Int. Ed.*, 2019, **58**, 5723–5728.
137 Q. Yu, Y. Zhang and J. P. Wan, *Green Chem.*, 2019, **21**, 3436–3441.
138 U. Wille, *Chem. Rev.*, 2013, **113**, 813–853.
139 J. Xuan and A. Studer, *Chem. Soc. Rev.*, 2017, **46**, 4329–4346.
140 M. H. Huang, W. J. Hao, G. Li, S. J. Tu and B. Jiang, *Chem. Commun.*, 2018, **54**, 10791–10811.
141 M. S. Kharasch and F. R. Mayo, *J. Am. Chem. Soc.*, 1933, **55**, 2468–2496.
142 M. S. Kharasch, H. Engelmann and F. R. Mayo, *J. Org. Chem.*, 1937, **2**, 288–302.
143 A. Singh, C. J. Fennell and J. D. Weaver, *Chem. Sci.*, 2016, **7**, 6796–6802.
144 H. Yue, C. Zhu, R. Kancherla, F. Liu and M. Rueping, *Angew. Chem., Int. Ed.*, 2020, **59**, 5738–5746.
145 W. Tian, Y. He, X. Song, H. Ding, J. Ye, W. Guo and Q. Xiao, *Adv. Synth. Catal.*, 2020, **362**, 1032–1038.
146 G. Zhang, Y. Lin, X. Luo, X. Hu, C. Chen and A. Lei, *Nat. Commun.*, 2018, **9**, 1225.

147 C. Song, X. Dong, Z. Wang, K. Liu, C. Chiang and A. Lei, *Angew. Chem., Int. Ed.*, 2019, **58**, 12206–12210.
148 X. Yang, J. Guo, H. Xiao, K. Feng, B. Chen, C. Tung and L. Wu, *Angew. Chem., Int. Ed.*, 2020, **59**, 5365–5370.
149 J. Chen, B. Q. He, P. Z. Wang, X. Y. Yu, Q. Q. Zhao, J. R. Chen and W. J. Xiao, *Org. Lett.*, 2019, **21**, 4359–4364.
150 J. Li, J. Zhang, H. Tan and D. Z. Wang, *Org. Lett.*, 2015, **17**, 2522–2525.
151 Z. Q. Song, Z. Liu, Q. C. Gan, T. Lei, C. H. Tung and L. Z. Wu, *Org. Lett.*, 2020, **22**, 832–836.
152 W. Dong, Y. Yuan, X. Xie and Z. Zhang, *Org. Lett.*, 2020, **22**, 528–532.
153 H. Wang, Q. Lu, C.-W. Chiang, Y. Luo, J. Zhou, G. Wang and A. Lei, *Angew. Chem., Int. Ed.*, 2017, **56**, 595–599.
154 H. Li, Z. Cheng, C. H. Tung and Z. Xu, *ACS Catal.*, 2018, **8**, 8237–8243.
155 Y. Ji, L. Wang, W. Guo, Q. Bi and B. Zhang, *Adv. Synth. Catal.*, 2020, **362**, 1131–1137.
156 Y. Li, T. Mou, L. Lu and X. Jiang, *Chem. Commun.*, 2019, **55**, 14299–14302.
157 Z. Wu, X. Liao, L. Yuan, Y. Wang, Y. Zheng, J. Zuo and Y. Pan, *Chem. – Eur. J.*, 2020, **26**, 5694–5700.
158 A. Studer and M. Bossart, *Radicals in Organic Synthesis*, Wiley-VCH Verlag GmbH, Weinheim, Germany, 2008, pp. 62–80.
159 Y. Zhao and W. Xia, *Org. Biomol. Chem.*, 2019, **17**, 4951–4963.
160 A. Sagadevan and M. F. Greaney, *Angew. Chem., Int. Ed.*, 2019, **58**, 9826–9830.
161 N. Holmberg-Douglas, N. P. R. Onuska and D. A. Nicewicz, *Angew. Chem., Int. Ed.*, 2020, **59**, 7425–7429.
162 D. A. Nagib and D. W. C. Macmillan, *Nature*, 2011, **480**, 224–228.
163 I. Abdiaj, C. Bottecchia, J. Alcazar and T. Noël, *Synthesis*, 2017, **49**, 4978–4985.
164 J. W. Beatty, J. J. Douglas, K. P. Cole and C. R. J. Stephenson, *Nat. Commun.*, 2015, **6**, 7919.
165 Y. Ouyang, X.-H. Xu and F.-L. Qing, *Angew. Chem., Int. Ed.*, 2018, **57**, 6926–6929.
166 J. Lin, Z. Li, J. Kan, S. Huang, W. Su and Y. Li, *Nat. Commun.*, 2017, **8**, 14353.
167 T. Zhang, X. Guo, Y. Shi, C. He and C. Duan, *Nat. Commun.*, 2018, **9**, 4024.
168 Y. Huang, Y. Y. Lei, L. Zhao, J. Gu, Q. Yao, Z. Wang, X. F. Li, X. Zhang and C. Y. He, *Chem. Commun.*, 2018, **54**, 13662–13665.
169 Y. Qiu, A. Scheremetjew, L. H. Finger and L. Ackermann, *Chem. – Eur. J.*, 2020, **26**, 3241–3246.
170 L. Wang, X. J. Wei, W. L. Jia, J. J. Zhong, L. Z. Wu and Q. Liu, *Org. Lett.*, 2014, **16**, 5842–5845.
171 M. D. Vanheyst, J. Qi, A. J. Roecker, J. M. E. Hughes, L. Cheng, Z. Zhao and J. Yin, *Org. Lett.*, 2020, **22**, 1648–1654.
172 R. Khan, S. Boonseng, P. D. Kemmitt, R. Felix, S. J. Coles, G. J. Tizzard, G. Williams, O. Simmonds, J.-L. Harvey, J. Atack, H. Cox and J. Spencer, *Adv. Synth. Catal.*, 2017, **359**, 3261–3269.
173 A. U. Meyer, T. Slanina, C. J. Yao and B. König, *ACS Catal.*, 2016, **6**, 369–375.
174 A. Arora and J. D. Weaver, *Org. Lett.*, 2016, **18**, 3996–3999.
175 A. Arora and J. D. Weaver, *Acc. Chem. Res.*, 2016, **49**, 2273–2283.
176 M. H. Aukland, M. Šiaučiulis, A. West, G. J. P. Perry and D. J. Procter, *Nat. Catal.*, 2020, **3**, 163–169.
177 Z. Wang, A. G. Herraiz, A. M. Del Hoyo and M. G. Suero, *Nature*, 2018, **554**, 86–91.
178 J. B. McManus and D. A. Nicewicz, *J. Am. Chem. Soc.*, 2017, **139**, 2880–2883.
179 L. J. Allen, P. J. Cabrera, M. Lee and M. S. Sanford, *J. Am. Chem. Soc.*, 2014, **136**, 5607–5610.
180 N. A. Romero, K. A. Margrey, N. E. Tay and D. A. Nicewicz, *Science*, 2015, **349**, 1326–1330.
181 L. Zhang, L. Liardet, J. Luo, D. Ren, M. Grätzel and X. Hu, *Nat. Catal.*, 2019, **2**, 366–373.
182 K. A. Margrey, A. Levens and D. A. Nicewicz, *Angew. Chem., Int. Ed.*, 2017, **56**, 15644–15648.
183 K. A. Margrey, J. B. McManus, S. Bonazzi, F. Zecri and D. A. Nicewicz, *J. Am. Chem. Soc.*, 2017, **139**, 11288–11299.
184 A. Ruffoni, F. Juliá, T. D. Svejstrup, A. J. McMillan, J. J. Douglas and D. Leonori, *Nat. Chem.*, 2019, **11**, 426–433.
185 P. S. Engl, A. P. Häring, F. Berger, G. Berger, A. Pérez-Bitrián and T. Ritter, *J. Am. Chem. Soc.*, 2019, **141**, 13346–13351.
186 S. L. Rössler, B. J. Jelier, P. F. Tripet, A. Shemet, G. Jeschke, A. Togni and E. M. Carreira, *Angew. Chem., Int. Ed.*, 2019, **58**, 526–531.
187 Y. Zhang, X. Dong, Y. Wu, G. Li and H. Lu, *Org. Lett.*, 2018, **20**, 4838–4842.
188 B. J. Jelier, P. F. Tripet, E. Pietrasiak, I. Franzoni, G. Jeschke and A. Togni, *Angew. Chem., Int. Ed.*, 2018, **57**, 13784–13789.
189 J. W. Lee, K. N. Lee and M. Ngai, *Angew. Chem., Int. Ed.*, 2019, **58**, 11171–11181.
190 W. Zheng, J. W. Lee, C. A. Morales-Rivera, P. Liu and M. Ngai, *Angew. Chem., Int. Ed.*, 2018, **57**, 13795–13799.
191 W. Zheng, C. A. Morales-Rivera, J. W. Lee, P. Liu and M.-Y. Ngai, *Angew. Chem., Int. Ed.*, 2018, **57**, 9645–9649.
192 J. W. Lee, D. N. Spiegowski and M. Y. Ngai, *Chem. Sci.*, 2017, **8**, 6066–6070.
193 L. Niu, J. Liu, H. Yi, S. Wang, X. A. Liang, A. K. Singh, C. W. Chiang and A. Lei, *ACS Catal.*, 2017, **7**, 7412–7416.
194 Y. Li, M. Wang and X. Jiang, *ACS Catal.*, 2017, **7**, 7587–7592.
195 F. Berger, M. B. Plutschack, J. Riegger, W. Yu, S. Speicher, M. Ho, N. Frank and T. Ritter, *Nature*, 2019, **567**, 223–228.
196 J. Li, J. Chen, R. Sang, W. S. Ham, M. B. Plutschack, F. Berger, S. Chabbra, A. Schnegg, C. Genicot and T. Ritter, *Nat. Chem.*, 2020, **12**, 56–62.
197 W. Chen, Z. Huang, N. E. S. Tay, B. Giglio, M. Wang, H. Wang, Z. Wu, D. A. Nicewicz and Z. Li, *Science*, 2019, **364**, 1170–1174.
198 I. Ghosh, J. Khamrai, A. Savateev, N. Shlapakov, M. Antonietti and B. König, *Science*, 2019, **365**, 360–366.
199 A. Lemos, C. Lemaire and A. Luxen, *Adv. Synth. Catal.*, 2019, **361**, 1500–1537.
200 A. Chatterjee and B. König, *Angew. Chem.*, 2019, **131**, 14427–14432.
201 F. Minisci, E. Vismara and F. Fontana, *Heterocycles*, 1989, **28**, 489–519.

202 R. S. J. Proctor and R. J. Phipps, *Angew. Chem., Int. Ed.*, 2019, **58**, 13666–13699.
203 A. C. Sun, R. C. McAtee, E. J. McClain and C. R. J. Stephenson, *Synthesis*, 2019, 1063–1072.
204 D. A. DiRocco, K. Dykstra, S. Krska, P. Vachal, D. V. Conway and M. Tudge, *Angew. Chem., Int. Ed.*, 2014, **53**, 4802–4806.
205 M. A. J. Duncton, *MedChemComm*, 2011, **2**, 1135–1161.
206 Y. Fujiwara, J. A. Dixon, F. O'hara, E. D. Funder, D. D. Dixon, R. A. Rodriguez, R. D. Baxter, B. Herlé, N. Sach, M. R. Collins, Y. Ishihara and P. S. Baran, *Nature*, 2012, **492**, 95–99.
207 G. A. Molander, V. Colombel and V. A. Braz, *Org. Lett.*, 2011, **13**, 1852–1855.
208 J. Jin and D. W. C. MacMillan, *Nature*, 2015, **525**, 87–90.
209 X. Wu, H. Zhang, N. Tang, Z. Wu, D. Wang, M. Ji, Y. Xu, M. Wang and C. Zhu, *Nat. Commun.*, 2018, **9**, 3343.
210 Z. Wang, J. Dong, Y. Hao, Y. Li, Y. Liu, H. Song and Q. Wang, *J. Org. Chem.*, 2019, **84**, 16245–16253.
211 P. Nuhant, M. S. Oderinde, J. Genovino, A. Juneau, Y. Gagné, C. Allais, G. M. Chinigo, C. Choi, N. W. Sach, L. Bernier, Y. M. Fobian, M. W. Bundesmann, B. Khunte, M. Frenette and O. O. Fadeyi, *Angew. Chem., Int. Ed.*, 2017, **56**, 15309–15313.
212 J. Dong, X. Lyu, Z. Wang, X. Wang, H. Song, Y. Liu and Q. Wang, *Chem. Sci.*, 2019, **10**, 976–982.
213 J. J. Perkins, J. W. Schubert, E. C. Streckfuss, J. Balsells and A. ElMarrouni, *Eur. J. Org. Chem.*, 2020, 1515–1522.
214 R. A. Garza-Sanchez, A. Tlahuext-Aca, G. Tavakoli and F. Glorius, *ACS Catal.*, 2017, **7**, 4057–4061.
215 J. Wang, G.-X. Li, G. He and G. Chen, *Asian J. Org. Chem.*, 2018, **7**, 1307–1310.
216 J. Genovino, Y. Lian, Y. Zhang, T. O. Hope, A. Juneau, Y. Gagné, G. Ingle and M. Frenette, *Org. Lett.*, 2018, **20**, 3229–3232.
217 X. Y. Zhang, W. Z. Weng, H. Liang, H. Yang and B. Zhang, *Org. Lett.*, 2018, **20**, 4686–4690.
218 T. C. Sherwood, N. Li, A. N. Yazdani and T. G. M. Dhar, *J. Org. Chem.*, 2018, **83**, 3000–3012.
219 Z. Wang, X. Ji, J. Zhao and H. Huang, *Green Chem.*, 2019, **21**, 5512–5516.
220 G. X. Li, C. A. Morales-Rivera, Y. Wang, F. Gao, G. He, P. Liu and G. Chen, *Chem. Sci.*, 2016, **7**, 6407–6412.
221 R. A. Garza-Sanchez, T. Patra, A. Tlahuext-Aca, F. Strieth-Kalthoff and F. Glorius, *Chem. – Eur. J.*, 2018, **24**, 10064–10068.
222 H. Yan, Z. Hou and H. Xu, *Angew. Chem., Int. Ed.*, 2019, **58**, 4592–4595.
223 H. Zhao and J. Jin, *Org. Lett.*, 2019, **21**, 6179–6184.
224 G. X. Li, X. Hu, G. He and G. Chen, *ACS Catal.*, 2018, **8**, 11847–11853.
225 Z. Sun, J. Zhao, H. Deng, L. Tian, B. Tang, K. K.-C. Liu and H. Y. Zhu, *Adv. Synth. Catal.*, 2020, **362**, 1502–1508.
226 W. Zhang, X. X. Xiang, J. Chen, C. Yang, Y. L. Pan, J. P. Cheng, Q. Meng and X. Li, *Nat. Commun.*, 2020, **11**, 638.
227 L. Trump, A. Lemos, B. Lallemand, P. Pasau, J. Mercier, C. Lemaire, A. Luxen and C. Genicot, *Angew. Chem., Int. Ed.*, 2019, **58**, 13149–13154.
228 Y. Quan, G. Lan, Y. Fan, W. Shi, E. You and W. Lin, *J. Am. Chem. Soc.*, 2020, **142**, 1746–1751.
229 W. M. Cheng, R. Shang and Y. Fu, *ACS Catal.*, 2017, **7**, 907–911.
230 R. S. J. Proctor, H. J. Davis and R. J. Phipps, *Science*, 2018, **360**, 419–422.
231 J. Dong, Q. Xia, X. Lv, C. Yan, H. Song, Y. Liu and Q. Wang, *Org. Lett.*, 2018, **20**, 5661–5665.
232 B. Bieszczad, L. A. Perego and P. Melchiorre, *Angew. Chem., Int. Ed.*, 2019, **58**, 16878–16883.
233 G. R. Park, J. Moon and E. J. Cho, *Chem. Commun.*, 2017, **53**, 12786–12789.
234 Z. Deng, G. X. Li, G. He and G. Chen, *J. Org. Chem.*, 2019, **84**, 15777–15787.
235 P. B. Arockiam, L. Guillemard and J. Wencel-Delord, *Adv. Synth. Catal.*, 2017, **359**, 2571–2579.
236 M. Ye, G. L. Gao, A. J. F. Edmunds, P. A. Worthington, J. A. Morris and J. Q. Yu, *J. Am. Chem. Soc.*, 2011, **133**, 19090–19093.
237 P. Guo, J. M. Joo, S. Rakshit and D. Sames, *J. Am. Chem. Soc.*, 2011, **133**, 16338–16341.
238 Z. Pan, Y. Liu, F. Hu, Q. Liu, W. Shang and C. Xia, *Chem. Commun.*, 2020, **56**, 4930–4933.
239 J. Dong, X. Wang, H. Song, Y. Liu and Q. Wang, *Adv. Synth. Catal.*, 2020, **362**, 2155–2159.
240 M. Jouffroy and J. Kong, *Chem. – Eur. J.*, 2019, **25**, 2217–2221.
241 J. Lu, X. He, X. Cheng, A. Zhang, G. Xu and J. Xuan, *Adv. Synth. Catal.*, 2020, **362**, 2178–2182.
242 L. Y. Xie, T. G. Fang, J. X. Tan, B. Zhang, Z. Cao, L. H. Yang and W. M. He, *Green Chem.*, 2019, **21**, 3858–3863.
243 H. Chen, H. Yi, Z. Tang, C. Bian, H. Zhang and A. Lei, *Adv. Synth. Catal.*, 2018, **360**, 3220–3227.
244 Y. Liang, X. Zhang and D. W. C. MacMillan, *Nature*, 2018, **559**, 83–88.
245 H. Huang and T. H. Lambert, *Angew. Chem., Int. Ed.*, 2020, **59**, 658–662.
246 S. Ye, T. Xiang, X. Li and J. Wu, *Org. Chem. Front.*, 2019, **6**, 2183–2199.
247 J. Dong, X. Wang, Z. Wang, H. Song, Y. Liu and Q. Wang, *Chem. Commun.*, 2019, **55**, 11707–11710.
248 B. Zhao, R. Shang, G. Z. Wang, S. Wang, H. Chen and Y. Fu, *ACS Catal.*, 2020, **10**, 1334–1343.
249 D. Fernandez Reina, A. Ruffoni, Y. S. S. Al-Faiyz, J. J. Douglas, N. S. Sheikh and D. Leonori, *ACS Catal.*, 2017, **7**, 4126–4130.
250 Q. Q. Zhou, S. J. S. Düsel, L. Q. Lu, B. König and W. J. Xiao, *Chem. Commun.*, 2019, **55**, 107–110.
251 Y.-Y. Liu, X.-Y. Yu, J.-R. Chen, M.-M. Qiao, X. Qi, D.-Q. Shi and W.-J. Xiao, *Angew. Chem., Int. Ed.*, 2017, **56**, 9527–9531.
252 Y. Shen, J. Cornella, F. Juliá-Hernández and R. Martin, *ACS Catal.*, 2017, **7**, 409–412.
253 J. Nugent, C. Arroniz, B. R. Shire, A. J. Sterling, H. D. Pickford, M. L. J. Wong, S. J. Mansfield, D. F. J. Caputo, B. Owen, J. J. Mousseau, F. Duarte and E. A. Anderson, *ACS Catal.*, 2019, **9**, 9568–9574.
254 Z. Z. Zhou, J. H. Zhao, X. Y. Gou, X. M. Chen and Y. M. Liang, *Org. Chem. Front.*, 2019, **6**, 1649–1654.

255 S. K. Kariofillis, B. J. Shields, M. A. Tekle-Smith, M. J. Zacuto and A. G. Doyle, *J. Am. Chem. Soc.*, 2020, **142**, 7683–7689.
256 J. Yi, S. O. Badir, L. M. Kammer, M. Ribagorda and G. A. Molander, *Org. Lett.*, 2019, **21**, 3346–3351.
257 I. B. Perry, T. F. Brewer, P. J. Sarver, D. M. Schultz, D. A. DiRocco and D. W. C. MacMillan, *Nature*, 2018, **560**, 70–75.
258 M. El Khatib, R. A. M. Serafim and G. A. Molander, *Angew. Chem., Int. Ed.*, 2016, **55**, 254–258.
259 Y. Sato, K. Nakamura, Y. Sumida, D. Hashizume, T. Hosoya and H. Ohmiya, *J. Am. Chem. Soc.*, 2020, **142**, 9938–9943.
260 L. Huang, T. Ji and M. Rueping, *J. Am. Chem. Soc.*, 2020, **142**, 3532–3539.
261 M. Ociepa, A. J. Wierzba, J. Turkowska and D. Gryko, *J. Am. Chem. Soc.*, 2020, **142**, 5355–5361.
262 M. Parasram, B. J. Shields, O. Ahmad, T. Knauber and A. G. Doyle, *ACS Catal.*, 2020, **10**, 5821–5827.
263 L. Huang, C. Zhu, L. Yi, H. Yue, R. Kancherla and M. Rueping, *Angew. Chem., Int. Ed.*, 2020, **59**, 457–464.
264 T. Constantin, M. Zanini, A. Regni, N. S. Sheikh, F. Juliá and D. Leonori, *Science*, 2020, **367**, 1021–1026.
265 C. Le, T. Q. Chen, T. Liang, P. Zhang and D. W. C. MacMillan, *Science*, 2018, **360**, 1010–1014.
266 V. Bacauanu, S. Cardinal, M. Yamauchi, M. Kondo, D. F. Fernández, R. Remy and D. W. C. MacMillan, *Angew. Chem., Int. Ed.*, 2018, **57**, 12543–12548.
267 M. K. Nielsen, B. J. Shields, J. Liu, M. J. Williams, M. J. Zacuto and A. G. Doyle, *Angew. Chem., Int. Ed.*, 2017, **56**, 7191–7194.
268 H. Huang, X. Li, C. Yu, Y. Zhang, P. S. Mariano and W. Wang, *Angew. Chem., Int. Ed.*, 2017, **56**, 1500–1505.
269 N. Alandini, L. Buzzetti, G. Favi, T. Schulte, L. Candish, K. D. Collins and P. Melchiorre, *Angew. Chem., Int. Ed.*, 2020, **59**, 5248–5253.
270 G. M. Torres, Y. Liu and B. A. Arndtsen, *Science*, 2020, **368**, 318–323.
271 B. J. Shields and A. G. Doyle, *J. Am. Chem. Soc.*, 2016, **138**, 12719–12722.
272 I. Karakaya, D. N. Primer and G. A. Molander, *Org. Lett.*, 2015, **17**, 3294–3297.
273 L. Yang, Z. Huang, G. Li, W. Zhang, R. Cao, C. Wang, J. Xiao and D. Xue, *Angew. Chem., Int. Ed.*, 2018, **57**, 1968–1972.
274 B. Liu, C. H. Lim and G. M. Miyake, *J. Am. Chem. Soc.*, 2017, **139**, 13616–13619.
275 M. Jouffroy, C. B. Kelly and G. A. Molander, *Org. Lett.*, 2016, **18**, 876–879.
276 S. Ye, Y. Li, J. Wu and Z. Li, *Chem. Commun.*, 2019, **55**, 2489–2492.
277 H. Kim, H. Kim, T. H. Lambert and S. Lin, *J. Am. Chem. Soc.*, 2020, **142**, 2087–2092.
278 A. Dumoulin, J. K. Matsui, Á. Gutiérrez-Bonet and G. A. Molander, *Angew. Chem., Int. Ed.*, 2018, **57**, 6614–6618.
279 J. L. Jeffrey, J. A. Terrett and D. W. C. MacMillant, *Science*, 2015, **349**, 1532–1536.
280 H. M. Huang, P. Bellotti, P. M. Pflüger, J. L. Schwarz, B. Heidrich and F. Glorius, *J. Am. Chem. Soc.*, 2020, **142**, 10173–10183.
281 S. Jana, Z. Yang, F. Li, C. Empel, J. Ho and R. M. Koenigs, *Angew. Chem., Int. Ed.*, 2020, **59**, 5562–5566.
282 X. Y. Yu, J. Chen, H. W. Chen, W. J. Xiao and J. R. Chen, *Org. Lett.*, 2020, **22**, 2333–2338.
283 A. Hossain, A. Bhattacharyya and O. Reiser, *Science*, 2019, 364.
284 B. Schweitzer-Chaput, M. A. Horwitz, E. de Pedro Beato and P. Melchiorre, *Nat. Chem.*, 2019, **11**, 129–135.
285 Z. J. Li, S. Li, E. Hofman, A. Hunter Davis, G. Leem and W. Zheng, *Green Chem.*, 2020, **22**, 1911–1918.
286 B. Liu, W. Z. Elder and G. M. Miyake, *J. Org. Chem.*, 2020, **85**, 3717–3727.
287 A. Varenikov and M. Gandelman, *Nat. Commun.*, 2018, **9**, 3566.
288 L. Chenneberg, A. Baralle, M. Daniel, L. Fensterbank, J.-P. Goddard and C. Ollivier, *Adv. Synth. Catal.*, 2014, **356**, 2756–2762.
289 J. P. Goddard, C. Ollivier and L. Fensterbank, *Acc. Chem. Res.*, 2016, **49**, 1924–1936.
290 C. C. Nawrat, C. R. Jamison, Y. Slutskyy, D. W. C. MacMillan and L. E. Overman, *J. Am. Chem. Soc.*, 2015, **137**, 11270–11273.
291 X. Zhang and D. W. C. MacMillan, *J. Am. Chem. Soc.*, 2016, **138**, 13862–13865.
292 F. J. Aguilar Troyano, F. Ballaschk, M. Jaschinski, Y. Özkaya and A. Gómez-Suárez, *Chem. – Eur. J.*, 2019, **25**, 14054–14058.
293 J. Wu, R. M. Bär, L. Guo, A. Noble and V. K. Aggarwal, *Angew. Chem., Int. Ed.*, 2019, **58**, 18830–18834.
294 Y. Zhao, B. Huang, C. Yang, B. Li, B. Gou and W. Xia, *ACS Catal.*, 2017, **7**, 2446–2451.
295 Y. Y. Gui, X. W. Chen, W. J. Zhou and D. G. Yu, *Synlett*, 2017, 2581–2586.
296 G. Zhao and T. Wang, *Angew. Chem., Int. Ed.*, 2018, **57**, 6120–6124.
297 B. Wang, D. C. Xiong and X. S. Ye, *Org. Lett.*, 2015, **17**, 5698–5701.
298 B. Ye, J. Zhao, K. Zhao, J. M. McKenna and F. D. Toste, *J. Am. Chem. Soc.*, 2018, **140**, 8350–8356.
299 W. Schilling, D. Riemer, Y. Zhang, N. Hatami and S. Das, *ACS Catal.*, 2018, **8**, 5425–5430.
300 N. F. Nikitas, D. I. Tzaras, I. Triandafillidi and C. G. Kokotos, *Green Chem.*, 2020, **22**, 471–477.
301 H. Fuse, H. Mitsunuma and M. Kanai, *J. Am. Chem. Soc.*, 2020, **142**, 4493–4499.
302 L.-M. Zhao, Q.-Y. Meng, X.-B. Fan, C. Ye, X.-B. Li, B. Chen, V. Ramamurthy, C.-H. Tung and L.-Z. Wu, *Angew. Chem., Int. Ed.*, 2017, **56**, 3020–3024.
303 W. Zhang, K. L. Carpenter and S. Lin, *Angew. Chem., Int. Ed.*, 2020, **59**, 409–417.
304 W. Guo, L. Q. Lu, Y. Wang, Y. N. Wang, J. R. Chen and W. J. Xiao, *Angew. Chem., Int. Ed.*, 2015, **54**, 2265–2269.
305 L. Ren, M. M. Yang, C. H. Tung, L. Z. Wu and H. Cong, *ACS Catal.*, 2017, **7**, 8134–8138.
306 L. Shi, H. Liu, L. Huo, Y. Dang, Y. Wang, B. Yang, S. Qiu and H. Tan, *Org. Chem. Front.*, 2018, **5**, 1312–1319.

307 W. Xu, J. Ma, X.-A. Yuan, J. Dai, J. Xie and C. Zhu, *Angew. Chem., Int. Ed.*, 2018, **57**, 10357–10361.
308 Q.-Y. Meng, S. Wang and B. König, *Angew. Chem., Int. Ed.*, 2017, **56**, 13426–13430.
309 P. Gandeepan, J. Koeller, K. Korvorapun, J. Mohr and L. Ackermann, *Angew. Chem., Int. Ed.*, 2019, **58**, 9820–9825.
310 J. J. Guo, A. Hu, Y. Chen, J. Sun, H. Tang and Z. Zuo, *Angew. Chem., Int. Ed.*, 2016, **55**, 15319–15322.
311 A. Hu, J. J. Guo, H. Pan, H. Tang, Z. Gao and Z. Zuo, *J. Am. Chem. Soc.*, 2018, **140**, 1612–1616.
312 J. Wang, B. Huang, C. Shi, C. Yang and W. Xia, *J. Org. Chem.*, 2018, **83**, 9696–9706.
313 J. Zhang, Y. Li, F. Zhang, C. Hu and Y. Chen, *Angew. Chem.*, 2016, **128**, 1904–1907.
314 G. G. Pawar, F. Robert, E. Grau, H. Cramail and Y. Landais, *Chem. Commun.*, 2018, **54**, 9337–9340.
315 K. Liang, T. Li, N. Li, Y. Zhang, L. Shen, Z. Ma and C. Xia, *Chem. Sci.*, 2020, **11**, 2130–2135.
316 K. Nakajima, Y. Miyake and Y. Nishibayashi, *Acc. Chem. Res.*, 2016, **49**, 1946–1956.
317 S. A. Morris, J. Wang and N. Zheng, *Acc. Chem. Res.*, 2016, **49**, 1957–1968.
318 J. T. José, V. A. Fernandes, B. T. Matsuo, J. A. C. Delgado, W. C. De Souza and M. W. Paixão, *Chem. Commun.*, 2020, **56**, 503–514.
319 A. Trowbridge, D. Reich and M. J. Gaunt, *Nature*, 2018, **561**, 522–527.
320 Y. Xiong, X. Ma and G. Zhang, *Org. Lett.*, 2019, **21**, 1699–1703.
321 K. P. Shing Cheung, D. Kurandina, T. Yata and V. Gevorgyan, *J. Am. Chem. Soc.*, 2020, **142**, 9932–9937.
322 Y. Zhang, D. Riemer, W. Schilling, J. Kollmann and S. Das, *ACS Catal.*, 2018, **8**, 6659–6664.
323 O. Yilmaz, M. S. Oderinde and M. H. Emmert, *J. Org. Chem.*, 2018, **83**, 11089–11100.
324 T. Wakaki, K. Sakai, T. Enomoto, M. Kondo, S. Masaoka, K. Oisaki and M. Kanai, *Chem. – Eur. J.*, 2018, **24**, 8051–8055.
325 B. Lu, Y. Cheng, L. Y. Chen, J. R. Chen and W. J. Xiao, *ACS Catal.*, 2019, **9**, 8159–8164.
326 L. Yang, J. Y. Zhang, X. H. Duan, P. Gao, J. Jiao and L. N. Guo, *J. Org. Chem.*, 2019, **84**, 8615–8629.
327 W. C. Wertjes, M. Okumura and D. Sarlah, *J. Am. Chem. Soc.*, 2019, **141**, 163–167.
328 J. Wu, L. He, A. Noble and V. K. Aggarwal, *J. Am. Chem. Soc.*, 2018, **140**, 10700–10704.
329 F. Sandfort, F. Strieth-Kalthoff, F. J. R. Klauck, M. J. James and F. Glorius, *Chem. – Eur. J.*, 2018, **24**, 17210–17214.
330 X. Jiang, M. Zhang, W. Xiong, L. Lu and W. Xiao, *Angew. Chem., Int. Ed.*, 2019, **58**, 2402–2406.
331 M. Ociepa, J. Turkowska and D. Gryko, *ACS Catal.*, 2018, **8**, 11362–11367.
332 J. Wu, P. S. Grant, X. Li, A. Noble and V. K. Aggarwal, *Angew. Chem., Int. Ed.*, 2019, **58**, 5697–5701.
333 Y. Xu, Z. J. Xu, Z. P. Liu and H. Lou, *Org. Chem. Front.*, 2019, **6**, 3902–3905.
334 J. Xie, X. Yuan, A. Abdukader, C. Zhu and J. Ma, *Org. Lett.*, 2014, **16**, 1768–1771.
335 T. C. Johnson, B. L. Elbert, A. J. M. Farley, T. W. Gorman, C. Genicot, B. Lallemand, P. Pasau, J. Flasz, J. L. Castro, M. Maccoss, D. J. Dixon, R. S. Paton, C. J. Schofield, M. D. Smith and M. C. Willis, *Chem. Sci.*, 2018, **9**, 629–633.
336 T. Ide, J. P. Barham, M. Fujita, Y. Kawato, H. Egami and Y. Hamashima, *Chem. Sci.*, 2018, **9**, 8453–8460.
337 C. Le, Y. Liang, R. W. Evans, X. Li and D. W. C. MacMillan, *Nature*, 2017, **547**, 79–83.
338 J. B. McManus, N. P. R. Onuska, M. S. Jeffreys, N. C. Goodwin and D. A. Nicewicz, *Org. Lett.*, 2020, **22**, 679–683.
339 J. Xie, J. Yu, M. Rudolph, F. Rominger and A. S. K. Hashmi, *Angew. Chem., Int. Ed.*, 2016, **55**, 9416–9421.
340 J. Davies, T. D. Svejstrup, D. Fernandez Reina, N. S. Sheikh and D. Leonori, *J. Am. Chem. Soc.*, 2016, **138**, 8092–8095.
341 T. D. Svejstrup, A. Ruffoni, F. Juliá, V. M. Aubert and D. Leonori, *Angew. Chem., Int. Ed.*, 2017, **56**, 14948–14952.
342 Q. Qin and S. Yu, *Org. Lett.*, 2015, **17**, 1894–1897.
343 Y. Y. Loh, K. Nagao, A. J. Hoover, D. Hesk, N. R. Rivera, S. L. Colletti, I. W. Davies and D. W. C. MacMillan, *Science*, 2017, **358**, 1182–1187.
344 J. Xuan, Z. G. Zhang and W. J. Xiao, *Angew. Chem., Int. Ed.*, 2015, **54**, 15632–15641.
345 J. D. Griffin, M. A. Zeller and D. A. Nicewicz, *J. Am. Chem. Soc.*, 2015, **137**, 11340–11348.
346 V. T. Nguyen, V. D. Nguyen, G. C. Haug, H. T. Dang, S. Jin, Z. Li, C. Flores-Hansen, B. S. Benavides, H. D. Arman and O. V. Larionov, *ACS Catal.*, 2019, **9**, 9485–9498.
347 K. C. Cartwright, A. M. Davies and J. A. Tunge, *Eur. J. Org. Chem.*, 2020, 1245–1258.
348 W. M. Cheng, R. Shang and Y. Fu, *Nat. Commun.*, 2018, **9**, 5212.
349 M. Koy, F. Sandfort, A. Tlahuext-Aca, L. Quach, C. G. Daniliuc and F. Glorius, *Chem. – Eur. J.*, 2018, **24**, 4552–4555.
350 H. Cao, H. Jiang, H. Feng, J. M. C. Kwan, X. Liu and J. Wu, *J. Am. Chem. Soc.*, 2018, **140**, 16360–16367.
351 J. L. Tu, J. L. Liu, W. Tang, M. Su and F. Liu, *Org. Lett.*, 2020, **22**, 1222–1226.
352 Q. Q. Zhou, W. Guo, W. Ding, X. Wu, X. Chen, L. Q. Lu and W. J. Xiao, *Angew. Chem., Int. Ed.*, 2015, **54**, 11196–11199.
353 J. R. Chen, X. Q. Hu, L. Q. Lu and W. J. Xiao, *Acc. Chem. Res.*, 2016, **49**, 1911–1923.
354 Y. Mao, W. Zhao, S. Lu, L. Yu, Y. Wang, Y. Liang, S. Ni and Y. Pan, *Chem. Sci.*, 2020, **11**, 4939–4947.
355 H. Wang, C. F. Liu, Z. Song, M. Yuan, Y. A. Ho, O. Gutierrez and M. J. Koh, *ACS Catal.*, 2020, **10**, 4451–4459.
356 V. T. Nguyen, V. D. Nguyen, G. C. Haug, N. T. H. Vuong, H. T. Dang, H. D. Arman and O. V. Larionov, *Angew. Chem., Int. Ed.*, 2020, **59**, 7921–7927.
357 W. Zhao, R. P. Wurz, J. C. Peters and G. C. Fu, *J. Am. Chem. Soc.*, 2017, **139**, 12153–12156.
358 R. Mao, A. Frey, J. Balon and X. Hu, *Nat. Catal.*, 2018, **1**, 120–126.
359 R. Mao, J. Balon and X. Hu, *Angew. Chem., Int. Ed.*, 2018, **57**, 9501–9504.
360 T. Patra, P. Bellotti, F. Strieth-Kalthoff and F. Glorius, *Angew. Chem., Int. Ed.*, 2020, **59**, 3172–3177.

361 V. K. Soni, S. Lee, J. Kang, Y. K. Moon, H. S. Hwang, Y. You and E. J. Cho, *ACS Catal.*, 2019, **9**, 10454–10463.
362 V. R. Yatham, P. Bellotti and B. König, *Chem. Commun.*, 2019, **55**, 3489–3492.
363 D. Wang, N. Zhu, P. Chen, Z. Lin and G. Liu, *J. Am. Chem. Soc.*, 2017, **139**, 15632–15635.
364 E. E. Stache, A. B. Ertel, T. Rovis and A. G. Doyle, *ACS Catal.*, 2018, **8**, 11134–11139.
365 M. Zhang, X.-A. Yuan, C. Zhu and J. Xie, *Angew. Chem., Int. Ed.*, 2019, **58**, 312–316.
366 C. L. Joe and A. G. Doyle, *Angew. Chem., Int. Ed.*, 2016, **55**, 4040–4043.
367 J. Amani and G. A. Molander, *Org. Lett.*, 2017, **19**, 3612–3615.
368 A. V. Davies, K. P. Fitzpatrick, R. C. Betori and K. A. Scheidt, *Angew. Chem., Int. Ed.*, 2020, **59**, 9143–9148.
369 Y. Q. Guo, R. Wang, H. Song, Y. Liu and Q. Wang, *Org. Lett.*, 2020, **22**, 709–713.
370 S. O. Badir, A. Dumoulin, J. K. Matsui and G. A. Molander, *Angew. Chem., Int. Ed.*, 2018, **57**, 6610–6613.
371 J. A. Kautzky, T. Wang, R. W. Evans and D. W. C. Macmillan, *J. Am. Chem. Soc.*, 2018, **140**, 6522–6526.
372 Q. Y. Han, K. L. Tan, H. N. Wang and C. P. Zhang, *Org. Lett.*, 2019, **21**, 10013–10017.
373 A. Fawcett, J. Pradeilles, Y. Wang, T. Mutsuga, E. L. Myers and V. K. Aggarwal, *Science*, 2017, **357**, 283–286.
374 D. Hu, L. Wang and P. Li, *Org. Lett.*, 2017, **19**, 2770–2773.
375 A. Noble, R. S. Mega, D. Pflästerer, E. L. Myers and V. K. Aggarwal, *Angew. Chem., Int. Ed.*, 2018, **57**, 2155–2159.
376 C. Shu, R. S. Mega, B. J. Andreassen, A. Noble and V. K. Aggarwal, *Angew. Chem., Int. Ed.*, 2018, **57**, 15430–15434.
377 G. Ernouf, E. Chirkin, L. Rhyman, P. Ramasami and J. Cintrat, *Angew. Chem., Int. Ed.*, 2020, **59**, 2618–2622.
378 N. A. Weires, Y. Slutskyy and L. E. Overman, *Angew. Chem., Int. Ed.*, 2019, **58**, 8561–8565.
379 L. Liu, J. Dong, Y. Yan, S. F. Yin, L. B. Han and Y. Zhou, *Chem. Commun.*, 2019, **55**, 233–236.
380 Z. He, M. Bae, J. Wu and T. F. Jamison, *Angew. Chem., Int. Ed.*, 2014, **53**, 14451–14455.
381 B. Pieber, J. A. Malik, C. Cavedon, S. Gisbertz, A. Savateev, D. Cruz, T. Heil, G. Zhang and P. H. Seeberger, *Angew. Chem., Int. Ed.*, 2019, **58**, 9575–9580.
382 R. Mao, J. Balon and X. Hu, *Angew. Chem., Int. Ed.*, 2018, **57**, 13624–13628.
383 S. Shibutani, T. Kodo, M. Takeda, K. Nagao, N. Tokunaga, Y. Sasaki and H. Ohmiya, *J. Am. Chem. Soc.*, 2020, **142**, 1211–1216.
384 T. Xu, T. Cao, M. Yang, R. Xu, X. Nie and S. Liao, *Org. Lett.*, 2020, **22**, 3692–3696.
385 T. Patra, S. Mukherjee, J. Ma, F. Strieth-Kalthoff and F. Glorius, *Angew. Chem., Int. Ed.*, 2019, **58**, 10514–10520.
386 Y. Sakakibara, E. Ito, T. Fukushima, K. Murakami and K. Itami, *Chem. – Eur. J.*, 2018, **24**, 9254–9258.
387 X. Huang, R. D. Webster, K. Harms and E. Meggers, *J. Am. Chem. Soc.*, 2016, **138**, 12636–12642.
388 M. A. Theodoropoulou, N. F. Nikitas and C. G. Kokotos, *Beilstein J. Org. Chem.*, 2020, **16**, 833–857.
389 Q. Q. Zhou, Y. Q. Zou, L. Q. Lu and W. J. Xiao, *Angew. Chem., Int. Ed.*, 2019, **58**, 1586–1604.
390 Q. Xia, J. Dong, H. Song and Q. Wang, *Chem. – Eur. J.*, 2019, **25**, 2949–2961.
391 X. Guo, Y. Okamoto, M. R. Schreier, T. R. Ward and O. S. Wenger, *Eur. J. Org. Chem.*, 2020, 1288–1293.
392 D. Liu, W. Ding, Q. Q. Zhou, Y. Wei, L. Q. Lu and W. J. Xiao, *Org. Lett.*, 2018, **20**, 7278–7282.
393 S. Mukherjee, R. A. Garza-Sanchez, A. Tlahuext-Aca and F. Glorius, *Angew. Chem., Int. Ed.*, 2017, **56**, 14723–14726.
394 L. Wang, T. Wang, G.-J. Cheng, X. Li, J. Wei, B. Guo, C. Zheng, G. Chen, C. Ran and C. Zheng, *ACS Catal.*, 2020, **10**(14), 7543–7551.
395 S. Jung, H. Lee, Y. Moon, H. Y. Jung and S. Hong, *ACS Catal.*, 2019, **9**, 9891–9896.
396 Y. Zhang, P. Ji, W. Hu, Y. Wei, H. Huang and W. Wang, *Chem. – Eur. J.*, 2019, **25**, 8225–8228.
397 S. Mukherjee, T. Patra and F. Glorius, *ACS Catal.*, 2018, **8**, 5842–5846.
398 P. F. Yuan, Q. B. Zhang, X. L. Jin, W. L. Lei, L. Z. Wu and Q. Liu, *Green Chem.*, 2018, **20**, 5464–5468.
399 K. N. Lee, Z. Lei and M. Y. Ngai, *J. Am. Chem. Soc.*, 2017, **139**, 5003–5006.
400 E. Arceo, A. Bahamonde, G. Bergonzini and P. Melchiorre, *Chem. Sci.*, 2014, **5**, 2438–2442.
401 M. D. Vu, M. Das, A. Guo, Z. E. Ang, M. Dokić, H. Sen Soo and X. W. Liu, *ACS Catal.*, 2019, **9**, 9009–9014.
402 J. Ma, A. R. Rosales, X. Huang, K. Harms, R. Riedel, O. Wiest and E. Meggers, *J. Am. Chem. Soc.*, 2017, **139**, 17245–17248.
403 D. Spinnato, B. Schweitzer-Chaput, G. Goti, M. Ošeka and P. Melchiorre, *Angew. Chem., Int. Ed.*, 2020, **59**, 9485–9490.
404 J. L. Schwarz, F. Schäfers, A. Tlahuext-Aca, L. Lückemeier and F. Glorius, *J. Am. Chem. Soc.*, 2018, **140**, 12705–12709.
405 Y. L. Li, W. D. Li, Z. Y. Gu, J. Chen and J. B. Xia, *ACS Catal.*, 2020, **10**, 1528–1534.
406 H. Yi, L. Niu, S. Wang, T. Liu, A. K. Singh and A. Lei, *Org. Lett.*, 2017, **19**, 122–125.
407 D. Liang, L. Rao, C. Xiao and J. R. Chen, *Org. Lett.*, 2019, **21**, 8783–8788.
408 N. Zhou, X.-A. Yuan, Y. Zhao, J. Xie and C. Zhu, *Angew. Chem., Int. Ed.*, 2018, **57**, 3990–3994.
409 E. M. Dauncey, S. P. Morcillo, J. J. Douglas, N. S. Sheikh and D. Leonori, *Angew. Chem., Int. Ed.*, 2018, **57**, 744–748.
410 X. Q. Hu, J. R. Chen and W. J. Xiao, *Angew. Chem., Int. Ed.*, 2017, **56**, 1960–1962.
411 J. C. K. Chu and T. Rovis, *Nature*, 2016, **539**, 272–275.
412 D. F. Chen, J. C. K. Chu and T. Rovis, *J. Am. Chem. Soc.*, 2017, **139**, 14897–14900.
413 D. Mazzarella, G. E. M. Crisenza and P. Melchiorre, *J. Am. Chem. Soc.*, 2018, **140**, 8439–8443.
414 Y. Shen, Y. Gu and R. Martin, *J. Am. Chem. Soc.*, 2018, **140**, 12200–12209.
415 J. Jia, R. Kancherla, M. Rueping and L. Huang, *Chem. Sci.*, 2020, **11**, 4954–4959.
416 Q. Guo, Q. Peng, H. Chai, Y. Huo, S. Wang and Z. Xu, *Nat. Commun.*, 2020, **11**, 1463.

417 S. Guo, D. I. AbuSalim and S. P. Cook, *J. Am. Chem. Soc.*, 2018, **140**, 12378–12382.
418 P. J. Sarver, V. Bacauanu, D. M. Schultz, D. A. DiRocco, Y. Hong Lam, E. C. Sherer and D. W. C. MacMillan, *Nat. Chem*, 2020, **12**, 459–467.
419 Y. Li, M. Lei and L. Gong, *Nat. Catal.*, 2019, **2**, 1016–1026.
420 S. Kamijo, K. Kamijo, K. Maruoka and T. Murafuji, *Org. Lett.*, 2016, **18**, 6516–6519.
421 H. Tian, Q. Xia, Q. Wang, J. Dong, Y. Liu and Q. Wang, *Org. Lett.*, 2019, **21**, 4585–4589.
422 J. D. Cuthbertson and D. W. C. MacMillan, *Nature*, 2015, **519**, 74–77.
423 H. Tanaka, K. Sakai, A. Kawamura, K. Oisaki and M. Kanai, *Chem. Commun.*, 2018, **54**, 3215–3218.
424 N. Tang, X. Wu and C. Zhu, *Chem. Sci.*, 2019, **10**, 6915–6919.
425 I. Kim, B. Park, G. Kang, J. Kim, H. Jung, H. Lee, M. Baik and S. Hong, *Angew. Chem., Int. Ed.*, 2018, **57**, 15517–15522.
426 N. Kim, C. Lee, T. Kim and S. Hong, *Org. Lett.*, 2019, **21**, 9719–9723.
427 L. K. G. Ackerman, J. I. Martinez Alvarado and A. G. Doyle, *J. Am. Chem. Soc.*, 2018, **140**, 14059–14063.
428 G. X. Li, C. A. Morales-Rivera, F. Gao, Y. Wang, G. He, P. Liu and G. Chen, *Chem. Sci.*, 2017, **8**, 7180–7185.
429 K. A. Hollister, E. S. Conner, M. L. Spell, K. Deveaux, L. Maneval, M. W. Beal and J. R. Ragains, *Angew. Chem., Int. Ed.*, 2015, **54**, 7837–7841.
430 F. Wu, J. P. Ariyarathna, N. Kaur, N. E. Alom, M. L. Kennell, O. H. Bassiouni and W. Li, *Org. Lett.*, 2020, **22**, 2135–2140.
431 Y. Wang, G. X. Li, G. Yang, G. He and G. Chen, *Chem. Sci.*, 2016, **7**, 2679–2683.
432 V. A. Schmidt, R. K. Quinn, A. T. Brusoe and E. J. Alexanian, *J. Am. Chem. Soc.*, 2014, **136**, 14389–14392.
433 R. Liu, J. Li, J. Sun, X. Liu, S. Qu, P. Li and B. Zhang, *Angew. Chem.*, 2020, **132**, 4458–4463.
434 B. J. Lee, K. S. DeGlopper and T. P. Yoon, *Angew. Chem., Int. Ed.*, 2020, **59**, 197–202.
435 D. Petzold, P. Singh, F. Almqvist and B. König, *Angew. Chem., Int. Ed.*, 2019, **58**, 8577–8580.
436 E. A. Wappes, A. Vanitcha and D. A. Nagib, *Chem. Sci.*, 2018, **9**, 4500–4504.
437 M. L. Czyz, G. K. Weragoda, T. H. Horngren, T. U. Connell, D. Gomez, R. A. J. O'Hair and A. Polyzos, *Chem. Sci.*, 2020, **11**, 2455–2463.
438 Y. Qin, Y. Han, Y. Tang, J. Wei and M. Yang, *Chem. Sci.*, 2020, **11**, 1276–1282.
439 J. Kim, B. Kang and S. H. Hong, *ACS Catal.*, 2020, **10**, 6013–6022.
440 S. Mukherjee, B. Maji, A. Tlahuext-Aca and F. Glorius, *J. Am. Chem. Soc.*, 2016, **138**, 16200–16203.
441 W. Xu, W. Wang, T. Liu, J. Xie and C. Zhu, *Nat. Commun.*, 2019, **10**, 4867.
442 W. L. Czaplyski, C. G. Na and E. J. Alexanian, *J. Am. Chem. Soc.*, 2016, **138**, 13854–13857.
443 C. G. Na and E. J. Alexanian, *Angew. Chem., Int. Ed.*, 2018, **57**, 13106–13109.
444 K. A. Margrey, W. L. Czaplyski, D. A. Nicewicz and E. J. Alexanian, *J. Am. Chem. Soc.*, 2018, **140**, 4213–4217.
445 W. Lecroq, P. Bazille, F. Morlet-Savary, M. Breugst, J. Lalevée, A. C. Gaumont and S. Lakhdar, *Org. Lett.*, 2018, **20**, 4164–4167.
446 S. Yang, M. Chen and P. Tang, *Angew. Chem., Int. Ed.*, 2019, **58**, 7840–7844.
447 J. Yi, S. O. Badir, R. Alam and G. A. Molander, *Org. Lett.*, 2019, **21**, 4853–4858.
448 J. X. Li, L. Li, M. D. Zhou and H. Wang, *Org. Chem. Front.*, 2018, **5**, 1003–1007.
449 I. D. Jurberg and H. M. L. Davies, *Chem. Sci.*, 2018, **9**, 5112–5118.
450 C. Shu, A. Noble and V. K. Aggarwal, *Angew. Chem., Int. Ed.*, 2019, **58**, 3870–3874.
451 Y. Fang, R. Zhao, Y. Yao, Y. Liu, D. Chang, M. Yao and L. Shi, *Org. Biomol. Chem.*, 2019, **17**, 7558–7563.
452 I. Kumar, R. Sharma, R. Kumar, R. Kumar and U. Sharma, *Adv. Synth. Catal.*, 2018, **360**, 2013–2019.
453 N. E. S. Tay and D. A. Nicewicz, *J. Am. Chem. Soc.*, 2017, **139**, 16100–16104.
454 L. Ge, D. X. Wang, R. Xing, D. Ma, P. J. Walsh and C. Feng, *Nat. Commun.*, 2019, **10**, 4367.
455 M. R. Becker, A. D. Richardson and C. S. Schindler, *Nat. Commun.*, 2019, **10**, 5095.
456 M. Ociepa, O. Baka, J. Narodowiec and D. Gryko, *Adv. Synth. Catal.*, 2017, **359**, 3560–3565.
457 W. Zhou, T. Miura and M. Murakami, *Angew. Chem., Int. Ed.*, 2018, **57**, 5139–5142.
458 H. L. Sun, F. Yang, W. T. Ye, J. J. Wang and R. Zhu, *ACS Catal.*, 2020, **10**, 4983–4989.
459 D. Petzold, P. Nitschke, F. Brandl, V. Scheidler, B. Dick, R. M. Gschwind and B. König, *Chem. – Eur. J.*, 2019, **25**, 361–366.
460 S. Wang, B.-Y. Cheng, M. Sršen and B. König, *J. Am. Chem. Soc.*, 2020, **142**, 7524–7531.
461 F. Song, F. Wang, L. Guo, X. Feng, Y. Zhang and L. Chu, *Angew. Chem., Int. Ed.*, 2020, **59**, 177–181.
462 A. J. Perkowski, C. L. Cruz and D. A. Nicewicz, *J. Am. Chem. Soc.*, 2015, **137**, 15684–15687.
463 F. Sandfort, T. Knecht, T. Pinkert, C. G. Daniliuc and F. Glorius, *J. Am. Chem. Soc.*, 2020, **142**, 6913–6919.
464 S. Shi, R. Li, L. Rao and Z. Sun, *Green Chem.*, 2020, **22**, 669–672.
465 H. E. Ho, A. Pagano, J. A. Rossi-Ashton, J. R. Donald, R. G. Epton, J. C. Churchill, M. J. James, P. O'Brien, R. J. K. Taylor and W. P. Unsworth, *Chem. Sci.*, 2020, **11**, 1353–1360.
466 A. K. Clarke, A. Parkin, R. J. K. Taylor, W. P. Unsworth and J. A. Rossi-Ashton, *ACS Catal.*, 2020, **10**, 5814–5820.
467 Z. Gan, G. Li, Q. Yan, W. Deng, Y. Y. Jiang and D. Yang, *Green Chem.*, 2020, **22**, 2956–2962.
468 J. B. I. Sap, N. J. W. Straathof, T. Knauber, C. F. Meyer, M. Médebielle, L. Buglioni, C. Genicot, A. A. Trabanco, T. Noël, C. W. am Ende and V. Gouverneur, *J. Am. Chem. Soc.*, 2020, **142**, 9181–9187.
469 J. Q. Liu, A. Shatskiy, B. S. Matsuura and M. D. Kärkäs, *Synthesis*, 2019, 2759–2791.

470 C. Bottecchia and T. Noël, *Chem. – Eur. J.*, 2019, **25**, 26–42.
471 S. P. Morcillo, E. M. Dauncey, J. H. Kim, J. J. Douglas, N. S. Sheikh and D. Leonori, *Angew. Chem., Int. Ed.*, 2018, **57**, 12945–12949.
472 M. Garreau, F. Le Vaillant and J. Waser, *Angew. Chem., Int. Ed.*, 2019, **58**, 8182–8186.
473 T. Brandhofer and O. G. Mancheño, *ChemCatChem*, 2019, **11**, 3797–3801.
474 Z. Yuan, M. B. Nodwell, H. Yang, N. Malik, H. Merkens, F. Bénard, R. E. Martin, P. Schaffer and R. Britton, *Angew. Chem., Int. Ed.*, 2018, **57**, 12733–12736.
475 X. Guo and O. S. Wenger, *Angew. Chem., Int. Ed.*, 2018, **57**, 2469–2473.
476 C. Wang, M. Guo, R. Qi, Q. Shang, Q. Liu, S. Wang, L. Zhao, R. Wang and Z. Xu, *Angew. Chem., Int. Ed.*, 2018, **57**, 15841–15846.
477 A. Noble and D. W. C. MacMillan, *J. Am. Chem. Soc.*, 2014, **136**, 11602–11605.
478 A. H. Jatoi, G. G. Pawar, F. Robert and Y. Landais, *Chem. Commun.*, 2019, **55**, 466–469.
479 T. Yamamoto, T. Iwasaki, T. Morita and Y. Yoshimi, *J. Org. Chem.*, 2018, **83**, 3702–3709.
480 A. Noble, S. J. McCarver and D. W. C. Macmillan, *J. Am. Chem. Soc.*, 2015, **137**, 624–627.
481 N. Chalotra, A. Ahmed, M. A. Rizvi, Z. Hussain, Q. N. Ahmed and B. A. Shah, *J. Org. Chem.*, 2018, **83**, 14443–14456.
482 K. Liang, X. Tong, T. Li, B. Shi, H. Wang, P. Yan and C. Xia, *J. Org. Chem.*, 2018, **83**, 10948–10958.
483 A. D. de Bruijn and G. Roelfes, *Chem. – Eur. J.*, 2018, **24**, 11314–11318.
484 Y. Tian, J. Li, H. Zhao, X. Zeng, D. Wang, Q. Liu, X. Niu, X. Huang, N. Xu and Z. Li, *Chem. Sci.*, 2016, **7**, 3325–3330.
485 N. Ichiishi, J. P. Caldwell, M. Lin, W. Zhong, X. Zhu, E. Streckfuss, H. Y. Kim, C. A. Parish and S. W. Krska, *Chem. Sci.*, 2018, **9**, 4168–4175.
486 M. Jiang, H. Yang and H. Fu, *Org. Lett.*, 2016, **18**, 1968–1971.
487 C. Wang, R. Qi, H. Xue, Y. Shen, M. Chang, Y. Chen, R. Wang and Z. Xu, *Angew. Chem., Int. Ed.*, 2020, **59**, 7461–7466.
488 Z. Zuo, D. T. Ahneman, L. Chu, J. A. Terrett, A. G. Doyle and D. W. C. MacMillan, *Science*, 2014, **345**, 437–440.
489 P. Ji, Y. Zhang, Y. Dong, H. Huang, Y. Wei and W. Wang, *Org. Lett.*, 2020, **22**, 1557–1562.
490 M. S. Santos, H. L. I. Betim, C. M. Kisukuri, J. A. Campos Delgado, A. G. Corrêa and M. W. Paixão, *Org. Lett.*, 2020, **22**, 4266–4271.
491 E. Speckmeier and K. Zeitler, *ACS Catal.*, 2017, **7**, 6821–6826.
492 Z. Liu, Y. Zhang, Z. Cai, H. Sun and X. Cheng, *Adv. Synth. Catal.*, 2015, **357**, 589–593.
493 N. Iqbal and E. J. Cho, *Adv. Synth. Catal.*, 2015, **357**, 2187–2192.
494 B. Reichart, G. Guedes de la Cruz, K. Zangger, C. O. Kappe and T. Glasnov, *Adv. Synth. Catal.*, 2016, **358**, 50–55.
495 D. J. Kunsberg, A. H. Kipping and D. E. Falvey, *Org. Lett.*, 2015, **17**, 3454–3457.
496 Y. Ma, S. Liu, Y. Xi, H. Li, K. Yang, Z. Cheng, W. Wang and Y. Zhang, *Chem. Commun.*, 2019, **55**, 14657–14660.
497 L. Anhäuser, N. Klöcker, F. Muttach, F. Mäsing, P. Špaček, A. Studer and A. Rentmeister, *Angew. Chem., Int. Ed.*, 2020, **59**, 3161–3165.
498 G. H. Lovett, S. Chen, X. S. Xue, K. N. Houk and D. W. C. MacMillan, *J. Am. Chem. Soc.*, 2019, **141**, 20031–20036.
499 A. Inial, F. Morlet-Savary, J. Lalevée, A. C. Gaumont and S. Lakhdar, *Org. Lett.*, 2020, **22**, 4404–4407.
500 S. O. Badir, J. Sim, K. Billings, A. Csakai, X. Zhang, W. Dong and G. A. Molander, *Org. Lett.*, 2020, **22**, 1046–1051.
501 D. K. Kölmel, A. S. Ratnayake, M. E. Flanagan, M. H. Tsai, C. Duan and C. Song, *Org. Lett.*, 2020, **22**, 2908–2913.
502 B. H. Lipshutz, S. Ghorai and M. Cortes-Clerget, *Chem. – Eur. J.*, 2018, **24**, 6672–6695.
503 M. J. Bu, G. P. Lu, J. Jiang and C. Cai, *Catal. Sci. Technol.*, 2018, **8**, 3728–3732.
504 J. P. Barham and B. König, *Angew. Chem., Int. Ed.*, 2020, **59**, 11732–11747.
505 L. Schmermund, V. Jurkaš, F. F. Özgen, G. D. Barone, H. C. Büchsenschütz, C. K. Winkler, S. Schmidt, R. Kourist and W. Kroutil, *ACS Catal.*, 2019, **9**, 4115–4144.